To the Graduate Council:

I am submitting herewith a dissertation written by Xueguang Jiang entitled "Synthesis and Solution Behavior of Doubly Responsive Hydrophilic Block Copolymers." I have examined the final electronic copy of this dissertation for form and content and recommend that it be accepted in partial fulfillment of the requirements for the degree of Doctor of Philosophy, with a major in Chemistry.

Bin Zhao, Major Professor

We have read this dissertation
and recommend its acceptance:

Mark Dadmun

Jamie Adcock

Qixin Zhong

Accepted for the council:

Carolyn R. Hodges
Vice Provost and Dean of the Graduate School

(Original signatures are on file with official student records.)

Synthesis and Solution Behavior of Doubly Responsive Hydrophilic Block Copolymers

A Dissertation

Presented for the

Doctor of Philosophy Degree

The University of Tennessee, Knoxville

Xueguang Jiang

August 2010

Acknowledgements

I would like to express my sincere gratitude to Dr. Bin Zhao for his guidance, encouragement, patience, and support throughout my graduate study. Dr. Zhao helped me get through the difficult time of my life and taught me how to be a professional and chemist.

I would also like to thank Dr. Jamie L. Adcock, Dr. Mark Dadmun, and Dr. Qixin Zhong for serving on my doctoral dissertation committee. In addition, I would like to thank Dr. Dadmun for his advice on light and neutron scattering experiments, Dr. Qixin Zhong of Department of Food Science and Technology at the University of Tennessee, Knoxville for teaching me how to use the rheometer, and Dr. Shi Jin of College of Staten Island at the City University of New York for performing small angle x-ray scattering and polarized light microscopy experiments.

I would like to thank all my group members in our research group who have been working with me during the past five years: Dr. Fengjun Hua, Dr. Dejin Li, Xiaoming Jiang, Thomas O′Lenick, Jeremiah Woodcock, Jonathan Horton, Naixiong Jin, Clark Moore, Christopher Lavender, and Roger Wright, for their cooperation and friendship.

Most importantly, I would like to thank my parents for their love, care, understanding, and support.

Finally, I appreciate the financial support from the University of Tennessee and National Science Foundation.

Abstract

This dissertation presents the synthesis of stimuli-sensitive hydrophilic polymers, particularly doubly responsive hydrophilic block copolymers, by controlled radical polymerizations and the study of their solution behavior in water. By incorporating a small amount of stimuli-responsive groups into the thermosensitive block of a hydrophilic block copolymer, the lower critical solution temperature (LCST) of the thermosensitive block can be tuned by a stimulus and multiple micellization/dissociation transitions can be achieved by combining two external triggers.

Chapter 1 describes the synthesis and thermosensitive properties of two new water-soluble polystyrenics with a short oligo(ethyl glycol) pendant from each repeat unit and the study of hydrophobic end group effects on cloud points of thermosensitive polystyrenics. Well-defined polymers were prepared from monomer-based initiators via nitroxide-mediated polymerization and the alkoxyamine end groups were removed by tri(*n*-butyl)tin hydride, yielding thermoresponsive polystyrenics with essentially no end groups. The results showed that hydrophobic end groups could significantly change the cloud points and the molecular weight dependences of cloud points of polystyrenics. Chapter 2 presents the synthesis of thermo- and light-sensitive hydrophilic block copolymers, poly(ethylene oxide)-*b*-poly(ethoxytri(ethylene glycol) acrylate-*co*-*o*-nitrobenzyl acrylate), and their responsive behavior in dilute aqueous solutions. Dynamic light scattering and fluorescence spectroscopy studies showed that these copolymers were molecularly dissolved in water at lower temperatures and self-assembled into micelles at temperatures above the LCST of the thermosensitive block. Upon UV irradiation, the *o*-

nitrobenzyl group was cleaved and the LCST of the thermosensitive block was increased, causing the dissociation of micelles into unimers. The resultant copolymers underwent thermo-induced reversible micellization at higher temperatures. Chapter 3 describes multiple micellization/dissociation transitions of thermo- and pH-sensitive hydrophilic block copolymers, poly(ethylene oxide)-*b*-poly(methoxydi(ethylene glycol) methacrylate-*co*-methacrylic acid), in response to temperature and pH changes. The LCST of the thermosensitive block can be reversibly tuned and precisely controlled by solution pH. Chapter 4 presents the study on multiple sol-gel-sol transitions of a 20.0 wt % aqueous solution of poly(ethylene oxide)-*b*-poly(ethoxytri(ethylene glycol) acrylate-*co*-*o*-nitrobenzyl acrylate) induced by temperature changes and UV irradiation. The solution underwent thermo-induced sol-gel-sol transitions. Upon UV irradiation to dissociate micelles, the gel was transformed into a free-flowing liquid, which upon heating underwent sol-gel-sol transitions again.

Contents

Chapter 1. Well-Defined Thermosensive Water-Soluble Polystyrenics with Short Pendant Oligo(ethylene glycol) Groups: Synthesis and End Group Effect on Thermosensitive Properties ……..…..1

Abstract……..2

1.1 Introduction……4

1.2 Experimental Section……..9

1.2.1 Materials……9

1.2.2 Characterization……..10

1.2.3 Synthesis of α-Hydro-ω-(4-vinylbenzyl)tris(oxyethylene) (HTEGSt)….11

1.2.4 Synthesis of α-Hydro-ω-(4-vinylbenzyl)tetrakis(oxyethylene) (HTrEGSt)……12

1.2.5 Nitroxide-Mediated Radical Polymerizations of HTEGSt and HTrEGSt Using 2,2,5-Trimethyl-3-(1-phenylethoxy)-4-phenyl-3-azahexane (TPPA) as Initiator……..12

1.2.6 Synthesis of 2,2,5-trimethyl-3-(1-(4′-(2,5,8,11-tetraoxadodecyl)phenyleth-oxy)-4-phenyl-3-azahexane (TEPPA)……..13

1.2.7 Synthesis of 2,2,5-trimethyl-3-(1-(4′-(2,5,8,11,14-pentaoxatetradecyl-phenylethoxy)-4-phenyl-3-azahexane (HTrEPPA)……..…14

1.2.8 Nitroxide-Mediated Radical Polymerization of TEGSt Using TEPPA as Initiator……..…15

1.2.9 Nitroxide-Mediated Radical Polymerization of HTrEGSt Using HTrEPPA as Initiator……16

1.2.10 Removal of the Alkoxyamine Group from the Chain End by Tri(*n*-butyl)tin Hydride……17
1.3 Results and Discussion……..17
1.3.1 Synthesis and Thermosensitive Properties of PHTEGSt and PHTrEGSt….17
1.3.1.1 Synthesis of Monomers……..…17
1.3.1.2 Nitroxide-Mediated Radical Polymerizations of HTEGSt and HTrEGSt Using TPPA as Initiator……18
1.3.1.3 Thermosensitive Properties of PHTEGSt and PHTrEGSt in Water…….22
1.3.2 End Group Effect on Thermosensitive Properties……24
1.3.2.1 Synthesis of Monomer-Based NMRP Initiators……...24
1.3.2.2 Nitroxide-Mediated Radical Polymerizations of TEGSt and HTrEGSt Using TEPPA and HTrEPPA as Initiator, Respectively..26
1.3.2.3 Removal of the Alkoxyamine Group from the Chain End of PTEGSt and PHTrEGSt……..….31
1.3.2.4 Thermosensitive Properties of PTEGSt Prepared by Use of TPPA and TEPPA as Initiators: Comparison of Cloud Points Before and After the Removal of the Alkoxyamine Group from Polymer Chain End……34
1.3.2.5 Molecular Weight Dependence of Cloud Point of PTEGSt with Different End Groups……39
1.3.2.6 Molecular Weight Dependence of Cloud Point of PHTrEGSt with Different End Groups……42

1.3.2.7 Molecular Weight Effect and End Group Effect on the Cloud Points of Polystyrenics……44

1.4 Conclusions……...…45

References……47

Chapter 2. Multiple Micellization and Dissociation Transitions of Thermo- and Light-Sensitive Poly(ethylene oxide)-*b*-Poly(ethoxytri(ethylene glycol) acrylate-*co*-*o*-nitrobenzyl acrylate) in Dilute Aqueous Solution…….....52

Abstract……53

2.1 Introduction……54

2.2 Experimental Section……56

2.2.1 Materials…….....56

2.2.2 General Characterization……..59

2.2.3 Preparation of Aqueous Polymer Solutions for Dynamic Light Scattering and Fluorescence Spectroscopy Studies……...60

2.2.4 Dynamic Light Scattering……61

2.2.5 Fluorescence Spectroscopy……...62

2.2.6 Synthesis of Ethoxytri(ethylene glycol) Acrylate (TEGEA)……....63

2.2.7 Synthesis of *o*-Nitrobenzyl Acrylate (NBA)……64

2.2.8 Synthesis of PEO Macroinitiator PEO-Br……65

2.2.9 Synthesis of PTEGEA by ATRP……..65

2.2.10 Synthesis of Random Copolymer of TEGEA and NBA by ATRP……66

2.2.11 Synthesis of Diblock Copolymer PEO-*b*-PTEGEA by ATRP from Macroinitiator PEO-Br……..67

2.2.12 Synthesis of Block Copolymer PEO-*b*-P(TEGEA-*co*-NBA) by ATRP Using Macroinitiator PEO-Br as Initiator…….68

2.2.13 Photo-Cleavage of *o*-Nitrobenzyl Group……69

2.3 Results and Discussion……..69

2.3.1 Synthesis of Monomers and Polymers……..70

2.3.2 Thermosensitive Properties of PTEGEA and P(TEGEA-*co*-NBA)…….73

2.3.3 Photocleavage of *o*-Nitrobenzyl Group of NBA in P(TEGEA-*co*-NBA) and the Cloud Point of the Obtained Polymer in Water……..76

2.3.4 Reversible Micellization of Block Copolymers in Water in Response to Temperature Changes……...78

2.3.5 UV-Irradiation-Induced Dissociation of Micelles of PEO-*b*-P(TEGEA-*co*-NBA)…….86

2.3.6 Temperature-Induced Reversible Formation and Dissociation of Micelles of PEO-*b*-P(TEGEA-*co*-AA)……92

2.4 Conclusion…….96

References……99

Chapter 3. Tuning Micellization and Dissociation Transitions of Thermo- and pH-Sensitive Poly(ethylene oxide)-*b*-poly(methoxydi(ethylene glycol) methacrylate-*co*-methacrylic acid) in Aqueous Solution by Combining Temperature and pH Triggers……105

Abstract……..106

3.1 Introduction……..108

3.2 Experimental Section……...111

3.2.1 Materials……111

3.2.2 General Characterization……...…….114

3.2.3 Preparation of Aqueous Buffer Solutions of Block Copolymers for Dynamic Light Scattering and Fluorescence Spectroscopy Studies…….….115

3.2.4 Titration of Aqueous Polymer Solutions with a KOH Solution…….116

3.2.5 Dynamic Light Scattering……...116

3.2.6 In Situ Dissociation and Re-formation of Micelles by Sequential Injection of 1.00 M KOH Solution and 1.00 M HCl Solution……...117

3.2.7 Fluorescence Spectroscopy…….118

3.2.8 Synthesis of Homopolymer of DEGMMA by ATRP…….119

3.2.9 Synthesis of Random Copolymer of DEGMMA and *t*BMA by ATRP…..120

3.2.10 Synthesis of Block Copolymer PEO-*b*-P(DEGMMA-*co*-*t*BMA) by ATRP Using Macroinitiator PEO-Br……...…..121

3.2.11 Removal of *t*-Butyl Group of P(DEGMMA-*co*-P*t*BMA) and PEO-*b*-P(DEGMMA-*co*-*t*BMA)…….121

3.2.12 Treatment of PDEGMMA with CF_3COOH……..123

3.3 Results and Discussion……123

3.3.1 Synthesis and Hydrolysis of Random Copolymer P(DEGMMA-*co*-*t*BMA) and Block Copolymer PEO-*b*-P(DEGMMA-*co*-*t*BMA)……123

3.3.2 Thermosensitive Properties of P(DEGMMA-*co*-MAA) and PDEGMMA126

3.3.3 Temperature-Induced Reversible Micellization/Dissociation Transitions of PEO-*b*-P(DEGMMA-*co*-MAA) in Aqueous Buffer Solutions……...127

3.3.4 KOH-Triggered Dissociation of Micelles and Subsequent Temperature-Induced Formation and Disassembly of Micelles……...133

3.3.5 HCl-Triggered Formation of Micelles and Subsequent Temperature-Induced Dissociation and Re-formation of Micelles……140

3.3.6 Three Cycles of Micellization and Dissociation Transitions of Thermo- and pH-Responsive Block Copolymer PEO-*b*-P(DEGMMA-*co*-MAA) Achieved by Judiciously Controlling Temperature and pH……...….142

3.3.7 Control Experiment…….148

3.4 Conclusion……...…150

References……..152

Chapter 4. Stimuli-Induced Multiple Sol-Gel-Sol Transitions of Aqueous Solution of a Thermo- and Light-Sensitive Hydrophilic Block Copolymer.....158

Abstract……..159

4.1 Introduction……..160

4.2 Experimental Section……...……162

4.2.1 Materials…….162

4.2.2 General Characterization……163

4.2.3 Preparation of 20.0 wt % Aqueous Solution of PEO-*b*-P(TEGEA-*co*-NBA)……163

4.2.4 Rheological Measurements…….……164

4.2.5 Photocleavage of *o*-Nitrobenzyl Group of NBA in PEO-*b*-P(TEGEA-*co*-NBA)…….…..164

4.2.6 Polarized Light Microscopy Experiments……..165

4.2.7 Dynamic Light Scattering Studies of Aqueous Solutions of PEO-*b*-P(TEGEA-*co*-NBA) and PEO-*b*-P(TEGEA-*co*-AA)…….165

4.2.8 Determination of Phase Diagrams of PEO-*b*-P(TEGEA-*co*-NBA) and PEO-*b*-P(TEGEA-*co*-AA) in Water by the Vial Inversion Test…….166

4.3 Results and Discussion……167

4.3.1 Multiple Sol-Gel-Sol Transitions of a 20.0 wt % Aqueous Solution of PEO-*b*-P(TEGEA-*co*-NBA) in Response to Temperature Changes and UV Irradiation……167

4.3.2 Rheological Properties of the 20.0 wt % Aqueous Solution of PEO-*b*-P(TEGEA-*co*-NBA) and the UV-Irradiated Solution…….171

4.3.3 Sol-Gel Phase Diagrams of PEO-*b*-P(TEGEA-*co*-NBA) and PEO-*b*-P(TEGEA-*co*-AA) in Water at Moderate Concentrations……..178

4.3.4 Mechanisms of Sol-to-Gel/Gel-to-Sol Transitions of the 20.0 wt % Aqueous Solution of the Thermo- and Light-Sensitive Block Copolymer Induced by Temperature Changes and UV Irradiation……..182

4.4 Conclusion……..…….187

References and Footnote……189

Chapter 5. Summary and Future Work……...……...……195

5.1 Summary……...…196

5.2 Future Work……..…198

5.2.1 Light-Induced Reversible Micellization/Dissociation Transitions of Thermo- and Light-Sensitive Block Copolymer in Water …….……...198

5.2.2 Structural Studies of Aqueous Solutions of Doubly Responsive Hydrophilic Block Copolymers by Small-Angle Neutron Scattering……201

References……....203

Appendix A……...……..……204

Appendix B……...……...……221

Vita……...……..……244

List of Tables

2.1 Characterization Data for PTEGEA, P(TEGEA-*co*-NBA), PEO-*b*-PTEGEA, and Two Samples of PEO-*b*-P(TEGEA-*co*-NBA) Used in this Work……74

2.2 Critical Micellization Temperatures, Critical Micelle Concentrations, and Micelle Characteristics of Three Block Copolymers……..83

2.3 Critical Micellization Temperatures and Micelle Characteristics of PEO-*b*-P(TEGEA-*co*-AA) Obtained from BR-**4** and -**5** by UV Irradiation……..97

3.1 Characterization Data for PDEGMMA, P(DEGMMA-*co*-*t*BMA) and the Corresponding P(DEGMMA-*co*-MAA), Two Samples of PEO-*b*-P(DEGMMA-*co*-*t*BMA) and the Corresponding PEO-*b*-P(DEGMMA-*co*-MAA) Used in this Work……....125

3.2 Critical Micellization Temperatures of Block Copolymer PEO-*b*-P(DEGMMA-*co*-MAA) (**BR3-H** and **BR4-H**), and the Hydrodynamic Sizes and Polydispersities of Their Micelles under Various Conditions……..……...132

3.3 Critical Micellization Temperatures (CMT) and Micelle Characteristics of PEO-*b*-P(DEGMMA-*co*-MAA) Obtained from Three Cycles of Micellization and Dissociation Transitions as Well as Critical Micelle Concentrations (CMC) at Different pH Values……..…147

List of Schemes

1.1 Synthesis of Thermosensitive, Water-Soluble PHTEGSt and PHTrEGSt by NMRP with TPPA as an Initiator in the Presence of TPANO……6

1.2 Synthesis of Thermosensitive Polystyrenics with "no" End Groups……...8

1.3 Molecular Structures of Alkoxyamine NMRP Initiators TPPA, TEPPA, and HTrEPPA and the Synthesis of TEPPA and HTrEPPA……27

2.1 Synthesis of Thermo- and Light-Sensitive Poly(ethylene oxide)-*b*-Poly(ethoxytri(ethylene glycol) acrylate-*co*-*o*-nitrobenzyl acrylate) and Cleavage of *o*-Nitrobenzyl Group by UV Irradiation……57

2.2 Multiple Micellization and Dissociation Transitions of Thermo- and Light-Sensitive Poly(ethylene oxide)-*b*-Poly(ethoxytri(ethylene glycol) acrylate-*co*-*o*-nitrobenzyl acrylate) in Water in Response to Temperature Changes and UV Irradiation.……..58

3.1 Synthesis of Thermo- and pH-Sensitive Water-Soluble Poly(ethylene oxide)-*b*-Poly(methoxydi(ethylene glycol) methacrylate-*co*-methacrylic acid) (PEO-*b*-P(DEGMMA-*co*-MAA))…….112

3.2 Multiple Reversible Micellization and Dissociation Transitions of Thermo- and pH-Sensitive Block Copolymer PEO-*b*-P(DEGMMA-*co*-MAA) by Controlling Temperature and pH……..……..113

4.1 Schematic Illustration of Thermo- and Light-Induced Multiple Sol-to-gel/gel-to-sol Transitions of the 20.0 wt % Aqueous Solution of PEO-*b*-P(TEGEA-*co*-NBA) under Different Conditions……..……185

5.1 Photoisomerization of spiropyran and azobenzene compounds and monomer structures of SPMA and AzoMA…….....199

List of Figures

1.1 (a) Relationship between $\ln([M]_o/[M])$ and time for the polymerization of HTEGSt using TPPA as an initiator in the presence of free nitroxide TPANO in anisole (1:1 w/w with respective to the monomer) at 120 ^oC ($[M]_o$ = 1.86 M, $[M]_o/[I]_o$ = 127, $[TPANO]_o$ = 0.72 mM), (b) evolution of GPC curves with the polymerization time, and (c) $M_{n,GPC}$ (■) and PDI (▼) versus the monomer conversion. The DP of the final polymer was 52……..…..20

1.2 (a) Relationship between $\ln[M]_o/[M]$ and time for the polymerization of HTrEGSt using TPPA as an initiator in the presence of free nitroxide TPANO in anisole (1:1 w/w with respect to the monomer) at 120 ^oC ($[M]_o$ = 1.72 M, $[M]_o/[I]_o$ = 119, $[TPANO]_o$ = 0.71 mM), and (b) $M_{n,GPC}$ (■) and PDI (▼) obtained from GPC analysis with respect to polystyrene standards versus the monomer conversion. The DP of the final polymer was 53……..21

1.3 Optical transmittances of aqueous solutions of PHTEGSt (▲, $M_{n,GPC}$ = 10400 g/mol, PDI = 1.08, DP = 52, 0.5 wt %) and PHTrEGSt (▼, $M_{n,GPC}$ = 11800 g/mol, PDI = 1.09, DP = 53, 1.0 wt %) as a function of temperature. The transmittances were recorded at wavelength of 490 nm by use of a UV-vis spectrometer……..23

1.4 ^1H NMR spectra of (a) PHTEGSt ($M_{n,GPC}$ = 10400 g/mol, DP = 52, PDI = 1.08) and (b) PHTrEGSt ($M_{n,GPC}$ = 11800 g/mol, PDI = 1.09, DP = 53) in D_2O (1.0 wt %) at various temperatures……..…25

1.5 (a) Relationship between $\ln([M]_0/[M])$ and time for the polymerization of TEGSt using TEPPA as initiator in the presence of free nitroxide TPANO in anisole

(1.1:1 w/w with respect to monomer) at 120 ^{o}C ($[TEGSt]_0$ = 1.66 M, $[M]_0/[I]_0$ = 121, $[TPANO]_0$ = 0.684 mM), (b) evolution of GPC curves with the polymerization time, and (c) $M_{n,GPC}$ (■) and PDI (▼), obtained from GPC analysis relative to polystyrene standards, versus monomer conversion. The DP of the final polymer was 54……...…….29

1.6 (a) Relationship between $\ln([M]_0/[M])$ and time for the polymerization of HTrEGSt using HTrEPPA as an initiator in the presence of free nitroxide TPANO in anisole (1.3:1 w/w with respect to monomer) at 120 ^{o}C ($[HTrEGSt]_0$ = 1.41 M, $[M]_0/[I]_0$ = 121, $[TPANO]_0$ = 0.580 mM), (b) evolution of GPC curves with the polymerization time, and (c) $M_{n,GPC}$ (■) and PDI (▼), obtained from GPC analysis relative to polystyrene standards, versus monomer conversion. The DP of the final polymer was 59……...…….30

1.7 (a) ^{1}H NMR spectra of PTEGSt that was synthesized using TEPPA as initiator ($M_{n,GPC}$ = 8300 g/mol, PDI = 1.09, DP = 41 (including one repeat unit from initiator TEPPA)) before and after the removal of the alkoxyamine end group with $(n\text{-Bu})_3SnH$, and (b) GPC traces of the same polymer before (solid line) and after (dotted line) the removal of the alkoxyamine group from the chain end…...……32

1.8 (a) ^{1}H NMR spectra of PHTrEGSt that was synthesized using HTrEPPA as initiator ($M_{n,GPC}$ = 8400 g/mol, PDI = 1.09, DP = 45) before and after the removal of the alkoxyamine group, and (b) GPC traces of the same polymer before (solid line) and after (dotted line) the removal of the alkoxyamine group from polymer chain end……..……..33

1.9 Optical transmittances of aqueous solutions of Ph-PTEGSt-ON (synthesized by use of TPPA initiator, $M_{n,GPC}$ = 8200 g/mol, PDI = 1.11, DP = 40, 1.0 wt %, ▲ heating process; ▼ cooling process) and the corresponding reduced polymer Ph-PTEGSt-H (1.0 wt %, ■ heating process; ● cooling process) as a function of temperature. The transmittances were recorded at wavelength of 500 nm by use of a UV-vis spectrometer..……...……..35

1.10 Optical transmittances of aqueous solutions of H-PTEGST-ON (synthesized by use of TEPPA as initiator, $M_{n,GPC}$ = 8300 g/mol, PDI = 1.09, DP = 40, 1.0 wt %, ▲ heating process, ▼ cooling process) and the corresponding reduced polymer H-PTEGSt-H (1.0 wt %, ■ heating process; ● cooling process) as a function of temperature. The transmittances were recorded at wavelength of 500 nm by use of a UV-vis spectrometer……...……36

1.11 Concentration effect on the cloud point of Ph-PTEGSt-ON (■, synthesized from TPPA initiator, DP = 40, $M_{n,GPC}$ = 8200 g/mol, PDI = 1.11), Ph-PTEGSt-H (●, reduced Ph-PTEGSt-ON by use of $(n\text{-Bu})_3SnH$), H-PTEGSt-ON (▲, synthesized from TEPPA initiator, DP = 41, $M_{n,GPC}$ = 8300 g/mol, PDI = 1.09), and H-PTEGSt-H (▼, reduced H-PTEGSt-ON by use of $(n\text{-Bu})_3SnH$)……..……38

1.12 Molecular weight dependence of cloud point of Ph-PTEGSt-ON (■, synthesized from TPPA initiator), Ph-PTEGSt-H (●, reduced from Ph-PTEGSt-ON using (n-Bu)$_3$SnH), H-PTEGSt-ON (▲, synthesized from initiator TEPPA), and H-PTEGSt-H (▼, reduced from H-PTEGSt-ON using (n-Bu)$_3$SnH) in water at a concentration of 1.0 wt %. The molecular weights were measured by GPC using polystyrene calibration……..…….40

1.13 Molecular weight dependence of cloud point of Ph-PHTrEGSt-ON (●, synthesized from initiator TPPA), H-PHTrEGSt-ON (▼, synthesized from initiator HTrEPPA), and H-PHTrEGSt-H (▲, reduced from H-PHTrEGSt-ON using (n-Bu)$_3$SnH) in water at a concentration of 1.0 wt %. The molecular weights were measured by GPC using polystyrene calibration…….….43

2.1 Gel permeation chromatography curves of macroinitiator PEO-Br and PEO-*b*-P(TEGEA-*co*-NBA) (BR-**4** in Table 2.1, $M_{n,GPC}$ = 18,300 g/mol, PDI = 1.07)....72

2.2 Optical transmittances at wavelength of 550 nm of an aqueous solution of PTEGEA (H-**1**, $M_{n,GPC}$ = 14,500 g/mol, PDI = 1.16, 0.2 wt %, heating ▲, cooling ▼) and an aqueous solution of P(TEGEA-*co*-NBA) (R-**2**, $M_{n,GPC}$ = 13,900 g/mol, PDI = 1.13, 0.2 wt %) before (heating ■, cooling ●) and after irradiation with 365 nm UV light at 13 ^{o}C for 485 min (heating ►, cooling ◄) as a function of temperature. The transmittances were recorded with a UV-visible spectrometer……...75

2.3 ^{1}H NMR spectra of (a) P(TEGEA-*co*-NBA) (R-**2**, $M_{n,GPC}$ = 13,900 g/mol, PDI = 1.13) and (b) the polymer obtained from the 0.2 wt % aqueous solution of R-**2** after irradiation with 365 nm UV light at 13 ^{o}C for 485 min. $CDCl_3$ was used as the solvent……..……77

2.4 The intensity of scattered light at a scattering angle of 90^{o} (a) and the hydrodynamic diameter (b) as a function of temperature (▲ heating, ▼ cooling) in a dynamic light scattering study of a 0.2 wt % aqueous solution of PEO-*b*-P(TEGEA-*co*-NBA) (BR-**4**, $M_{n,GPC}$ = 18,300 g/mol, PDI = 1.07)……80

2.5 (a) Hydrodynamic diameter (D_h) distribution of micelles of PEO-*b*-P(TEGEA-*co*-NBA) (BR-**4**, $M_{n,GPC}$ = 18,300 g/mol, PDI = 1.07) at 50 ^oC and (b) plot of Γ/q^2 of micelles of BR-**4** (●) and the corresponding PEO-*b*-P(TEGEA-*co*-AA) (▲) vs. q^2 at 50 ^oC. The polydispersity of micelles of BR-**4** at 50 ^oC was 0.048. PEO-*b*-P(TEGEA-*co*-AA) was obtained by UV irradiation of a 0.2 wt % aqueous solution of BR-**4** at 32 ^oC for 480 min……..…..81

2.6 Fluorescence spectra of Nile Red (a) in a 0.2 wt % aqueous solution of PEO-*b*-P(TEGEA-*co*-NBA) (BR-**4**, $M_{n,GPC}$ = 18,300 g/mol, PDI = 1.07) at various temperatures during the heating process and (b) in a series of aqueous solutions of BR-**4** with different concentrations at 32 ^oC. The inset in (a) is the plot of maximum fluorescence intensity versus temperature, from which the critical micellization temperature (CMT_1) was determined. The inset in (b) is the plot of maximum fluorescence intensity versus polymer concentration at 32 ^oC, from which the critical micelle concentration (CMC) was determined…….……84

2.7 The intensity of scattered light at scattering angle of 90^o (a) and hydrodynamic diameter (b) as a function of temperature in a dynamic light scattering study of multiple micellization and dissociation transitions of PEO-*b*-P(TEGEA-*co*-NBA) (BR-**4**, $M_{n,GPC}$ = 18,300 g/mol, PDI = 1.07, 0.2 wt % aqueous solution – the same solution used in Figure 4) in response to temperature changes and UV irradiation. The data points from 15 to 32 ^oC before UV irradiation were from the heating process in Figure 4. At 32 ^oC, the polymer solution was irradiated with 365 nm UV light for 480 min. The collection of light scattering data was resumed thereafter……..……..88

2.8 Fluorescence spectra of Nile Red in a 0.2 wt % aqueous solution of PEO-*b*-P(TEGEA-*co*-NBA) (BR-**4**, $M_{n,GPC}$ = 18,300 g/mol, PDI = 1.07) after exposure to 365 nm UV light at 32 ^{o}C for 0, 145, 199, 253, 311, and 480 min. The inset is the plot of maximum fluorescence emission intensity versus UV irradiation time. The wavelengths of the maximum peak were 617 nm (0 min), 625 nm (145 min), 626 nm (199 min), 625 nm (253 min), 628.5 nm (311 min), and 625 nm (480 min).....89

2.9 Fluorescence spectra of (a) Nile Red in a 0.2 wt % aqueous solution of PEO-*b*-PTEGEA (B-**3**, $M_{n,GPC}$ = 21,400 g/mol, PDI = 1.07) after exposure to 365 nm UV irradiation for 0, 58, 180, 244, 319, 403, and 500 min and (b) photobleached Nile Red in the UV-irradiated solution of B-**3** at various temperatures during the heating process. The inset in (a) is the plot of maximum fluorescence emission intensity versus UV irradiation time. The inset in (b) is the plot of maximum fluorescence intensity versus temperature, from which the CMT was determined……..……91

2.10 The intensity of scattered light at scattering angle of 90^{o} (a) and hydrodynamic diameter (b) as a function of temperature (▲ heating, ▼ cooling) in a dynamic light scattering study of thermo-induced reversible formation and dissociation of micelles of PEO-*b*-P(TEGEA-*co*-AA), which was obtained in situ by UV irradiation of a 0.2 wt % aqueous solution of PEO-*b*-P(TEGEA-*co*-NBA) (BR-**4**, $M_{n,GPC}$ = 18,300 g/mol, PDI = 1.07) for 480 min……..93

2.11 Fluorescence spectra of (a) photobleached Nile Red and (b) photobleached dye plus reloaded fresh Nile Red in an aqueous solution of PEO-*b*-P(TEGEA-*co*-AA)

at various temperatures in the heating process. The aqueous solution of PEO-*b*-P(TEGEA-*co*-AA) was obtained in situ by UV irradiation of a 0.2 wt % aqueous solution of PEO-*b*-P(TEGEA-*co*-NBA) (BR-**4**, $M_{n,GPC}$ = 18,300 g/mol, PDI = 1.07) at 32 ^{o}C for 480 min. The insets are the plots of maximum fluorescence emission intensity versus temperature, which are used to determine the CMT_2……94

3.1 (a) Optical transmittances at wavelength of 550 nm of 0.2 wt % aqueous solutions of P(DEGMMA-*co*-MAA) (**R2-H**) in 10 mM potassium hydrogen phthalate buffers with pH values of 4.0 (■ heating; □ cooling), 5.5 (▲ heating; △ cooling), 6.0 (▼ heating; ▽ cooling), and 6.5 (● heating) as a function of temperature. The transmittances were recorded with a UV-visible spectrometer. (b) Dependence of the cloud point of **R2-H** on the solution pH……...…128

3.2 The intensity of scattered light at scattering angle of 90^{o} (a) and the hydrodynamic diameter (b) as a function of temperature (■ heating, □ cooling) in a DLS study of a 0.2 wt % aqueous buffer solution of PEO-*b*-P(DEGMMA-*co*-MAA) (**BR3-H**) at pH = 4.0. In (b), at 30 ^{o}C in both heating and cooling processes, two size distributions, one ascribed to the unimers and one to the micelles, were observed and the reported hydrodynamic diameters for this temperature were the average values over two hydrodynamic size distributions……130

3.3 The plot of solution pH versus number of μmols of KOH injected into a 0.2 wt % solution of PEO-*b*-P(DEGMMA-*co*-MAA) (**BR3-H**) in 10 mM KHP buffer (2.50 g). The KOH solution was added stepwise; each time, 10 μL of a 0.20 M aqueous

KOH solution was injected via a microsyringe, followed by the measurement of pH with a pH meter……..135

3.4 The intensity of scattered light at scattering angle of 90^{o} (a) and the apparent hydrodynamic diameter (b) as a function of temperature (■ heating, □ cooling) in a DLS study of multiple micellization and dissociation transitions of a 0.2 wt % solution of PEO-*b*-P(DEGMMA-*co*-MAA) (**BR3-H**) in 10 mM KHP buffer solution (2.50 g, the same solution used in Figure 3.2) in response to addition of KOH (19 μL of 1.00 M KOH at 34 ^{o}C) and subsequent temperature changes. The data points from 20 ^{o}C to 34 ^{o}C were from the heating process in Figure 3.2…137

3.5 Maximum fluorescence emission intensity of Nile Red in a 0.2 wt % solution of **BR3-H** (PEO-*b*-P(DEGMMA-*co*-MAA)) in 10 mM KHP buffer in response to pH and subsequent temperature changes (■ heating, □ cooling). In (a), at 34 ^{o}C, 7.5 μmol of KOH was injected into the fluorescence quartz cuvette that contained 1.00 g of a 0.2 wt % polymer buffer solution (the pH increased from 4.0 to 5.4). In (b), the data points from 50 to 34 ^{o}C were from the cooling process in (a). At 34 ^{o}C, 7.5 μmol of HCl was injected into the solution (1.00 g) to change the pH from 5.4 to 4.0……..139

3.6 The intensity of scattered light at a scattering angle of 90^{o} (a) and the hydrodynamic diameter (b) as a function of temperature (□ cooling, ■ heating) in a DLS study of multiple micellization/dissociation transitions of a 0.2 wt % solution of PEO-*b*-P(DEGMMA-*co*-MAA) (**BR3-H**) in 10 mM KHP buffer solution (2.50 g, the same solution used in Figure 3.3) in response to addition of HCl (19 μL of 1.00 M HCl solution at 34 ^{o}C) and subsequent temperature changes.

The data points in the cooling curve from 50 to 34 ^{o}C were from the cooling process in Figure 3.3. In (b), at 30 ^{o}C in both cooling and heating processes, two size distributions were observed and the reported hydrodynamic diameters for this temperature were the average values over two hydrodynamic size distributions……...……..141

3.7 The intensity of scattered light at a scattering angle of 90^{o} (a) and the hydrodynamic diameter (b) as a function of temperature in a DLS study of multiple micellization and dissociation transitions of a 0.2 wt % solution of PEO-*b*-P(DEGMMA-*co*-MAA) (**BR3-H**) in 10 mM KHP buffer solution (2.50 g) in response to temperature and pH changes. At 34 ^{o}C, 16 μL of a 1.00 M KOH solution was injected into the solution (the pH changed to 5.2). At 40 ^{o}C, 11 μL of a 1.00 M KOH solution was injected (the pH changed to 5.9). At 48 ^{o}C, 7.0 μL of a 1.00 M KOH solution was injected (the pH changed to ~ 8.6). In (b), at 30 ^{o}C, two size distributions were observed, and the reported hydrodynamic diameter for this temperature was the average value over two hydrodynamic size distributions……..…143

3.8 Maximum fluorescence emission intensity of Nile Red in a 0.2 wt % solution of PEO-*b*-P(DEGMMA-*co*-MAA) (**BR3-H**) in 10 mM KHP buffer solution in response to the temperature and pH changes. At 34 ^{o}C, 6.3 μmol of KOH was injected into the solution (the pH changed to 5.2); the λ_{max} shifted from 617 to 621.5 nm. At 40 ^{o}C, 4.5 μL of 1.00 M KOH was added (the pH changed to 5.9); the λ_{max} changed from 615.5 nm to 623 nm. At 48 ^{o}C: 2.7 μL of 1.00 M KOH was

injected (the pH changed to ~ 8.6); the λ_{max} shifted from 616.5 nm to 625 nm……144

3.9 The intensity of scattered light at a scattering angle of 90^{o} (a) and the hydrodynamic diameter (b) as a function of temperature in a DLS study of a 0.2 wt % solution of PEO-*b*-P(DEGMMA-*co*-MAA) (**BR3-H**) in 10 mM KHP buffer solution (2.50 g) in response to temperature and pH changes. At 45 ^{o}C, 25 μL of 1.00 M KOH solution was injected to bring the pH to 5.7 from 4.0. In (b), at 30 ^{o}C in the heating process and at 39 and 40 ^{o}C during the cooling process, two size distributions were observed, and the reported hydrodynamic diameters for these temperatures were the average values over two hydrodynamic size distributions……149

4.1 Digital optical pictures of a 20.0 wt % aqueous solution of poly(ethylene oxide)-*b*-poly(ethoxytri(ethylene oxide) acrylate-*co*-*o*-nitrobenzyl acrylate) (PEO-*b*-P(TEGEA-*co*-NBA) at (a) 25 ^{o}C, (b) 33 ^{o}C, and (c) 52 ^{o}C before UV irradiation, and at (d) 33 ^{o}C, (e) 40 ^{o}C, and (f) 52 ^{o}C after UV irradiation. At 33 ^{o}C, the 20.0 wt % aqueous solution of PEO-*b*-P(TEGEA-*co*-NBA) was irradiated for six days with 365 nm UV light from a Spectroline ENF-240C hand-held UV lamp..…..168

4.2 ^{1}H NMR spectra of (a) PEO-*b*-P(TEGEA-*co*-NBA) and (b) PEO-*b*-P(TEGEA-*co*-AA), which was formed from PEO-*b*-P(TEGEA-*co*-NBA) after UV irradiation at 33 ^{o}C for 6 days. $CDCl_3$ was used as the solvent…….170

4.3 Plot of dynamic storage modulus G' (■), loss modulus G" (□), and tan δ versus temperature for (a) the 20.0 wt % aqueous solution of PEO-*b*-P(TEGEA-*co*-NBA) and (b) the UV-irradiated solution (a 18.9 wt % aqueous solution of PEO-*b*-

P(TEGEA-*co*-AA). The data were collected from temperature ramp experiments with a heating rate of 3 ^{o}C/min. A strain amplitude of 0.2 % and an oscillation frequency of 1 Hz were used……..…….172

4.4 Frequency dependences of dynamic storage modulus G' (■) and dynamic loss modulus G" (□) of the 20.0 wt % aqueous solution of PEO-*b*-P(TEGEA-*co*-NBA) at (a) 33 °C and (b) 31 °C. A strain amplitude of 0.2 % was used in the frequency sweep experiments……...174

4.5 Frequency dependences of dynamic storage modulus G' (■) and dynamic loss modulus G" (□) of the UV-irradiated solution (a 18.9 wt % aqueous solution of PEO-*b*-P(TEGEA-*co*-AA)) at (a) 41 °C and (b) 37 °C. A strain amplitude of 0.2 % was used in the frequency sweep experiments……...……..……..175

4.6 Flow curves of (a) a 20.0 wt % aqueous solution of block copolymer PEO-*b*-P(TEGEA-*co*-NBA) and (b) the UV-irradiated solution (a 18.9 wt % aqueous solution of PEO-*b*-P(TEGEA-*co*-AA) at various temperatures)…….177

4.7 Temperature dependence of the apparent viscosity of (a) the 20.0 wt % aqueous solution of PEO-*b*-P(TEGEA-*co*-NBA) and (b) the irradiated solution at a shear rate of 10 s^{-1}…….179

4.8 Sol-Gel phase diagrams for aqueous solutions of PEO-*b*-P(TEGEA-*co*-NBA) (●) and PEO-*b*-P(TEGEA-*co*-AA) (■), formed from PEO-*b*-P(TEGEA-*co*-NBA) after UV irradiation at 33 °C for six days, at moderate concentrations……...181

4.9 Scattered light intensity of (a) the 20.0 wt % aqueous solution of PEO-*b*-P(TEGEA-*co*-NBA) and (b) the 18.9 wt % aqueous solution of PEO-*b*-

P(TEGEA-*co*-AA) at a scattering angle of 90° as a function of temperature. The data were collected from dynamic light scattering studies. The 18.9 wt % solution of PEO-*b*-P(TEGEA-*co*-AA) was obtained from the 20.0 wt % aqueous solution of PEO-*b*-P(TEGEA-*co*-NBA) after UV irradiation at 33 °C for six days. The insets in (a) and (b) show the enlarged plots of scattering intensity versus temperature……..……183

A.1 UV-vis spectra of an aqueous solution of P(TEGEA-*co*-NBA) ($M_{n,GPC}$ = 13,900 g/mol and PDI = 1.13) with a concentration of 0.2 wt % after irradiation with 365 nm UV light at 13 ^{o}C for 0, 63, 120, 180, 284, 414, and 485 min. The inset is the plot of the absorbance of polymer solution at wavelength of 330 nm versus UV irradiation time……...……..205

A.2 Hydrodynamic diameter (D_h) distribution function of PEO-*b*-P(TEGEA-*co*-NBA) (BR-**4**, $M_{n,GPC}$ = 18,300 g/mol, PDI = 1.07, 0.2 wt % aqueous solution) at 27 ^{o}C in the cooling process…….……..206

A.3 The intensity of scattered light at scattering angle of 90^{o} (a) and hydrodynamic diameter (b) as a function of temperature in a dynamic light scattering study of multiple micellization and dissociation transitions of PEO-*b*-P(TEGEA-*co*-NBA) (BR-**5**, $M_{n,GPC}$ = 24,700 g/mol, PDI = 1.11, 0.2 wt %) in water in response to temperature changes and UV irradiation. At 30 ^{o}C, the polymer solution was irradiated with 365 nm UV light for 480 min. The collection of light scattering data was resumed thereafter…….207

A.4 (a) Hydrodynamic diameter (D_h) distribution function of PEO-*b*-P(TEGEA-*co*-NBA) (BR-**5**, $M_{n,GPC}$ = 24,700 g/mol, PDI = 1.11, 0.2 wt % aqueous solution) at

30 ^{o}C in the heating process and (b) plot of Γ/q^2 of micelles of BR-**5** versus q^2 at 30 ^{o}C. The polydispersity of micelles of BR-**5** was 0.030 at 30 ^{o}C……208

A.5 The intensity of scattered light at scattering angle of 90^{o} (a) and hydrodynamic diameter (b) as a function of temperature in both heating and cooling processes in a dynamic light scattering study of thermo-induced formation and dissociation of micelles of PEO-*b*-PTEGEA (B-**3**, $M_{n,GPC}$ = 21,400 g/mol, PDI = 1.07, 0.2 wt %) in water……...……..209

A.6 (a) Hydrodynamic diameter (D_h) distribution function of micelles of PEO-*b*-PTEGEA (B-**3**, $M_{n,GPC}$ = 21,400 g/mol, PDI = 1.07) at 50 ^{o}C and (b) plot of Γ/q^2 of micelles of B-**3** versus q^2 at 50 ^{o}C. The polydispersity of micelles at 50 ^{o}C was 0.044……210

A.7 Fluorescence emission spectra of Nile Red in a 0.2 wt % aqueous solution of PEO-*b*-P(TEGEA-*co*-NBA) (BR-**4**, $M_{n,GPC}$ = 18,300 g/mol, PDI = 1.07) at different temperatures during the cooling process. The inset is the plot of maximum fluorescence emission intensity versus temperature……...211

A.8 Fluorescence spectra of Nile Red (a) in a 0.2 wt % aqueous solution of PEO-*b*-PTEGEA) (B-**3**, $M_{n,GPC}$ = 21,400 g/mol, PDI = 1.07) at various temperatures during the heating process and (b) in a series of aqueous solutions of B-**3** with different concentrations at 45 ^{o}C. The inset in (a) is the plot of maximum fluorescence intensity versus temperature, from which the critical micellization temperature (CMT) was determined. The inset in (b) is the plot of maximum fluorescence emission intensity versus the logarithm of polymer concentration at 45 ^{o}C, from which the critical micelle concentration (CMC) was determined…212

A.9 Fluorescence spectra of Nile Red (a) in a 0.2 wt % aqueous solution of PEO-*b*-P(TEGEA-*co*-NBA) (BR-**5**, $M_{n,GPC}$ = 24,700 g/mol, PDI = 1.11) at various temperatures during the heating and (b) cooling processes, and (c) in a series of aqueous solutions of BR-**5** with different concentrations at 30 ^{o}C. The insets in (a) and (b) are the plots of maximum fluorescence emission intensity versus temperature, from which the critical micellization temperature (CMT) was determined. The inset in (c) is the plot of maximum fluorescence emission intensity versus the logarithm of polymer concentration at 30 ^{o}C, from which the critical micelle concentration (CMC) was determined……...….213

A.10 UV-vis spectra of an aqueous solution of PEO-*b*-P(TEGEA-*co*-NBA) (BR-**4**, $M_{n,GPC}$ = 18,300 g/mol, PDI = 1.07) with a concentration of 0.2 wt % after irradiation with 365 nm UV light for 0, 83, 183, 247, 322, and 400 min at 32 ^{o}C. The inset is the plot of the absorbance of polymer solution at wavelength of 330 nm versus UV irradiation time……...……..214

A.11 ^{1}H NMR spectra of block copolymer PEO-*b*-P(TEGEA-*co*-NBA) (BR-**4**, $M_{n,GPC}$ = 18,300 g/mol, PDI = 1.07) and the corresponding polymer PEO-*b*-P(TEGEA-*co*-AA) obtained after UV irradiation at 32 ^{o}C for 400 min……...…….215

A.12 Hydrodynamic diameter (D_h) distribution function of micelles of PEO-*b*-P(TEGEA-*co*-AA) at 50 ^{o}C. The polymer solution was obtained in situ from the UV irradiation of a 0.2 wt % aqueous solution of BR-**4** ($M_{n,GPC}$ = 18,300 g/mol, PDI = 1.07) at 32 ^{o}C for 480 min. The hydrodynamic diameter was calculated by use of the CONTIN method. The polydispersity of micelles at 50 ^{o}C was 0.062…….216

A.13 Fluorescence spectra of photobleached Nile Red in the aqueous solution of PEO-*b*-P(TEGEA-*co*-AA) at various temperatures in the cooling process. The aqueous solution of PEO-*b*-P(TEGEA-*co*-AA) was obtained in situ by UV irradiation of a 0.2 wt % aqueous solution of PEO-*b*-P(TEGEA-*co*-NBA) (BR-**4**, $M_{n,GPC}$ = 18,300 g/mol, PDI = 1.07) at 32 ^{o}C for 480 min. The inset is the plot of emission intensity of the maximum peak versus temperature……...…..217

A.14 Fluorescence spectra of Nile Red (photobleached dye plus reloaded fresh Nile Red dye) in the aqueous solution of PEO-*b*-P(TEGEA-*co*-AA) at various temperatures in the cooling process. The aqueous solution of PEO-*b*-P(TEGEA-*co*-AA) was obtained in situ by UV irradiation of a 0.2 wt % aqueous solution of PEO-*b*-P(TEGEA-*co*-NBA) (BR-**4**, $M_{n,GPC}$ = 18,300 g/mol, PDI = 1.07) at 32 ^{o}C for 480 min. The inset is the plot of emission intensity of the maximum peak versus temperature…….……..218

A.15 (a) Hydrodynamic diameter (D_h) distribution function of PEO-*b*-P(TEGEA-*co*-AA) at 50 ^{o}C in the heating process and (b) plot of Γ/q^2 of micelles of PEO-*b*-P(TEGEA-*co*-AA) versus q^2 at 50 ^{o}C. The aqueous solution of PEO-*b*-P(TEGEA-*co*-AA) was obtained in situ by UV irradiation of a 0.2 wt % aqueous solution of PEO-*b*-P(TEGEA-*co*-NBA) (BR-**5**, $M_{n,GPC}$ = 24,700 g/mol, PDI = 1.11) loaded with Nile Red at 30 ^{o}C for 480 min. The polydispersity of micelles at 50 ^{o}C was 0.013…….219

A.16 Fluorescence spectra of photobleached Nile Red in the aqueous solution of PEO-*b*-P(TEGEA-*co*-AA) at various temperatures in (a) the heating process and (b) the cooling process. The aqueous solution of PEO-*b*-P(TEGEA-*co*-AA) was

obtained in situ by UV irradiation of a 0.2 wt % aqueous solution of PEO-*b*-P(TEGEA-*co*-NBA) (BR-**5**, $M_{n,GPC}$ = 24,700 g/mol, PDI = 1.11) loaded with Nile Red at 30 ^{o}C for 480 min. The inset is the plot of emission intensity of the maximum peak versus temperature…….……220

B.1 Gel permeation chromatography traces of macroinitiator PEO-Br and a block copolymer PEO-*b*-P(DEGMMA-*co*-*t*BMA) (**BR3** in Table 3.1)……..……..222

B.2 ^{1}H NMR spectra of (i) PEO-*b*-P(DEGMMA-*co*-*t*BMA) (**BR3**, $M_{n,GPC}$ = 21800 Da, PDI = 1.06) and (ii) PEO-*b*-P(DEGMMA-*co*-MAA) (**BR3-H**). $CDCl_3$ was used as solvent in the ^{1}H NMR spectroscopy analysis…….223

B.3 Gel permeation chromatography traces of PDEGMMA (**H1**, $M_{n,GPC}$ = 16200 Da, PDI = 1.11) before and after treatment with CF_3COOH in a control experiment……..……..224

B.4 ^{1}H NMR spectra of PDEGMMA (**H1**, $M_{n,GPC}$ = 16200 Da, PDI = 1.11) before (a) and after treatment with CF_3COOH (b) in a control experiment…….……....225

B.5 Optical transmittances at wavelength of 550 nm of 0.2 wt % aqueous solutions of PDEGMMA (**H1**, $M_{n,GPC}$ = 16200 Da, PDI = 1.11) in 10 mM potassium hydrogen phthalate buffer with pH values of 4.1 (■), 5.3 (◆),and 6.1 (●) as a function of temperature upon heating. The transmittances were recorded with a UV-visible spectrometer…….226

B.6 (a) Hydrodynamic diameter (D_h) distribution of micelles of PEO-*b*-P(DEGMMA-*co*-MAA) (**BR3-H**) at pH = 4.0 and T = 50 ^{o}C and (b) plot of Γ/q^2 of micelles of **BR3-H** vs. q^2 at pH = 4.0 and T = 50 ^{o}C. The polydispersity of micelles at 50 ^{o}C was 0.018……...……..227

B.7 The intensity of scattered light at scattering angle of 90^{o} (a) and the hydrodynamic diameter (b) as a function of temperature (■ heating, □ cooling) in a dynamic light scattering study of a 0.2 wt % aqueous buffer solution of PEO-*b*-P(DEGMMA-*co*-MAA) (**BR4-H**) at pH = 4.0. In (b), at 26 ^{o}C in the heating process and at 25 ^{o}C in the cooling process, two size distributions, one ascribed to the unimers and one to the micelles, were observed and the reported hydrodynamic diameters for these temperatures were the average values over two hydrodynamic size distributions…….…….228

B.8 (a) Hydrodynamic diameter (D_h) distribution of micelles of PEO-*b*-P(DEGMMA-*co*-MAA) (**BR4-H**) at pH = 4.0 and T = 50 ^{o}C and (b) plot of Γ/q^2 of micelles of **BR4-H** vs. q^2 at pH = 4.0 and T = 50 ^{o}C. The polydispersity of micelles at 50 ^{o}C was 0.004…….……229

B.9 Fluorescence emission spectra of Nile Red in a 0.2 wt % aqueous buffer solution of PEO-*b*-P(DEGMMA-*co*-MAA) (**BR3-H**) with a pH of 4.0 at various temperatures during heating. The inset is the plot of maximum fluorescence intensity versus temperature, from which the critical micellization temperature ($CMT_{4.0\text{-}I}$) was determined. The excitation wavelength was 550 nm……..…230

B.10 Fluorescence emission spectra of Nile Red in a 0.2 wt % solution of PEO-*b*-P(DEGMMA-*co*-MAA) (**BR3-H**) in 10 mM KHP buffer with a pH of 4.0 at various temperatures during cooling. The inset is the plot of maximum fluorescence intensity versus temperature, from which the critical micellization temperature was determined. The excitation wavelength is 550 nm……...231

B.11 Fluorescence emission spectra of Nile Red in a 0.2 wt % solution of PEO-*b*-P(DEGMMA-*co*-MAA) (**BR4-H**) in 10 mM KHP buffer with a pH of 4.0 at various temperatures in both heating (a) and cooling (b) processes. The insets are the plots of maximum fluorescence intensity versus temperature, from which the critical micellization temperature ($CMT_{4.0\text{-}I}$) was determined. The excitation wavelength is 550 nm……..232

B.12 The plot of solution pH versus number of μmols of KOH injected into a 0.2 wt % solution of PEO-*b*-P(DEGMMA-*co*-MAA) (**BR4-H**) in 10 mM KHP buffer (2.50 g). The KOH solution was added stepwise; each time, 10 μL of a 0.20 M aqueous KOH solution was injected via a microsyringe, followed by the measurement of pH with a pH meter. The volume of the solution increased by 6.8 % after the titration was finished…….……..233

B.13 (a) Hydrodynamic diameter (D_h) distribution of micelles of PEO-*b*-P(DEGMMA-*co*-MAA) (**BR3-H**) at pH = 5.4 and T = 50 ^oC and (b) plot of Γ/q^2 of micelles of BR3-H vs. q^2 at pH = 5.4 and T = 50 ^oC. The polydispersity of micelles at 50 ^oC was 0.055…….……234

B.14 The intensity of scattered light at scattering angle of 90^o (a) and the hydrodynamic diameter (b) as a function of temperature (■ heating, □ cooling) in a dynamic light scattering study of multiple micellization/dissociation transitions of 0.2 wt % PEO-*b*-P(DEGMMA-*co*-MAA) (**BR4-H**) in 10 mM KHP buffer solution (the same solution used in Figure B.7) in response to addition of KOH and subsequent temperature changes. At 30 ^oC, 19 μmol of KOH (19 μL 1.00 M KOH) was injected into the polymer solution (2.50 g) to break the micelles in situ.

The data points from 20 ^{o}C to 30 ^{o}C were from the heating process in Figure B.7. In (b), at 26 ^{o}C in the heating process, two size distributions were observed and the reported hydrodynamic diameter for this temperature was the average value over two hydrodynamic size distributions.....235

B.15 Fluorescence emission intensity of Nile Red in a 0.2 wt % solution of **BR4-H** (PEO-*b*-P(DEGMMA-*co*-MAA)) in 10 mM KHP buffer (the same solution used in Figure B.11) in response to addition of KOH and subsequent temperature changes. The data points from 20 to 30 ^{o}C were from the heating process in Figure B.11. At 30 ^{o}C, 7.6 μmol of KOH (7.6 μL 1.00 M KOH) was injected into the fluorescence quartz cuvette that contained 1.00 g of a 0.2 wt % polymer buffer solution (the pH increased from 4.0 to 5.4) and the fluorescence emission intensity was recorded at a function of temperature (■ heating, □ cooling). The excitation wavelength was 550 nm……..236

B.16 (a) Hydrodynamic diameter (D_h) distribution of micelles of PEO-*b*-P(DEGMMA-*co*-MAA) (**BR3-H**) at pH = 4.0 and T = 50 ^{o}C and (b) plot of Γ/q^2 of micelles of BR3-H vs. q^2 at pH = 4.0 and T = 34 ^{o}C. The polydispersity of micelles at 50 ^{o}C was 0.004. A predetermined amount of HCl (7.5 μmol) was added into the polymer solution to change the pH back to 4.0 from 5.4 and subsequent cooling and heating to 50 ^{o}C…….237

B.17 The intensity of scattered light at a scattering angle of 90^{o} (a) and the hydrodynamic diameter (b) as a function of temperature (□ cooling, ■ heating) in a dynamic light scattering study of multiple micellization/dissociation transitions of a 0.2 wt % solution of PEO-*b*-P(DEGMMA-*co*-MAA) (**BR4-H**) in 10 mM

KHP buffer solution (the same solution used in Figure B.14) in response to addition of HCl and subsequent temperature changes. At 30 ^{o}C, 19 μL of 1.00 M HCl solution was injected into the DLS tube which contained 2.50 g of the polymer solution. The data points in the cooling curve from 50 to 30 ^{o}C were from the cooling curve of Figure B.14…….238

B.18 Fluorescence emission intensity of Nile Red in a 0.2 wt % solution of PEO-*b*-P(DEGMMA-*co*-MAA) (**BR4-H**) in 10 mM KHP buffer (the same solution used in Figure B.15) in response to addition of HCl and subsequent temperature changes. The data points from 50 to 30 ^{o}C were from the cooling process in Figure B.15. At 30 ^{o}C, 7.6 μmol of HCl (7.6 μL of 1.00 M HCl) was injected into the solution (1.00 g) to change the pH from 5.4 to 4.0 and the fluorescence emission intensity was recorded at a function of temperature (□ cooling, ■ heating). The excitation wavelength was 550 nm……...…….239

B.19 The intensity of scattered light at a scattering angle of 90^{o} (a) and the hydrodynamic diameter (b) as a function of temperature in a dynamic light scattering study of multiple micellization/dissociation transitions of a 0.2 wt % solution of PEO-*b*-P(DEGMMA-*co*-MAA) (**BR4-H**) in 10 mM KHP buffer (2.50 g) in response to temperature and pH changes. At 30 ^{o}C, 16 μL of 1.00 M KOH solution was injected into the solution (the pH changed to 5.2). At 37 ^{o}C, 11.0 μL of 1.00 M KOH solution was injected (the pH changed to 5.9). At 45 ^{o}C, 7.0 μL of 1.00 M KOH solution was injected into the solution (the pH changed to ~ 8.3). In (b), at 26 ^{o}C, two size distributions were observed and the reported

hydrodynamic diameter for this temperature was the average value over two hydrodynamic size distributions……..……240

B.20 Fluorescence emission intensity of Nile Red in a 10 mM KHP buffer solution that contained 0.2 wt % PEO-*b*-P(DEGMMA-*co*-MAA) (**BR4-H**) in response to the temperature and pH changes. The excitation wavelength was 550 nm. At 30 ^{o}C, 6.6 μL of a 1.00 M KOH solution was injected into the solution (the pH changed to 5.2). At 37 ^{o}C, 4.5 μL of 1.00 M KOH was added (the pH changed to 5.9). At 45 ^{o}C: 3.0 μL of 1.00 M KOH was injected (the pH changed to ~ 8.3)…….……..241

B.21 Plots of maximum fluorescence emission intensity of Nile Red in 10 mM KHP buffer solutions of **BR3-H** at T= 50 ^{o}C and pH = 4.0 (a), T = 50 ^{o}C and pH = 5.2 (b), T = 50 ^{o}C and pH = 5.9 (c) versus the logarithm of polymer concentration, from which the critical micelle concentrations (CMC) were determined……...242

B.22 Plots of maximum fluorescence emission intensity of Nile Red in 10 mM KHP buffer solutions of **BR4-H** at T= 50 ^{o}C and pH = 4.0 (a), T = 50 ^{o}C and pH = 5.2 (b), T = 50 ^{o}C and pH = 5.9 (c) versus the logarithm of polymer concentration, from which the critical micelle concentrations (CMC) were determined……...243

Chapter 1. Well-Defined Thermosensive Water-Soluble Polystyrenics with Short Pendant Oligo(ethylene glycol) Groups: Synthesis and End Group Effect on Thermosensitive Properties

Abstract

This chapter presents the synthesis and thermosensitive properties of well-defined water-soluble polystyrenics with short pendant oligo(ethylene glycol) groups. Two monomers, α-hydro-ω-(4-vinylbenzyl)tris(oxyethylene) (HTEGSt) and α-hydro-ω-(4-vinylbenzyl)tetrakis(oxyethylene) (HTrEGSt), were prepared and polymerized by nitroxide-mediated radical polymerization using 2,2,5-trimethyl-3-(1-phenylethoxy)-4-phenyl-3-azahexane as initiator. Kinetics and gel permeation chromatography analysis showed that the polymerizations were controlled, yielding polymers with controlled molecular weights and narrow polydispersities. The polymers can be dissolved in water forming transparent solutions and undergo phase transitions when the temperature is above a critical point. The thermosensitive properties were studied by turbidimetry and variable temperature ^{1}H NMR spectroscopy. The cloud points of the polymers of HTEGSt and HTrEGSt were around 13 and 64 ^{o}C, respectively. The effects of hydrophobic chain end groups on the cloud points of thermosensitive water-soluble polystyrenics were investigated. Well-defined poly(4-vinylbenzyl methoxytris(oxyethylene) ether) (PTEGSt) and poly(HTrEGSt) (PHTrEGSt) were prepared by nitroxide-mediated radical polymerization using α-hydrido alkoxyamine initiators including two monomer-based initiators. The polymers were reduced with (n-Bu)$_3$SnH to replace the alkoxyamine end group with hydrogen. In the studied molecular weight range ($M_{n,GPC}$ = 3000 to 28000 g/mol), we found that the hydrophobic end groups decreased the cloud point by 1 – 20 ^{o}C depending on the molecular weight and the largest depression was observed at the lowest molar mass. The cloud points of PTEGSt and

PHTrEGSt with two hydrophobic end groups, phenylethyl and alkoxyamine, exhibited a monotonic increase with the increase of molecular weight. For polymers with only one hydrophobic end group, either phenylethyl or alkoxyamine, the cloud point initially increased with the increase of molecular weight but leveled off/decreased slightly with further increasing molar mass. For polymers with essentially no end groups, the cloud point decreased with the increase of chain length, which represents the "true" molecular weight dependence of cloud point. The observed molecular weight dependences of cloud points of polystyrenics with hydrophobic end group(s) are believed to result from the combined end group effect and "true" molecular weight effect.

1.1 Introduction

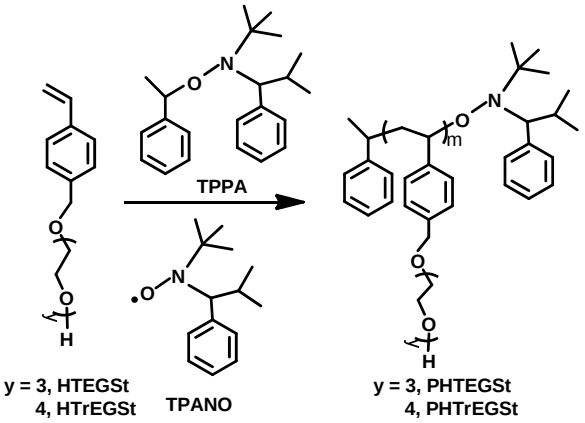
Thermosensitive water-soluble polymers exhibit a phase transition from a soluble to an insoluble state in water when the temperature is above a critical point, known as lower critical solution temperature (LCST).[1,2] The macroscopic phase separation of aqueous polymer solutions above LCST reflects the release of water molecules from the hydrated layer around polymer chains to bulk water, the collapse of polymer molecules from a random coil to a tightly packed globule, and the aggregation of collapsed polymer chains into larger colloidal particles. These polymers have been intensively studied from both scientific and technological standpoints in the past decades[1-31] and a wide variety of applications have been reported ranging from drug delivery,[3,4] to smart surfaces/smart particles,[5-15] to microfluidic systems,[16] to catalysis,[17] and environmentally responsive Pickering emulsions.[18] One of the most studied thermoresponsive water-soluble polymers is poly(*N*-isopropylacrylamide) (PNIPAm).[1,2,6-10,19-24] By introduction of a short oligo(ethylene glycol) group to the polymer backbone as pendant from each repeat unit, one can create new thermosensitive water-soluble polymers. This concept has been demonstrated in recent reports on the preparation of thermoresponsive polymers of oligo(ethylene glycol) vinyl ethers by living cationic polymerization,[32-36] of methoxyoligo(ethylene glycol) methacrylates by living anionic polymerization[37] and atom transfer radical polymerization (ATRP),[14,15,38-40] of styrenics and acrylates with short oligo(ethylene glycol) pendants by nitroxide-mediated radical polymerization (NMRP),[41,42] and thermosensitive dendrimers.[43] Homopolymers, block and random copolymers, dendrimers, and polymer brushes on silica particles have been synthesized and interesting phenomena have been observed.[14,15,32-43]

Our group previously reported the synthesis of thermosensitive water-soluble polystyrenics with short oligo(ethylene glycol) pendant groups,[41] poly(4-vinylbenzyl methoxytris(oxyethylene) ether) (PTEGSt), poly(4-vinylbenzyl methoxytetrakis-(oxyethylene) ether) (PTrEGSt), and poly(4-vinylbenzyl methoxypentakis(oxyethylene) ether) (PPEGSt), by NMRP using 2,2,5-trimethyl-3-(1-phenylethoxy)-4-phenyl-3-azahexane (TPPA)[44-47] as initiator. TPPA, an α-hydrido alkoxyamine that contains a hydrogen atom attached to a carbon located α to the nitrogen atom, has been proven to be highly effective in the controlled polymerizations of a wide variety of monomers.[44-46] The cloud points of these polystyrenics in water were found to be dependent on the length of oligo(ethylene glycol) pendant.

Here, two new monomers, *α*-hydro-*ω*-(4-vinylbenzyl)tris(oxyethylene) (HTEGSt), and *α*-hydro-*ω*-(4-vinylbenzyl)tetrakis(oxyethylene) (HTrEGSt) as shown in Scheme 1.1, were synthesized and polymerized by NMRP using TPPA and 0.05 equiv. of free nitroxide 2,2,5-trimethyl-4-phenyl-3-azahexane-3-nitroxide (TPANO) relative to TPPA as the initiator system. The thermoresponsive properties of these two polymers in aqueous solutions were studied.

In the study of molecular weight effects, our group found that the cloud points of thermosensitive water-soluble polymers prepared by NMRP using TPPA as initiator in water increased with the increase of molecular weight. This is different from the common observation that the cloud point is lower when the molecular weight is higher.[34,38,48,49] The observation might be due to the hydrophobic end groups of polymer chains, which are from the initiator TPPA. The end groups of thermosensitive water-soluble polymers

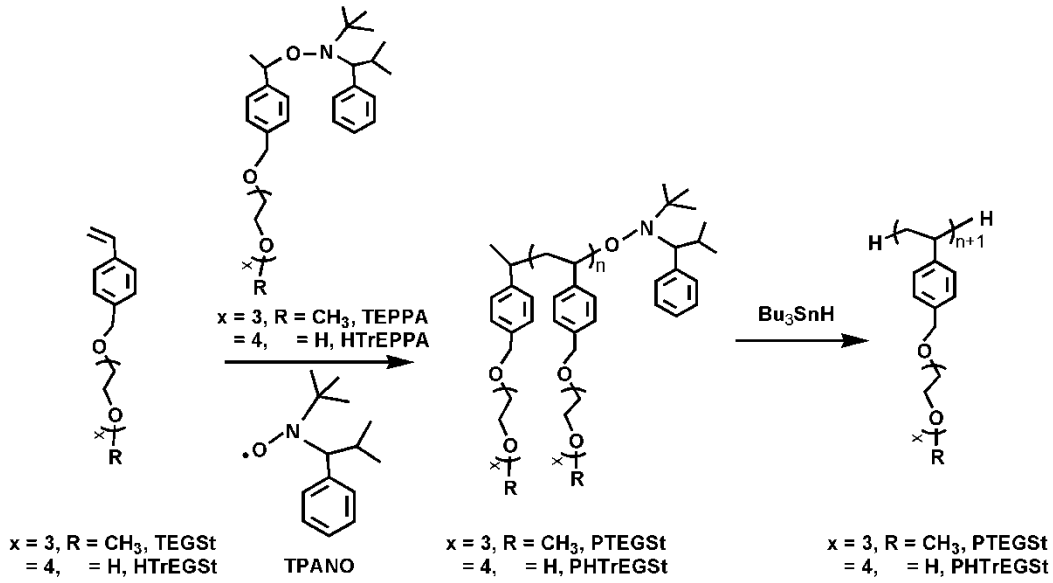
Scheme 1.1. Synthesis of Thermosensitive, Water-Soluble PHTEGSt and PHTrEGSt by NMRP with TPPA as an Initiator in the Presence of TPANO



are known to affect the cloud points and in some situations could change or even reverse the molecular weight dependence of cloud point.[50-60] While hydrophobic end groups decrease the cloud points due to the increased degree of ordering of water molecules, hydrophilic ones tend to increase them because they decrease the degree of ordering of water molecules. Stöver and coworkers reported the synthesis of narrow-disperse PNIPAm with various end groups by ATRP.[50] Their study showed that the magnitude of the molecular weight dependence decreased when using more hydrophobic end groups. If the end groups are hydrophobic enough, they may facilitate the micellization. For example, Winnik *et al.* examined the influence of polymer chain length on the cloud point of aqueous solutions of telechelic PNIPAm with *n*-octodecyl termini.[51,52] Separate transitions of micellization and chain dehydration were observed. While the cloud point decreased significantly with decreasing polymer molar mass, the coil-to-globule collapse was only slightly affected by polymer molecular weight. The end group effects are most pronounced for low molecular weight polymers.

To study how and to what degree the end groups affect the thermoresponsive properties of water-soluble polystyrenics with short oligo(ethylene glycol) pendants, two monomer-based NMRP initiators, TEPPA and HTrEPPA, were synthesized and used to prepare the polystyrenics with controlled molecular weights, narrow polydispersities, and defined end groups, respectively (Scheme 1.2). Tri(*n*-butyl)tin hydride was used to remove the alkoxyamine group from polymer chain end, yielding polymers with essentially "no" end groups (two hydrogen atoms). It was found that while the cloud points of polymers with two hydrophobic end groups, synthesized from initiator TPPA, exhibited a monotonic increase with the increase of chain length, the transition point of

Scheme 1.2. Synthesis of Thermosensitive Polystyrenics with "no" End Groups



polystyrenics with one hydrophobic end group, prepared from new initiators, increased initially with the increase of chain length but leveled off/decreased slightly at higher molecular weights. In contrast, the cloud points of polymers with essentially no end groups decreased with increasing molar mass.

1.2 Experimental Section

1.2.1 Materials

Tri(ethylene glycol) monomethyl ether (95%), tri(ethylene glycol) (99%), and tetra(ethylene glycol) (99%) were purchased from Aldrich and used without further purification. Anisole was dried over CaH_2 and distilled under reduced pressure. 4-vinylbenzyl chloride (tech. 90%), NaH (60% dispersion in mineral oil), and tri(*n*-butyl)tin hydride (97%) were obtained from Acros and used as received. Tetrahydrofuran (THF) was distilled from sodium and benzophenone and stored in a solvent storage bottle prior to use. 2,2,5-Trimethyl-4-phenyl-3-azahexane-3-nitroxide (TPANO), 2,2,5-trimethyl-3-(1-phenylethoxy)-4-phenyl-3-azahexane (TPPA), and 2,2,5-trimethyl-3-(1-(4′-chloromethyl)phenylethoxy)-4-phenyl-3-azahexane (TCPPA) were synthesized according to the procedures reported in the literature.[44] The synthesis of monomers, 4-vinylbenzyl methoxytris(oxyethylene) ether (TEGSt) and the polymerizations of TEGSt using TPPA as initiator followed the procedures reported in the literature.[41] All other chemical reagents were purchased from either Aldrich or Fisher and used without further purification.

1.2.2 Characterization

Gel permeation chromatography (GPC) was carried out at room temperature using PL-GPC 20 (an integrated GPC system from Polymer Laboratories, Inc) with a refractive index detector, one PLgel 5 μm guard column (50 × 7.5 mm), and two PLgel 5 μm mixed-C columns (each 300 × 7.5 mm, linear range of molecular weight from 200 to 2,000,000 according to Polymer Laboratories). The data were processed using Cirrus^{TM} GPC/SEC software (Polymer Laboratories). THF was used as the carrier solvent at a flow rate of 1.0 mL/min. Polystyrene standards (Polymer Laboratories) were used for calibration. The ^{1}H (300 MHz) and ^{13}C NMR (75 MHz) spectra were recorded on a Varian Mercury 300 NMR spectrometer and the residual solvent proton signal was used as the internal standard. Mass spectroscopy was performed at the Mass Spectrometry Center of the Department of Chemistry at the University of Tennessee at Knoxville using a PE Sciex QSTAR XL triple quadrupole time-of-flight (QTOF) mass spectrometer (Concord, Ontario, Canada) with an electrospray ionization source.

The cloud points of thermosensitive polymers in aqueous solutions were measured by two methods. The first one used UV-vis spectrometry. The optical transmittances of aqueous polymer solutions at various temperatures were recorded at wavelength of 490 or 500 nm with a UV-vis spectrometer (Biomate 5 from Thermospectronic). The sample cell was thermostated with an external water bath of a Fisher Scientific Isotemp refrigerated circulator. At each temperature, the solutions were equilibrated for 5 min. In the second method, 3.5 mL vials that contained aqueous polymer solutions were placed in the water bath of a Fisher Scientific Isotemp refrigerated circulator. The temperature was increased

at a step of 1 ^{o}C. At each temperature, the polymer solutions were allowed to equilibrate with the water bath for 5 min. The cloud point was recorded when the polymer solution turned cloudy. The difference between the cloud points determined by these two methods was within one degree.

1.2.3 Synthesis of α-Hydro-ω-(4-vinylbenzyl)tris(oxyethylene) (HTEGSt)

Tri(ethylene glycol) (29.25 g, 0.195 mol) and dry THF (35 mL) were added into a three-necked flask, followed by gradual addition of NaH (3.32 g, 0.083 mol). The mixture was stirred under N_2 atmosphere for 1 h. A solution of 4-vinylbenzyl chloride (6.02 g, 39.4 mmol) in dry THF (15 mL) was added dropwise. After being refluxed at 65 ^{o}C overnight, the reaction mixture was quenched with water (100 mL) and poured into a separatory funnel. The organic layer was separated and the aqueous layer was extracted with chloroform four times. The organic phase and extracts were combined and dried over anhydrous Na_2SO_4. After removal of solvents by a rotavapor, the crude product was purified by silica gel column chromatography with ethyl acetate as eluent affording a light yellow liquid (7.24 g, 69% yield). ^{1}H NMR ($CDCl_3$) δ (ppm): 7.36 (d, 2H, aromatic), 7.27 (d, 2H, aromatic), 6.68 (dd, 1H, CH_2=C*H*-), 5.71 (dd, 1H, C*H*H=CH-), 5.20 (dd, 1H, CH*H*=CH-), 4.52 (s, 2H, $(CH)_2CCH_2O$-), 3.55-3.70 (m, 12H, -OCH_2CH_2O-), 2.88 (br, 1H, -O*H*); ^{13}C NMR ($CDCl_3$) δ (ppm): 137.59 ($OCH_2C(CH)_2$), 136.78 (CH_2=*C*HC$(CH)_2$), 136.34 (CH_2=CH*C*$(CH)_2$), 127.79 ((*C*H)$_2$CCH$_2$O-), 126.03 (CH_2=CHC(*C*H)$_2$), 113.60 (*C*H$_2$=CHC$(CH)_2$), 72.75 ((CH)$_2$CH*C*H$_2$O-), 72.35, 70.46, 70.41, 70.16, 69.14 (*C*H$_2$O), 61.48 (-*C*H$_2$OH). MS (ES) m/z 288.9 ([M + Na]$^{+}$).

1.2.4 Synthesis of α-Hydro-ω-(4-vinylbenzyl)tetrakis(oxyethylene) (HTrEGSt)

α-Hydro-ω-(4-vinylbenzyl)tetrakis(oxyethylene) (HTrEGSt) was prepared from tetra(ethylene glycol) and 4-vinylbenzyl chloride by use of a procedure similar to that for the synthesis of HTEGSt. A light yellow liquid was obtained (54% yield). ^{1}H NMR ($CDCl_3$) δ (ppm): 7.37 (d, 2H, aromatic), 7.29 (d, 2H, aromatic), 6.69 (dd, 1H, CH_2=C*H*-), 5.73 (dd, 1H, C*H*H=CH-), 5.22 (dd, 1H, CH*H*=CH-), 4.54 (s, 2H, $(CH)_2CCH_2$-), 3.57-3.72 (m, 16H, -OCH_2CH_2O-), 2.72 (t, 1H, -O*H*); ^{13}C NMR ($CDCl_3$) δ (ppm): 137.73 (-$OCH_2C(CH)_2$), 136.84 (CH_2=*C*HC$(CH)_2$), 136.42 (CH_2=CH*C*$(CH)_2$), 127.88 ((*C*H)$_2$CHCH_2O), 126.10 (CH_2=CHC(*C*H)$_2$), 113.68 (*C*H_2=CHC$(CH)_2$), 72.84 ((CH)$_2$CH*C*H_2O-), 72.40, 70.53, 70.51, 70.48, 70.24, 69.27 (*C*H_2O), 61.62 (-*C*H_2OH). MS (ES) m/z 333.0 ([M + Na]$^+$).

1.2.5 Nitroxide-Mediated Radical Polymerizations of HTEGSt and HTrEGSt Using 2,2,5-Trimethyl-3-(1-phenylethoxy)-4-phenyl-3-azahexane (TPPA) as Initiator

A typical procedure for nitroxide-mediated radical polymerization of HTEGSt is described below. A similar procedure was used to polymerize HTrEGSt. TPPA (14.2 mg, 43.7 μmol), HTEGSt (1.481 g, 5.57 mmol), anisole (1.478 g), and a solution of 2,2,5-trimethyl-4-phenyl-3-azahexane-3-nitroxide (TPANO) in anisole (100 μL, concentration: 0.472 mg/100 μL) were added into a 25 mL two-necked flask. The concentrations were: $[HTEGSt]_o$ = 1.86 M; $[I]_o$ = 14.6 mM; $[TPANO]_o$ = 0.72 mM. The flask was then degassed by freeze-pump-backfilling with nitrogen six times. After warming to room temperature, the reaction flask was placed in a 120 ^{o}C oil bath. A sample was taken immediately (t = 0 min) for kinetics study. During the polymerization, samples were

taken via an argon-exchanged syringe at regular intervals for ^{1}H NMR spectroscopy and GPC analysis. After polymerization proceeded for 273 min, the flask was removed from the oil bath. The mixture was allowed to cool naturally to room temperature, diluted with THF, and precipitated in diethyl ether. The polymer was purified by reprecipitation of its THF solution in diethyl ether. The polymer was then transferred to a flask and dried in vacuum overnight at room temperature. A viscous polymer was obtained (0.324 g, 22 % yield). GPC analysis results: $M_{n,GPC}$ = 10400 g/mol, PDI = 1.08.

1.2.6 Synthesis of 2,2,5-trimethyl-3-(1-(4′-(2,5,8,11-tetraoxadodecyl)phenylethoxy)-4-phenyl-3-azahexane (TEPPA)

To a 50 mL three-necked flask were added tri(ethylene glycol) monomethyl ether (4.91 g, 29.9 mmol) and dry THF (20 mL). The flask was then placed in an ice/water bath and NaH (0.92 g, 23 mmol) was gradually added under N_2 atmosphere. After the mixture turned clear, a solution of TCPPA (1.00 g, 2.68 mmol) in dry THF (5 mL) was added dropwise. The reaction mixture was stirred at 50 ^{o}C under N_2 atmosphere for 24 h, and was then quenched with water (50 mL). The organic phase was separated and the aqueous layer was extracted with CH_2Cl_2 (15 mL × 3). The organic extracts were combined and dried over anhydrous sodium sulfate overnight. The solvents were removed by a rotavapor. Purification by silica gel column chromatography (ethyl acetate : hexanes = 1 : 1, v/v) afforded a light yellow liquid (1.09 g, 81 % yield). ^{1}H NMR (300 MHz, $CDCl_3$, both diastereomers) δ (ppm): 7.47-7.15 (m, 18H, aromatic), 4.92 (q + q, 2H, CH_3CHON), 4.58 and 4.54 (each s, 4H, $(CH)_2CCH_2O$, both diastereomers), 3.70-3.53 (m, 24H, CH_2O), 3.42 and 3.31 (each d, 2H, NCH(Ph)CH, both diastereomers),

3.37 (each s, 6H, OCH_3), 2.36 and 1.40 (each m, 2H, NCH(Ph)CH, both diastereomers), 1.62 and 1.54 (each d, 6H, CH_3CHON, both diastereomers), 1.31, 0.94, 0.55, and 0.22 (each d, CH(CH_3)$_2$, 12H, both diastereomers), 1.05 and 0.79 (each s, C(CH_3)$_3$, 18H, both diastereomers); ^{13}C NMR ($CDCl_3$) δ (ppm): 145.03, 144.28 (NCHC(CH)$_2$), 142.30, 142.08 ((CH)$_2C$CHON), 137.08, 136.42 ((CH)$_2C$CH$_2$O), 130.84, 130.77, 130.39, 129.03, 127.69, 127.47, 127.43, 127.23, 127.06, 126.88, 126.21, and 126.03 (aromatic), 83.17 ((CH)$_2$CCHON), 82.37 ((CH)$_2$CCH$_2$O), 73.04, 72.94, 72.06, 72.01, 71.82, 70.54, 70.52, 70.41, 69.31, 69.09 (CH$_2$O), 60.38 (NCH(Ph)CH), 60.29 (NC(CH$_3$)$_3$), 58.88 (OCH$_3$), 31.88, 31.48 (CHCH(CH$_3$)$_2$), 28.27, 28.11 (NC(CH$_3$)$_3$), 24.59, 23.01 (CH$_3$CHON), 22.06, 21.83, 21.03, 20.94 (CH(CH$_3$)$_2$); MS (ES) m/z 502.4 ([M + H]$^+$).

1.2.7 Synthesis of 2,2,5-trimethyl-3-(1-(4′-(2,5,8,11,14-pentaoxatetradecyl)phenyleth-oxy)-4-phenyl-3-azahexane (HTrEPPA)

To a solution of HTrEGSt (6.00 g, 19.4 mmol) and TPANO (2.49 g, 11.3 mmol) in 1:1 toluene and ethanol (75 mL) was added (*S,S*)-(+)-*N,N*′-bis(3,5-di-*tert*-butylsalicylidene)-1,2-cyclohexanediaminomanganese(III) chloride (Jacobsen's catalyst, 1.29 g, 2.03 mmol), followed by di-*tert*-butyl peroxide (2.68 g, 18.4 mmol) and sodium borohydride (1.30 g, 34.2 mmol). The reaction mixture was then stirred at room temperature under N_2 atmosphere for 20 h, evaporated to dryness, and partitioned between dichloromethane (30 mL) and water (50 mL). The organic layer was separated and the aqueous layer was extracted with dichloromethane (15 mL × 4). The organic layers were combined and dried over anhydrous sodium sulfate. After the removal of solvents by a rotavapor, purification by silica gel column chromatography with a mixture

of hexanes and ethyl acetate (2 : 1, v/v) as eluent gave a light green viscous liquid (0.89 g, yield 15%). ^{1}H NMR (300 MHz, $CDCl_3$, both diastereomers) δ (ppm): 7.40-7.13 (m, 18H, aromatic), 4.87 (q + q, 2H, CH_3CHON, both diastereomers), 4.55 and 4.51 (each s, 4H, $(CH)_2CCH_2O$, both diastereomers), 3.68-3.57 (m, 32H, CH_2O), 3.38 and 3.26 (each d, 2H, NCH(Ph)CH, both diastereomers), 2.58 (s, 2H, OH), 2.30 and 1.36 (each m, 2H, NCH(Ph)CH, both diastereomers), 1.58 and 1.50 (each d, 6H, CH_3CHO, both diastereomers), 1.27, 0.89, 0.50, and 0.17 (each d, 12H, $CH(CH_3)_2$, both diastereomers), 1.01 and 0.74 (each s, 18H, $C(CH_3)_3$, both diastereomers); ^{13}C NMR ($CDCl_3$) δ (ppm): 145.14, 144.37 ($NCHC(CH)_2$), 142.36, 142.15 ($(CH)_2CCHO$), 136.97, 136.30 ($(CH)_2CCH_2O$), 130.86, 130.80, 127.57, 127.53, 127.28, 127.11, 126.95, 126.23, and 126.07 (aromatic), 83.18 ($(CH)_2CCHO$), 82.41 ($(CH)_2CCH_2O$), 73.09, 72.99, 72.46, 72.03, 71.97, 70.54, 70.49, 70.22, 69.29, and 69.04 (CH_2O), 61.63 (NCH(Ph)CH), 60.41 (CH_2OH), 60.30 ($NC(CH_3)_3$), 31.91, 31.50 ($CHCH(CH_3)_2$), 28.29, 28.13 ($NC(CH_3)_3$), 24.68, 23.06 (CH_3CHON), 22.10, 21.86, 21.08, 20.99 ($CH(CH_3)_2$); MS (ES) m/z 532.4 ($[M + H]^+$).

1.2.8 Nitroxide-Mediated Radical Polymerization of TEGSt Using TEPPA as Initiator

Described below is a typical procedure for nitroxide-mediated radical polymerization of TEGSt using TEPPA as initiator. TEPPA (0.0141 g, 0.0281 mmol), TEGST (0.950 g, 3.393 mmol), dry anisole (1.05 g), and a solution of TPANO in anisole (0.063 mL, concentration: 0.0049 g/1.00 mL) were added into a 25 mL two-necked flask. The concentrations were: $[TEPPA]_0$ = 13.7 mM; $[TEGSt]_0$ = 1.66 M; $[TPANO]_0$ = 0.684

mM. The mixture was degassed by freeze-pump-backfilling with nitrogen six times. The flask was then placed in a 120 ^{o}C oil bath. A sample was taken immediately (t = 0 min) for kinetics study. During the polymerization, samples were taken via an argon-exchanged syringe at various time intervals for ^{1}H NMR spectroscopy and GPC analysis. After the polymerization proceeded for 300 min, the flask was removed from the oil bath. The polymerization mixture was allowed to cool naturally to room temperature, diluted with THF, and precipitated in hexanes. After re-precipitation in hexanes, the polymer was transferred to a flask and dried in vacuum overnight at room temperature. A viscous polymer was obtained (0.266 g, 28 % yield). GPC analysis results (relative to polystyrene standards): $M_{n,GPC}$ = 11100 g/mol, PDI = 1.10.

1.2.9 Nitroxide-Mediated Radical Polymerization of HTrEGSt Using HTrEPPA as Initiator

A procedure similar to the NMRP of TEGSt was used to polymerize HTrEGSt with HTrEPPA as initiator. A typical polymerization is described below. HTrEPPA (0.0148 g, 0.0278 mmol), HTrEGSt (1.04 g, 3.35 mmol), anisole (1.34 g), and a solution of TPANO in anisole (0.062 mL, concentration: 0.0049 mg/1.00 mL) were added into a 25 mL two-necked flask. The concentrations were: $[HTrEPPA]_0$ = 11.7 mM; $[HTrEGSt]_0$ = 1.41 M; $[TPANO]_0$ = 0.580 mM. The mixture was degassed by freeze-pump-backfilling with nitrogen six times. The flask was then placed in a 120 ^{o}C oil bath. Samples were taken via an argon-exchanged syringe at various time intervals for ^{1}H NMR spectroscopy and GPC analysis. After the polymerization proceeded for 303 min, the flask was removed from the oil bath. The polymerization mixture was diluted with THF and precipitated in

diethyl ether (100 mL). After reprecipitation in diethyl ether, the polymer was dried in vacuum overnight at room temperature (0.389 g, 37% yield). GPC analysis results (relative to polystyrene standards): $M_{n,GPC}$ = 10400 g/mol, PDI = 1.08.

1.2.10 Removal of the Alkoxyamine Group from the Chain End by Tri(*n*-butyl)tin Hydride

A typical procedure for the removal of the alkoxyamine group from PTEGSt chain end is described below. A similar procedure was used to reduce PHTrEGSt. Anisole (4.98 g) was added into a 25 mL two-necked flask that contained PTEGSt (prepared by use of TEPPA as initiator, 0.230 g, $M_{n,GPC}$ = 8300 g/mol, PDI = 1.09, DP = 41, 0.0197 mmol). After the polymer was completely dissolved in anisole, tri(*n*-butyl)tin hydride (0.25 g, 0.86 mmol) was injected into the polymer solution. The flask was placed in a 120 ^{o}C oil bath. After 6 h, the flask was removed from the oil bath and the light yellow solution was precipitated in hexanes (100 mL). After re-precipitation in hexanes, the polymer was dried in vacuum (0.197 g, 86 % yield). GPC analysis results (relative to polystyrene standards): $M_{n,GPC}$ = 8300 g/mol, PDI = 1.09.

1.3 Results and Discussion

1.3.1 Synthesis and Thermosensitive Properties of PHTEGSt and PHTrEGSt

1.3.1.1 Synthesis of Monomers

HTEGSt and HTrEGSt were prepared by reaction of 4-vinylbenzyl chloride with tri(ethylene glycol) and tetra(ethylene glycol), respectively, in the presence of NaH in dry THF. Two monomers were thoroughly purified by vacuum distillation and/or silica gel

column chromatography, and the molecular structures were confirmed by ^{1}H NMR, ^{13}C NMR, and mass spectroscopy.

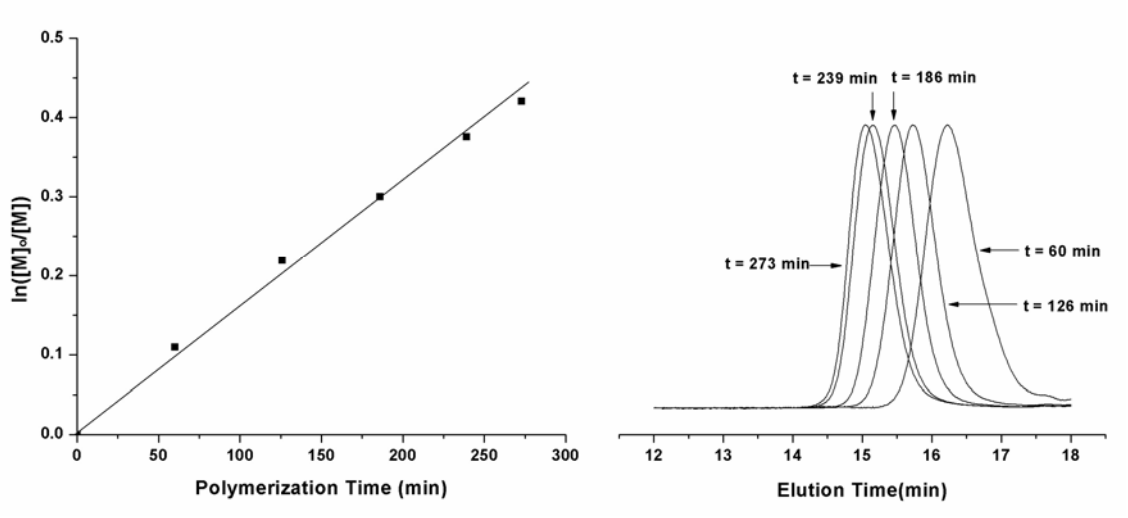
1.3.1.2 Nitroxide-Mediated Radical Polymerizations of HTEGSt and HTrEGSt Using TPPA as Initiator

TPPA and the corresponding nitroxide radical, 2,2,5-trimethyl-4-phenyl-3-azahexane-3-nitroxide (TPANO), were prepared according to the procedures described in the literature.[44] TPPA, a second-generation NMRP initiator, has been used for the controlled polymerizations of styrenics, acrylates, and acrylamides, producing polymers with accurately controlled molecular weights, narrow polydispersities, and well-defined architectures.[44-47,61-63] The key feature of NMRP is the operation of a special kinetic phenomenon termed the persistent radical effect. According to the mechanism, a small fraction of the initiating radicals formed from decomposition of the initiator undergo radical-radical coupling reaction in the initial stage of the polymerization, leading to a small amount of excess mediating free radical (persistent radical) that gives rise to the persistent radical effect and to eventual control over the polymerization process.[46] Artificial persistent radical effect may be created by addition of a few percent of mediating radical relative to the initiator. Our lab previously showed that a better control over the polymerization of styrenic monomers was obtained with addition of 0.05 equiv. of free nitroxide radical TPANO.[41] In the present work, a few percent of TPANO relative to the initiator TPPA was used in the NMRPs of HTEGSt and HTrEGSt.

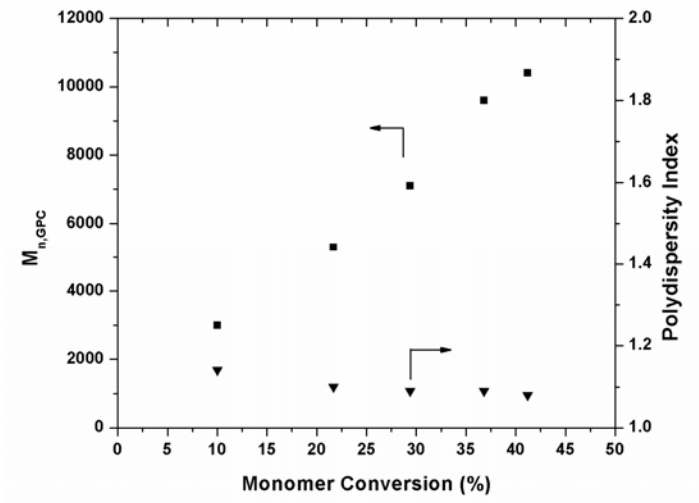
To confirm that the polymerizations of HTEGSt and HTrEGSt initiated by TPPA in the presence of a few percent of free nitroxide were controlled processes, ^{1}H NMR

spectroscopy was employed to monitor the polymerizations. The peaks at 4.30 - 4.70 ppm, which were from -CH_2- of the benzyl groups of the monomer and the polymer, were used as internal standard. The sum of the integral values of the two peaks was a constant during the course of polymerization. The monomer conversions were calculated by use of the integral value of the peaks at 5.7 ppm at time *t* and the value of the same peaks at *t* = 0. The molecular weights and polydispersities of the polymers obtained at different polymerization times were measured by GPC relative to polystyrene standards. After desired conversions/molecular weights were reached, the polymerizations were stopped by cooling the mixtures to room temperature. The polymers were precipitated in diethyl ether and then dried in vacuum at room temperature.

Figures 1.1 and 1.2 show the kinetics analysis and GPC results for the NMRPs of HTEGSt and HTrEGSt. A linear relationship between $\ln([M]_o/[M])$ and the reaction time was observed for the two monomers, suggesting that the polymerizations were a first-order reaction with respect to the monomer and the number of growing polymer chains was a constant during the course of the polymerization. GPC analysis shows that the molecular weight increased with the reaction time in a nearly linear fashion and the polydispersity index decreased progressively. For example, for the NMRP of HTEGSt (Figure 1.1), the $M_{n,GPC}$ increased from 3000 (*t* = 60 min), to 5300 (*t* = 126 min), to 7100 (*t* = 186 min), to 9600 (*t* = 219 min), to 10400 g/mol (*t* = 273 min), while the polydispersity index decreased gradually from 1.14 (*t* = 60 min), to 1.10 (*t* = 126 min), to 1.09 (*t* = 186 and 219 min), to 1.08 (*t* = 273 min).

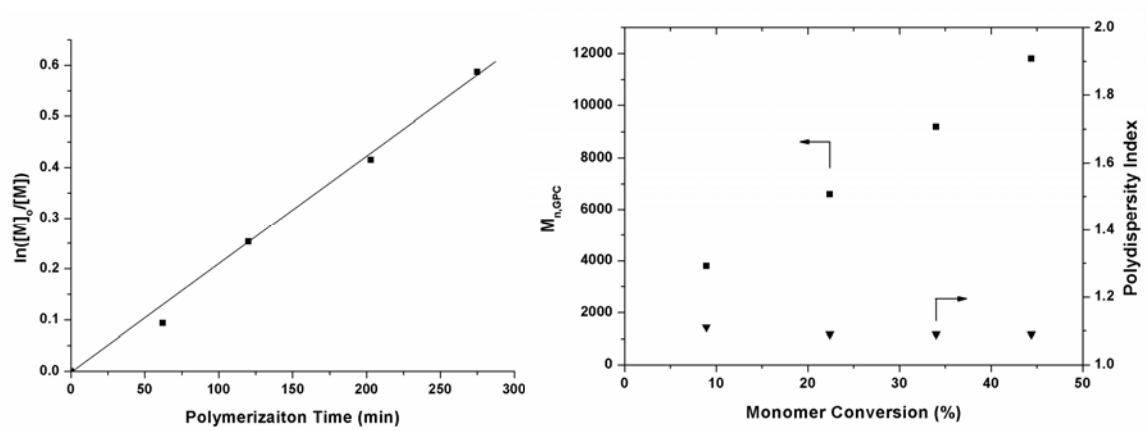


(a) (b)



(c)

Figure 1.1. (a) Relationship between $\ln([M]_o/[M])$ and time for the polymerization of HTEGSt using TPPA as an initiator in the presence of free nitroxide TPANO in anisole (1:1 w/w with respective to the monomer) at 120 ^oC ($[M]_o$ = 1.86 M, $[M]_o/[I]_o$ = 127, $[TPANO]_o$ = 0.72 mM), (b) evolution of GPC curves with the polymerization time, and (c) $M_{n,GPC}$ (■) and PDI (▼) versus the monomer conversion. The DP of the final polymer was 52.



(a) (b)

Figure 1.2. (a) Relationship between $\ln[M]_o/[M]$ and time for the polymerization of HTrEGSt using TPPA as an initiator in the presence of free nitroxide TPANO in anisole (1:1 w/w with respect to the monomer) at 120 ^oC ($[M]_o$ = 1.72 M, $[M]_o/[I]_o$ = 119, $[TPANO]_o$ = 0.71 mM), and (b) $M_{n,GPC}$ (■) and PDI (▼) obtained from GPC analysis with respect to polystyrene standards versus the monomer conversion. The DP of the final polymer was 53.

Since the kinetics and GPC analysis showed that the polymerizations were controlled processes, the degrees of polymerization (DP) of the polymers can be calculated by use of monomer-to-initiator ratios and monomer conversions. The DPs of the final PHTEGSt in Figure 1.1, and PHTrEGSt in Figure 1.2 were 52 and 53, respectively. The polymers were then used for the study of thermoresponsive properties in aqueous solutions by UV-vis spectrometry and variable temperature ^{1}H NMR spectroscopy.

1.3.1.3 Thermosensitive Properties of PHTEGSt and PHTrEGSt in Water

Homopolymers of HTEGSt and HTrEGSt could be dissolved in water, forming transparent solutions as long as the temperature was below a critical point. To determine the cloud points, aqueous solutions of two polymers (PHTEGSt, $M_{n,GPC}$ = 10400 g/mol, PDI = 1.08; PHTrEGSt $M_{n,GPC}$ = 11800 g/mol, PDI = 1.09) were prepared. The optical transmittances of the two polymer solutions at wavelength of 490 nm were recorded as a function of temperature by use of a UV-vis spectrometer, and the results are shown in Figure 1.3. The aqueous solutions of PHTEGSt, and PHTrEGSt turned cloudy at 13 and 64 ^{o}C, respectively. Apparently, the cloud point for polystyrenics increases with the length of oligo(ethylene glycol) group. The longer the pendant oligo(ethylene glycol), the stronger the interaction between polymer molecules and water, and the higher the cloud point. Our lab reported before that poly(4-vinylbenzyl methoxytris(oxyethylene) ether) (PTEGSt) and poly(4-vinylbenzyl methoxytetrakis(oxyethylene) ether) (PTrEGSt) underwent a phase transition in aqueous solutions at 13 and 39 ^{o}C, respectively.[41] Although no noticeable difference was observed between the cloud points of PTEGSt and

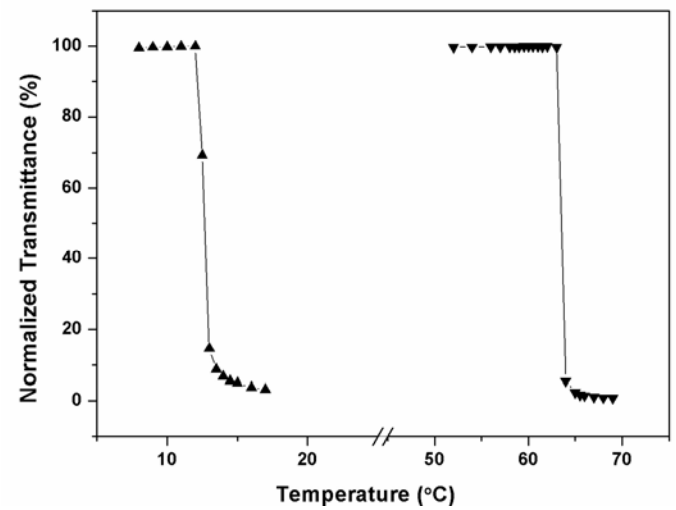


Figure 1.3. Optical transmittances of aqueous solutions of PHTEGSt (▲, $M_{n,GPC}$ = 10400 g/mol, PDI = 1.08, DP = 52, 0.5 wt %) and PHTrEGSt (▼, $M_{n,GPC}$ = 11800 g/mol, PDI = 1.09, DP = 53, 1.0 wt %) as a function of temperature. The transmittances were recorded at wavelength of 490 nm by use of a UV-vis spectrometer.

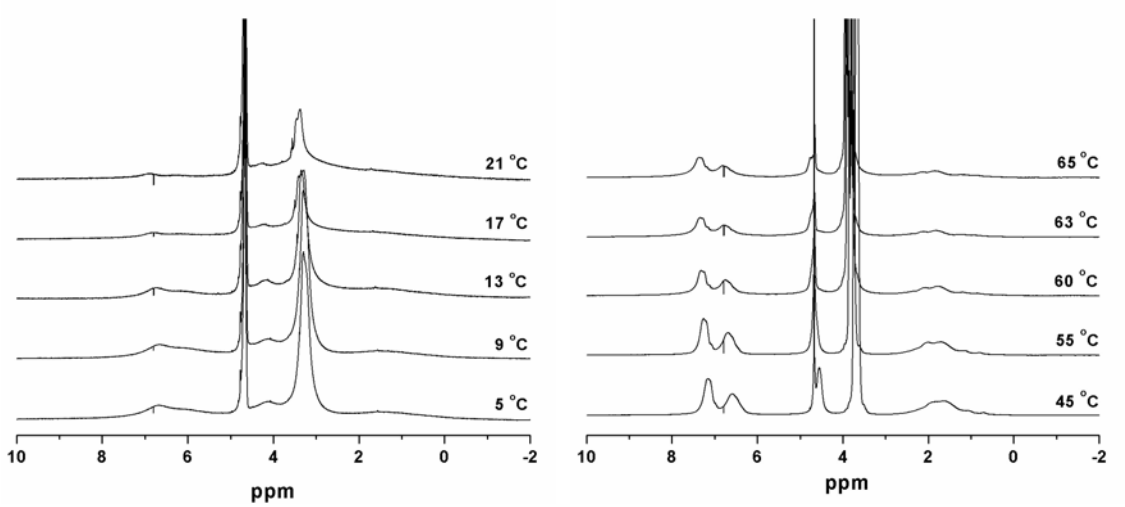
PHTEGSt, the transition temperature of PHTrEGSt was 25 ^{o}C higher than that of PTrEGSt. The only difference between PHTrEGSt and PTrEGSt is that the pendant tetra(ethylene glycol) group is end-capped with methyl group in PTrEGSt.

The phase transitions of these polymers in water were further studied by variable temperature ^{1}H NMR spectroscopy. Figure 1.4 shows the ^{1}H NMR spectra of PHTEGSt and PHTrEGSt in D_2O with concentrations of 1.0 wt % at various temperatures. For PHTEGSt, the aromatic peak decreased when the temperature was raised from 9 to 13 ^{o}C and almost disappeared at 17 and 21 ^{o}C. The transition can also be appreciated from the height of the peak at 2.5 – 4.0 ppm, which decreased significantly from 9 to 17 ^{o}C. This observation is consistent with the result from UV-vis spectrometry study. For PHTrEGSt, when the temperature was increased from 55 to 63 ^{o}C, the peak at 1.0 - 2.5 ppm decreased appreciably.

1.3.2 End Group Effect on Thermosensitive Properties

1.3.2.1 Synthesis of Monomer-Based NMRP Initiators

A new class of well-defined thermosensitive water-soluble polymers, polystyrenics with short oligo(ethylene glycol) pendants, were synthesized by NMRP using TPPA as initiator.[41] The cloud points of these polymers in water were found to increase with the increase of molecular weight, which is presumably due to the presence of hydrophobic groups, phenylethyl and alkoxyamine from initiator TPPA, at the two ends of polymer chains. To clarify how and to what degree the two hydrophobic end groups affect the cloud points of polystyrenics in water, two monomer-based NMRP initiators, TEPPA and HTrEPPA (Scheme 1.2), were designed, synthesized, and used to polymerize TEGSt and



(a) (b)

Figure 1.4. ^{1}H NMR spectra of (a) PHTEGSt ($M_{n,GPC}$ = 10400 g/mol, DP = 52, PDI = 1.08) and (b) PHTrEGSt **(**$M_{n,GPC}$ = 11800 g/mol, PDI = 1.09, DP = 53) in D_2O (1.0 wt %) at various temperatures.

HTrEGSt, respectively (Scheme 1.2). The alkoxyamine groups were then removed from polymer chain ends by use of tri(*n*-butyl)tin hydride, yielding thermosensitive polystyrenics with essentially "no" end groups other than two hydrogen atoms. Thus, the cloud points of such polymers with different molecular weights reflect the "true" molecular weight effect on the thermoresponsive properties.

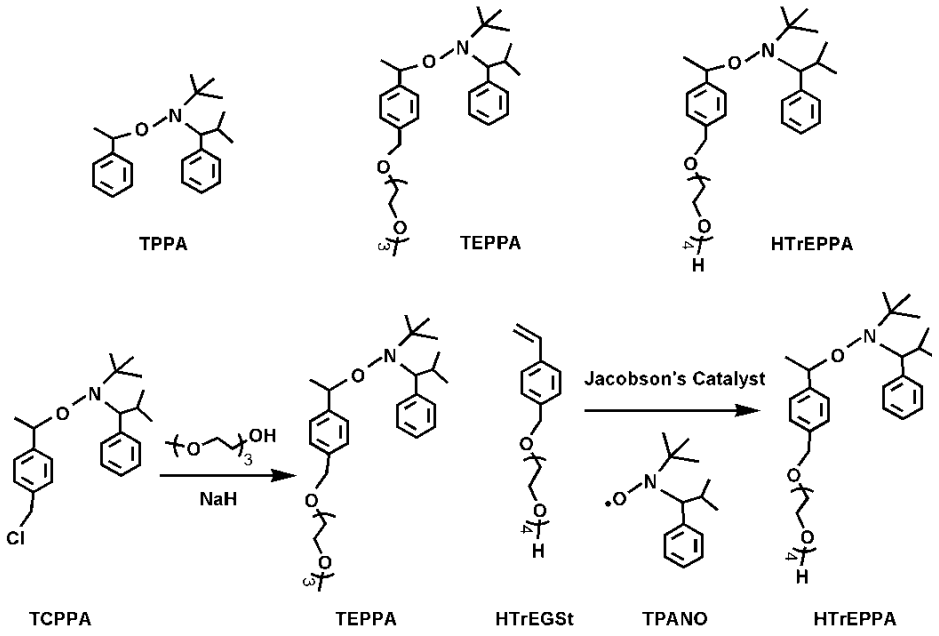
The two initiators, TEPPA and HTrEPPA, were prepared by use of different synthetic routes (Scheme 1.3). TEPPA was synthesized by the reaction of TCPPA with sodium salt of tri(ethylene glycol) monomethyl ether. HTrEPPA was synthesized from HTrEGSt, which was reacted with nitroxide radical TPANO in the presence of Jacobsen's catalyst. The new alkoxyamine initiators TEPPA and HTrEPPA were thoroughly purified by silica gel column chromatography, and the molecular structures were confirmed by ^{1}H NMR, ^{13}C NMR, and mass spectroscopy. It should be noted that the separation of the desired product was easier in the synthetic route for TEPPA than for HTrEPPA.

1.3.2.2 Nitroxide-Mediated Radical Polymerizations of TEGSt and HTrEGSt Using TEPPA and HTrEPPA as Initiator, Respectively

TEPPA and HTrEPPA were used to polymerize TEGSt and HTrEGSt, respectively. 0.05 Equiv. of free nitroxide TPANO with respect to the initiator was added into the reaction mixture to create an artificial persistent radical effect, which was shown to provide further control over the polymerization.[41]

To confirm that the NMRPs of TEGSt and HTrEGSt initiated by TEPPA and HTrEPPA, respectively, in the presence of 0.05 equiv. of free nitroxide were controlled

Scheme 1.3. Molecular Structures of Alkoxyamine NMRP Initiators TPPA, TEPPA, and HTrEPPA and the Synthesis of TEPPA and HTrEPPA



processes, ^{1}H NMR spectroscopy was used to monitor the polymerizations. The peaks located in the range of 4.30 – 4.70 ppm, which were from -CH_2- of the benzyl groups of monomer and polymer, were used as internal standard. The sum of the integral values of the two peaks was a constant during the course of polymerization. The monomer conversions were calculated by use of the integral value of the peaks at 5.2 ppm (1H from the double bond of styrenic monomers) at time *t* and the value of the same peaks at $t = 0$. The molecular weights and polydispersities of the polymers obtained at different polymerization times were measured by GPC relative to polystyrene standards.

Figures 1.5 and 1.6 show the kinetic analysis and GPC results of typical NMRPs of TEGSt and HTrEGSt with TEPPA and HTrEPPA as initiators, respectively. A nearly linear relationship between $\ln([M]_0/[M])$ and reaction time was observed for both monomers, suggesting that the polymerization was a first-order reaction with respect to the monomer and the number of growing polymer chains was a constant throughout the course of polymerization. GPC analysis shows that the molecular weight $M_{n,GPC}$ increased with the monomer conversion in a linear fashion and the polydispersity index decreased progressively. For instance, for the NMRP of TEGSt (Figure 1.5), the $M_{n,GPC}$ increased from 4300 ($t = 60$ min), to 6800 ($t = 129$ min), to 8400 ($t = 183$ min), to 10100 ($t = 255$ min), to 11100 g/mol ($t = 300$ min), while the polydispersity index decreased gradually from 1.14 ($t = 60$ min), to 1.12 ($t = 129$ and 183 min), to 1.11 ($t = 255$ min), to 1.10 ($t = 300$ min).

To study the effect of molecular weight on thermosensitive properties, a series of poly(TEGSt) (PTEGSt) and poly(HTrEGSt) (PHTrEGSt) with $M_{n,GPC}$ from 3000 to

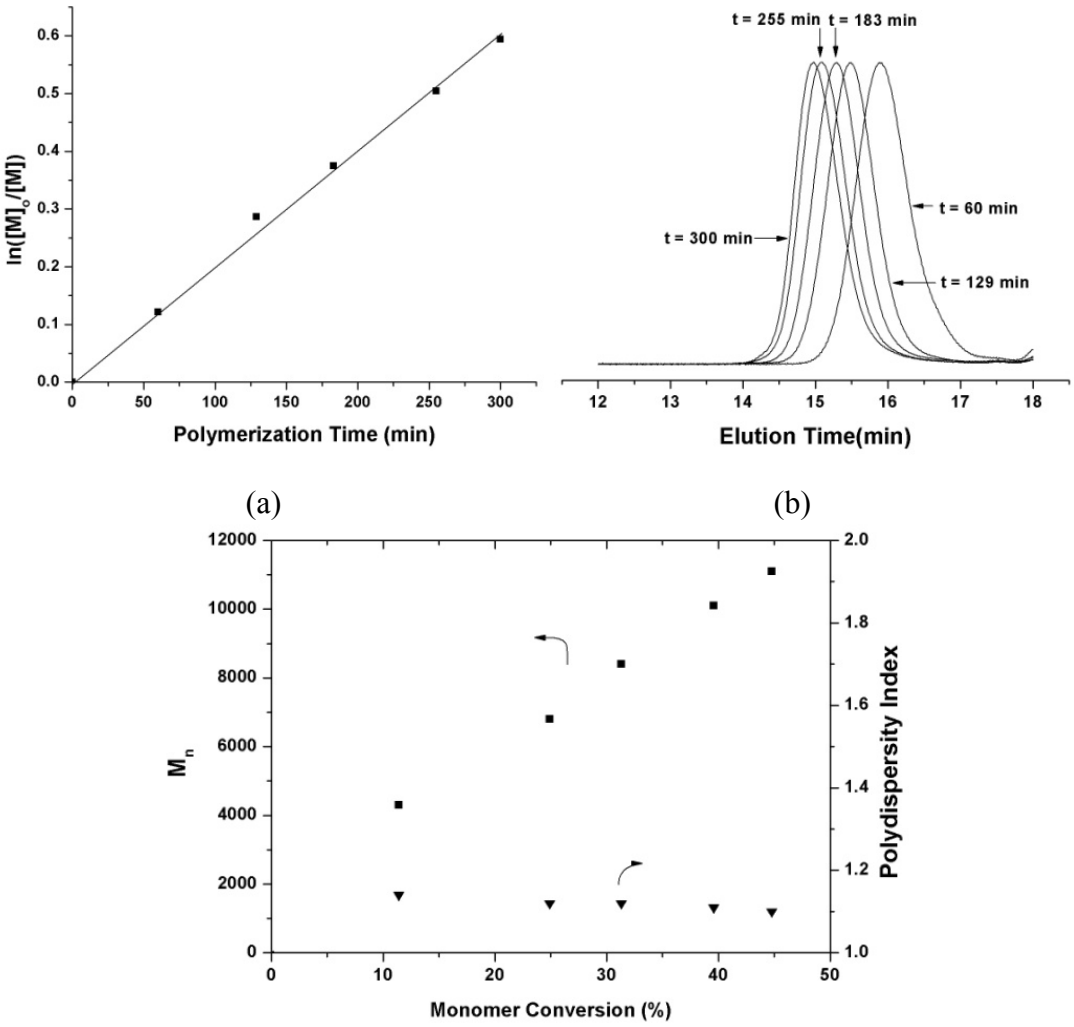
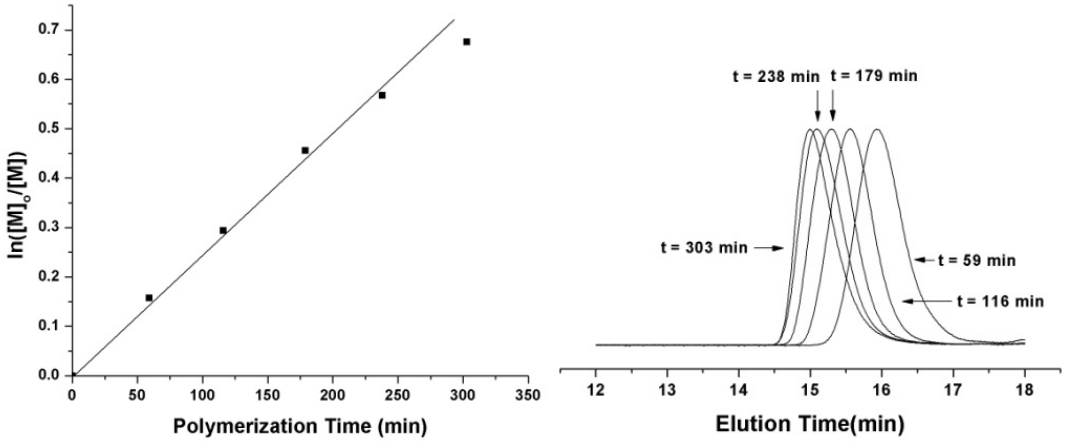
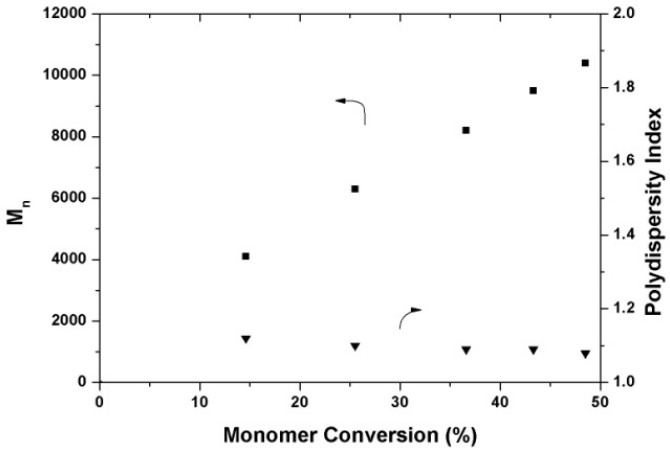


Figure 1.5. (a) Relationship between $\ln([M]_0/[M])$ and time for the polymerization of TEGSt using TEPPA as initiator in the presence of free nitroxide TPANO in anisole (1.1:1 w/w with respect to monomer) at 120 ^{o}C ($[TEGSt]_0$ = 1.66 M, $[M]_0/[I]_0$ = 121, $[TPANO]_0$ = 0.684 mM), (b) evolution of GPC curves with the polymerization time, and (c) $M_{n,GPC}$ (■) and PDI (▼), obtained from GPC analysis relative to polystyrene standards, versus monomer conversion. The DP of the final polymer was 54.



(a) (b)



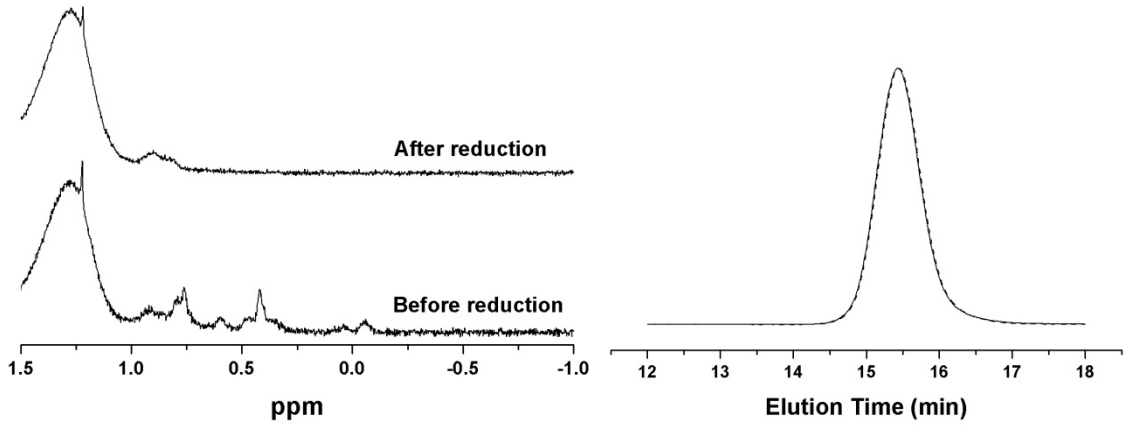
(c)

Figure 1.6. (a) Relationship between $\ln([M]_0/[M])$ and time for the polymerization of HTrEGSt using HTrEPPA as an initiator in the presence of free nitroxide TPANO in anisole (1.3:1 w/w with respect to monomer) at 120 ^{o}C ($[HTrEGSt]_0$ = 1.41 M, $[M]_0/[I]_0$ = 121, $[TPANO]_0$ = 0.580 mM), (b) evolution of GPC curves with the polymerization time, and (c) $M_{n,GPC}$ (■) and PDI (▼), obtained from GPC analysis relative to polystyrene standards, versus monomer conversion. The DP of the final polymer was 59.

28000 g/mol were synthesized by use of new alkoxyamine initiators. These polymers are designated as H-PTEGSt-ON and H-PHTrEGSt-ON, where the two ends of polymer chains are hydrogen (H) and alkoxyamine group (ON). For all these polystyrenics, the polydispersity indices were in the range of 1.08 and 1.13.[64] For comparison study of end group effect, six polymers of TEGSt with $M_{n,GPC}$ from 3900 to 26400 g/mol were prepared using TPPA as initiator with addition of 0.05 equiv of free nitroxide TPANO. These polystyrenics were designated as Ph-PTEGSt-ON, where the two ends of PTEGSt were phenylethyl (Ph) and the alkoxyamine group (ON).

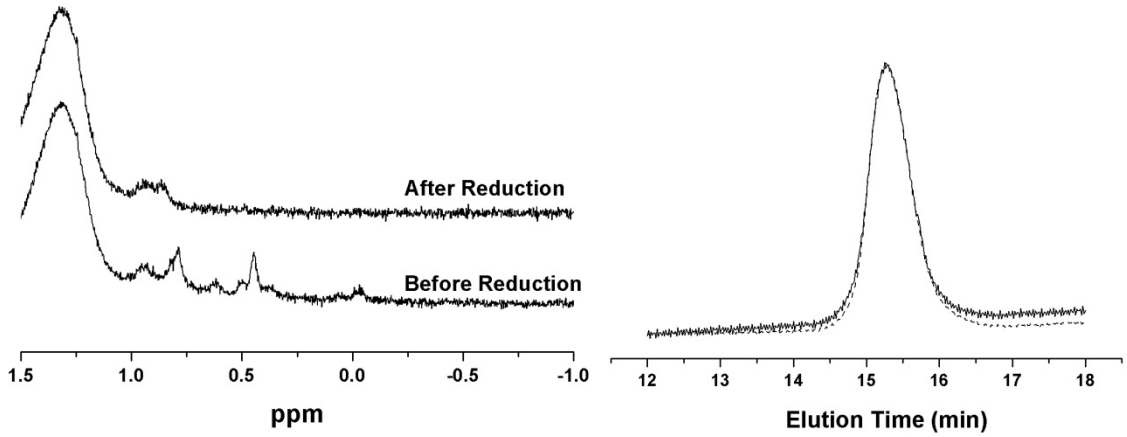
1.3.2.3 Removal of the Alkoxyamine Group from the Chain End of PTEGSt and PHTrEGSt

By use of monomer-based initiators TEPPA and HTrEPPA, the hydrophobic phenylethyl end group of the polymers prepared with TPPA as initiator was effectively "eliminate" (Scheme 1.2). The other chain end of the polymers is terminated by the alkoxyamine group, which is also hydrophobic. To study its effects on the thermosensitive properties of PTEGSt and PHTrEGSt and on the molecular weight dependences of cloud points, tri(*n*-butyl)tin hydride was used to remove it from polymer chain end. It has been reported that this method is very effective for the removal of the alkoxyamine group.[65] Figures 1.7 and 1.8 show the ^{1}H NMR spectra and GPC traces of PTEGSt and PHTrEGSt, respectively, before and after reduction with $(n\text{-Bu})_3\text{SnH}$. From ^{1}H NMR spectra, the peaks in the range of 0 – 1 ppm, which are from the alkoxyamine end group, completely disappeared, indicating that the alkoxyamine group was replaced with hydrogen (Figures 1.7a and 1.8a). GPC analysis showed that there were no changes



(a) (b)

Figure 1.7. (a) ^{1}H NMR spectra of PTEGSt that was synthesized using TEPPA as initiator ($M_{n,GPC}$ = 8300 g/mol, PDI = 1.09, DP = 41 (including one repeat unit from initiator TEPPA)) before and after the removal of the alkoxyamine end group with (*n*-Bu)$_3$SnH, and (b) GPC traces of the same polymer before (solid line) and after (dotted line) the removal of the alkoxyamine group from the chain end.



(a) (b)

Figure 1.8. (a) ^{1}H NMR spectra of PHTrEGSt that was synthesized using HTrEPPA as initiator ($M_{n,GPC}$ = 8400 g/mol, PDI = 1.09, DP = 45) before and after the removal of the alkoxyamine group, and (b) GPC traces of the same polymer before (solid line) and after (dotted line) the removal of the alkoxyamine group from polymer chain end.

in the molecular weights after reduction (Figure 1.7b and 1.8b), which means that the reduction reactions did not degrade the polymer chains but only removed the alkoxyamine group (the actual change in the polymer molecular weight due to the removal of alkoxyamine end group (220 amu) was too small to be detected by GPC). The reduced polymers of TEGSt and HTrEGSt synthesized from TEPPA and HTrEPPA were designated as H-PTEGSt-H and H-PHTrEGSt-H, where the two ends were hydrogen atoms. Similarly, the polymers of TEGSt synthesized from TPPA were reduced with (*n*-Bu)$_3$SnH and the reduced polymers were designated as Ph-PTEGSt-H, where the two ends were phenylethyl (Ph) and hydrogen (H).

1.3.2.4 Thermosensitive Properties of PTEGSt Prepared by Use of TPPA and TEPPA as Initiators: Comparison of Cloud Points Before and After the Removal of the Alkoxyamine Group from Polymer Chain End

All polymers of TEGSt prepared by use of TPPA and the monomer-based initiator TEPPA can be dissolved in cold water, yielding transparent solutions. Upon heating to a certain temperature, the clear solutions turn cloudy. Figures 1.9 and 1.10 show the optical transmittances of the aqueous solutions (1.0 wt %) of PTEGSt synthesized from TPPA and TEPPA (Ph-PTEGSt-ON and H-PTEGSt-ON, respectively) and the corresponding reduced polymers (Ph-PTEGSt-H and H-PTEGSt-H) as a function of temperature. The two original polymers, Ph-PTEGSt-ON and H-PTEGSt-ON, are essentially identical in chain length (for Ph-PTEGSt-ON, DP = 40 and $M_{n,GPC}$ = 8200 g/mol; for H-PTEGSt-ON, DP = 41 (including one repeat unit from initiator TEPPA) and $M_{n,GPC}$ = 8300 g/mol). The transmittance of aqueous solution of Ph-PTEGSt-ON decreased dramatically at ~ 10 ^{o}C.

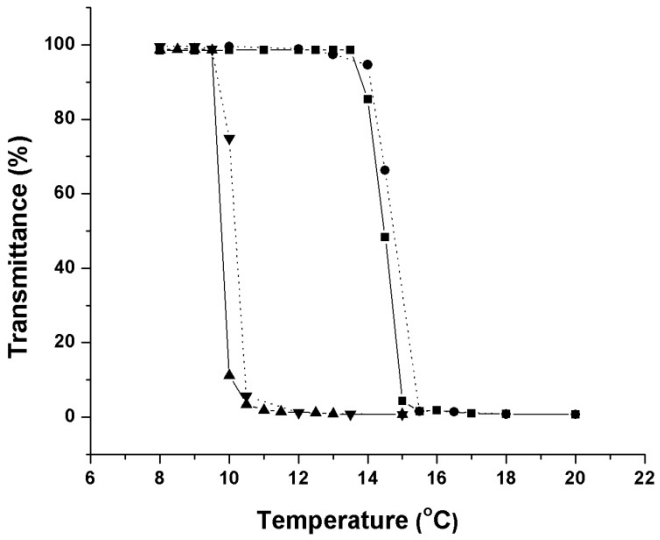


Figure 1.9. Optical transmittances of aqueous solutions of Ph-PTEGSt-ON (synthesized by use of TPPA initiator, $M_{n,GPC}$ = 8200 g/mol, PDI = 1.11, DP = 40, 1.0 wt %, ▲ heating process; ▼ cooling process) and the corresponding reduced polymer Ph-PTEGSt-H (1.0 wt %, ■ heating process; ● cooling process) as a function of temperature. The transmittances were recorded at wavelength of 500 nm by use of a UV-vis spectrometer.

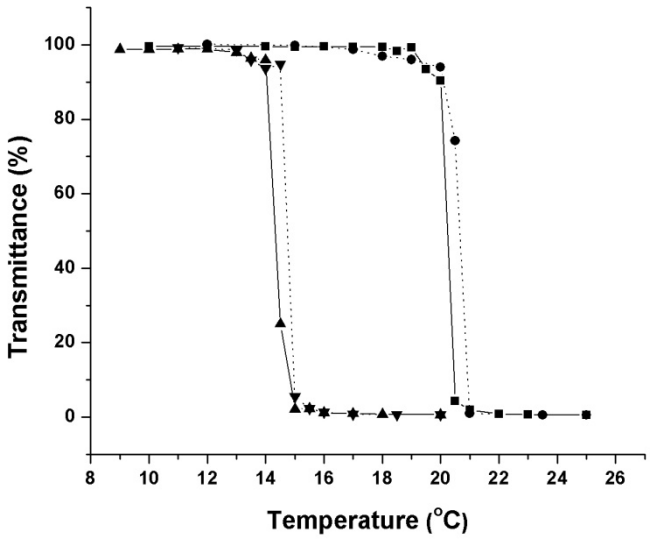


Figure 1.10. Optical transmittances of aqueous solutions of H-PTEGST-ON (synthesized by use of TEPPA as initiator, $M_{n,GPC}$ = 8300 g/mol, PDI = 1.09, DP = 40, 1.0 wt %, ▲ heating process, ▼ cooling process) and the corresponding reduced polymer H-PTEGSt-H (1.0 wt %, ■ heating process; ● cooling process) as a function of temperature. The transmittances were recorded at wavelength of 500 nm by use of a UV-vis spectrometer.

If 50 % of transmittance is used, the cloud point is 9.7 ^{o}C. The transparent-to-cloudy transition was sharp and the transition zone from Figure 1.9 was ~ 1 ^{o}C. After the replacement of alkoxyamine end group with hydrogen, the cloud point increased to 14.5 ^{o}C, which was 4.8 ^{o}C higher than that of Ph-PTEGSt-ON. For H-PTEGSt-ON (Figure 1.10), the cloud point was 14.3 ^{o}C (50 % transmittance), which was 4.6 ^{o}C higher than that of Ph-PTEGSt-ON with essentially the same molecular weight. After the removal of the alkoxyamine group from the chain end, the cloud point increased from 14.3 to 20.2 ^{o}C. Since GPC analysis showed that there was no change in the molecular weight after reduction, the difference in the cloud points can be attributed to the influence of a single alkoxyamine group at the chain end. Note that the cloud point of Ph-PTEGSt-H (14.5 ^{o}C) is very similar to that of H-PTEGSt-ON (14.3 ^{o}C), suggesting that phenylethyl and alkoxyamine groups have very similar effects on the cloud point of PTEGSt, though the alkoxyamine end group is slightly stronger because of a slightly lower cloud point observed for H-PTEGSt-ON.

The concentration effect on the cloud points of these polymers in water was further investigated. The results are summarized in Figure 1.11. For all four polymers (Ph-PTEGSt-ON, Ph-PTEGSt-H, H-PTEGSt-ON, and H-PTEGSt-H), the cloud points were found to increase gradually with the decrease of polymer concentration. For instance, the cloud points of H-PTEGSt-ON were 13 and 21 ^{o}C at concentrations of 2.03 % and 0.05 %, respectively. While the cloud point difference between Ph-PTEGSt-ON and Ph-PTEGSt-H) (4 – 5 ^{o}C) was maintained at all concentrations, the transition temperature difference between H-PTEGSt-ON and H-PTEGSt-H increased slightly with decreasing concentration, from 4 ^{o}C at 2.0 % to 7 ^{o}C at 0.05 wt %. It is interesting to note that the

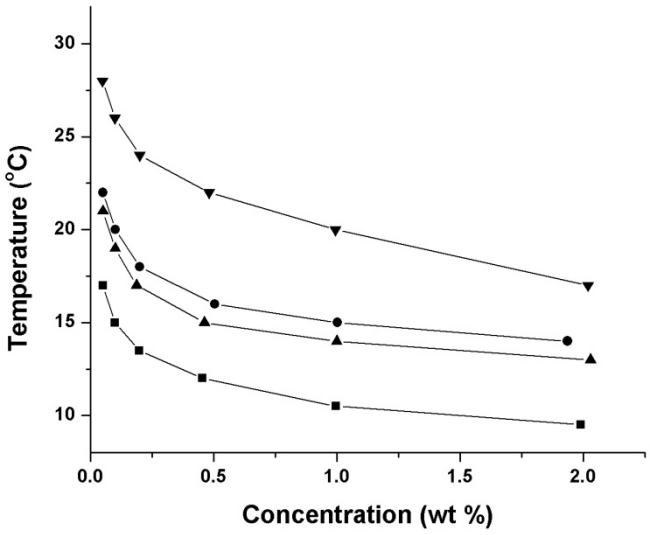


Figure 1.11. Concentration effect on the cloud point of Ph-PTEGSt-ON (■, synthesized from TPPA initiator, DP = 40, $M_{n,GPC}$ = 8200 g/mol, PDI = 1.11), Ph-PTEGSt-H (●, reduced Ph-PTEGSt-ON by use of $(n\text{-Bu})_3SnH$), H-PTEGSt-ON (▲, synthesized from TEPPA initiator, DP = 41, $M_{n,GPC}$ = 8300 g/mol, PDI = 1.09), and H-PTEGSt-H (▼, reduced H-PTEGSt-ON by use of $(n\text{-Bu})_3SnH$)).

cloud point of Ph-PTEGSt-H was consistently higher by 1 ^{o}C than that of H-PTEGSt-ON at all concentrations (a different method was used here to record the cloud points and there was a slight difference (within 1 ^{o}C) between the cloud points from these two methods), indicating that the phenylethyl and alkoxyamine groups have similar effects but the alkoxyamine group is slightly stronger in depressing the cloud point. All these further support that a hydrophobic end group could decrease the cloud point of a thermosensitive polymer appreciably. The hydrophobic end groups increase the degree of ordering of water molecules that surround the polymer chain and thus increase the entropy penalty,[50] resulting in a lower cloud point.

1.3.2.5 Molecular Weight Dependence of Cloud Point of PTEGSt with Different End Groups

To study the molecular weight effect on cloud point, a series of Ph-PTEGSt-ON and H-PTEGSt-ON with various molecular weights and narrow polydispersities were synthesized from initiators TPPA and TEPPA, respectively. These polymers were reacted with tri(*n*-butyl)tin hydride to remove the alkoxyamine group from the chain end, yielding corresponding Ph-PTEGSt-H and H-PTEGSt-H. The cloud points of these polymers in water at a concentration of 1.0 wt % were measured, and the results are summarized in Figure 1.12.

In the investigated molecular weight range from $M_{n,GPC}$ = 3000 to 28000 g/mol, the cloud point of Ph-PTEGSt-ON increased with the increase of molecular weight, from 6 ^{o}C at $M_{n,GPC}$ of 3900 g/mol to 15 ^{o}C at $M_{n,GPC}$ of 26400 g/mol. For H-PTEGSt-ON, the cloud point increased with the increase of $M_{n,GPC}$ up to 16700 g/mol and then decreased

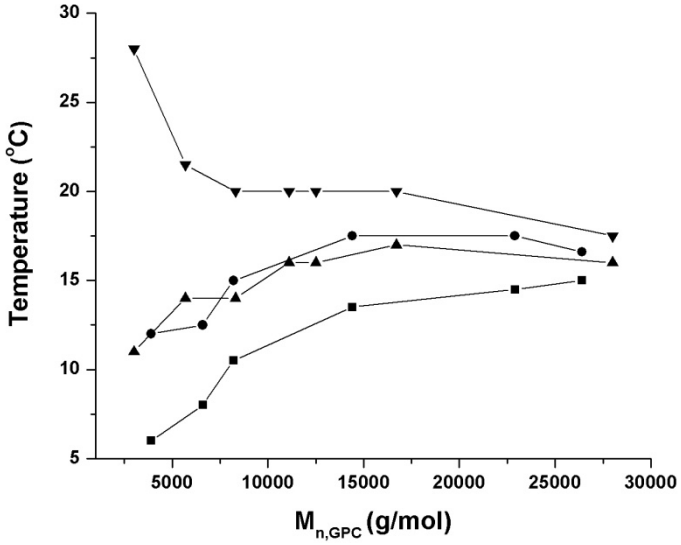


Figure 1.12. Molecular weight dependence of cloud point of Ph-PTEGSt-ON (■, synthesized from TPPA initiator), Ph-PTEGSt-H (●, reduced from Ph-PTEGSt-ON using $(n\text{-Bu})_3\text{SnH}$), H-PTEGSt-ON (▲, synthesized from initiator TEPPA), and H-PTEGSt-H (▼, reduced from H-PTEGSt-ON using $(n\text{-Bu})_3\text{SnH}$) in water at a concentration of 1.0 wt %. The molecular weights were measured by GPC using polystyrene calibration.

slightly with further increasing molecular weight, from 17 ^{o}C at $M_{n,GPC}$ of 16700 g/mol to 16 ^{o}C at $M_{n,GPC}$ of 28000 g/mol. The cloud points of PTEGSt synthesized from the monomer-based initiator TEPPA (H-PTEGSt-ON) are higher than those of Ph-PTEGSt-ON with similar molecular weights. This is most pronounced in the low molecular weight range and the difference can be 5 – 6 ^{o}C. Since the kinetics and GPC analysis showed that the polymerizations were well-controlled processes yielding well-defined polymers, the only difference in the molecular structures of Ph-PTEGSt-ON and H-PTEGSt-ON is the terminal group at one end, phenylethyl versus one hydrogen atom. Thus, the observed difference in the cloud points of Ph-PTEGSt-ON and H-PTEGSt-ON with similar molecular weights is caused by the hydrophobic phenylethyl group. With the increase of $M_{n,GPC}$, the cloud point difference at a particular molecular weight became smaller, ~ 1 ^{o}C at $M_{n,GPC}$ > 26000 g/mol. At even higher molecular weight, the cloud points are expected to be essentially the same for Ph-PTEGSt-ON and H-PTEGSt-ON, that is the phenylethyl group has a negligible effect on the thermosensitive property of PTEGSt if the chain length is long enough.

After the removal of the alkoxyamine group from chain end, the cloud points of the polymers prepared from both TPPA and TEPPA increased, with the largest change at the lowest molecular weight. While the cloud point of Ph-PTEGSt-ON with $M_{n,GPC}$ of 3900 g/mol was only 6 ^{o}C lower than that of Ph-PTEGSt-H, a cloud point difference of 17 ^{o}C was observed between H-PTEGSt-ON and H-PTEGSt-H at $M_{n,GPC}$ of 3000 g/mol. For all PTEGSt, the cloud point change before and after reduction decreased with the increase of molecular weight. An increase of only 1.5 ^{o}C in cloud point was found for H-PTEGSt-ON with $M_{n,GPC}$ of 28000 g/mol after reduction. Thus, similar to phenylethyl, the effect

of TPANO group on the thermosensitive property of PTEGSt becomes negligible if the molecular weight is high enough. It should be emphasized that the cloud point of H-PTEGSt-H decreased with the increase of molecular weight, which is completely different from Ph-PTEGSt-ON. It is also worth noting here that the cloud point of Ph-PTEGSt-H is slightly higher than that of H-PTEGSt-ON at a similar molecular weight except one data point in Figure 1.12, consistent with the observations in Figures 1.9 – 1.11. This further supports that the alkoxyamine group is stronger than phenylethyl in depressing the cloud point, which is reasonable because the alkoxyamine group is a larger hydrophobic group than phenylethyl.[66]

1.3.2.6 Molecular Weight Dependence of Cloud Point of PHTrEGSt with Different End Groups

Similarly, a series of H-PHTrEGSt-ON and the corresponding H-PHTrEGSt-H with various molecular weights and narrow molecular weight distributions were prepared and the cloud points of their aqueous solutions at a concentration of 1.0 wt % were measured. The results are summarized in Figure 1.13. For comparison, the cloud points of PHTrEGSt synthesized from TPPA initiator are also included. A monotonic increase in the cloud point with the increase of molecular weight was observed for Ph-PHTrEGSt-ON in the $M_{n,GPC}$ range from 4000 to 26000 g/mol. For H-PHTrEGSt-ON, a trend similar to that of H-PTEGSt-ON was found, though the cloud points for the two polymers were very different. When the molecular weight was higher than 16700 g/mol, the cloud point began to decrease, from 72 ^{o}C at $M_{n,GPC}$ of 16700 g/mol to 67 ^{o}C at $M_{n,GPC}$ of 25600 g/mol. After the removal of alkoxyamine group from the chain end, the cloud point was

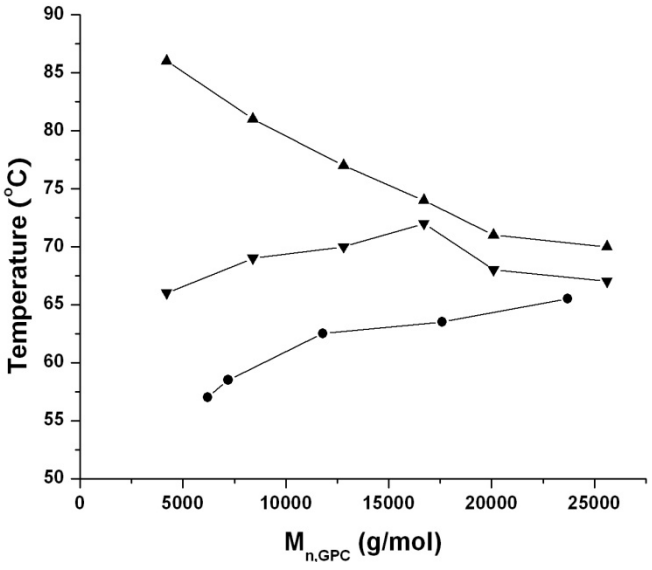


Figure 1.13. Molecular weight dependence of cloud point of Ph-PHTrEGSt-ON (●, synthesized from initiator TPPA), H-PHTrEGSt-ON (▼, synthesized from initiator HTrEPPA), and H-PHTrEGSt-H (▲, reduced from H-PHTrEGSt-ON using $(n\text{-Bu})_3\text{SnH}$) in water at a concentration of 1.0 wt %. The molecular weights were measured by GPC using polystyrene calibration.

found to be higher at all molecular weights. The largest increase, from 66 to 86 ^{o}C, was observed at $M_{n,GPC}$ of 4200 g/mol. Moreover, H-PHTrEGSt-H exhibited a monotonic decrease in cloud point with increasing molecular weight, which is totally different from Ph-PHTrEGSt-ON. The studies of both PTEGSt and PHTrEGSt conclude that the hydrophobic end groups can lower the cloud point appreciably, especially in the low molecular weight range, and can reverse the molecular weight dependence of cloud point.

1.3.2.7 Molecular Weight Effect and End Group Effect on the Cloud Points of Polystyrenics

Since H-PTEGSt-H and H-PHTrEGSt-H essentially have no end groups, their cloud points at various $M_{n,GPC}$ reflect the "true" molecular weight effect on the thermosensitive properties of PTEGSt and PHTrEGSt, i.e., the LCST decreases with the increase of polymer chain length. For other polymers (Ph-PTEGSt-ON, Ph-PTEGSt-H, H-PTEGSt-ON, H-PHTrEGSt-ON, and Ph-PHTrEGSt-ON), the observed molecular weight dependences are actually the results of combined end group effect and "true" molecular weight effect. Thus, at low molecular weights, the end group effect outweighs the molecular weight effect and the situation is reversed when molecular weight is high enough. This can be seen in the molecular weight dependences of cloud points of Ph-PTEGSt-H, H-PTEGSt-ON, and H-PHTrEGSt-ON, where the cloud point initially increased with $M_{n,GPC}$ but leveled off/decreased slightly at higher molecular weights. For Ph-PTEGSt-ON and Ph-PHTrEGSt-ON, there are two hydrophobic groups at the two ends of polymer chains making the end group effect stronger than molecular weight effect in the studied molecular weight range. If the chain length is further increased, the

cloud point may level off or decrease slightly.

1.4 Conclusions

Two monomers HTEGSt and HTrEGSt were prepared and polymerized by nitroxide-mediated radical polymerization using an alkoxyamine as initiator. Kinetics study and GPC analysis showed that the polymerizations were living processes, producing polymers with controlled molecular weights and narrow polydispersities. The thermosensitive properties of the two polymers in aqueous solutions were studied by UV-vis spectrometry and variable temperature ^{1}H NMR spectroscopy. The cloud points of PHTEGSt and PHTrEGSt in water were around 13 and 64 ^{o}C, respectively, which were supported by variable temperature ^{1}H NMR spectroscopy analysis. Thermosensitive water-soluble PTEGSt and PHTrEGSt with controlled molecular weights, narrow polydispersities, and defined chain end groups were prepared by NMRP using α-alkoxyamine initiators and were used to study the end group effect and molecular weight effect on cloud points. Two new initiators, TEPPA and HTrEPPA, with molecular structures resembling TEGSt and HTrEGSt, respectively, were synthesized. Kinetics and GPC analysis showed that the polymerizations were controlled, producing well-defined polystyrenics. The alkoxyamine group was removed from polymer chain end by use of (*n*-Bu)$_3$SnH. The cloud points of these polymers in aqueous solutions were measured. It was found that in the studied molecular weight range ($M_{n,GPC}$ = 3000 to 28000 g/mol) the hydrophobic end groups, phenylethyl and alkoxyamine, could depress the cloud point by 1 – 20 ^{o}C depending on the molecular weight and the largest change was observed at the lowest molecular weight. The cloud points of PTEGSt and PHTrEGSt with two

hydrophobic groups at the two ends, phenylethyl and alkoxyamine, showed a monotonic increase with the increase of molecular weight. For polymers with only one hydrophobic chain end group (Ph-PTEGSt-H, H-PTEGSt-ON, and H-PHTrEGSt-ON), the cloud point initially increased with the increase of molecular weight but leveled off/decreased slightly with further increasing polymer molar mass. For polymers with essentially no end groups (H-PTEGSt-H and H-PHTrEGSt-H), the cloud point decreased with the increase of chain length in the low molecular weight range and exhibited little change when the molecular weight was high enough, which represents the "true" molecular weight dependence of cloud point. The observed molecular weight dependences of cloud points of polymers with hydrophobic end group(s) were explained by the end group effect and the "true" molecular weight effect. This study shows that the hydrophobic end groups can change the apparent molecular weight dependence of cloud point of a thermosensitive water-soluble polymer.

References:

1. Gil, E. S; Hudson, S. M. *Prog. Polym. Sci.* **2004**, *29*, 1173-1222.
2. Schild , H. G. *Prog. Polym. Sci.* **1992**, *17*, 163-249.
3. Chung, J. E.; Yokoyama, M.; Yamato, M.; Aoyagi, T.; Sakurai, Y.; Okano, T. *J. Controlled Release* **1999**, *62*, 115-127.
4. Langer, R. *Nature* **1998**, *392*, 5-10 (suppl.).
5. Nath, N.; Chilkoti, A. *Adv. Mater.* **2002**, *14*, 1243-1247.
6. Kushida, A.; Yamato, M.; Konno, C.; Kikuchi, A.; Sakurai, Y.; Okano, T. *J. Biomed. Mater. Res.* **1999**, *45*, 355-362.
7. Tu, H.; Heitzman, C. E.; Braun, P. V. *Langmuir* **2004**, *20*, 8313-8320.
8. Plunkett, K. N.; Zhu, X.; Moore, J. S.; Leckband, D. E. *Langmuir* **2006**, *22*, 4259-4266.
9. Raula, J.; Shan, J.; Nuopponen, M.; Niskanen, A. Jiang, H.; Kauppinen, E. I.; Tenhu, H. *Langmuir* **2003**, *19*, 3499-3504.
10. Kizhakkedathu, J. N.; Norris-Jones, R.; Brooks, D. E. *Macromolecules* **2004**, *37*, 734-743.
11. Perruchot, C.; Khan, M. A.; Kamitsi, A.; Armes, S. P.; von Werne, T.; Patten, T. E. *Langmuir* **2001**, *17*, 4479-4481.
12. Tsuji, S.; Kawaguchi, H. *Langmuir* **2004**, *20*, 2449-2455.
13. Tsuji, S.; Kawaguchi, H. *Macromolecules* **2006**, *39*, 4338-4344.
14. Li, D. J.; Jones, G. J.; Dunlap, J. R.; Hua, F. J.; Zhao, B. *Langmuir* **2006**, *22*, 3344-3351.
15. Li, D. J.; Zhao, B. *Langmuir* **2007**, *23*, 2208-2217.

16. Saitoh, T.; Sekino, A.; Hiraide, M. *Chemistry Letters* **2004**, *33*, 912-913.

17. Bergbreiter, D. E. *Chem. Rev.* **2002**, *102*, 3345-3384.

18. Fujii, S.; Read, E. S.; Binks, R. P.; Armes, S. P. *Adv. Mater.* **2005**, *17*, 1014-1018.

19. Wu, C.; Zhou, S. Q. *Macromolecules* **1995**, *28*, 8381-8387.

20. Wu, C.; Wang, X. H. *Phys. Rev. Lett.* **1998**, *80*, 4092-4094.

21. Kubota, K.; Fujishige, S.; Ando, I. *J. Phys. Chem.* **1990**, *94*, 5154-5158.

22. Convertine, A. J.; Ayres, N.; Scales, C. W.; Lowe, A. B.; McCormick, C. L. *Biomacromolecues* **2004**, *5*, 1177-1180.

23. Schilli, C. M.; Zhang, M.; Rizzardo, E.; Thang, S. H.; Chong, Y. K.; Edwards, K.; Karlsson, G.; Müller, A. H. E. *Macromolecules* **2004**, *37*, 7861-7866.

24. Qin, S. H.; Geng, Y.; Discher, D. E.; Yang, S. *Adv. Mater.* **2006**, *18*, 2905-2909.

25. Liu, B.; Perrier, S. *J. Polym. Sci. Part A: Polym. Chem.* **2005**, *43*, 3643-3654.

26. Aubrecht, K. B.; Grubbs, R. B. *J. Polym. Sci. Part A: Polym. Chem.* **2005**, *43*, 5156-5167.

27. Jones, J. A.; Novo, N.; Flagler, K.; Pagnucco, C. D.; Carew, S.; Cheong, C.; Kong, X. Z.; Burke, N. A. D.; Stöver, H. D. H. *J. Polym. Sci. Part A: Polym. Chem.* **2005**, *43*, 6095-6104.

28. Duan, Q.; Miura, Y.; Narumi, A.; Shen, X.; Sato, S.-I.; Satoh, T.; Kakuchi, T. *J. Polym. Sci. Part A: Polym. Chem.* **2006**, *44*, 1117-1124.

29. Ge, Z.; Luo, S.; Liu, S. *J. Polym. Sci. Part A: Polym. Chem.* **2006**, *44*, 1357-1371.

30. Kim, M. S.; Hyun, H.; Seo, K. S.; Cho, Y. H.; Lee, J. W.; Lee, C. R.; Khang, G.; Lee, H. B. *J. Polym. Sci. Part A: Polym. Chem.* **2006**, *44*, 5413-5423.

31. Gibbons, O.; Carroll, W. M.; Aldabbagh, F.; Yamada, B. *J. Polym. Sci. Part A: Polym. Chem.* **2006**, *44*, 6410-6418.

32. Aoshima, S.; Sugihara, S. *J. Polym. Sci. Part A: Polym. Chem.* **2000**, *38*, 3962-3965.

33. Aoshima, S.; Sugihara, S.; Shibayama, M.; Kanaoka, S. *Macromol. Symp.* **2004**, *215*, 151-163.

34. Sugihara, S.; Kanaoka, S.; Aoshima, S. *Macromolecules* **2005**, *38*, 1919-1927.

35. Sugihara, S.; Kanaoka, S.; Aoshima, S. *J. Polym. Sci. Part A: Polym. Chem.* **2004**, *42*, 2601-2611.

36. Shibata, T.; Kanaoka, S.; Aoshima, S. *J. Am. Chem. Soc.* **2006**, *128*, 7497-7504.

37. Han, S.; Hagiwara, M.; Ishizone, T. *Macromolecules* **2003**, *36*, 8312-8319.

38. Ali, M. M.; Stöver, H. D. H. *Macromolecules* **2004**, *37*, 5219-5227.

39. Lutz, J.-F.; Hoth, A. *Macromolecules* **2006**, *39*, 893-896.

40. Lutz, J.-F.; Akdemir, O.; Hoth, A. *J. Am. Chem. Soc.* **2006**, *128*, 13046-13047.

41. Zhao, B.; Li, D. J.; Hua, F. J.; Green, D. R. *Macromolecules* **2005**, *38*, 9509-9517.

42. Hua, F. J.; Jiang, X. G.; Zhao, B. *Macromolecules* **2006,** *39*, 3476-3479.

43. Aathimanikandan, S. V.; Savariar, E. N. Thayumanavan, S. *J. Am. Chem. Soc.* **2005**, 127, 14922-14929.

44. Benoit, D.; Chaplinski, V.; Braslau, R.; Hawker, C. J. *J. Am. Chem. Soc.* **1999**, *121*, 3904-3920.

45. Benoit, D.; Harth, E.; Fox, P.; Waymouth, R. M.; Hawker, C. J. *Macromolecules* **2000**, *33*, 363-370.

46. Hawker, C. J.; Bosman, A. W.; Harth, E. *Chem. Rev.* **2001**, *101*, 3661-3688.

47. Hawker, C. J.; Wooley, K. L. *Science* **2005**, *309*, 1200-1205.

48. Xia, Y.; Yin, X.; Burke, N. A. D; Stöver, H. D. H. *Macromolecules* **2005**, *38*, 5937-5943.

49. Huang, J.; Matyjaszewski, K. *Macromolecules* **2005**, *38*, 3577-3583.

50. Xia, Y.; Burke, N. A. D.; Stöver, H. D. H. *Macromolecules* **2006**, *39*, 2275-2283.

51. Kujawa, P.; Segui, F.; Shaban, S.; Diab, C.; Okada, Y.; Tanaka, F.; Winnik, F. M. *Macromolecules* **2006**, *39*, 341-348.

52. Kujuwa, P.; Tanak, F.; Winnik, F. M. *Macromolecules* **2006**, *39*, 3048-3055.

53. Fujishige, S.; Kubota, K.; Ando, I. *J. Phys. Chem.* **1989**, *93*, 3311-3313.

54. Chung, J. E.; Yokoyama, M.; Suzuki, K.; Aoyagi, T.; Sakurai, Y.; Okano, T. *Colloids and Surfaces B: Biointerfaces* **1997**, *9*, 37-48.

55. Yamazaki, A.; Song, J. M.; Winnik, F. M.; Brash, J. L. *Macromolecules* **1998**, *31*, 109-115.

56. Ringsdorf, H.; Venzmer, J.; Winnik, F. M. *Macromolecules* **1991**, *24*, 1678-1686.

57. Kujawa, P.; Winnik, F. M. *Macromolecules* **2001**, *34*, 4130-4135.

58. Bütün, V.; Armes, S. P.; Billingham, N. C. *Polymer* **2001**, *42*, 5993-6008.

59. Chung, J. E.; Yokoyama, M.; Aoyagi, T.; Sakurai, Y.; Okano, T. *J. Controlled Release* **1998**, *53*, 119-130.

60. Furyk, S.; Zhang, Y.; Ortiz-Acosta, D.; Cremer, P. S.; Bergbreiter, D. E. *J. Polym. Sci. Part A: Polym. Chem.* **2006**, *44*, 1492-1501.

61. Bosman, A. W.; Vestberg, R.; Heumann, A.; Fréchet, J. M. J.; Hawker, C. J. *J. Am. Chem. Soc.* **2003**, *125*, 715-728.

62. Wegrzyn, J. K.; Stephan, T.; Lau, R.; Grubbs, R. B. *J. Polym. Sci. Part A: Polym. Chem.* **2005**, *43*, 2977-2984.

63. Lacroix-Desmazes, P.; Andre, P.; Desimone, J. M.; Ruzette, A.; Boutevin, B. *J. Polym. Sci. Part A: Polym. Chem.* **2004**, *42*, 3537-3552.

64. The polydispersity index (PDI) could affect the thermosensitive properties of water-soluble polystyrenics (e.g., the transition zone might be broader if the PDI is higher).

65. Gotz, H.; Harth, E.; Schiller, S. M.; Frank, C. W.; Knoll, W.; Hawker, C. J. *J. Polym. Sci. Part A: Polym. Chem.* **2002**, *40*, 3379-3391.

66. The logP values of phenylethyl and the alkoxyamine groups were calculated by use of the software Molinspiration Interactive logP Calculator (P: partition coefficient of a compound between octanol and water, which is generally used as a measure of molecular hydrophobicity), and they are 2.852 and 3.951, respectively. Clearly, the alkoxyamine group is more hydrophobic than phenylethyl, which is consistent with our observations in the study of their effects on the cloud point of PTEGSt.

Chapter 2. Multiple Micellization and Dissociation Transitions of Thermo- and Light-Sensitive Poly(ethylene oxide)-*b*-Poly(ethoxytri(ethylene glycol) acrylate-*co*-*o*-nitrobenzyl acrylate) in Dilute Aqueous Solution

Abstract

This chapter presents the synthesis of thermo- and light-sensitive hydrophilic block copolymers, poly(ethylene oxide)-*b*-poly(ethoxytri(ethylene glycol) acrylate-*co*-*o*-nitrobenzyl acrylate), and the study of their micellization/dissociation transitions in water in response to temperature changes and UV irradiation. The block copolymers with controlled molecular weights and narrow polydispersities were synthesized by atom transfer radical polymerization of a mixture of ethoxytri(ethylene glycol) acrylate and *o*-nitrobenzyl acrylate with a molar ratio of 100 : 10 from a PEO macroinitiator. Dynamic light scattering and fluorescence spectroscopy studies showed that these copolymers were molecularly dissolved in water at lower temperatures and self-assembled into micelles with the thermosensitive block associating into the core and the PEO block forming the corona when the temperature was above the lower critical solution temperature (LCST) of the thermosensitive block. Upon UV irradiation, the *o*-nitrobenzyl group was cleaved and the LCST of the thermosensitive block was increased, causing the dissociation of micelles into unimers and the release of encapsulated fluorescent dye Nile Red into water. Further increasing the temperature induced the formation of micelles again and the re-encapsulation of Nile Red. The thermo-induced formation and dissociation of micelles were reversible.

2.1 Introduction

Environmentally responsive micelles or vesicles formed from the self-assembly of stimuli-sensitive block copolymers or low mass amphiphiles in solution have received growing interest in recent years.[1-3] These micellar aggregates can spontaneously dissociate into the molecularly dissolved unimers or undergo morphology changes upon application of external stimuli.[1-49] Thus, they are particularly suitable for controlled encapsulation and triggered release of substances, and have potential applications in targeted drug delivery, cosmetics, etc.[1] A common principle for destabilizing micelles or vesicles involves the modification of the polarity or hydrophobicity/hydrophilicity balance of the core-forming component by the use of an environmental trigger. When the core-forming component becomes soluble in the medium, the driving force for the formation of micellar aggregates is eliminated, causing the micelles or vesicles to disassemble. Depending on the response mechanism, dissociation of micellar aggregates can be reversible or irreversible.[1-3] In some applications, the reversible dissociation and micellization can be advantageous or are desired because the re-formation of micellar aggregates enables the re-encapsulation of the released substance.[35,36]

Various chemical and physical stimuli including pH,[1-16] specific molecules,[1,17-19] redox,[1,20-27] light,[28-36] and temperature[37-49] have been employed to induce the disassembly or morphology changes of micellar aggregates. Light is an especially attractive external stimulus because the triggered release of encapsulated substances can be controlled at a specific time and location.[28-36] For examples, Jiang et al. synthesized photo-responsive poly(ethylene oxide)-*b*-poly(pyrenyl methacrylate) (PEO-*b*-poly(pyrenyl methacrylate))

and PEO-*b*-poly(*o*-nitrobenzyl methacrylate), and prepared the micelles by addition of water into their THF solutions.[31,32] Upon UV irradiation, the pyrenyl or *o*-nitrobenzyl group was cleaved, converting the core-forming hydrophobic block into hydrophilic. Consequently, the micelles dissociated into the unimers. Goodwin et al. used IR light to trigger the release of Nile Red from the micelles of a low mass nonionic surfactant that contained a photoresponsive 2-diazo-1,2-naphthoquinone (DNQ) group.[33] Light irradiation of DNQs induced Wolff rearrangement, resulting in a drastic increase in water solubility and thus the dissociation of micelles. Jiang et al. reported the assembly and disassembly of vesicles formed by a light-responsive PEO-terminated malachite green derivative.[35] Lee et al. synthesized a diblock copolymer of ethylene glycol and a spiropyran-containing methacrylate.[36] The block copolymer micellar aggregates were disrupted by UV irradiation and regenerated by exposure to visible light.

Temperature is another attractive environmental trigger.[37-52] The behaviors of hydrophilic block copolymers with one or more blocks exhibiting thermosensitive properties in water are intriguing.[37-49] These block copolymers undergo reversible micellization and dissociation in response to temperature changes. It should be emphasized here that one advantage of the preparation of micelles from doubly hydrophilic diblock copolymers is the elimination of the use of organic solvents. It is known that the lower critical solution temperature (LCST) of a thermosensitive polymer can be modified by incorporation of a different monomer.[1-3,52-59] Hennink et al. recently developed a series of diblock copolymers composed of PEO and thermosensitive polymers that contained lactate side chains.[1,54-57] Hydrolysis of lactate groups caused an

increase of the LCST of the thermosensitive block. When the polymer became soluble in water, dissociation of micelles occurred and the encapsulated molecules were released.

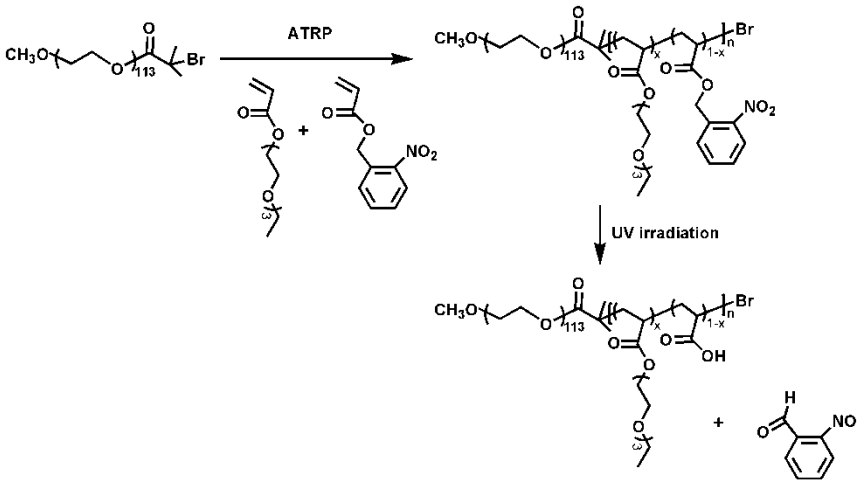
In this work, thermo- and light-sensitive hydrophilic block copolymers, PEO-*b*-poly(ethoxytri(ethylene glycol) acrylate-*co*-*o*-nitrobenzyl acrylate) (PEO-*b*-P(TEGEA-*co*-NBA), Scheme 2.1), were synthesized by atom transfer radical polymerization (ATRP) and their micellization and dissociation transitions in water in response to temperature changes and UV irradiation were investigated. PTEGEA is a thermosensitive water soluble polymer. Above the LCST of the thermosensitive block ($LCST_1$), the copolymers self-assemble into micelles in water. Upon UV irradiation, the hydrophobic *o*-nitrobenzyl group is cleaved[32] and the LCST of the thermosensitive block increases, causing the dissociation of micelles into unimers (Scheme 2.2). Further increasing the temperature to above the LCST of the new thermosensitive block ($LCST_2$) induces the formation of micelles again. The temperature-induced micellization is reversible. As a demonstration, the hydrophobic dye Nile Red can be encapsulated by micelles when $T > LCST_1$, released into H_2O upon UV irradiation, and re-encapsulated when $T > LCST_2$.

2.2 Experimental Section

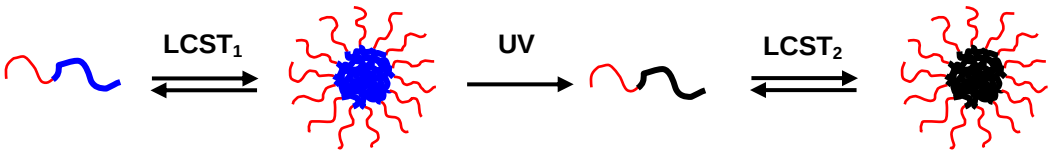
2.2.1 Materials

Tri(ethylene glycol) monoethyl ether (technical grade) and poly(ethylene glycol) monomethyl ether (PEO-OH, MW = 5,000 g/mol) were purchased from Aldrich and used as received. 2-Nitrobenzyl alcohol (98%), triethylamine (99%), acetone (HPLC grade), and Nile Red (99%) were obtained from Acros and used without further purification. Acryloyl chloride (96%, Alfa Aesar) was used as received. Dichloromethane and anisole

Scheme 2.1. Synthesis of Thermo- and Light-Sensitive Poly(ethylene oxide)-*b*-Poly(ethoxytri(ethylene glycol) acrylate-*co*-*o*-nitrobenzyl acrylate) and Cleavage of *o*-Nitrobenzyl Group by UV Irradiation



Scheme 2.2. Multiple Micellization and Dissociation Transitions of Thermo- and Light-Sensitive Poly(ethylene oxide)-*b*-Poly(ethoxytri(ethylene glycol) acrylate-*co*-*o*-nitrobenzyl acrylate) in Water in Response to Temperature Changes and UV Irradiation



(99%, Acros) were distilled from calcium hydride and stored in solvent storage flasks prior to use. Toluene was distilled from sodium and benzophenone and used immediately. *N,N,N′,N′,N″*-pentamethyldiethylenetriamine (PMDETA, Aldrich) and ethyl 2-bromoisobutyrate (EBiB, Aldrich) were distilled over calcium hydride under reduced pressure. CuBr (98%, Aldrich) was stirred in glacial acetic acid overnight, filtered, and washed with absolute ethanol and ethyl ether. The salt was then collected, dried under vacuum, and stored in a desiccator. All other chemicals were purchased from either Aldrich or Fisher and used without purification.

2.2.2 General Characterization

Gel permeation chromatography (GPC) was carried out at room temperature using PL-GPC 20 (an integrated GPC system from Polymer Laboratories, Inc) with a refractive index detector, one PLgel 5 μm guard column (50 × 7.5 mm), and two PLgel 5 μm mixed-C columns (each 300 × 7.5 mm, linear range of molecular weight from 200 to 2,000,000 according to Polymer Laboratories). The data were processed using Cirrus™ GPC/SEC software (Polymer Laboratories). THF was used as the carrier solvent at a flow rate of 1.0 mL/min. Polystyrene standards (Polymer Laboratories) were used for calibration. The ^{1}H (300 MHz) and ^{13}C (75 MHz) spectra were recorded on a Varian Mercury 300 NMR spectrometer and the residual solvent proton signal was used as the internal standard. Mass spectroscopy was performed at the Mass Spectrometry Center of the Department of Chemistry at the University of Tennessee at Knoxville using a PE Sciex QSTAR XL triple quadrupole time-of-flight (QTOF) mass spectrometer (Concord, Ontario, Canada) with an electrospray ionization source. The cloud points of

thermosensitive polymers in water were measured by turbidimetry. The optical transmittances of aqueous polymer solutions at various temperatures were recorded at wavelength of 550 nm with a UV-vis spectrometer (Biomate 5 from Thermospectronic). The sample cell was thermostated with an external water bath of a Fisher Scientific Isotemp refrigerated circulator. At each temperature, the solutions were equilibrated for 5 min.

2.2.3 Preparation of Aqueous Polymer Solutions for Dynamic Light Scattering and Fluorescence Spectroscopy Studies

The polymers were dried under vacuum at 40 ^{o}C for > 3 h. An aqueous solution of a polymer with a desired concentration was prepared either by direct addition of water into the small vial that contained the weighed polymer or by dilution of a polymer solution with a known concentration. The polymer solutions were sonicated in an ultrasonic ice/water bath for 5 min to ensure complete dissolution. The polymer solutions that contained Nile Red for fluorescence spectroscopy studies were made by the following procedure. 10 μL of a stock solution of Nile Red in acetone (concentration: 0.042 mg/mL) was added into an empty vial via a microsyringe, which was then placed in vacuum for > 3 h to remove the solvent. A calculated amount of a stock aqueous polymer solution (1.0 wt %) was added into the vial and a certain amount of deionized water was added to bring the total weight of the solution to 2.00 g. The nominal concentration of Nile Red was 6.6×10^{-7} M. The solution was allowed to equilibrate at a specific temperature for > 3 h before the fluorescence spectroscopy study.

2.2.4 Dynamic Light Scattering

Dynamic light scattering (DLS) measurements were conducted with a Brookhaven Instruments BI-200SM goniometer equipped with a PCI BI-9000AT digital correlator, a temperature controller, and a solid-state laser (model 25-LHP-928-249, λ = 633 nm) at a scattering angle of 90°. The copolymer solutions were filtered into borosilicate glass tubes with an inner diameter of 7.5 mm by the use of Millipore Teflon filters (0.2 μm pore size). The glass tubes were then sealed with a PE stopper. At each temperature, the solutions were equilibrated for 15 min prior to data recording. The second-order correlation function of the scattered light intensity, $g^{(2)}(t)$, was analyzed by the CONTIN method. $g^{(2)}(t)$ can be expressed by the following equation:

$$g^{(2)}(t) = A(1 + \beta|g^{(1)}(t)|^2)$$

where A is the baseline, β is the coherence factor determined by the geometry of the detection, $g^{(1)}(t)$ is the normalized electric field correlation function. Generally, $g^{(1)}(t)$ is expressed by the distribution function $G(\Gamma)$ as

$$|g^{(1)}(t)| = \int G(\Gamma)\exp(-\Gamma t)\, d\Gamma$$

For a translational diffusion mode, Γ can be used to determine the diffusion coefficient D through $\Gamma = Dq^2$, where q is the scattering vector. The hydrodynamic diameter D_h is related to the diffusion coefficient D by the Stokes-Einstein equation:

$$D = k_B T/(3\pi\eta D_h)$$

where k_B is the Boltzmann constant, T is the absolute temperature, and η is the viscosity of the solvent.

2.2.5 Fluorescence Spectroscopy (FS)

Fluorescence emission spectra were recorded from Perkin Elmer LS 55 fluorescence spectrometer equipped with a 20 kW Xenon discharge lamp. The excitation wavelength was 550 nm and the fluorescence emission spectra were recorded from 560 to 720 nm. The slit width was 10 nm. The sample cell was thermostated with an external water bath of a Fisher Scientific Isotemp refrigerated circulator. At each temperature, the sample was equilibrated for 10 min.

(1) Determination of critical micellization temperature (CMT). The fluorescence emission spectra of Nile Red in a 0.2 wt % aqueous polymer solution at various temperatures were recorded. At each temperature, the solution was equilibrated for 10 min. The maximum fluorescence intensities were plotted against temperatures for the determination of CMT.

(2) Determination of critical micelle concentration (CMC). A series of aqueous polymer solutions with different concentrations that were loaded with the same amounts of Nile Red were made. The fluorescence emission spectra of Nile Red in these solutions at a specific temperature were recorded. The maximum fluorescence intensities were then plotted against the logarithm of polymer concentrations for the determination of CMC.

(3) Reloading of Nile Red into the polymer solution after UV irradiation for 480 min and the determination of CMT. 10 μL of a stock solution of Nile Red in acetone

(concentration: 0.042 mg/mL) was added into an empty vial via a microsyringe, which was then placed in high vacuum for > 3 h to remove the solvent. The 0.2 wt % aqueous solution of PEO-*b*-P(TEGEA-*co*-NBA) (M_n = 18,300 g/mol, PDI = 1.07, n_{EO}:n_{TEGEA}:n_{NBA} = 113:70:9) that was irradiated with 365 nm UV light for 480 min was transferred into the vial. The solution was allowed to equilibrate at 32 ^oC for > 3 h. The fluorescence emission spectra were then recorded at various temperatures for the determination of CMT.

2.2.6 Synthesis of Ethoxytri(ethylene glycol) Acrylate (TEGEA)

A solution of tri(ethylene glycol) monoethyl ether (40.8 g, 0.229 mol) and triethylamine (21.6 g, 0.214 mol) in dichloromethane (50 mL) was stirred under nitrogen atmosphere in a 250 mL three-necked flask in an ice/water bath. A solution of acryloyl chloride (16.1 g, 0.178 mol) in dichloromethane (20 mL) was added dropwise into the flask from an addition funnel. The reaction mixture was warmed to room temperature and stirred overnight. The precipitate was filtered off, and the filtrate was washed sequentially with an aqueous solution of sodium bicarbonate (50 mL), water (50 mL), and a saturated aqueous solution of NaCl. The organic layer was separated and dried over anhydrous sodium sulfate. The crude product was purified by silica gel column chromatography with ethyl acetate as eluent. The product was further purified by vacuum distillation (90 ^oC/30 mTorr) with addition of a small amount of hydroquinone as inhibitor. The monomer was then dissolved in dichloromethane (150 mL) and washed with 0.1 M aqueous solution of NaOH until the aqueous layer became colorless. The organic layer was subsequently washed with water to neutral and dried over anhydrous sodium sulfate.

The product was obtained as a colorless liquid (25.5 g, yield: 62 %). ^{1}H NMR ($CDCl_3$): δ (ppm) 6.37 (dd, 1H, C*H*H=CH-), 6.10 (dd, CHH=C*H*-), 5.78 (dd, CH*H*=CH-), 4.25 (t, 2H, -COOC*H*$_2$-), 3.70-3.50 (m, 10H, -C*H*$_2$O-), 3.46 (q, 2H, -OC*H*$_2$CH$_3$), 1.14 (t, 3H, -OCH$_2$C*H*$_3$); ^{13}C NMR ($CDCl_3$): δ (ppm) 166.04 (-*C*OOCH$_2$-), 130.93 (*C*H$_2$=CH-), 128.14 (CH$_2$=*C*H-), 70.58, 70.49, 70.46, 69.69, 68.97 (-*C*H$_2$O-), 66.51 (-O*C*H$_2$CH$_3$), 63.58 (-COO*C*H$_2$-), 15.05 (-OCH$_2$*C*H$_3$). MS (ES): 255.0 ([M + Na$^+$]).

2.2.7 Synthesis of *o*-Nitrobenzyl Acrylate (NBA)

2-Nitrobenzyl alcohol (2.56 g, 16.7 mmol) and triethylamine (2.59 g, 25.6 mmol) were dissolved in dichloromethane (30 mL) in a 100 mL flask, which was then placed in an ice/water bath. A solution of acryloyl chloride (2.02 g, 22.3 mmol) in CH_2Cl_2 (10 mL) was added dropwise into the flask under N_2 from an addition funnel over a period of 10 min. After 24 h, the reaction mixture was poured into a separatory funnel and sequentially washed with an aqueous solution of $NaHCO_3$ (30 mL), H_2O (30 mL), and a saturated aqueous solution of NaCl (40 mL). The organic layer was separated and dried over anhydrous Na_2SO_4 overnight. The solvent was removed by a rotavapor and the crude product was purified by silica gel column chromatography with ethyl acetate and hexanes (v/v, 1 : 4) as eluent. The pure product was obtained as a light yellow liquid (3.16 g, yield: 92 %). ^{1}H NMR ($CDCl_3$): δ (ppm) 8.09 (d, 1H, aromatic), 7.66-7.44 (m, 3H, aromatic), 6.47 (dd, 1H, C*H*H=CH-), 6.19 (dd, 1H, CHH=C*H*-), 5.90 (dd, 1H, CH*H*=CH-), 5.58 (s, 2H, -C*H*$_2$O-); ^{13}C NMR ($CDCl_3$): δ (ppm) 165.38 (-*C*OO-), 147.07, 133.73, 132.09, 128.81, 127.70, 125.01 (aromatic), 131.84 (CH$_2$=*C*H-), 128.72 (*C*H$_2$=CH-), 62.88 (-COO*C*H$_2$-); MS (ES): 229.9 ([M + Na$^+$]).

2.2.8 Synthesis of PEO Macroinitiator PEO-Br

Poly(ethylene glycol) monomethyl ether (PEO-OH, MW = 5,000 g/mol, 13.0 g, 2.60 mmol) was added into a 500 mL three-necked flask. The trace amount of water was removed by azeotropic distillation with toluene (40 mL) under reduced pressure. The polymer was then dissolved in toluene (250 mL), followed by addition of triethylamine (1.05 g, 10.4 mmol). The flask was placed in an ice/water bath. 2-Bromoisobutyryl bromide (1.45 g, 6.31 mmol) was added dropwise into the flask through an addition funnel. After being stirred at room temperature for 24 h, the solution was treated with charcoal, which was subsequently removed by filtration. The solvent was removed by the use of a rotavapor and the concentrated solution was precipitated in diethyl ether (100 mL). The crude product was dried under vacuum, re-dissolved in water, and then extracted with dichloromethane. The organic extracts were combined and dried over anhydrous sodium sulfate. The pure product was obtained after the solvent was removed in vacuum. ^{1}H NMR ($CDCl_3$): δ (ppm) 4.28 (t, 2H, -CH_2CH_2OC=O-), 3.90-3.36 (m, -CH_2O-), 3.34 (s, 3H, -OCH_3), 1.90 (s, 6H, -CBr(CH_3)$_2$).

2.2.9 Synthesis of PTEGEA by ATRP

A typical procedure for the synthesis of PTEGEA by ATRP using ethyl 2-bromoisobutyrate (EBiB) as initiator is described below. CuBr (6.3 mg, 0.044 mmol), TEGEA (2.50 g, 10.8 mmol), anisole (1.27 g), PMDETA (6.8 mg, 0.039 mmol), and EBiB (9.3 mg, 0.048 mmol) were added into a two-necked flask. The mixture was stirred under N_2 atmosphere and degassed by three freeze-pump-thaw cycles. A sample was taken for ^{1}H NMR spectroscopy analysis and the flask was immediately placed in a 90 ^{o}C

oil bath. After the polymerization proceeded for 210 min, a sample was taken for ^{1}H NMR spectroscopy analysis of monomer conversion. The reaction mixture was opened to air, diluted with THF, and passed through a neutral Al_2O_3 column with THF as eluent to remove the catalyst. The obtained polymer solution was concentrated and precipitated in hexanes (100 mL). The polymer was then dissolved in THF (3 mL) and precipitated again in hexanes. A colorless polymer was obtained. GPC analysis results (polystyrene standards): $M_{n,GPC}$ = 14,500 g/mol, polydispersity index (PDI) = 1.16. The degree of polymerization (DP) of the polymer was calculated from the monomer conversion and the monomer to initiator ratio. The integral values of the peak located at 4.25 ppm (from -C*H*$_2$OOC- of monomer) and the peak at 4.15 ppm (from -C*H*$_2$OOC- of polymer) were used for the calculation of monomer conversion. The calculated DP was 74.

2.2.10 Synthesis of Random Copolymer of TEGEA and NBA by ATRP

A typical procedure for the synthesis of P(TEGEA-*co*-NBA) by ATRP using EBiB as initiator is described below. CuBr (7.5 mg, 0.052 mmol), TEGEA (2.06 g, 8.88 mmol), NBA (0.182 g, 0.88 mmol), EBiB (8.9 mg, 0.046 mmol), anisole (0.91 g), and PMDETA (8.3 mg, 0.048 mmol) were added into a 25 mL two-necked flask. The mixture was stirred under N_2 atmosphere and degassed by three freeze-pump-thaw cycles. A sample was taken for ^{1}H NMR spectroscopy analysis and the flask was immediately placed in a 90 ^{o}C oil bath. After the polymerization proceeded for 305 min, a sample was taken for analysis of monomer conversion and the reaction mixture was then diluted with THF. The catalyst was removed by passing the reaction mixture through a neutral Al_2O_3 column with THF as eluent. The obtained polymer solution was concentrated and

precipitated in a mixture of hexanes and diethyl ether (v/v = 80 : 20, 100 mL). The polymer was then dissolved in THF (3 mL) and precipitated again in the mixture of hexanes and diethyl ether (v/v = 80 : 20, 100 mL). A nearly colorless polymer was obtained. GPC analysis results (polystyrene standards): $M_{n,GPC}$ = 13,900 g/mol, polydispersity index (PDI) = 1.13. The DP of the polymer was determined from the monomer conversion and the monomer-to-initiator ratio. The peaks located in the range of 4.0 – 4.6 ppm, which were from -C*H*$_2$OOC- of monomer TEGEA and the TEGEA units in the polymer, were used as internal standard. The conversion was calculated from the integral values of the peaks from 6.0 to 5.7 ppm (CH*H*=CH- from both NBA and TEGEA monomers) at t = 0 min and 305 min. The DP was 75. The molar ratio of TEGEA and NBA units in the copolymer was calculated from the integral values of the peaks at 4.15 (-C*H*$_2$OC=O- of the TEGEA unit in the copolymer) and 5.44 ppm (-C*H*$_2$OC=O- of the NBA unit in the copolymer). The obtained value was 100 : 13.

2.2.11 Synthesis of Diblock Copolymer PEO-*b*-PTEGEA by ATRP from Macroinitiator PEO-Br

A typical procedure for the synthesis of PEO-*b*-PTEGEA by ATRP using macroinitiator PEO-Br is described below. CuBr (11.1 mg, 0.077 mmol), TEGEA (2.06 g, 8.88 mmol), PEO-Br (0.28 g, 0.054 mmol), anisole (0.90 g), and PMDETA (9.8 mg, 0.057 mmol) were added into a two-necked flask. The mixture was stirred under nitrogen atmosphere and degassed by three freeze-pump-thaw cycles. The flask was then placed in a 90 ^{o}C oil bath. The polymerization was stopped after 193 min. The reaction mixture was diluted with THF and passed through a neutral Al_2O_3 column with THF as eluent to

remove the catalyst. The obtained polymer solution was concentrated and precipitated in hexanes (100 mL). The solvent was discarded, and THF (3 mL) was added to dissolve the polymer. The polymer was precipitated again in hexanes (100 mL). A colorless polymer was obtained. GPC analysis results (polystyrene standards): $M_{n,GPC}$ = 21,400 g/mol, PDI = 1.07. The DP of PTEGEA in the diblock copolymer was calculated from the NMR spectrum using the integral values of the peak from 4.0 to 4.5 ppm (-C*H*$_2$OOC- of TEGEA unit) and the peaks from 3.2 to 3.9 ppm (-OC*H*$_2$- from PEO and PTEGEA). The DP of PEO was 113. The calculated DP of PTEGEA was 92.

2.2.12 Synthesis of Block Copolymer PEO-*b*-P(TEGEA-*co*-NBA) by ATRP Using Macroinitiator PEO-Br as Initiator

A typical procedure for the synthesis of PEO-*b*-P(TEGEA-*co*-NBA) is described below. CuBr (7.1 mg, 0.049 mmol), TEGEA (2.14 g, 9.22 mmol), PEO-Br (0.23 g, 0.045 mmol), NBA (0.186 g, 0.90 mmol), anisole (1.17 g), and PMDETA (9.9 mg, 0.057 mmol) were added into a 25 mL two-necked flask. After the mixture was degassed by three freeze-pump-thaw cycles, the flask was placed in a 90 ^{o}C oil bath. The polymerization was allowed to proceed for 172 min. The mixture was diluted with THF and passed through a neutral Al_2O_3 column with THF as eluent to remove the catalyst. The obtained polymer solution was concentrated and precipitated in a mixture of hexanes and diethyl ether (v/v = 60 : 40). The polymer was re-dissolved in THF and precipitated again in the mixture of hexanes and diethyl ether (v/v = 60 : 40). This purification process was repeated one more time. The polymer was then dried in high vacuum and obtained as a partially solidified liquid. GPC analysis results (polystyrene standards): $M_{n,GPC}$ = 18,300

g/mol, PDI = 1.07. The composition of the block copolymer was determined from the NMR spectrum. The number of TEGEA units in the block copolymer was calculated using the integral values of the peak from 4.0 to 4.5 ppm (-C*H*$_2$OCO- of TEGEA unit) and the peaks from 3.2 to 4.0 ppm (-OC*H*$_2$- from the PEO block and TEGEA unit). The obtained number of TEGEA units was 70. The number of NBA units was calculated from the integral values of the peak from 5.2 to 5.7 ppm (-C*H*$_2$OOC- of NBA unit) and the peaks from 3.2 to 4.0 ppm (-OC*H*$_2$- in the PEO block and TEGEA unit). The obtained number of NBA units was 9.

2.2.13 Photo-Cleavage of *o*-Nitrobenzyl Group

The long wavelength (365 nm) UV light from a Spectroline ENF-240C hand-held UV lamp equipped with one 4-watt long wavelength tube filtered at 365 nm and one short wavelength tube filtered at 254 nm was used for photocleavage of *o*-nitrobenzyl group. The typical intensity of the 365 nm UV light from this lamp is 300 μw/cm^2 at a distance of 15 cm. The vials or cuvettes or glass tubes that contained polymer solutions were placed in a water bath with a preset temperature, and were irradiated with 365 nm UV light at a distance of ~ 2 cm. UV-visible spectrometry was used to monitor the photocleavage reaction by recording the UV-vis spectra at various irradiation times at a specific temperature.

2.3 Results and Discussion

By introducing a short oligo(ethylene glycol) group onto the polymer backbone as a pendant from each repeat unit, a class of new thermosensitive water-soluble polymers, including poly(vinyl ether)s,[37-40] polymethacrylates,[60-64] polystyrenics,[44,65-67]

polyacrylates,[44,66] and dendritic polymers,[68] have been developed recently. The cloud point can be easily tuned by varying the type of polymer backbone, the length and end group of oligo(ethylene glycol) pendant as well as the chain end group.[37-40,60-68] This chapter presents the synthesis of thermo- and light-responsive block copolymers, PEO-*b*-P(TEGEA-*co*-NBA), and the study of their micellization/dissociation behavior in water in response to temperature changes and UV irradiation. At first, a homopolymer of TEGEA and a random copolymer of TEGEA and NBA (P(TEGEA-*co*-NBA)) were synthesized by ATRP. Their thermosensitive properties were studied and the effect of photocleavage of *o*-nitrobenzyl group on the cloud point of the random copolymer in water was investigated. For comparison with PEO-*b*-P(TEGEA-*co*-NBA), a thermosensitive diblock copolymer PEO-*b*-PTEGEA was prepared and its temperature-induced micellization/dissociation transitions in water were studied.

2.3.1 Synthesis of Monomers and Polymers

TEGEA and NBA were synthesized by the reactions of acryloyl chloride with tri(ethylene glycol) monoethyl ether and *o*-nitrobenzyl alcohol, respectively, in the presence of triethylamine. The two monomers were thoroughly purified by vacuum distillation and/or silica gel column chromatography. Their molecular structures were confirmed by ^{1}H NMR, ^{13}C NMR, and mass spectroscopy analysis. The macroinitiator, PEO with one end functionalized with an ATRP initiator (PEO-Br), was prepared according to a literature procedure.[69] Prior to the reaction of poly(ethylene glycol) monomethyl ether (PEO-OH) with excess 2-bromoisobutyryl bromide, the trace amount of water in PEO-OH was removed by azeotropic distillation with dry toluene. The

macroinitiator was purified by precipitation in diethyl ether, dissolution in water and extraction with methylene chloride. After drying in high vacuum, it was used for the synthesis of block copolymers.

A homopolymer of TEGEA with $M_{n,GPC}$ of 14,500 g/mol and PDI of 1.16 was prepared by ATRP of TEGEA in anisole at 90 ^{o}C using ethyl 2-bromoisobutyrate (EBiB) as initiator and CuBr/*N*,*N*,*N*′,*N*′,*N*″-pentamethyldiethylenetriamine (PMDETA) as catalyst. The DP, calculated from the monomer conversion and the monomer-to-initiator ratio, was 74. Similarly, a random copolymer of TEGEA and NBA, P(TEGEA-*co*-NBA), with $M_{n,GPC}$ of 13,900 g/mol and PDI of 1.13 was prepared by ATRP of a mixture of TEGEA and NBA with a molar ratio of 100 : 10. The composition of the random copolymer was determined from its ^{1}H NMR spectrum using the peaks located at 5.44 ppm (–C*H*$_2$– of the benzyl group in NBA unit) and 4.15 ppm (–C*H*$_2$OOC– of TEGEA unit). The molar ratio of TEGEA and NBA was 100 : 13, close to the feed composition. Block copolymers, PEO-*b*-PTEGEA and PEO-*b*-P(TEGEA-*co*-NBA), were synthesized from macroinitiator PEO-Br by ATRP of either pure TEGEA or a mixture of TEGEA and NBA with a molar ratio of 100 : 10 at 90 ^{o}C using CuBr/PMDETA as catalyst. The polymers were purified by repetitive precipitation in hexanes (for PEO-*b*-PTEGEA) or in a mixture of hexanes and diethyl ether (v/v, 60 : 40, for PEO-*b*-P(TEGEA-*co*-NBA)). Figure 2.1 shows the GPC curves of macroinitiator PEO-Br and one sample of PEO-*b*-P(TEGEA-*co*-NBA). The peak completely shifted to the high molecular weight side and remained narrow, indicating that the block copolymerization was a well controlled process. The DP of TEGEA units in the PEO-*b*-PTEGEA and the numbers of TEGEA and NBA units in the two samples of PEO-*b*-P(TEGEA-*co*-NBA) were determined from

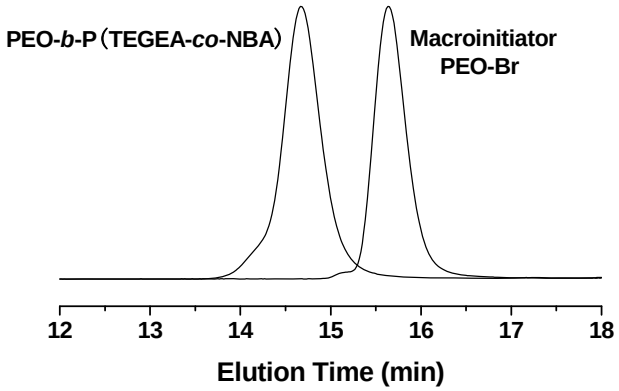


Figure 2.1. Gel permeation chromatography curves of macroinitiator PEO-Br and PEO-*b*-P(TEGEA-*co*-NBA) (BR-**4** in Table 2.1, $M_{n,GPC}$ = 18,300 g/mol, PDI = 1.07).

^{1}H NMR spectra. The molar ratio of TEGEA to NBA units in PEO-*b*-P(TEGEA-*co*-NBA)s was 100 : 13, essentially identical to the composition of P(TEGEA-*co*-NBA). The characterization data for the polymers used in the present work are summarized in Table 2.1. The PDIs of all these polymers, determined by GPC using polystyrene calibration, were ≤ 1.16.

2.3.2 Thermosensitive Properties of PTEGEA and P(TEGEA-*co*-NBA)

The cloud points of PTEGEA (H-**1**) and P(TEGEA-*co*-NBA) (R-**2**) in water were determined by turbidimetry. Figure 2.2 shows the optical transmittances of 0.2 wt % aqueous solutions of H-**1** and R-**2** at wavelength of 550 nm as a function of temperature in both heating and cooling processes. For PTEGEA, the solution turned cloudy at ~ 35 ^{o}C during the course of increasing temperature. The transparent-to-cloudy transition was relatively sharp and the transition zone was ~ 4 ^{o}C. If 50 % of the transmittance change is used for the determination of cloud point (CP), the CP of H-**1** in water is 36 ^{o}C. The CP of P(TEGEA-*co*-NBA) in a 0.2 wt % aqueous solution was 18.5 ^{o}C; therefore, the incorporation of 13 mol % of hydrophobic monomer NBA with respect to TEGEA into the polymer chain decreased the CP by 17.5 ^{o}C. From Figure 2.2, one can also find that there was essentially no hysteresis for H-**1** and R-**2** between heating and cooling. The thermo-induced LCST transitions of both polymers were reversible. Note that Lutz et al. also observed that there was no hysteresis between heating and cooling in the LCST transitions of copolymers of 2-(2-methoxyethoxy)ethyl methacrylate and oligo(ethylene glycol) methacrylate in water.[63,64]

Table 2.1. Characterization Data for PTEGEA, P(TEGEA-*co*-NBA), PEO-*b*-PTEGEA, and Two Samples of PEO-*b*-P(TEGEA-*co*-NBA) Used in this Work

No.	Polymer	$M_{n,GPC}$ (g/mol)[a]	PDI[b]	n_{EO} : n_{TEGEA} : n_{NBA}[c]
H-**1**	PTEGEA	14,500	1.16	0 : 74[d] : 0
R-**2**	P(TEGEA-*co*-NBA)	13,900	1.13	0 : 66 : 9[d,e]
B-**3**	PEO-*b*-PTEGEA	21,400	1.07	113 : 92 : 0
BR-**4**	PEO-*b*-P(TEGEA-*co*-NBA)	18,300	1.07	113 : 70 : 9
BR-**5**	PEO-*b*-P(TEGEA-*co*-NBA)	24,700	1.11	113 : 109 : 14

[a,b]The number average molecular weight ($M_{n,GPC}$) and polydispersity index (PDI) were determined by gel permeation chromatography using polystyrene calibration. [c]n_{EO}, n_{TEGEA}, and n_{NBA} are the numbers of EO (in the PEO block), TEGEA, and NBA units in the polymers, respectively. The values of n_{TEGEA} and n_{NBA} in the block copolymers were determined from ^{1}H NMR spectra. [d]The degrees of polymerization (DPs) of PTEGEA and P(TEGEA-*co*-NBA) were calculated from the monomer conversion and the monomer-to-initiator ratio. [e]The DP of P(TEGEA-*co*-NBA) was 75. The molar ratio of TEGEA and NBA in the random copolymer was determined from ^{1}H NMR spectrum.

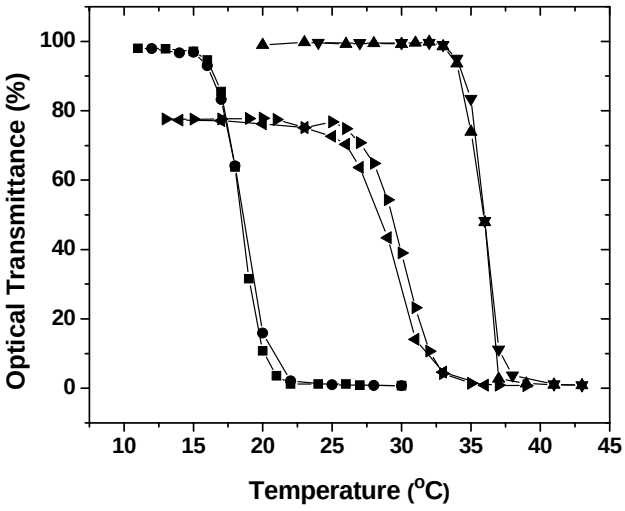


Figure 2.2. Optical transmittances at wavelength of 550 nm of an aqueous solution of PTEGEA (H-**1**, $M_{n,GPC}$ = 14,500 g/mol, PDI = 1.16, 0.2 wt %, heating ▲, cooling ▼) and an aqueous solution of P(TEGEA-*co*-NBA) (R-**2**, $M_{n,GPC}$ = 13,900 g/mol, PDI = 1.13, 0.2 wt %) before (heating ■, cooling ●) and after irradiation with 365 nm UV light at 13 °C for 485 min (heating ►, cooling ◄) as a function of temperature. The transmittances were recorded with a UV-vis spectrometer.

2.3.3 Photocleavage of *o*-Nitrobenzyl Group of NBA in P(TEGEA-*co*-NBA) and the Cloud Point of the Obtained Polymer in Water

o-Nitrobenzyl has been widely used as a protective group;[32,70-73] it can be removed by long wavelength UV irradiation. To study the photocleavage of *o*-nitrobenzyl group in the random copolymer, a 0.2 wt % aqueous solution of R-**2** was irradiated with 365 nm UV light from a Spectroline ENF-240C hand-held UV lamp at 13 ^{o}C, which was below the CP of R-**2**. Initially, the solution was colorless. With the increase of irradiation time, the solution gradually turned slightly yellow. To determine the time that was needed to achieve the maximum degree of cleavage of *o*-nitrobenzyl groups, UV-vis spectrometry was used to monitor the photolysis reaction.[74] The absorbances in the wavelength range of 330 to 550 nm increased rapidly in the first 180 min and then leveled off with further increasing the irradiation time. To confirm that the *o*-nitrobenzyl group was cleaved, ^{1}H NMR spectroscopy was employed. Figure 2.3 shows the ^{1}H NMR spectra of R-**2** and the polymer obtained from the 0.2 wt % aqueous solution of R-**2** after UV irradiation for 485 min. Clearly, the aromatic peaks and the peak located at 5.44 ppm, which were from the NBA unit, disappeared. By comparing the two ^{1}H NMR spectra, one can also find that the peaks from the TEGEA units did not undergo any changes, indicating that the TEGEA units were stable under UV irradiation.

Figure 2.2 shows the optical transmittance of a 0.2 wt % aqueous solution of R-**2** after UV irradiation for 485 min (i.e., the aqueous solution of P(TEGEA-*co*-acrylic acid) (P(TEGEA-*co*-AA))) as a function of temperature in both heating and cooling processes. The slightly lower transmittances (~78 %) of the polymer solution below the LCST

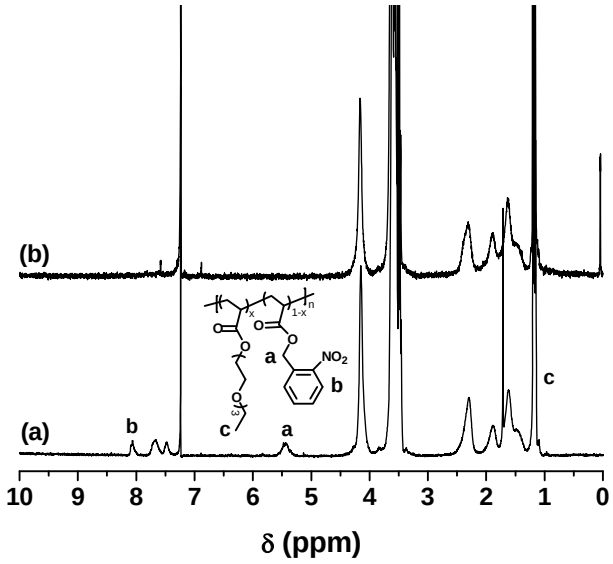


Figure 2.3. ^{1}H NMR spectra of (a) P(TEGEA-*co*-NBA) (R-**2**, $M_{n,GPC}$ = 13,900 g/mol, PDI = 1.13) and (b) the polymer obtained from the 0.2 wt % aqueous solution of R-**2** after irradiation with 365 nm UV light at 13 ^{o}C for 485 min. $CDCl_3$ was used as the solvent.

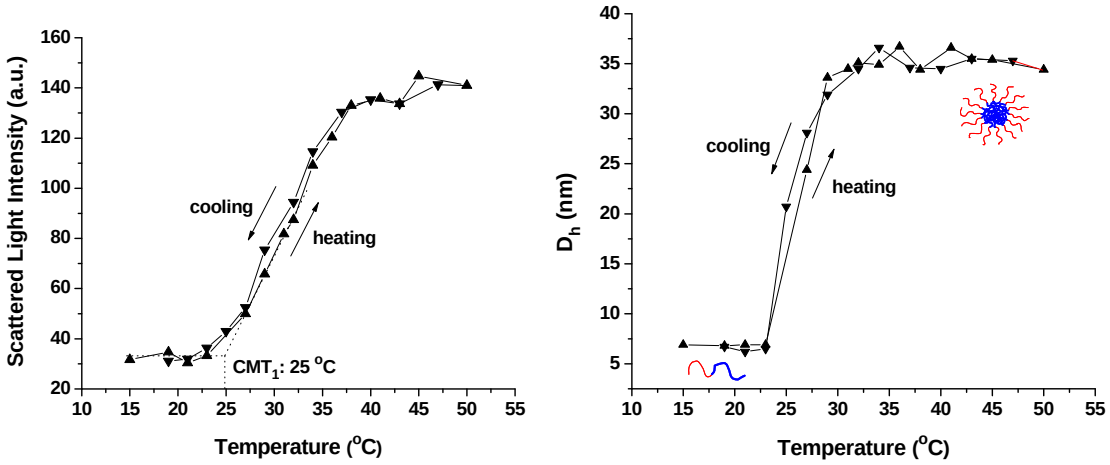
transition were due to the absorbance of the colored product formed from the photocleavage reaction. The CP, determined from the heating curve at 50 % of the transmittance change, was 30 ^{o}C, which was only 11.5 ^{o}C higher than that of P(TEGEA-*co*-NBA). Since the AA units in P(TEGEA-*co*-AA) are hydrophilic, a CP higher than that of PTEGEA (36 ^{o}C) was expected.[75] However, the observed CP of P(TEGEA-*co*-AA) was 6 ^{o}C lower. It was found that the pH of a 0.2 wt % copolymer solution after UV irradiation was ~ 4.2 (note that deionized water was used to prepare the polymer solution). It is known that pH can affect the cloud point of an acid-containing thermosensitive polymer in water.[75,76] Calculations show that only a few percent of AA units in the P(TEGEA-*co*-AA) are needed to be ionized to produce a pH of ~ 4.2. The remaining unionized AA units are likely to form hydrogen bonds with neighboring TEGEA units, which would depress the CP. Another possible reason is the presence of an organic compound, *o*-nitrosobenzaldehyde, generated from the photo-cleavage reaction in the solution. Organic additives are known to affect the cloud points of thermosensitive polymers in water.[52]

2.3.4 Reversible Micellization of Block Copolymers in Water in Response to Temperature Changes

Two samples of PEO-*b*-P(TEGEA-*co*-NBA) with different molecular weights but essentially the same compositions for the thermosensitive blocks (BR-**4** and BR-**5**) were used for demonstration of thermo- and light-induced multiple micellization and dissociation transitions in water. Their reversible micellizations in response to temperature changes were studied by dynamic light scattering (DLS) and fluorescence

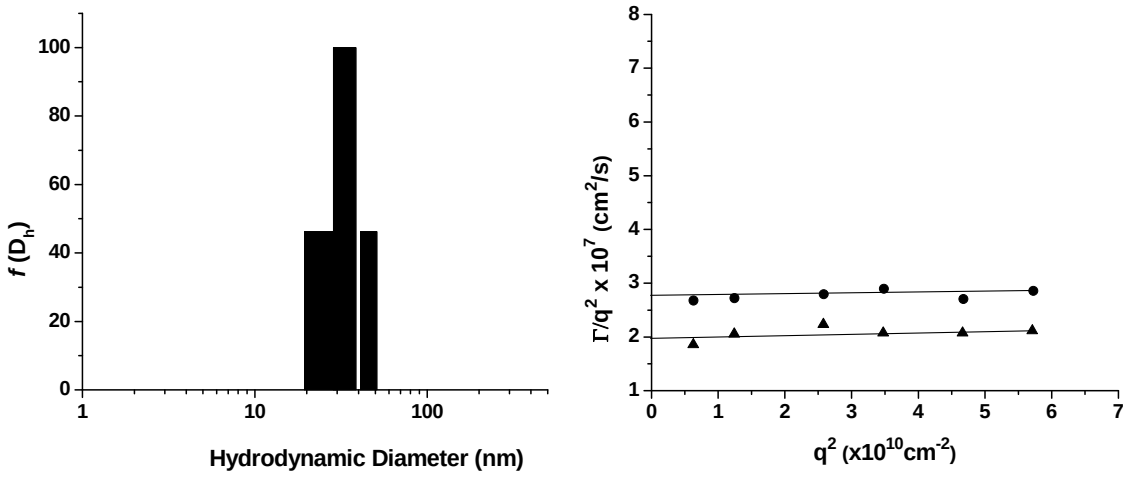
spectroscopy (FS). For comparison, PEO-*b*-PTEGEA (B-**3**) was also investigated. Figure 2.4 shows the intensity of scattered light at scattering angle of 90° and the hydrodynamic size as a function of temperature for a 0.2 wt % aqueous solution of BR-**4**. When the temperature was ≤ 23 °C, the intensity of scattered light was very low and the hydrodynamic size was < 7 nm, indicating that the block copolymer was molecularly dissolved in water. With the increase of temperature, the scattered light intensity gradually increased, and two size distributions, one attributed to the unimers and one to the micelles, were observed at 27 °C with an average hydrodynamic size of 24.4 nm, suggesting that the thermosensitive block was undergoing a hydration-to-dehydration transition.[74] The critical micellization temperature (CMT_1), determined from the plot of the intensity of scattered light versus temperature (Figure 2.4a), was 25 °C, which was 6.5 °C higher than the CP of P(TEGEA-*co*-NBA) with the same composition. It is known that the LCST transition temperature is slightly higher when a thermosensitive polymer is attached to a hydrophilic block.[1-3]

When the temperature reached 29 °C, only micelles were observed. With further increasing the temperature, the average size of micelles remained at ~ 35 nm, but the intensity of scattered light continued to increase. A similar phenomenon was observed by Zhou and Chu in the study of thermo-induced micellization of poloxamer 188 (PEO-*b*-PPO-*b*-PEO) in water, and was considered to result from the decreased micellar hydration and the increased aggregation number at higher temperatures.[77] The polydispersity of micelles at 50 °C was 0.048, indicating that the micelles were uniform in size (Figure 2.5a). Moreover, it was found that the value of Γ/q^2 was nearly



(a) (b)

Figure 2.4. Intensity of scattered light at a scattering angle of 90° (a) and the hydrodynamic diameter (b) as a function of temperature (▲ heating, ▼ cooling) in a dynamic light scattering study of a 0.2 wt % aqueous solution of PEO-*b*-P(TEGEA-*co*-NBA) (BR-**4**, $M_{n,GPC}$ = 18,300 g/mol, PDI = 1.07).[74]



(a) (b)

Figure 2.5. (a) Hydrodynamic diameter (D_h) distribution of micelles of PEO-*b*-P(TEGEA-*co*-NBA) (BR-**4**, $M_{n,GPC}$ = 18,300 g/mol, PDI = 1.07) at 50 ^oC and (b) plot of Γ/q^2 of micelles of BR-**4** (●) and the corresponding PEO-*b*-P(TEGEA-*co*-AA) (▲) vs. q^2 at 50 ^oC. The polydispersity of micelles of BR-**4** at 50 ^oC was 0.048. PEO-*b*-P(TEGEA-*co*-AA) was obtained by UV irradiation of a 0.2 wt % aqueous solution of BR-**4** at 32 ^oC for 480 min.

independent of scattering angle (Figure 2.5b), suggesting that the micelles were spherical.[5] This thermo-induced micellization was reversible. Decreasing the temperature caused the micelles to dissociate into the unimers (Figure 2.4).

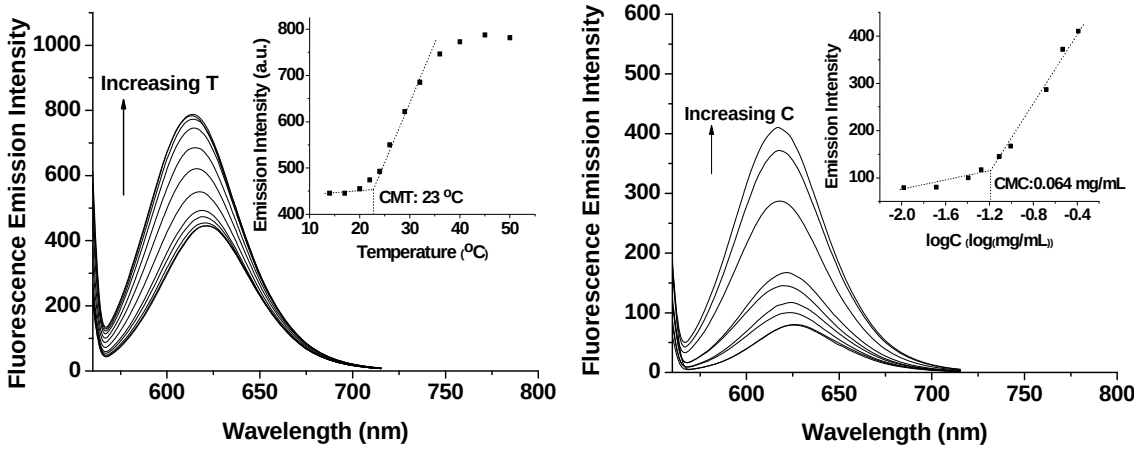
The thermo-induced reversible micellization behaviors of BR-**5** and B-**3** were also investigated by DLS[74] and the results are summarized in Table 2.2. The CMT_1 of BR-**5** at the same concentration (0.2 wt %) was 21 ^oC, 4 ^oC lower than that of BR-**4**, which is reasonable because the molecular weight of the thermosensitive block in BR-**5** is higher than that in BR-**4**. For B-**3**, the CMT was found at 39 ^oC, which was 3 ^oC higher than the CP of PTEGEA. For all three block copolymers, the micelles had similar hydrodynamic sizes (~ 35 nm), narrow polydispersities, and spherical shapes (as suggested by the independence of Γ/q^2 on scattering angle).

The thermo-induced reversible formation and dissociation of micelles of BR-**4**, BR-**5,** and B-**3** in water were further studied by FS. Nile Red was used as the hydrophobic fluorescence probe because its fluorescence is negligible in water but is known to increase substantially in a hydrophobic environment such as the core of micelles.[7,8,32] Furthermore, its absorption λ_{max} is at 553 nm, far from the interfering absorptions of the block copolymers. Figure 2.6 shows the fluorescence emission spectra of Nile Red in a 0.2 wt % aqueous solution of BR-**4** at various temperatures in the heating process. The noticeable fluorescence intensity at lower temperatures (< 18 ^oC) might be due to the enhanced solubilization of Nile Red by the polymer in water. A similar observation was reported by Jiang et al.[32] When the temperature was increased to above 20 ^oC, the fluorescence emission intensity increased significantly, indicating that the molecularly

Table 2.2. Critical Micellization Temperatures, Critical Micelle Concentrations, and Micelle Characteristics of Three Block Copolymers

No.	$CMT_{1\text{-}DLS}$[a]	Micelle size[b]	PD[c]	$CMT_{1\text{-}FS}$[d]	CMC (mg/mL)[e]
B-**3**	39 ^{o}C	35.4 nm (50 ^{o}C)	0.044 (50 ^{o}C)	39 ^{o}C	0.33 (45 ^{o}C)
BR-**4**	25 ^{o}C	34.4 nm (50 ^{o}C)	0.048 (50 ^{o}C)	23 ^{o}C	0.064 (32 ^{o}C)
BR-**5**	21 ^{o}C	33.9 nm (30 ^{o}C)	0.030 (30 ^{o}C)	20 ^{o}C	0.025 (30 ^{o}C)

[a]The critical micellization temperature ($CMT_{1\text{-}DLS}$) was determined by dynamic light scattering study of a 0.2 wt % aqueous polymer solution. [b]The average size of micelles at a specific temperature was obtained by the use of the CONTIN method. [c]The polydispersity (PD) of micelles at a specific temperature. [d]The $CMT_{1\text{-}FS}$ determined by fluorescence spectroscopy (FS) analysis of a 0.2 wt % aqueous polymer solution. [e]Critical micelle concentration (CMC) at a specific temperature determined by FS.



(a) (b)

Figure 2.6. Fluorescence spectra of Nile Red (a) in a 0.2 wt % aqueous solution of PEO-*b*-P(TEGEA-*co*-NBA) (BR-**4**, $M_{n,GPC}$ = 18,300 g/mol, PDI = 1.07) at various temperatures during the heating process and (b) in a series of aqueous solutions of BR-**4** with different concentrations at 32 ^{o}C. The inset in (a) is the plot of maximum fluorescence intensity versus temperature, from which the critical micellization temperature (CMT_1) was determined. The inset in (b) is the plot of maximum fluorescence intensity versus polymer concentration at 32 ^{o}C, from which the critical micelle concentration (CMC) was determined.

dissolved polymer chains began to associate into micelles and the dye molecules were sequestered into the core. The maximum peak underwent a blue shift with the increase of temperature, from 621 nm at 14 ^{o}C to 615 nm at 50 ^{o}C, which further supported that the dye molecules moved from a hydrophilic to a hydrophobic environment.[7,8,32] The CMT_1, determined from the plot of maximum fluorescence intensity versus temperature, was 23 ^{o}C, close to that obtained from DLS study (25 ^{o}C). When the temperature decreased to 16 ^{o}C, the fluorescence emission intensity gradually decreased,[74] implying that the micelles dissociated into the unimers and the dye was released into water. Thus, consistent with DLS study, the thermo-induced micellization was reversible.

Since the micelles of BR-**4** were well developed at 32 ^{o}C from both DLS and FS studies, the critical micelle concentration (CMC) of this block copolymer was determined at this temperature. A series of aqueous solutions of BR-**4** with different concentrations that were loaded with the same amounts of Nile Red were made. After equilibration for > 3 h, the fluorescence emission spectra were recorded at 32 ^{o}C and are shown in Figure 5b. From the plot of maximum emission intensity versus the logarithm of copolymer concentration, the CMC of this polymer at 32 ^{o}C was determined to be 0.064 mg/mL. With the increase of polymer concentration above the CMC, the maximum peak also underwent a blueshift from 625.5 nm at concentration of 0.0104 mg/mL to 617 nm at concentration of 0.407 mg/mL, consistent with the formation of micelles.

Similarly, the temperature-induced reversible micellization of BR-**5** and B-**3** at concentration of 0.2 wt % were studied by FS,[74] and the CMTs were found to be 20 and 39 ^{o}C, respectively (Table 2.2). While the CMT of B-**3** determined from FS was identical

to that from DLS, the values of CMT_1 for BR-**4** and -**5** were slightly lower than those obtained by DLS. The CMC was 0.33 mg/mL for B-**3** at 45 ^oC and 0.025 mg/mL for BR-**5** at 30 ^oC (Table 2.2). The CMC of B-**3** at 45 ^oC was much higher than those of BR-**4** and BR-**5**, which can be attributed to that the thermosensitive random copolymer block P(TEGEA-*co*-NBA) is more hydrophobic than PTEGEA making the association of copolymer molecules occur at a lower concentration. The slightly lower CMC of BR-**5** compared with that of BR-**4** is likely due to the longer thermosensitive block in BR-**5**.

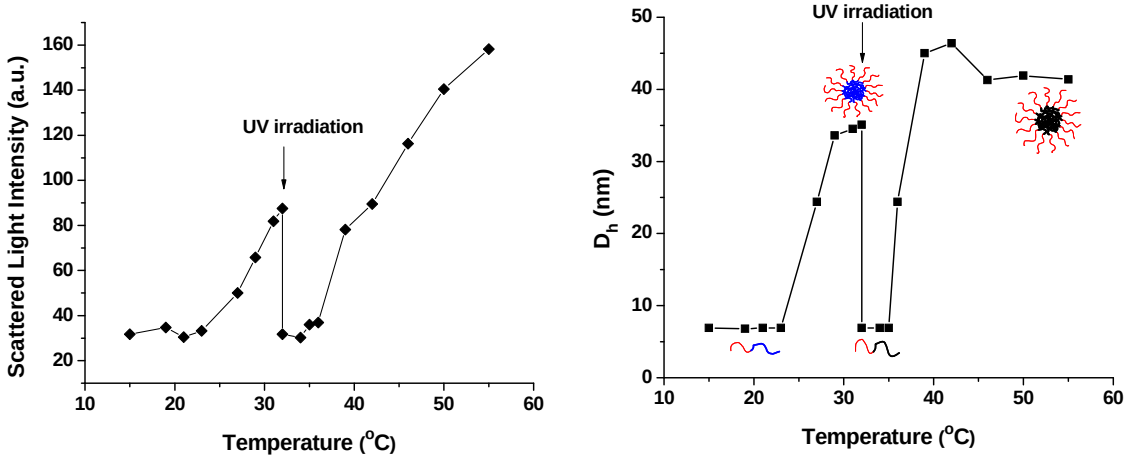
2.3.5 UV-Irradiation-Induced Dissociation of Micelles of PEO-*b*-P(TEGEA-*co*-NBA)

The study of the photocleavage of *o*-nitrobenzyl group in the random copolymer P(TEGEA-*co*-NBA) showed that the cloud point increased by 11.5 ^oC. The CMT of BR-**4** at concentration of 0.2 wt % was 25 ^oC ($CMT_{1\text{-}DLS}$). If the photocleavage of *o*-nitrobenzyl in BR-**4** increases the CMT by the same magnitude as for the random copolymer, the CMT of the new block copolymer (CMT_2) would be 36.5 ^oC. Considering that well-defined spherical micelles of BR-**4** were observed at 32 ^oC from DLS, UV irradiation at this temperature is expected to induce the dissociation of micelles. Because at 32 ^oC the *o*-nitrobenzyl groups were located in the core of micelles, the irradiation time that was needed to achieve a maximum degree of cleavage might be different from that for P(TEGEA-*co*-NBA) below the LCST. Therefore, UV-vis spectrometry was used to monitor the photocleavage reaction. A 0.2 wt % aqueous micellar solution of BR-**4** was irradiated with 365 nm UV light at 32 ^oC and the UV-vis spectra at various times were recorded.[74] It appeared that there was no further change in the absorbances from 330 to 650 nm after 183 min. The polymer after UV irradiation for 400 min was isolated and the

^{1}H NMR spectroscopy analysis showed that the aromatic peaks and the peak at 5.44 ppm, which were from NBA, were no longer present in the spectrum. To ensure that the photocleavage of *o*-nitrobenzyl groups in the micelle core reached the maximum degree, the micellar solutions were irradiated for 480 min in the following DLS and FS studies.

DLS study provided direct evidence for the UV irradiation-induced dissociation of micelles of BR-**4** at 32 ^{o}C. The 0.2 wt % aqueous solution of BR-**4** used in the DLS study shown in Figure 2.4 was irradiated with 365 nm UV light at 32 ^{o}C for 480 min. The intensity of scattered light at scattering angle of 90^o decreased to the level for the solution of BR-**4** below 22 ^{o}C before UV irradiation (Figure 2.7a). Meanwhile, the hydrodynamic diameter decreased to < 7 nm (Figure 2.7b). These confirmed that the micelles were disrupted by the UV irradiation. When the solution temperature was increased from 32 ^{o}C to above 36 ^{o}C, the intensity of scattered light increased significantly. Two size distributions were observed in the range of 36 – 42 ^{o}C: one attributed to the unimers and one to the micelles. With further increasing the temperature, the micelle size was found to be stabilized at ~ 41 nm, slightly larger than that of the micelles of BR-**4** (~ 35 nm). This might be the result of more water being retained in the core due to the hydrophilic carboxylic acid groups. The intensity of scattered light continued to increase with the increase of temperature, similar to the observations for the micelles of BR-**4**, BR-**5**, and B-**3**. The polydispersity of micelles at 50 ^{o}C was 0.062.[74] The nearly independence of Γ/q^2 on scattering angle at 50 ^{o}C suggested that the micelles were spherical (Figure 2.5b).

The UV-induced dissociation of micelles of BR-**4** was further studied by FS. Figure 2.8 shows the fluorescence emission spectra of Nile Red in a 0.2 wt % aqueous micellar



(a) (b)

Figure 2.7. The intensity of scattered light at scattering angle of 90° (a) and hydrodynamic diameter (b) as a function of temperature in a dynamic light scattering study of multiple micellization and dissociation transitions of PEO-*b*-P(TEGEA-*co*-NBA) (BR-**4**, $M_{n,GPC}$ = 18,300 g/mol, PDI = 1.07, 0.2 wt % aqueous solution – the same solution used in Figure 2.4) in response to temperature changes and UV irradiation. The data points from 15 to 32 °C before UV irradiation were from the heating process in Figure 2.4. At 32 °C, the polymer solution was irradiated with 365 nm UV light for 480 min. The collection of light scattering data was resumed thereafter.

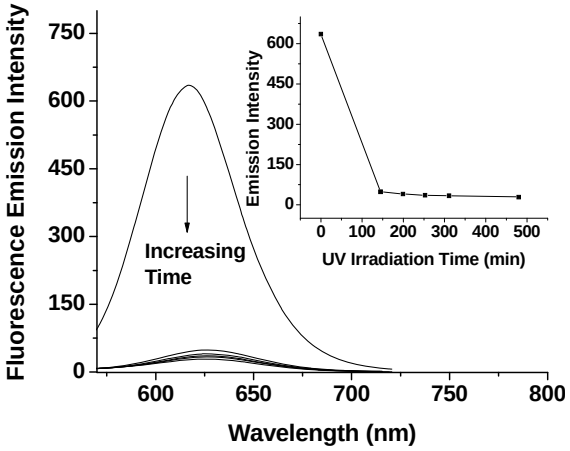
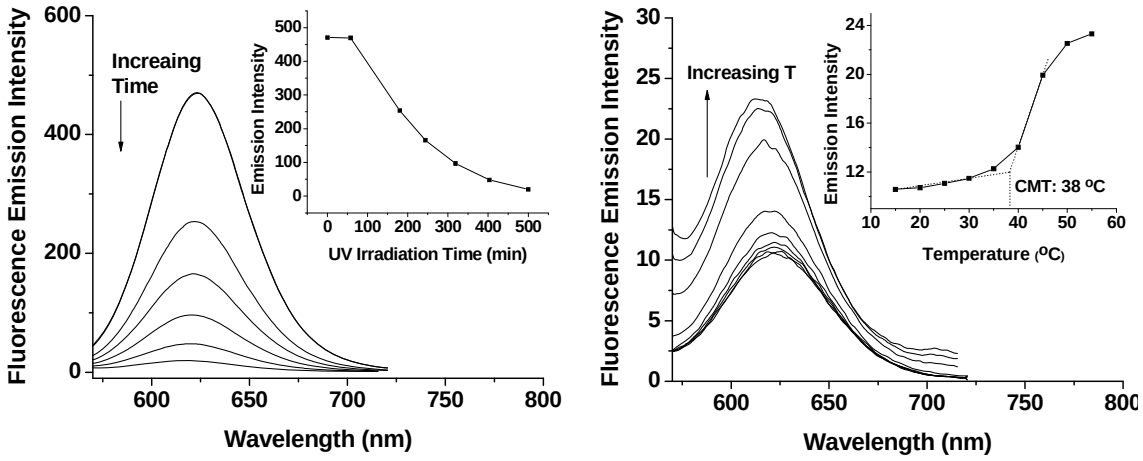


Figure 2.8. Fluorescence spectra of Nile Red in a 0.2 wt % aqueous solution of PEO-*b*-P(TEGEA-*co*-NBA) (BR-**4**, $M_{n,GPC}$ = 18,300 g/mol, PDI = 1.07) after exposure to 365 nm UV light at 32 ^{o}C for 0, 145, 199, 253, 311, and 480 min. The inset is the plot of maximum fluorescence emission intensity versus UV irradiation time. The wavelengths of the maximum peak were 617 nm (0 min), 625 nm (145 min), 626 nm (199 min), 625 nm (253 min), 628.5 nm (311 min), and 625 nm (480 min).

solution of BR-**4** at 32 ^{o}C after UV irradiation for various times. In only 140 min, the fluorescence intensity at the maximum peak decreased dramatically. Further increasing the irradiation time did not change the emission intensity significantly. The maximum peak underwent a red-shift from 617 nm at 0 min to 625 nm at 480 min, which indicated that the dye molecules were transferred from a hydrophobic to a hydrophilic environment. Note that the maximum fluorescence intensity after UV irradiation for 140 min was much lower than that of Nile Red in the solution of BR-**4** below the CMT before UV irradiation (Figure 2.6a), which is likely due to the photobleaching. To confirm it, a control experiment was conducted. A 0.2 wt % aqueous micellar solution of B-**3** loaded with Nile Red was irradiated at 45 ^{o}C with 365 nm UV light for 500 min. Figure 2.9 shows the fluorescence emission spectra at various irradiation times. No change was observed at 58 min. With increasing the irradiation time, the fluorescence intensity decreased but at a slower pace compared with that in Figure 2.8. The temperature was decreased to 15 ^{o}C, then gradually increased and the fluorescence spectra of the photobleached Nile Red dye were recorded. The CMT was found at 38 ^{o}C (Figure 2.9b), essentially identical to that of B-**3** before UV irradiation, indicating that the photobleaching did not affect the determination of CMT, though the emission intensity was much lower.

The UV irradiation-induced dissociation of micelles of BR-**5** was conducted at 30 ^{o}C.[74] After 480 min, the intensity of scattered light at scattering angle of 90^{o} decreased to the level for the polymer solution below the CMT_1 before UV irradiation, and the hydrodynamic size decreased to < 7 nm, indicating that the micelles dissociated into the unimers. Further increasing temperature induced the formation of micelles again, similar



(a) (b)

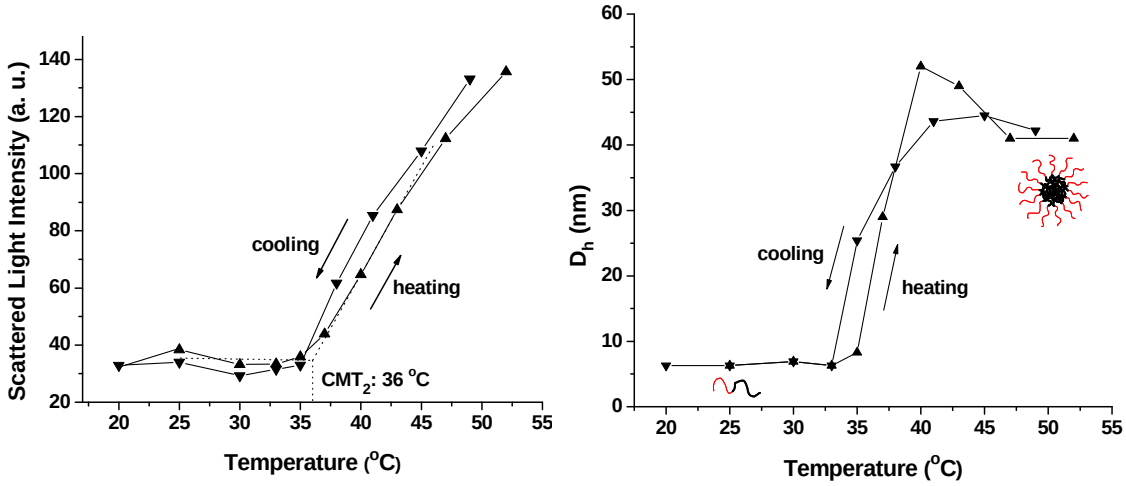
Figure 2.9. Fluorescence spectra of (a) Nile Red in a 0.2 wt % aqueous solution of PEO-*b*-PTEGEA (B-**3**, $M_{n,GPC}$ = 21,400 g/mol, PDI = 1.07) after exposure to 365 nm UV irradiation for 0, 58, 180, 244, 319, 403, and 500 min and (b) photobleached Nile Red in the UV-irradiated solution of B-**3** at various temperatures during the heating process. The inset in (a) is the plot of maximum fluorescence emission intensity versus UV irradiation time. The inset in (b) is the plot of maximum fluorescence intensity versus temperature, from which the CMT was determined.

to the observation for thermo- and light- induced micellization and dissociation of BR-**4**.

2.3.6 Temperature-Induced Reversible Formation and Dissociation of Micelles of PEO-*b*-P(TEGEA-*co*-AA)

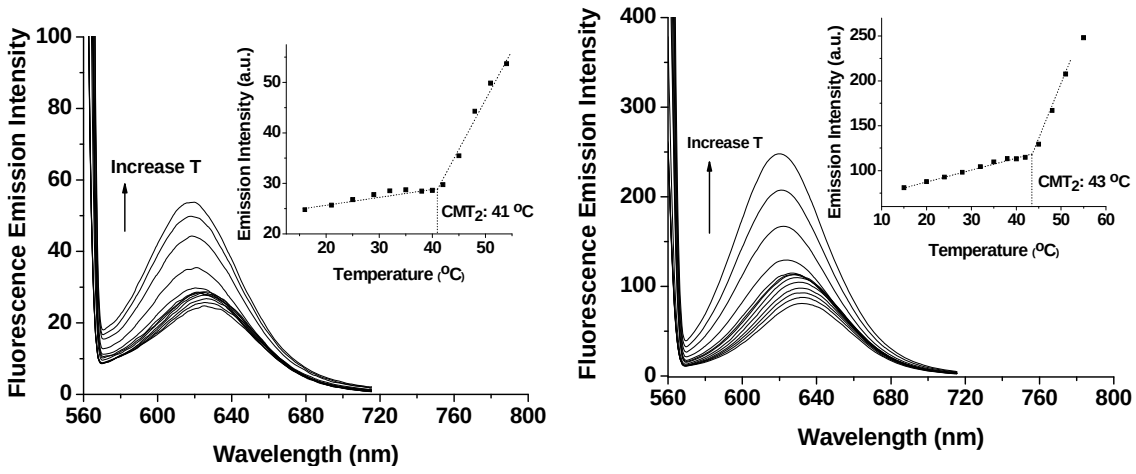
As for the micellization of BR-**4**, the thermo-induced formation of micelles of PEO-*b*-P(TEGEA-*co*-AA) was reversible. Figure 2.10 shows the DLS data for the cooling-induced dissociation of micelles and the heating-induced micellization. In the heating process, when the temperature was above 35 ^{o}C, the intensity of scattered light at scattering angle of 90^{o} began to increase. The CMT_2 was found at 36 ^{o}C. At temperatures > 43 ^{o}C, only micelles were observed and the hydrodynamic size became stabilized at ~ 41 nm with further increasing the temperature.

The thermo-induced reversible formation and dissociation of micelles of PEO-*b*-P(TEGEA-*co*-AA) was then studied by FS. The 0.2 wt % aqueous micellar solution of BR-**4** loaded with Nile Red was irradiated at 32 ^{o}C for 480 min (Figure 2.7), and then cooled to 16 ^{o}C. Figure 2.11a shows the fluorescence spectra of photobleached Nile Red in this solution at various temperatures in the heating process. Above 40 ^{o}C, the fluorescence emission intensity began to increase. The maximum peak shifted from 625.5 nm at 16 ^{o}C to 618 nm at 51 ^{o}C, suggesting that the dye molecules were re-encapsulated in the hydrophobic core of the micelles. The control experiment with PEO-*b*-PTEGEA showed that the UV-induced photobleaching did not affect the determination of CMT. However, the CMT_2 determined from FS analysis was 41 ^{o}C (Figure 2.11a), 5 ^{o}C higher than that from DLS. Since the core contained hydrophilic carboxylic acid groups and the fluorescence intensity of Nile Red is sensitive to the polarity of the environment, a higher



(a) (b)

Figure 2.10. The intensity of scattered light at scattering angle of 90° (a) and hydrodynamic diameter (b) as a function of temperature (▲ heating, ▼ cooling) in a dynamic light scattering study of thermo-induced reversible formation and dissociation of micelles of PEO-*b*-P(TEGEA-*co*-AA), which was obtained in situ by UV irradiation of a 0.2 wt % aqueous solution of PEO-*b*-P(TEGEA-*co*-NBA) (BR-**4**, $M_{n,GPC}$ = 18,300 g/mol, PDI = 1.07) for 480 min.



(a) (b)

Figure 2.11. Fluorescence spectra of (a) photobleached Nile Red and (b) photobleached dye plus reloaded fresh Nile Red in an aqueous solution of PEO-*b*-P(TEGEA-*co*-AA) at various temperatures in the heating process. The aqueous solution of PEO-*b*-P(TEGEA-*co*-AA) was obtained in situ by UV irradiation of a 0.2 wt % aqueous solution of PEO-*b*-P(TEGEA-*co*-NBA) (BR-**4**, $M_{n,GPC}$ = 18,300 g/mol, PDI = 1.07) at 32 ^{o}C for 480 min. The insets are the plots of maximum fluorescence emission intensity versus temperature, which are used to determine the CMT_2.

temperature might be required for the fluorescence emission intensity of the dye to begin to increase. The micellization was reversible. Decreasing the temperature resulted in the dissociation of micelles and the decrease of fluorescence emission intensity.[74] The maximum peak underwent a redshift from 619 nm at 48 ^{o}C to 625 nm at 25 ^{o}C, which indicated that Nile Red was released into water.

Because of the photobleaching, the fluorescence emission intensity in Figure 2.11a was very low even at T > 50 ^{o}C. To better demonstrate the re-encapsulation of Nile Red by the micelles of PEO-*b*-P(TEGEA-*co*-AA) at temperatures higher than CMT_2, the polymer solution was transferred into a vial that contained fresh Nile Red. Figure 2.11b shows the fluorescence spectra of the reloaded Nile Red plus the photobleached dye at various temperatures in the heating process. The emission intensity of the dye was much higher at 20 ^{o}C than that of the photobleached dye (Figure 2.11a) and increased substantially with the increase of temperature to 55 ^{o}C. The CMT_2 determined from this plot was 43 ^{o}C, slightly higher than that determined from Figure 2.11a. Moreover, the maximum peak shifted from 633 nm at 15 ^{o}C to 620 nm at 55 ^{o}C, implying that the dye molecules were encapsulated in the micelle core. Lowering the temperature caused the fluorescence emission intensity to decrease with the release of dye into water.[74]

The PEO-*b*-P(TEGEA-*co*-AA) obtained from the photocleavage of BR-**5** was also investigated.[74] DLS study showed that the CMT_2 was 34 ^{o}C. The size of micelles at 50 ^{o}C was 45.6 nm, which was about 10 nm larger than that of micelles of BR-**5** at 30 ^{o}C before UV irradiation. The micelles were spherical as implied by the nearly independence of Γ/q^2 on q^2 at 50 ^{o}C. These observations were similar to the results obtained from BR-**4**.

The CMT_2, determined by FS, was 39 ^oC, which was 5 ^oC higher than that from DLS. Regardless of what technique was used for the determination of CMT, the CMT_2 of the higher molecular weight block copolymer was lower, which is reasonable because higher molecular weight thermosensitive water-soluble polymers tend to undergo the hydration-to-dehydration transition at a lower temperature.[67] Table 2.3 summarizes the values of CMT_2 and micelle characteristics for the two samples after UV irradiation.[74]

2.4 Conclusion

In summary, thermo- and light-induced multiple formation and dissociation of micelles of PEO-*b*-P(TEGEA-*co*-NBA) in water were demonstrated in this work. Well-defined block copolymers that contained photosensitive NBA units in the thermosensitive blocks were synthesized by ATRP of a mixture of TEGEA and NBA with a molar ratio of 100 : 10 from macroinitiator PEO-Br. DLS and FS studies showed that the block copolymers underwent reversible micellization of micelles in response to temperature changes. The micelles had hydrodynamic sizes of ~ 35 nm, narrow polydispersities, and spherical shapes. The CMCs were found to be much lower than that of PEO-*b*-PTEGEA. Upon UV irradiation, the *o*-nitrobenzyl groups were cleaved and the LCST of the thermosensitive block was increased by ≥ 11 ^oC, triggering the dissociation of micelles into unimers and the release of encapsulated molecules into water at appropriate temperatures. With further increasing the temperature above the LCST of the new thermosensitive block, micellization occurred again and the released Nile Red was re-encapsulated by the micelles. Since *o*-nitrobenzyl group can be cleaved via two-photon absorption of near IR light,[32] these thermo- and light-sensitive block copolymers might

Table 2.3. Critical Micellization Temperatures and Micelle Characteristics of PEO-*b*-P(TEGEA-*co*-AA) Obtained from BR-4 and -5 by UV Irradiation

PEO-*b*-P(TEGEA-*co*-AA)	$CMT_{2\text{-}DLS}$[a]	Micelle size[b]	PD[c]	$CMT_{2\text{-}FS}$[d]
obtained from BR-**4**	36 ^{o}C	41.9 nm (50 ^{o}C)	0.062 (50 ^{o}C)	41 ^{o}C
obtained from BR-**5**	34 ^{o}C	45.6 nm (50 ^{o}C)	0.013 (50 ^{o}C)	39 ^{o}C

[a]The critical micellization temperature of PEO-*b*-P(TEGEA-*co*-AA) ($CMT_{2\text{-}DLS}$) was determined by dynamic light scattering (DLS). [b]The size of micelles was obtained by the use of the CONTIN method. [c]The polydispersity (PD) of micelles at a specific temperature. [d]The critical micellization temperature ($CMT_{2\text{-}FS}$) was determined by fluorescence spectroscopy (FS).

be of interest for targeted drug delivery.

References:

1. Rijcken, C. J. F.; Soga, O.; Hennink, W. E.; van Nostrum, C. F. *J. Controlled Release* **2007**, *120*, 131-148.
2. Dimitrov, I.; Trzebicka, B.; Müller, A. H. E.; Dworak, A.; Tsvetanov, C. B. *Prog. Polym. Sci.* **2007**, *32*, 1275-1343.
3. Gil, E. S; Hudson, S. M. *Prog. Polym. Sci.* **2004**, *29*, 1173-1222.
4. Bütün, V.; Billingham, N. C.; Armes, S. P. *J. Am. Chem. Soc.* **1998**, *120*, 11818-11819.
5. Liu, S. Y.; Billingham, N. C.; Armes, S. P. *Angew. Chem. Int. Ed.* **2001**, *40*, 2328-2331.
6. Gohy, J. F.; Antoun, S.; Jérome, R. *Macromolecules* **2001**, *34*, 7435-7440.
7. Gillies, E. R.; Fréchet, J. M. J. *Chem. Commun.* **2003**, *14*, 1640-1641.
8. Gillies, E. R.; Jonsson, T. B.; Fréchet, J. M. J. *J. Am. Chem. Soc.* **2004**, *126*, 11936-11943.
9. Gillies, E. R.; Fréchet, J. M. J. *Bioconjugate Chem.* **2005**, *16*, 361-368.
10. Bae, Y.; Fukushima, S.; Harada, A.; Kataoka, K. *Angew. Chem. Int. Ed.* **2003**, *42*, 4640-4643.
11. Bae, Y.; Nishiyama, N.; Fukushima, S.; Hoyama, H.; Yasuhori, M.; Kataoka, K. *Bioconjugate Chem.* **2005**, *16*, 122-130.
12. Schilli, C. M.; Zhang, M. F.; Rizzardo, E.; Thang, S. H.; Chong, Y. K.; Edwards, K.; Karlsson, G.; Müller, A. H. E. *Macromolecules* **2004**, *37*, 7861-7866.
13. André, X.; Zhang, M. F.; Müller, A. H. E *Macromol. Rapid Commun.* **2005**, *26*, 558-563.

14. Bellomo, E. G.; Wyrsta, M. D.; Pakstis, L.; Pochan, D. J.; Deming, T. J. *Nature Materials* **2004**, *3*, 244-248.

15. Borchert, U.; Lipprandt, U.; Bilang, M.; Kimpfler, A.; Rank, A.; Peschka, R.; Schubert, R.; Lindner, P.; Forster, S. *Langmuir* **2006**, *22*, 5843-5847.

16. Xu, J.; Ge, Z. S.; Zhu, Z. Y.; Luo, S. Z.; Liu, H. W.; Liu, S. Y. *Macromolecules* **2006**, *39*, 8178-8185.

17. Katayama, Y.; Sonoda, T.; Maeda, M. *Macromolecules* **2001**, *34*, 8569-8573.

18. Ishihara, Y.; Bazzi, H. S.; Toader, V.; Godin, F.; Sleiman, H. F. *Chem. Eur. J.* **2007**, *13*, 4560-4570.

19. Joseph, J.; Dreiss, C. A.; Cosgrove, T. *Langmuir* **2007**, *23*, 460-466.

20. Saji, T.; Hoshino, K.; Aoyagi, S. *J. Am. Chem. Soc.* **1985**, *107*, 6865-6868.

21. Anton, P.; Heinze, , J.; Laschewsky, A. *Langmuir* **1993**, *9*, 77-85.

22. Takeoka, Y.; Aoki, T.; Sanui, K.; Ogata, N.; Yokoyama, M.; Okano, T.; Sakurai, Y.; Watanabe, M. *J. Controlled Release* **1995**, *33*, 79-87.

23. Kakizawa, Y.; Sakai, H.; Nishiyama, K. Abe, M. *Langmuir* **1996**, *12*, 921-924.

24. Jong, J. I.; Abbott, N. L. *Langmuir* **2000**, *16*, 5553-5561.

25. Napoli, A.; Valentini, M.; Tirelli, N.; Muller, M.; Hubbell, J. A. *Nature Materials* **2004**, *3*, 183-189.

26. Napoli, A.; Boerakker, M. J.; Tirelli, N.; Muller, M.; Sommerdijk, N. A.; Hubbell, J. A. *Langmuir* **2004**, *20*, 3487-3491.

27. Ghosh, S.; Irvin, K.; Thayumanavan, S. *Langmuir* **2007**, *23*, 7916-7919.

28. Orihara, Y.; Matsumura, A.; Saito, Y.; Ogawa, N.; Saji, T.; Yamaguchi, A.; Sakai, H.; Abe, M. *Langmuir* **2001**, *17*, 6072-6076.

29. Wang, G.; Tong, X.; Zhao. Y. *Macromolecules* **2004**, *37*, 8911-8917.

30. Tong, X.; Wang, G.; Soldera, A.; Zhao. Y. *J. Phys. Chem. B.* **2005**, *109*, 20281-20287.

31. Jiang, J. Q.; Tong, X.; Zhao, Y. *J. Am. Chem. Soc.* **2005**, *127*, 8290-8291.

32. Jiang, J. Q.; Tong, X.; Morris, D.; Zhao. Y. *Macromolecules* **2006**, *39*, 4633-4640.

33. Goodwin, A. P.; Mynar, J. L.; Ma, Y.; Fleming, G. R.; Fréchet, J. M. J. *J. Am. Chem. Soc.* **2005**, *127*, 9952-8853.

34. Lee, H.-I, Pietrasik, J.; Matyjaszewski, K. *Macromolecules* **2006**, *39*, 3914-3920.

35. Jiang, Y.; Wang, Y.; Ma, N.; Wang, Z.; Smet, M.; Zhang, X. *Langmuir* **2007**, *23*, 4029-4034.

36. Lee, H-I; Wu, W.; Oh, J. K.; Mueller, L.; Sherwood, G.; Peteanu, L.; Kowalewski, T.; Matyjaszewski, K. *Angew. Chem. Int. Ed.* **2007**, *46*, 2453-2457.

37. Aoshima, S.; Sugihara, S. *J. Polym. Sci. Part A: Polym. Chem.* **2000**, *38*, 3962-3965.

38. Sugihara, S.; Kanaoka, S.; Aoshima, S. *J. Polym. Sci. Part A: Polym. Chem.* **2004**, *42*, 2601-2611.

39. Aoshima, S.; Sugihara, S.; Shibayama, M.; Kanaoka, S. *Macromol. Symp.* **2004**, *215*, 151-163.

40. Sugihara, S.; Kanaoka, S.; Aoshima, S. *Macromolecules* **2005**, *38*, 1919-1927.

41. Arotcarena, M.; Heise, B.; Ishaya, S.; Laschewsky, A. *J. Am. Chem. Soc.* **2002**, *124*, 3787-3793.

42. Mertoglu, M.; Garnier, S.; Laschewsky, A.; Skrabania, K.; Sorsberg, J. *Polymer* **2005**, *46*, 7726-7740.

43. Skrabania, K.; Juliane, K.; Laschewsky, A.; Akdemir, O.; Hoth, A. ; Lutz, J.-F. *Langmuir* **2007**, *23*, 84-93.

44. Hua, F. J.; Jiang, X. G.; Zhao, B. *Macromolecules* **2006,** *39*, 3476-3479.

45. Qin, S. H.; Geng, Y.; Discher, D. E.; Yang, S. *Adv. Mater.* **2006**, *18*, 2905-2909.

46. Zhang, W. Q.; Shi, L. Q.; Wu, K.; An. Y. G. *Macromolecules* **2005**, *38*, 5743-5747.

47. Dimitrov, P.; Rangelov, S.; Dworak, A.; Tsvetanov, C. B. *Macromolecules* **2004**, *37*, 1000-1008.

48. Convertine, A. J.; Lokitz, B. S.; Vasileva, Y.; Myrick, L. J.; Scales, C. W.; Lowe, A. B.; McCormick, C. L. *Macromolecules* **2006**, *39*, 1724-1730.

49. Li, Y. T.; Lokitz, B. S.; McCormick, C. L. *Macromolecules* **2006**, *39*, 81-89.

50. Wu, C.; Wang, X. H. *Phys. Rev. Lett.* **1998**, *80*, 4092-4094.

51. Plamper, F. A.; Schmalz, A.; Ballauff, M.; Müller, A. H. E. *J. Am. Chem. Soc.* **2007**, *129*, 14538-14539.

52. Schild , H. G. *Prog. Polym. Sci.* **1992**, *17*, 163-249.

53. Huang, X. N.; Du, F. S.; Ju, R.; Li, Z. C. *Macromol. Rapid Commun.* **2007**, *28*, 597-603.

54. Neradovic, D.; van Nostrum, C. F.; Hennink, W. E. *Macromolecules* **2001**, *34*, 7589-7591.

55. Neradovic, D.; van Steenbergen, M. J.; Vansteelant, L.; Meijer, Y. J.; van Nostrum, C. F.; Hennink, W. E. *Macromolecules* **2003**, *36*, 7491-7498.

56. Soga, O.; van Nostrum, C. F.; Ramzi, A.; Visser, T.; Soulimani, F.; Frederik, P. M.; Bomans, P. H. H.; Hennink, W. E. *Langmuir* **2004**, *20*, 9388-9395.

57. Rijicken, C. J. F.; Veldhuis, T. F. J.; Ramzi, A.; Meeldijk, J. D.; van Nostrum, C. F.; Hennink, W. E. *Biomacromolecules* **2005**, *6*, 2343-2351.

58. Kohori, F.; Sakai, K.; Aoyagi, T.; Yokoyama, M.; Yamato, M.; Sakurai, Y.; Okano, T. *Colloids and Surfaces B: Biointerfaces* **1999**, *16*, 195-205.

59. Gotzamanis, G.; Tsitsilianis, C. *Polymer* **2007**, *48*, 6226-6233.

60. Han, S.; Hagiwara, M.; Ishizone, T. *Macromolecules* **2003**, *36*, 8312-8319.

61. Li, D. J.; Jones, G. J.; Dunlap, J. R.; Hua, F. J.; Zhao, B. *Langmuir* **2006**, *22*, 3344-3351.

62. Li, D. J.; Zhao, B. *Langmuir* **2007**, *23*, 2208-2217.

63. Lutz, J.-F.; Hoth, A. *Macromolecules* **2006**, *39*, 893-896.

64. Lutz, J. F.; Weichenhan, K.; Akdemir, O.; Hoth, A. *Macromolecules* **2007**, *40*, 2503-2508.

65. Zhao, B.; Li, D. J.; Hua, F. J.; Green, D. R. *Macromolecules* **2005**, *38*, 9509-9517.

66. Hua, F. J.; Jiang, X.G.; Li, D. J.; Zhao, B. *J. Polym. Sci. Part A: Polym. Chem.* **2006**, *44*, 2454-2467.

67. Jiang, X. G.; Zhao, B. *J. Polym. Sci. Part A: Polym. Chem.* **2007**, *45*, 3707-3721.

68. Aathimanikandan, S. V.; Savariar, E. N. Thayumanavan, S. *J. Am. Chem. Soc.* **2005**, *127*, 14922-14929.

69. Liu, S.; Weaver, J. V. M.; Save, M.; Armes, S. P. *Langmuir* **2002**, *18*, 8350-8357.

70. Zhao, B.; Moore, J. S.; Beebe, D. J. *Science* **2001**, *291*, 1023-1026.

71. Zhao, B.; Viernes, N. O. L.; Moore, J. S.; Beebe, D. J. *J. Am. Chem. Soc.* **2002**, *124*, 5284-5285.

72. Zhao, B.; Moore, J. S.; Beebe, D. J. *Langmuir* **2003**, *19*, 1873-1879.

73. Greene, T. W.; Wuts, P. G. M. "Protective Groups in Organic Synthesis", John Wiley & Sons: New York, 3rd Ed., **1999**.

74. Details can be found in appendix A.

75. Bulmus, V.; Ding, Z.; Long, C. J.; Stayton, P. S.; Hoffman, A. S. *Bioconjugate Chem.* **2000**, *11*, 78-83.

76. Yin, X.; Hoffman, A. S.; Stayton, P. S. *Biomacromolecules* **2006**, *7*, 1381-1385.

77. Zhou, Z.; Chu, B. *J. Colloid & Interface Sci.* **1988**, *126*, 171-180.

Chapter 3. Tuning Micellization and Dissociation Transitions of Thermo- and pH-Sensitive Poly(ethylene oxide)-*b*-poly(methoxydi(ethylene glycol) methacrylate-*co*-methacrylic acid) in Aqueous Solution by Combining Temperature and pH Triggers

Abstract

This chapter presents the active control of multiple micellization and dissociation transitions of thermo- and pH-sensitive water-soluble block copolymers, poly(ethylene oxide)-*b*-poly(methoxydi(ethylene glycol) methacrylate-*co*-methacrylic acid) (PEO-*b*-P(DEGMMA-*co*-MAA)), in aqueous solutions by combining temperature and pH triggers. Two block copolymers and one random copolymer P(DEGMMA-*co*-MAA) were prepared by atom transfer radical polymerization of a mixture of methoxydi(ethylene glycol) methacrylate (DEGMMA) and *t*-butyl methacrylate (*t*-BMA) with a molar ratio of 100 : 13 from a PEO macroinitiator and a small molecule initiator, respectively, and subsequent removal of *t*-butyl group. PDEGMMA is a thermosensitive water-soluble polymer exhibiting a lower critical solution temperature in water at 25 ^{o}C. The cloud point of P(DEGMMA-*co*-MAA) in water can be readily tuned from 24 to 60 ^{o}C by changing the solution pH. The block copolymers dissolved molecularly in cold aqueous buffer solutions with a pH of 4.0 and underwent micellization when the temperature was raised to a critical value. Upon judiciously changing the solution pH by injection of a predetermined amount of a KOH solution, the block copolymer micelles were dissociated into the unimers, which subsequently re-formed micelles at the same temperature in response to the addition of a predetermined amount of an HCl solution or heating to a higher temperature. These temperature- and pH-induced micellization/dissociation transitions were reversible. By continuously increasing temperature from 20 to 57 ^{o}C and simultaneously controlling the pH, three cycles of micellization and disassembly transitions of these block copolymers in aqueous solutions were realized, demonstrating the possibility of achieving on-demand micellization and dissociation transitions by

combining temperature and pH triggers. Fluorescence spectroscopy studies showed that a hydrophobic fluorescence dye, Nile Red, can be repeatedly encapsulated by block copolymer molecules upon micellization and released upon dissociation of micelles under different combinations of pH and temperature.

3.1 Introduction

Block copolymer micelles that can dissociate into the molecularly dissolved unimers upon application of an external stimulus are of great interest for controlled encapsulation and triggered release of substances in many technological applications including targeted drug delivery and cosmetics.[1-45] A common principle for destabilizing micellar assemblies involves the modification of the polarity or hydrophobicity/ hydrophilicity balance of the core-forming component by the use of an external trigger.[1] When the core-forming block becomes soluble in the medium, the driving force for the micellization is eliminated and the micellar assemblies are dissociated into the unimers. The dissociation process can be reversible or irreversible depending on the response mechanism. In many applications, reversible dissociation/micellization transitions induced by external stimuli can be advantageous or are desired because the re-formation of micelles allows the re-encapsulation of the released substance.[38,39]

Various chemical and physical stimuli including pH,[1-23] temperature,[1-3,24-35] light,[36-40] specific molecules,[1,41-43] redox[1,44,45], or their combinations[7-8,21,22,40] have been employed to induce the formation and dissociation of block copolymer micelles or vesicles. Among them, pH and temperature are the most commonly used external triggers.[1-3] In general, there are two types of pH-sensitive block copolymer micelles: (i) those in which the core-forming blocks contain weak acid or base moieties (e.g., carboxylic acid, tertiary amine, etc.),[4-15] and (ii) those in which the core-forming blocks contain hydrolyzable pendant groups.[16-23] In the first type, deprotonation or protonation of weak acid or base groups modifies the polarity of the core-forming block upon pH

changes, triggering the formation/dissociation of micellar assemblies. For example, Armes et al. reported a series of schizophrenic diblock copolymers that formed conventional and inverted micelles by varying the solution pH.[4-7] In the second type of pH-sensitive micelles, pH change-induced hydrolysis of pendant groups converts the core-forming hydrophobic block into hydrophilic. For example, Frétchet et al. developed block copolymers with one block functionalized with acid-labile cyclic benzylidene acetal groups.[16-18] The micelles were stable at physiological pH, but once the pH was lowered to 5, hydrolysis of acetal bonds occurred and the micelles disassembled. Lee et al. reported a diblock copolymer containing citraconic amide side groups, which were stable at pH ≥ 7 but became unstable at acidic pH.[21] They observed that the micelles underwent fast dissociation at pH = 5.5.

Temperature is a very attractive physical stimulus for the formation and dissociation of micelles.[1-3,24-35] Thermosensitive water-soluble polymers undergo a transition from a hydrated to a dehydrated state when the temperature is above a critical point, known as lower critical solution temperature (LCST).[1-3,46-49] Water-soluble block copolymers with one or more blocks exhibiting thermoresponsive properties in water have attracted growing interest in recent years.[24-35] These block copolymers undergo reversible micellization and dissociation in water in response to temperature changes. Note that one advantage of stimuli-responsive water-soluble block copolymers for the preparation of micelles is the elimination of the use of organic solvents. It is known that the LCST of a thermosensitive polymer can be modified by copolymerization with a second monomer,[1-3,48-57] which has been utilized to design block copolymer micelles with controlled instability.[1,50-53] Hennink et al. developed a series of block copolymers composed of

poly(ethylene oxide) (PEO) and thermosensitive polymers that contained lactate side chains.[1,50-53] Hydrolysis of lactate side groups caused an increase of the LCST of the thermosensitive block. When the polymer became soluble in water, dissociation of micelles occurred and the encapsulated molecules were released. The LCST of a thermosensitive water-soluble polymer can also be tuned by changing the solution pH if the polymer contains a small amount of weak acid or base groups.[58-66] The transition temperature is higher if more charges reside on the polymer chain, which is in turn controlled by the solution pH. For example, Yin et al. reported that the LCST of poly(*N*-isopropylacrylamide-*co*-propylacrylic acid) copolymers can be tuned from 4.8 to 63.8 ^{o}C by varying the acid content in the copolymer and the solution pH.[58] The pH dependence of the LCST has been exploited by Lokitz et al. to control the critical micellization temperature (CMT) of a thermosensitive block copolymer in aqueous solution.[66]

Our group has been interested in developing multi-responsive water-soluble block copolymers that can undergo multiple micellization and dissociation transitions by combining two external stimuli. The previous chapter has showed a thermo- and light-sensitive block copolymer, which dissolved molecularly in cold water but formed micelles when the temperature was above the CMT. Upon UV irradiation, the micelles were dissociated into the unimers, which on further increasing temperature formed micelles again. Although the thermo-induced micellization/dissociation transitions were reversible, the UV-triggered disassembly of micelles of this block copolymer was irreversible.[40] For many applications, it is more desired if stimuli-induced dissociation transitions are reversible. In this chapter, two stimuli, pH and temperature, are employed to achieve multiple reversible micellization and dissociation transitions of thermo- and

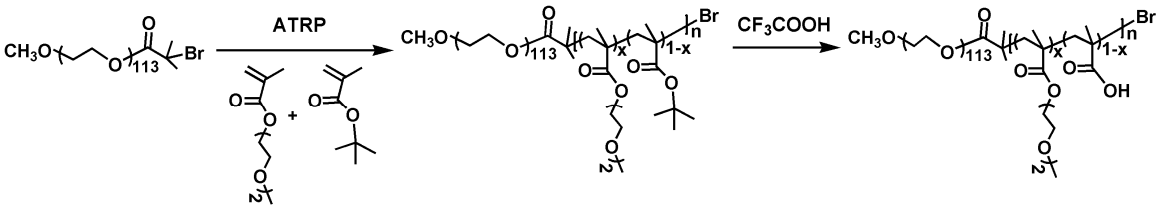
pH-sensitive poly(ethylene oxide)-*b*-poly(methoxydi(ethylene glycol) methacrylate-*co*-methacrylic acid) (PEO-*b*-P(DEGMMA-*co*-MAA), Scheme 3.1). PDEGMMA is a thermosensitive water-soluble polymer with a LCST reportedly at 25 ^{o}C in water.[67,68] By continuously increasing temperature and simultaneously controlling the pH of the solution, three complete cycles of micellization and dissociation transitions of PEO-*b*-P(DEGMMA-*co*-MAA) were realized (Scheme 3.2), demonstrating the possibility of achieving on-demand reversible micellization/dissociation transitions by combining two external triggers.

3.2 Experimental Section

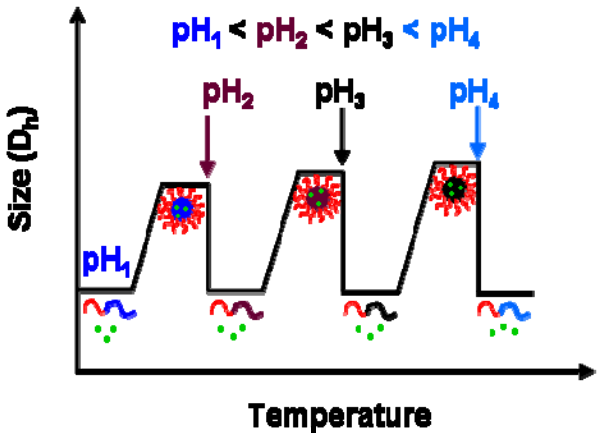
3.2.1 Materials

Poly(ethylene glycol) monomethyl ether (PEO-OH, MW = 5000 Da, Aldrich) was dried by azeotropic distillation with anhydrous toluene to remove the trace amount of water before the synthesis of the macroinitiator. Potassium hydrogen phthalate (KHP), trifluoroacetic acid (99%), acetone (HPLC grade), and Nile Red (99%) were obtained from Acros and used without further treatment. Dichloromethane and anisole (99%, Acros) were dried with calcium hydride, distilled, and stored in solvent storage flasks prior to use. Toluene was distilled from sodium and benzophenone and used immediately. Methoxydi(ethylene glycol) methacrylate (DEGMMA, or di(ethylene glycol) methyl ether methacrylate, 95%, Aldrich), *N,N,N′,N′,N″*-pentamethyldiethylenetriamine (PMDETA, Aldrich), and ethyl 2-bromoisobutyrate (EBiB, Aldrich) were dried over

Scheme 3.1. Synthesis of Thermo- and pH-Sensitive Water-Soluble Poly(ethylene oxide)-*b*-Poly(methoxydi(ethylene glycol) methacrylate-*co*-methacrylic acid) (PEO-*b*-P(DEGMMA-*co*-MAA))



Scheme 3.2. Multiple Micellization and Dissociation Transitions of Thermo- and pH-Sensitive Block Copolymer PEO-*b*-P(DEGMMA-*co*-MAA) by Controlling Temperature and pH



calcium hydride and distilled under reduced pressure. CuBr (98%, Aldrich) was stirred in glacial acetic acid overnight, filtered, and washed with absolute ethanol and ethyl ether. The salt was then collected, dried under vacuum, and stored in a desiccator. *tert*-Butyl methacrylate (99%, Aldrich) was passed through a basic aluminum oxide column prior to use. All other chemicals were purchased from either Aldrich or Fisher and used without further purification.

3.2.2 General Characterization

Gel permeation chromatography (GPC) was carried out at room temperature using PL-GPC 20 (an integrated GPC system from Polymer Laboratories, Inc) with a differential refractive index detector, one PLgel 5 μm guard column (50 × 7.5 mm), and two PLgel 5 μm mixed-C columns (each 300 × 7.5 mm, linear range of molecular weight from 200 to 2,000,000 according to Polymer Laboratories). The data were processed using Cirrus^{TM} GPC/SEC software (Polymer Laboratories). THF was used as the carrier solvent at a flow rate of 1.0 mL/min. Polystyrene standards (Polymer Laboratories) were used for calibration. The ^{1}H (300 MHz) spectra were recorded on a Varian Mercury 300 NMR spectrometer and the residual solvent proton signal was used as the internal standard. The cloud points of thermosensitive polymers in 10 mM potassium hydrogen phthalate (KHP) buffers with various pH values were measured by turbidimetry. The pH value of the polymer solution in 10 mM KHP buffer was adjusted by addition of a KOH solution and was measured by the use of a pH meter (Accumet AB15 pH meter from Fisher Scientific, calibrated with pH = 4.01, 7.00, and 10.01 standard buffer solutions). The optical transmittances of aqueous polymer solutions at various temperatures were

recorded at wavelength of 550 nm using a UV-vis spectrometer (Biomate 5 from Thermospectronic). The sample cell was thermostated with an external water bath of a Fisher Scientific Isotemp refrigerated circulator. At each temperature, the solutions were equilibrated for 5 min.

3.2.3 Preparation of Aqueous Buffer Solutions of Block Copolymers for Dynamic Light Scattering and Fluorescence Spectroscopy Studies

The polymers were dried in vacuum for > 3 h. An aqueous buffer solution of a block copolymer with a desired concentration was prepared either by direct addition of 10 mM aqueous solution of potassium hydrogen phthalate (KHP) into the small vial that contained the weighed polymer or by dilution of a polymer buffer solution of a known concentration with 10 mM KHP solution. The polymer solutions were sonicated in an ultrasonic ice/water bath for 5 min to ensure complete dissolution. The aqueous polymer solutions that contained Nile Red for fluorescence spectroscopy studies were made by the following procedure. 10 μL of a stock solution of Nile Red in acetone (concentration: 0.042 mg/mL) was added into an empty vial via a microsyringe, which was then placed in vacuum for > 3 h to remove the solvent. A calculated amount of a stock polymer buffer solution (1.0 wt % or 0.2 wt %) was injected into the vial and 10 mM KHP buffer was added to bring the total weight of the solution to 2.00 g. The nominal concentration of Nile Red was 6.6×10^{-7} M. The solution was allowed to equilibrate at a specific temperature for > 3 h before the fluorescence spectroscopy experiments.

3.2.4 Titration of Aqueous Polymer Solutions with a KOH Solution

A typical procedure is described below. A 0.2 wt % solution of PEO-*b*-P(DEGMMA-*co*-MAA) ($M_{n,GPC}$ = 21800 Da, PDI = 1.06) in 10 mM KHP buffer (2.50 g) was added into a vial and the pH was measured by a pH meter (Accumet AB 15). 10 μL of 0.2 M aqueous KOH solution was injected into the vial via a microsyringe. The solution was gently shaken and the pH value was recorded. This process was repeated until a total of 170 μL of 0.20 M KOH solution was added. The total volume increased by 6.8 %. A plot of pH versus the number of μmol of KOH was made. The pH values of the polymer buffer solutions in dynamic light scattering and fluorescence spectroscopy experiments after injection of a certain amount of KOH were obtained from the plot.

3.2.5 Dynamic Light Scattering

Dynamic light scattering (DLS) measurements were conducted with a Brookhaven Instruments BI-200SM goniometer equipped with a PCI BI-9000AT digital correlator, a temperature controller, and a solid-state laser (model 25-LHP-928-249, λ = 633 nm) at a scattering angle of 90°. The block copolymer buffer solutions were filtered into borosilicate glass tubes with an inner diameter of 7.5 mm by the use of Millipore Teflon filters (0.2 μm pore size). The glass tubes were then sealed with a PE stopper. At each temperature, the solutions were equilibrated for 15 min prior to data recording. The second-order correlation function of the scattered light intensity, $g^{(2)}(t)$, was analyzed by the CONTIN method. $g^{(2)}(t)$ can be expressed by the following equation:

$$g^{(2)}(t) = A(1 + \beta|g^{(1)}(t)|^2)$$

where A is the baseline, β is the coherence factor determined by the geometry of the detection, $g^{(1)}(t)$ is the normalized electric field correlation function.

Generally, $g^{(1)}(t)$ is expressed by the distribution function $G(\Gamma)$ as

$$|g^{(1)}(t)| = \int G(\Gamma)\exp(-\Gamma t)\, d\Gamma$$

For a translational diffusion mode, Γ can be used to determine the diffusion coefficient D through $\Gamma = Dq^2$, where q is the scattering vector. The hydrodynamic diameter D_h is related to the diffusion coefficient D by the Stokes-Einstein equation:

$$D = k_B T/(3\pi\eta D_h)$$

where k_B is the Boltzmann constant, T is the absolute temperature, and η is the viscosity of the solvent.

3.2.6 In Situ Dissociation and Re-formation of Micelles by Sequential Injection of 1.00 M KOH Solution and 1.00 M HCl Solution

A typical procedure is described below for DLS experiments. A similar procedure was used in the fluorescence spectroscopy study of in situ dissociation and re-formation of micelles. A glass tube that contained 2.50 g of a 2.5 wt % filtered buffer solution of PEO-*b*-P(DEGMMA-*co*-MAA) ($M_{n,GPC}$ = 21800 Da, PDI = 1.06) for light scattering study was placed in the tube holder of the light scattering instrument. The solution was gradually heated and cooled for study of thermo-induced micellization and dissociation transitions. At each temperature, the solution was equilibrated for 15 min prior to data recording. The solution was then equilibrated at 34 ^{o}C for 30 min and the scattering data

were recorded. 19 μL of a 1.00 M KOH solution which was pre-filtered through a 0.2 μm filter was injected into the tube by the use of a microsyringe with the needle penetrating through a pre-made tiny hole in the PE stopper. The solution was gradually heated to 50 ^{o}C and then cooled to 33 ^{o}C for study of the temperature-induced micellization and dissociation, respectively. After the solution was equilibrated at 34 ^{o}C for 30 min, 19 μL of a 1.00 M HCl solution which was passed through a 0.2 μm filter was injected into the tube by the use of a microsyringe with the needle penetrating through the PE stopper. The solution was then gradually heated and cooled for study of thermo-induced formation and dissociation.

3.2.7 Fluorescence Spectroscopy

Fluorescence emission spectra were recorded from Perkin Elmer LS 55 fluorescence spectrometer equipped with a 20 kW Xenon discharge lamp. The excitation wavelength was 550 nm and the fluorescence emission spectra were recorded from 560 to 720 nm. The slit width was 10 nm. The sample cell was thermostated with an external water bath of a Fisher Scientific Isotemp refrigerated circulator. At each temperature, the sample was equilibrated for 10 min.

(1). Determination of critical micellization temperature (CMT). The fluorescence emission spectra of Nile Red in a 0.2 wt % aqueous polymer buffer solution at various temperatures were recorded. At each temperature, the solution was equilibrated for 10 min. The maximum fluorescence intensities were plotted against temperatures for the determination of CMT.

(2) Determination of critical micelle concentration (CMC). A series of solutions of a block copolymer in 10 mM aqueous KHP buffer with different concentrations that were loaded with the same amount of Nile Red were made. The fluorescence emission spectra of Nile Red in these solutions at a specific temperature were recorded. The maximum fluorescence intensities were then plotted against the logarithm of polymer concentrations for the determination of CMC.

3.2.8 Synthesis of Homopolymer of DEGMMA by ATRP

A typical procedure for the synthesis of PDEGMMA by ATRP using ethyl 2-bromoisobutyrate (EBiB) as initiator is described below. CuBr (7.5 mg, 0.052 mmol), DEGMMA (1.86 g, 9.89 mmol), EBiB (15.9 mg, 0.082 mmol), anisole (3.95 g), and PMDETA (18.0 mg, 0.104 mmol) were added into a 25 mL two-necked flask. The mixture was stirred under nitrogen atmosphere and then degassed by three freeze-pump-thaw cycles. A sample was taken for ^{1}H NMR spectroscopy analysis and the flask was placed immediately in a 60 ^{o}C oil bath. After the polymerization proceeded for 225 min, a sample was taken for ^{1}H NMR spectroscopy analysis of monomer conversion and the reaction mixture was opened to the air and diluted with THF. The catalyst was removed by passing the reaction mixture through a neutral Al_2O_3 column with THF as eluent. The obtained polymer solution was concentrated and precipitated in hexanes (100 mL). The polymer was then dissolved in THF (3 mL) and precipitated again in hexanes (100 mL). This process was repeated one more time. A nearly colorless viscous liquid was obtained. GPC analysis results (polystyrene standards): $M_{n,GPC}$ = 16200 Da, polydispersity index (PDI) = 1.11. The DP of the polymer was calculated from the monomer conversion and

the monomer-to-initiator ratio assuming that the initiator efficiency was 100%. The peaks located in the range of 4.6 – 4.0 ppm, which were from -CH_2OOC- of monomer DEGMMA and the DEGMMA units in the polymer, were used as internal standard. The conversion was calculated from the integral values of the peaks from 5.8 to 5.3 ppm (C*H*H=CCH_3- from DEGMMA monomer) at t = 0 min and 225 min. The DP was 85.

3.2.9 Synthesis of Random Copolymer of DEGMMA and *t*BMA by ATRP

A typical procedure for the synthesis of P(DEGMMA-*co*-*t*BMA) by ATRP using ethyl 2-bromoisobutyrate (EBiB) as initiator is described below. CuBr (7.3 mg, 0.051 mmol), DEGMMA (1.25 g, 6.65 mmol), *t*BMA (0.125 g, 0.88 mmol), EBiB (13.8 mg, 0.071 mmol), anisole (2.39 g), and PMDETA (10.6 mg, 0.061 mmol) were added into a 25 mL two-necked flask. The mixture was stirred under nitrogen atmosphere and then degassed by three freeze-pump-thaw cycles. A sample was taken for ^{1}H NMR spectroscopy analysis and the flask was placed immediately in a 60 ^oC oil bath. After the polymerization proceeded for 171 min, a sample was taken for ^{1}H NMR spectroscopy analysis of monomer conversion and the reaction mixture was opened to the air and diluted with THF. The catalyst was removed by passing the reaction mixture through a neutral Al_2O_3 column with THF as eluent. The obtained polymer solution was concentrated and precipitated in hexanes. The polymer was then dissolved in THF (3 mL) and precipitated again in hexanes (100 mL). This process was repeated one more time. A nearly colorless viscous liquid was obtained. GPC analysis results (polystyrene standards): $M_{n,GPC}$ = 15000 Da, polydispersity index (PDI) = 1.14. The DP of the polymer was calculated from the monomer conversion and the monomer-to-initiator ratio

assuming that the initiator efficiency was 100%. The peaks located in the range of 4.6 – 4.0 ppm, which were from -CH_2OOC- of monomer DEGMMA and the DEGMMA units in the polymer, were used as internal standard. The conversion was calculated from the integral values of the peaks from 5.8 to 5.3 ppm (C*H*H=CCH_3- from both DEGMMA and *t*BMA monomers) at t = 0 min and 171 min. The DP was 82. The molar ratio of DEGMMA and *t*BMA units in the copolymer was calculated from ^{1}H NMR spectrum of the polymer. The obtained value was 100 : 16.

3.2.10 Synthesis of Block Copolymer PEO-*b*-P(DEGMMA-*co*-*t*BMA) by ATRP Using Macroinitiator PEO-Br

A typical procedure for the synthesis of PEO-*b*-P(DEGMMA-*co*-*t*BMA) is described below. CuBr (8.3 mg, 0.058 mmol), DEGMMA (1.96 g, 10.4 mmol), PEO-Br (0.31 g, 0.060 mmol), *t*BMA (0.196 g, 1.38 mmol), anisole (4.81 g), and PMDETA (17.3 mg, 0.10 mmol) were added into a 25 mL two-necked flask. After the mixture was degassed by three freeze-pump-thaw cycles, the flask was placed in a 60 ^oC oil bath. After the polymerization proceeded for 63 min, the reaction mixture was diluted with THF and passed through a neutral Al_2O_3 column with THF as eluent to remove the catalyst. The obtained polymer solution was concentrated and precipitated in a mixture of hexanes and diethyl ether (v/v = 80 : 20). The polymer was re-dissolved in THF and precipitated again in the mixture of hexanes and diethyl ether (v/v = 80 : 20). This purification process was repeated one more time. The polymer was then dried in high vacuum and obtained as a viscous liquid. GPC analysis results (polystyrene standards): $M_{n,GPC}$ = 21800 Da, PDI = 1.06. The composition of the block copolymer was determined

from the ^{1}H NMR spectrum. The number of DEGMMA units in the block copolymer was calculated using the integral values of the peak from 4.5 to 4.0 ppm (-CH_2OCO- of DEGMMA unit) and the peaks from 4.0 to 3.2 ppm (-OCH_2- from the PEO block and DEGMMA unit). The obtained number of DEGMMA units was 100. The number of *t*BMA units was calculated from the integral values of the peak from 1.6 to 1.4 ppm (-C(CH_3)$_3$of *t*BMA unit) and the peaks from 4.0 to 3.2 ppm (-OCH_2- in the PEO block and DEGMMA unit). The obtained number of *t*BMA units was 18.

3.2.11 Removal of *t*-Butyl Group of P(DEGMMA-*co*-P*t*BMA) and PEO-*b*-P(DEGMMA-*co*-*t*BMA)

The following is a typical procedure for removing *t*-butyl groups from the random and block copolymers. PEO-*b*-P(DEGMMA-*co*-MAA-*t*BMA) (0.22 g, $M_{n,GPC}$ = 21800 Da, PDI = 1.06) was dissolved in dry dichloromethane (4.0 mL) in a 20 mL scintillation vial. After addition of trifluoroacetic acid (2.01 g), the reaction mixture was stirred at room temperature for 24 h. The solvent was then removed by the use of a rotavapor. The residue was dissolved in 20 mL dichloromethane and the solvent was evaporated again by the use of a rotavapor. This process was repeated one more time to remove most of trifluoroacetic acid. The polymer was then dissolved in THF (5 mL) and precipitated in a mixture of hexanes and diethyl ether (v/v = 80 : 20, 100 mL) twice. The polymer was obtained as a viscous liquid (0.20 g, yield: 91 %). The successful removal of *tert*-butyl group was supported by the disappearance of the peak at 1.6 - 1.4 ppm in the ^{1}H NMR spectrum.

3.2.12 Treatment of PDEGMMA with CF_3COOH

To confirm that CF_3COOH will not affect the ester group of PDEGMMA, a control experiment was conducted as follows. PDEGMMA (0.19 g, $M_{n,GPC}$ = 16200 Da, PDI = 1.11) and CF_3COOH (2.1 g) were dissolved in dry dichloromethane (4 mL) in a 20 mL scintillation vial. The mixture was stirred at room temperature for 24 h. The solvent was then removed by the use of a rotavapor. The residue was dissolved in dichloromethane (20 mL) and the solvent was evaporated again by the use of a rotavapor. This process was repeated one more time to remove most of CF_3COOH. The polymer was then dissolved in THF (5 mL) and precipitated in a mixture of hexanes and diethyl ether (v/v = 80 : 20, 100 mL) twice. ^{1}H NMR spectroscopy and GPC analysis confirmed that there was no change of PDEGMMA after treatment with CF_3COOH.

3.3 Results and Discussion

3.3.1 Synthesis and Hydrolysis of Random Copolymer P(DEGMMA-*co*-*t*BMA) and Block Copolymer PEO-*b*-P(DEGMMA-*co*-*t*BMA)

Poly(methoxydi(ethylene glycol) methacrylate) (PDEGMMA) belongs to a new family of thermosensitive water-soluble polymers in which short oligo(ethylene glycol) groups are covalently bonded to the polymer backbone as a pendant group from each repeating unit.[24-30,40,56,57,67-80] The cloud point can be readily tuned by varying the type of polymer backbone, the length and end group of oligo(ethylene glycol) pendant, or the chain end group, or by copolymerizing with a second monomer. One advantage of these thermosensitive water-soluble polymers is that the short oligo(ethylene glycol) pendant groups render the polymers a property of biocompatibility.[81] In this work, thermo- and

pH-sensitive water-soluble block copolymers, PEO-*b*-P(DEGMMA-*co*-MAA), with controlled molecular weights and narrow polydispersities were prepared and used to pursue multiple reversible micellization and dissociation transitions by controlling both temperature and pH. PDEGMMA was chosen in this work because its reported cloud point in water is 25 ^{o}C, which is located in a convenient temperature range.

The macroinitiator, PEO with a molecular weight of 5000 Da and one end functionalized with an ATRP initiator (PEO-Br), was prepared by following the same procedure in the chapter 2. Block copolymers PEO-*b*-P(DEGMMA-*co*-*t*-butyl methacrylate) (PEO-*b*-P(DEGMMA-*co*-*t*BMA), **BR3** and **BR4** in Table 3.1) were synthesized from macroinitiator PEO-Br by ATRP of a mixture of DEGMMA and *t*BMA with a molar ratio of 100 : 13 at 60 ^{o}C in anisole using CuBr/*N,N,N′,N′,N″*-pentamethyldiethylenetri-amine as catalyst. The polymers were purified by repeated precipitation in a mixture of hexanes and diethyl ether (v/v, 80 : 20). Gel permeation chromatography (GPC) analysis showed that the peaks of block copolymers shifted to the high molecular weight side compared with that of the macroinitiator PEO-Br and were narrow.[82] For the study of pH effect on cloud point, one homopolymer PDEGMMA (**H1**) and one random copolymer P(DEGMMA-*co*-*t*BMA) (**R2**) were prepared by the use of ethyl 2-bromoisobutyrate as initiator. The degrees of polymerization (DPs) of **H1** and **R2** were calculated from the monomer conversion and the monomer-to-initiator ratio, assuming that the initiator efficiency was 100%. The numbers of DEGMMA and *t*BMA units in the two samples of PEO-*b*-P(DEGMMA-*co*-*t*BMA) (**BR3** and **BR4**) were determined from ^{1}H NMR spectra. The molar ratios of DEGMMA to *t*BMA units in the two block copolymers were essentially identical (~ 100 : 18), and were also close to that

Table 3.1. Characterization Data for PDEGMMA, P(DEGMMA-*co*-*t*BMA) and the Corresponding P(DEGMMA-*co*-MAA), Two Samples of PEO-*b*-P(DEGMMA-*co*-*t*BMA) and the Corresponding PEO-*b*-P(DEGMMA-*co*-MAA) Used in this Work

No.	Polymers	$M_{n,GPC}$ (Da)[a]	PDI[a]	n_{EO} : n_{DEGMMA} : n_{tBMA}[b]
H1	PDEGMMA	16200	1.11	0 : 85 : 0 [c]
R2	P(DEGMMA-*co*-*t*BMA)	15000	1.14	0 : 71 : 11[c,d]
R2-H	P(DEGMMA-*co*-MAA)	NA	NA	0 : 71 : 11
BR3	PEO-*b*-P(DEGMMA-*co*-*t*BMA)	21800	1.06	113 : 100 : 18
BR3-H	PEO-*b*-P(DEGMMA-*co*-MAA)	NA	NA	113 : 100 : 18
BR4	PEO-*b*-P(DEGMMA-*co*-*t*BMA)	30200	1.07	113 : 144 : 25
BR4-H	PEO-*b*-P(DEGMMA-*co*-MAA)	NA	NA	113 : 144 : 25

[a]The number average molecular weight ($M_{n,GPC}$) and polydispersity index (PDI) were determined by gel permeation chromatography using polystyrene calibration. [b]n_{EO}, n_{DEGMMA}, and n_{tBMA} (or n_{MAA}) are the numbers of EO (in the PEO block), DEGMMA, and *t*BMA units (or the corresponding MAA units) in the polymers, respectively. The values of n_{DEGMMA} and n_{tBMA} in the block copolymers were determined from ^{1}H NMR spectra. [c]The degrees of polymerization of PDEGMMA and P(DEGMMA-*co*-*t*BMA) were calculated from the monomer conversion and the monomer-to-initiator ratio assuming that the initiator efficiencies were 100 % in the polymerizations. [d]The molar ratio of DEGMMA and *t*BMA in the random copolymer was determined from ^{1}H NMR spectrum.

in the random copolymer **R2** (~ 100 : 16). The molecular characteristics of the polymers used in this work are summarized in Table 3.1. The polydispersities of all these polymers, determined from GPC using PS standards, were < 1.15.

The *t*-butyl groups of P(DEGMMA-*co*-*t*BMA) and PEO-*b*-P(DEGMMA-*co*-*t*BMA) were removed by the use of CF_3COOH, which has been shown to selectively cleave the *t*-butyl ester group without affecting other types of esters.[73] ^1H NMR spectroscopy analysis of **BR3** and **BR4** before and after treatment with CF_3COOH revealed that the peak located at 1.40 ppm, which is characteristic for *t*-butyl group, disappeared, indicating that the hydrolysis was essentially complete. To confirm that the ester group of PDEGMMA was not affected by CF_3COOH, a control experiment was carried out by treating PDEGMMA (**H1**) with CF_3COOH under the same condition. No changes were observed from ^1H NMR spectra and GPC analysis.[82]

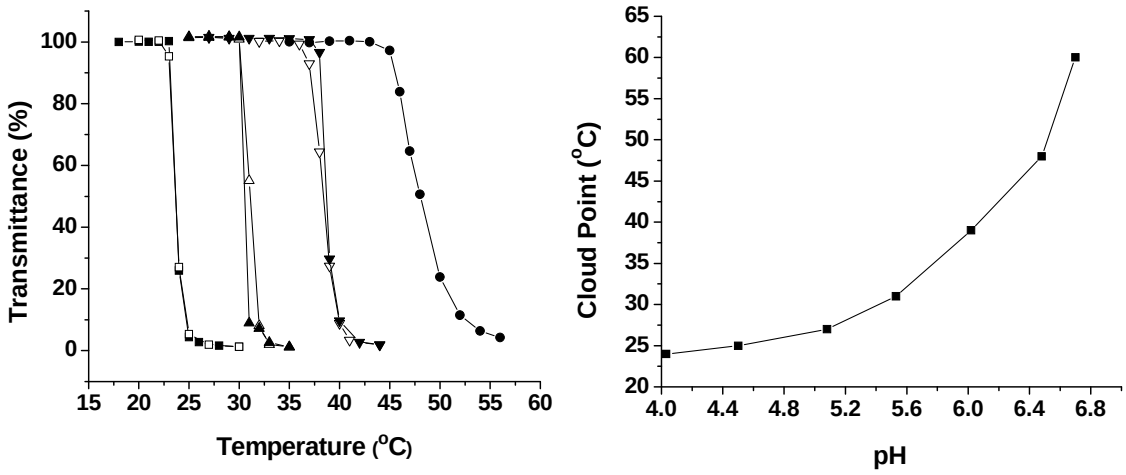
3.3.2 Thermosensitive Properties of P(DEGMMA-*co*-MAA) and PDEGMMA

The hypothesis of achieving multiple reversible micellization and dissociation transitions as shown in Scheme 3.2 is based on that the LCST transition temperature of the thermosensitive block that contains a small amount of carboxylic acid groups can be tuned in a large temperature range by changing the solution pH. To be able to readily tune and precisely control the pH, the KHP buffers instead of pure water were used to make polymer solution. Thus, the thermoresponsive properties of P(DEGMMA-*co*-MAA) (**R2-H**) in 10 mM aqueous KHP buffer solutions with pH ranging from 4.0 – 7.0 were studied first. The pH was adjusted by addition of an aqueous KOH solution and was measured by a pH meter.

Figure 3.1a shows the optical transmittances of 0.2 wt % aqueous buffer solutions of **R2-H** with pH values of 4.0, 5.5, 6.0, and 6.5 at wavelength of 550 nm as a function of temperature. At pH values of 4.0, 5.5, and 6.0, the thermo-induced phase transitions were sharp and there were essentially no hystereses between heating and cooling processes. Apparently, the cloud point (CP) increases with the increase of pH (Figure 3.1b, the CP is defined as the temperature at which the optical transmittance drops by 50 %). A higher pH results in a higher degree of ionization of carboxylic acid groups, which shifts the hydrophobic/hydrophilic balance of the thermosensitive block, making the transition occur at a higher temperature. The LCST transition of **R2-H** in the buffer with pH = 6.5 is noticeably broader than in other three buffers, indicating that the transition at this pH is weaker, which is likely because more charges residing on the polymer chains at a higher pH result in less structured or "frozen" water being released from hydrated polymer chains during the transition as discussed by Urry.[83] At pH = 7.0, no LCST transition was observed up to 70 ^{o}C. Figure 3.1 shows that the CP of **R2-H** can be tuned in a temperature range from 24 to 60 ^{o}C, providing great flexibility in controlling the micellization and dissociation transitions of the corresponding block copolymers in water. In contrast, the pH has little effect on the CP of PDEGMMA (CP of **H1** = 27.5 ^{o}C at pH = 4.1, 27 ^{o}C at pH = 5.3, and 26.5 ^{o}C at pH = 6.1).[82]

3.3.3 Temperature-Induced Reversible Micellization/Dissociation Transitions of PEO-*b*-P(DEGMMA-*co*-MAA) in Aqueous Buffer Solutions

Two samples of PEO-*b*-P(DEGMMA-*co*-MAA) with different molecular weights but essentially the same compositions for the thermosensitive blocks (**BR3-H** and **BR4-H**)

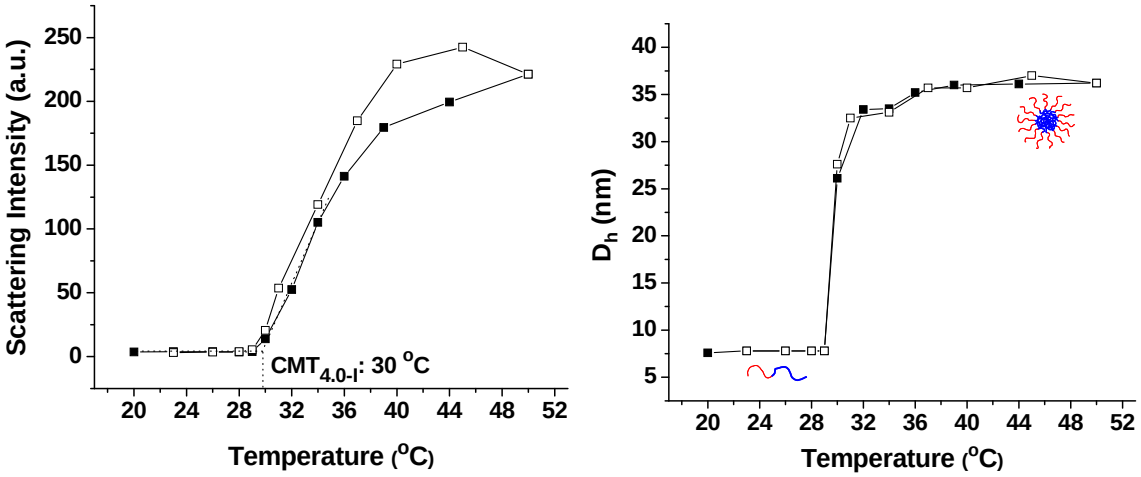


(a) (b)

Figure 3.1. (a) Optical transmittances at wavelength of 550 nm of 0.2 wt % aqueous solutions of P(DEGMMA-*co*-MAA) (**R2-H**) in 10 mM potassium hydrogen phthalate buffers with pH values of 4.0 (■ heating; □ cooling), 5.5 (▲ heating; △ cooling), 6.0 (▼ heating; ▽ cooling), and 6.5 (● heating) as a function of temperature. The transmittances were recorded with a UV-visible spectrometer. (b) Dependence of the cloud point of **R2-H** on the solution pH.

were used for the study of thermo- and pH-induced multiple reversible micellization and dissociation transitions in aqueous KHP buffer solutions. Their reversible micellization in response to temperature changes at pH = 4.0 were first studied by dynamic light scattering (DLS) and fluorescence spectroscopy (FS).

Figure 3.2 shows the intensity of scattered light at scattering angle of 90^{o} and the hydrodynamic size as a function of temperature for a 0.2 wt % aqueous buffer solution of **BR3-H** with a pH of 4.0. When the temperature was ≤ 29 ^{o}C, the scattering intensity was very low and the hydrodynamic size was < 8 nm, indicating that the block copolymer was dissolved molecularly in water. With the increase of temperature, the scattering intensity gradually increased, and two size distributions, one ascribed to the unimers and one to the micelles, were observed at 30 ^{o}C with an average hydrodynamic size of 26.1 nm, indicating that the thermosensitive block was undergoing a hydration-to-dehydration transition at 30 ^{o}C. The critical micellization temperature ($CMT_{4.0\text{-}I}$), determined from the plot of intensity of scattered light versus temperature in the heating process (Figure 3.2a), was 30 ^{o}C, which was 6 ^{o}C higher than the CP of P(DEGMMA-*co*-MAA) at the same pH. This observation is similar to that of thermo- and light-sensitive block copolymer PEO-*b*-poly(ethoxytri(ethylene glycol) acrylate-*co*-*o*-nitrobenzyl acrylate) in the previous chapter. It is known that the LCST transition temperature is slightly higher when a thermosensitive polymer is attached to a hydrophilic block.[1-3] When the temperature reached 32 ^{o}C, only micelles with apparent hydrodynamic diameter (D_h) of 33.4 nm were observed. The micelle size became stabilized around 36 nm. The polydispersity of micelles at 50 ^{o}C was 0.018, indicating that the micelles were uniform in size.[82] Moreover, it was found that the value of Γ/q^2 was essentially independent of scattering



(a) (b)

Figure 3.2. The intensity of scattered light at scattering angle of 90° (a) and the hydrodynamic diameter (b) as a function of temperature (■ heating, □ cooling) in a DLS study of a 0.2 wt % aqueous buffer solution of PEO-*b*-P(DEGMMA-*co*-MAA) (**BR3-H**) at pH = 4.0. In (b), at 30 °C in both heating and cooling processes, two size distributions, one ascribed to the unimers and one to the micelles, were observed and the reported hydrodynamic diameters for this temperature were the average values over two hydrodynamic size distributions.

angle,[82] suggesting that the micelles were of a spherical shape. The thermo-induced micellization was reversible; decreasing the temperature caused the micelles to dissociate into the unimers (Figure 3.2).

The thermo-induced reversible micellization of **BR4-H** in a 10 mM KHP buffer with a pH of 4.0 was also studied by DLS[82] and the results are summarized in Table 3.2 along with those from **BR3-H**. The $CMT_{4.0\text{-}I}$ of **BR4-H** at the same concentration (0.2 wt %) and same pH (4.0) was 26 ^{o}C, which was 4 ^{o}C lower than that of **BR3-H** but 2 ^{o}C higher than the CP of **R2-H**. This is understandable because the molecular weight of the thermosensitive block in **BR4-H** is higher than that in **BR3-H** and a higher molecular weight thermosensitive polymer tends to undergo a LCST transition at a lower temperature.[72] The hydrodynamic diameter of micelles of **BR4-H** at 50 ^{o}C was ~ 46 nm, which was ~ 10 nm larger than that of **BR3-H** under the same condition (Table 3.2). The micelles of **BR4-H** also had narrow polydispersities, and a spherical shape (as suggested by the independence of Γ/q^2 on scattering angle).[82]

The thermo-induced reversible formation and dissociation of micelles of **BR3-H** and **BR4-H** were further studied by FS.[82] Nile Red was used as the fluorescence probe because its fluorescence is known to increase substantially in a hydrophobic environment such as the core of micelles.[16,17,37,40] The fluorescence emission spectra of Nile Red in a 0.2 wt % aqueous buffer solution of **BR3-H** with a pH of 4.0 at various temperatures upon heating were recorded (Figure B.9 in Appendix B).[82] The noticeable fluorescence intensity at temperatures < 30 ^{o}C might be due to the enhanced solubilization of Nile Red by the polymer in water.[37,40] When the temperature was raised above 30 ^{o}C, the

Table 3.2. Critical Micellization Temperatures of Block Copolymer PEO-*b*-P(DEGMMA-*co*-MAA) (BR3-H and BR4-H), and the Hydrodynamic Sizes and Polydispersities of Their Micelles under Various Conditions

Buffer pH	Description	**BR3-H**	**BR4-H**
pH = 4.0	$CMT_{4.0\text{-}I}$	30 °C, [a] 30 °C [b]	26 °C, [a] 26 °C [b]
	Size [c] and PD [d] of Micelles at 50 °C	36.2 nm, 0.018	45.8 nm, 0.004
pH = 5.4 (the buffer pH after addition of KOH)	$CMT_{5.4}$	37 °C, [a] 36 °C [b]	33 °C, [a] 33 °C [b]
	Size and PD of Micelles at 50 °C	38.3 nm, 0.055	65.3 nm, 0.034
pH = 4.0 (the buffer pH after addition of HCl)	$CMT_{4.0\text{-}II}$	29 °C, [a] 29 °C [b]	25 °C, [a] 25 °C [b]
	Size and PD of Micelles at 50 °C	36.2 nm, 0.004	46.6 nm, 0.003

[a] Critical micellization temperature (CMT) determined by DLS; [b] CMT determined by FS; [c] the hydrodynamic diameter of micelles at a specific temperature was obtained by the use of the CONTIN method; [d] The polydispersity (PD) of micelles at a specific temperature obtained by the use of the CONTIN method. The concentration of block copolymers in the buffer was 0.2 wt %.

fluorescence emission intensity increased significantly, indicating that the molecularly dissolved polymer chains began to associate into micelles and the dye molecules were sequestered into the core. The maximum peak underwent a blueshift with the increase of temperature, from 623.5 nm at 20 ^{o}C to 615.5 nm at 50 ^{o}C, which further supported that the dye molecules moved from a hydrophilic to a hydrophobic environment and thus the micelles formed in the solution.[16,17,37,40] The $CMT_{4.0\text{-}I}$, determined from the plot of maximum fluorescence intensity versus temperature, was 30 ^{o}C, same as that obtained from DLS study. When the temperature was decreased to 22 ^{o}C, the fluorescence emission intensity decreased and the λ_{max} underwent a redshift from 615.5 nm at 50 ^{o}C to 623 nm at 22 ^{o}C,[82] indicating that the micelles were dissociated into the unimers and the dye molecules were released into water. Thus, consistent with DLS study, the thermo-induced micellization was reversible. Similarly, the thermo-induced reversible micellization of **BR4-H** under the same conditions was studied by FS. The $CMT_{4.0\text{-}I}$[82] was found to be at 26 ^{o}C, consistent with the results obtained from DLS study (Table 3.2).

3.3.4 KOH-Triggered Dissociation of Micelles and Subsequent Temperature-Induced Formation and Disassembly of Micelles

As shown in the preceding section, when the temperature is above $CMT_{4.0\text{-}I}$, the thermosensitive block of **BR3-H** or **BR4-H** underwent a hydration-to-dehydration transition and the block copolymer molecules self-assembled into the micelles. If a condition is chosen under which the LCST of the thermosensitive block becomes higher than the solution temperature, dissociation of micelles will occur. Since we were especially interested in disassembling micelles in situ by changing the solution pH and it

was not practical and convenient to measure the pH of a solution in a DLS tube or a fluorescence quartz cuvette, how the solution pH varied with the addition of KOH was investigated and used as a guide for determining how much KOH needs to be added to achieve a particular pH. The titration experiment was conducted on a 0.2 wt % aqueous solution of **BR3-H** in 10 mM KHP buffer (2.50 g) by injecting 10 μL of a 0.20 M KOH solution each time and subsequently measuring the pH with a pH meter. A plot of solution pH versus number of μmol of added KOH was obtained, and is shown in Figure 3.3. Note that after the completion of titration, the volume increased by only 6.8 %, which had a negligible effect on the concentrations of KHP and the polymer. The titration curve of a 0.2 wt % aqueous solution of **BR4-H** in 10 mM KHP buffer was also obtained, which is identical to the one shown in Figure 3.3.[82] Figures 3.1b and 3.3 were used as a guide for effecting dissociation of micelles in situ in the DLS and FS experiments.

In Figure 3.2b, at 34 ^{o}C, the micelles of **BR3-H** were well developed and only one size distribution was observed from DLS. Thus, this temperature was well suited for effecting dissociation of micelles by injection of an aqueous KOH solution. Figure 3.2 shows that at pH = 4.0 the $CMT_{4.0\text{-}I}$ of **BR3-H** is 6 ^{o}C higher than the CP of **R2-H**. Assuming that the difference between the CP of **R2-H** and the CMT of **BR3-H** at a higher pH is the same as that at pH = 4.0, to disrupt the micelles at 34 ^{o}C, a pH value must be chosen at which the CP of **R2-H** is at least 28 ^{o}C. From Figure 3.1b, a CP of 28 ^{o}C corresponds to a pH value of 5.2, and from Figure 3.3, 16 μmol of KOH needs to be added to bring the pH to 5.2. To ensure that the micelles were disrupted, 19 μmol of KOH was injected via a microsyringe into DLS tube and the solution pH increased to 5.4.

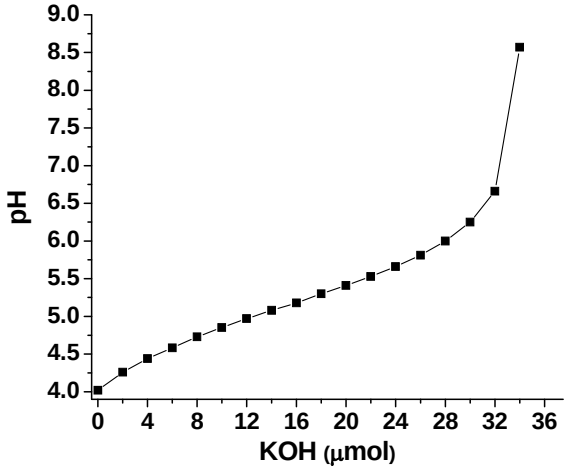
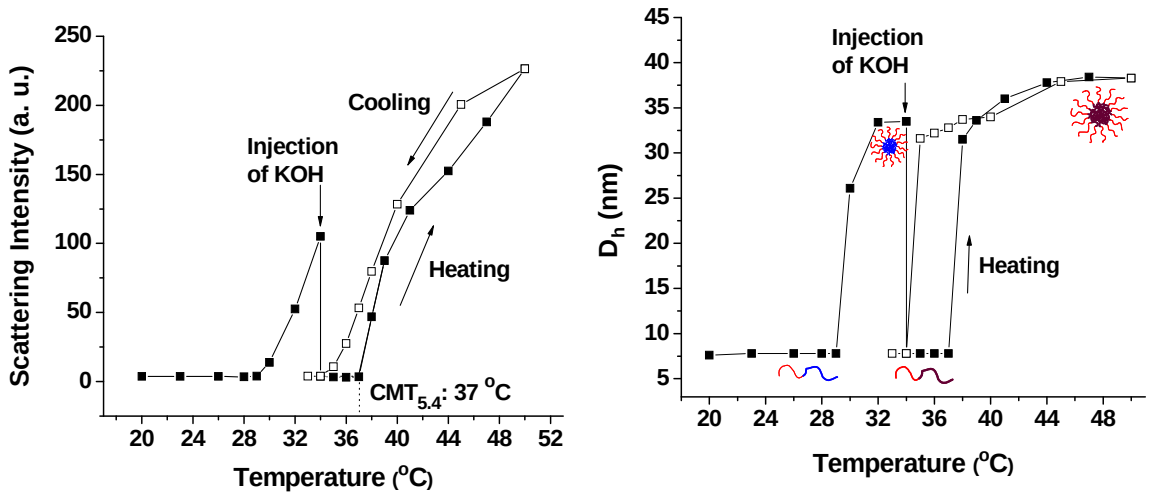


Figure 3.3. The plot of solution pH versus number of μmols of KOH injected into a 0.2 wt % solution of PEO-*b*-P(DEGMMA-*co*-MAA) (**BR3-H**) in 10 mM KHP buffer (2.50 g). The KOH solution was added stepwise; each time, 10 μL of a 0.20 M aqueous KOH solution was injected via a microsyringe, followed by the measurement of pH with a pH meter.

Figure 3.4 shows the DLS data. The scattering intensity dropped immediately to the level before the micellization of the polymer solution at pH = 4.0 and the hydrodynamic size decreased from 33.5 nm to 7.8 nm, clearly indicating that the micelles disassembled into the individually dissolved block copolymer molecules in the solution.

The solution was then gradually heated from 34 to 50 ^{o}C. When the temperature was above 37 ^{o}C, the scattering intensity began to increase, and the average hydrodynamic size jumped from 7.8 nm at 37 ^{o}C to 31.5 nm at 38 ^{o}C and eventually became stabilized around 38 nm with the increase of temperature. These observations indicate that when the temperature was > 37 ^{o}C, the thermosensitive block of **BR3-H** became dehydrated again and the micelles re-formed. The CMT of **BR3-H** at the new pH ($CMT_{5.4}$), determined from the heating curve in Figure 3.4a, was 37 ^{o}C. Note that at pH = 5.4, the CP of **R2-H** is 30 ^{o}C. Thus, the predicted CMT of **BR3-H** at this pH would be 36 ^{o}C (30 + 6 ^{o}C), only 1 ^{o}C different from the experimentally observed value, 37 ^{o}C . The hydrodynamic size of the micelles at 50 ^{o}C was 38.3 nm, which was slightly larger than that of the micelles of **BR3-H** at pH = 4.0 and T = 50 ^{o}C (36.2 nm), likely because more carboxylic acid groups on the thermosensitive block were ionized at pH = 5.4, resulting in charge-charge repulsive interactions in the core and/or more molecules being assembled in each micelle. The micelles at 50 ^{o}C had narrow polydispersities, and a spherical shape.[82] As shown in Figure 3.4, upon cooling, both the scattering intensity and the hydrodynamic size decreased, and at 34 ^{o}C, the observed hydrodynamic size was < 8 nm, indicating that the micelles were completely dissociated. However, unlike the transitions in Figure 3.2b where the cooling and heating curves superimposed each other, there was a hysteresis between heating and cooling in Figure 3.4 (~ 3 ^{o}C difference).

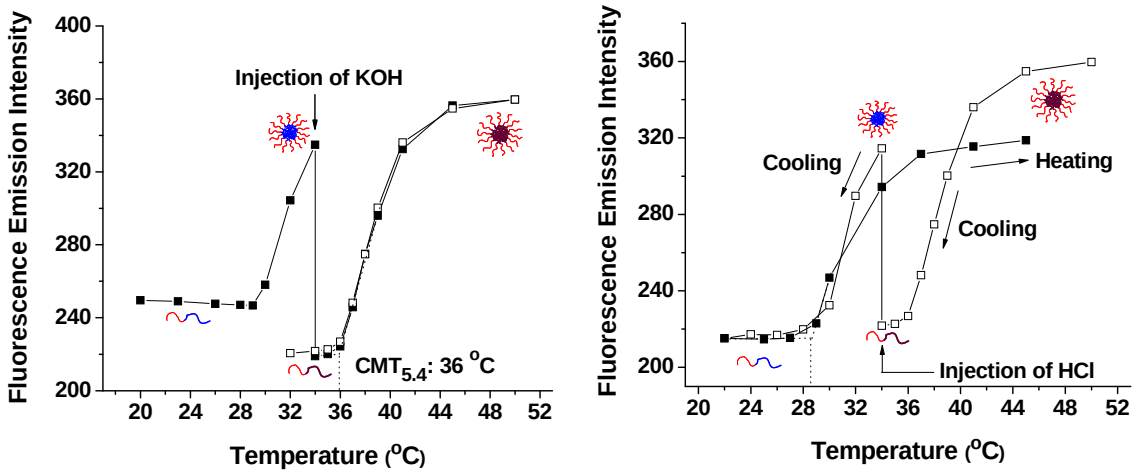


(a) (b)

Figure 3.4. Intensity of scattered light at scattering angle of 90° (a) and the apparent hydrodynamic diameter (b) as a function of temperature (■ heating, □ cooling) in a DLS study of multiple micellization and dissociation transitions of a 0.2 wt % solution of PEO-*b*-P(DEGMMA-*co*-MAA) (**BR3-H**) in 10 mM KHP buffer solution (2.50 g, the same solution used in Figure 3.2) in response to addition of KOH (19 μL of 1.00 M KOH at 34 °C) and subsequent temperature changes. The data points from 20 °C to 34 °C were from the heating process in Figure 3.2.

Similar results were obtained from **BR4-H** (Table 3.2 and Appendix B, KOH was injected at 30 ^{o}C), and there was also a hysteresis of 3 ^{o}C between the heating and cooling curves.[82] However, the average hydrodynamic diameter of micelles of **BR4-H** at T = 50 ^{o}C and pH = 5.4 (65.3 nm) was ~ 20 nm larger than that of **BR4-H** at the same temperature but a pH of 4.0 (45.8 nm). This is in contrast to a difference of only 2 nm for the micelles of **BR3-H** at the two different pH values (Table 3.2). Likely, the chain length of the thermosensitive block plays an important role here; the longer chain of **BR4-H** had more charges at the same pH, resulting in larger micelles.

FS studies showed that after the injection of KOH at 34 ^{o}C to increase the pH of the **BR3-H** solution to 5.4, the fluorescence emission intensity of Nile Red decreased dramatically (Figure 3.5a) and the maximum peak position shifted from 618 nm to 623 nm, indicating that the micelles were dissociated into the unimers. Further increasing temperature resulted in the re-formation of micelles, as evidenced by the increase of fluorescence emission intensity and the blueshift of λ_{max} (from 623 nm at 34 ^{o}C to 615 nm at 50 ^{o}C). The transition is reversible; cooling from 50 to 32 ^{o}C triggered the disassembly of micelles. The CMT ($CMT_{5.4}$) determined from the plot of maximum emission intensity versus temperature was 36 ^{o}C, very close to that from DLS (37 ^{o}C). Unlike the observations from DLS, there was no hysteresis between cooling and heating curves in Figure 3.5a. Since the fluorescence property of Nile Red is very sensitive to the microenvironment, this observation suggests that the micelles in the range of 35-37 ^{o}C in the cooling curve of Figure 3.4 were in a metastable state. For **BR4-H**, KOH was added at 30 ^{o}C and the CMT at pH = 5.4 ($CMT_{5.4}$) from FS studies was 33 ^{o}C, identical to that from the DLS experiment (Table 3.2).

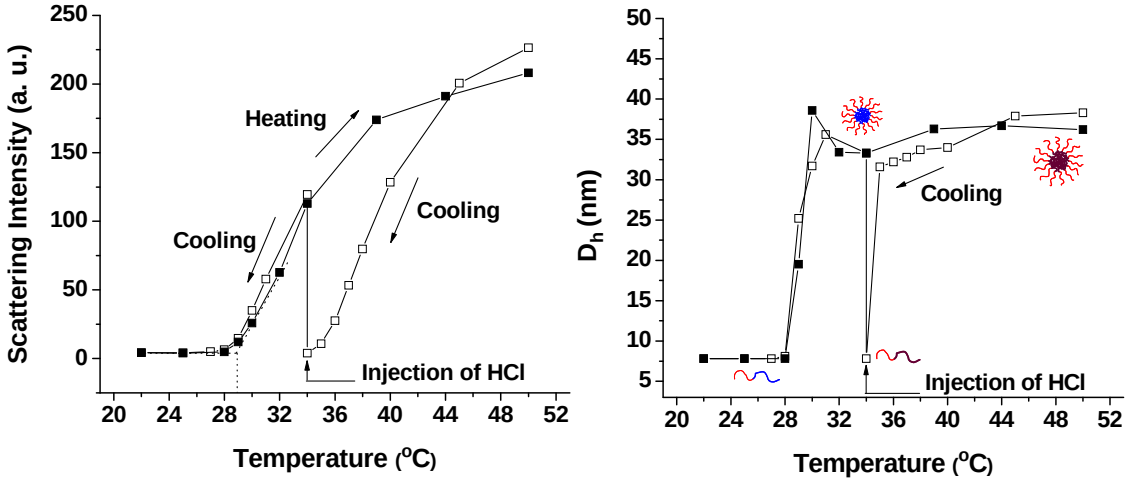


(a) (b)

Figure 3.5. Maximum fluorescence emission intensity of Nile Red in a 0.2 wt % solution of **BR3-H** (PEO-*b*-P(DEGMMA-*co*-MAA)) in 10 mM KHP buffer in response to pH and subsequent temperature changes (■ heating, □ cooling). In (a), at 34 °C, 7.5 μmol of KOH was injected into the fluorescence quartz cuvette that contained 1.00 g of a 0.2 wt % polymer buffer solution (the pH increased from 4.0 to 5.4). In (b), the data points from 50 to 34 °C were from the cooling process in (a). At 34 °C, 7.5 μmol of HCl was injected into the solution (1.00 g) to change the pH from 5.4 to 4.0.

3.3.5 HCl-Triggered Formation of Micelles and Subsequent Temperature-Induced Dissociation and Re-formation of Micelles

To find out whether the KOH-triggered dissociation of micelles was a reversible process, the same amount of HCl as that of KOH was injected into the solution of **BR3-H** at 34 ^{o}C. The pH changed back to 4.0 from 5.4. The intensity of scattered light at scattering angle of 90^{o} jumped up immediately and micelles with a hydrodynamic size of 33.3 nm were observed (Figure 3.6). The micelle size and the scattering intensity were essentially identical to those obtained by heating the 0.2 wt % polymer solution with a pH of 4.0 from 20 ^{o}C to 34 ^{o}C in Figure 3.2, which conclusively demonstrated the reversibility of pH-induced transition of **BR3-H**. Furthermore, the micelles were dissociated when the temperature was decreased below 28 ^{o}C. Subsequent heating induced micellization and the hydrodynamic size and the scattering intensity at 34 ^{o}C were essentially identical to those observed right after the addition of HCl. From the plot of scattering intensity versus temperature in the heating curve, the CMT ($CMT_{4.0\text{-}II}$) was found at 29 ^{o}C, which was only 1 ^{o}C different from $CMT_{4.0\text{-}I}$ in Figure 3.2 (Table 3.2). The size of the micelles at 50 ^{o}C was 36.2 nm. Also, the micelles had narrow polydispersities, and a spherical shape.[82] The pH- and temperature-induced reversible micellization processes were also supported by the results from FS studies (Figure 3.5b). After the addition of HCl at 34 ^{o}C, the fluorescence emission intensity of Nile Red jumped from the level for the unimers to the level for the micelles, and the maximum peak shifted from 622.5 to 617 and to 622 nm upon cooling to 22 ^{o}C, which indicated the formation and the subsequent dissociation of micelles. Upon heating, the fluorescence emission intensity gradually increased and the λ_{max} underwent a blueshift from 622 nm



(a) (b)

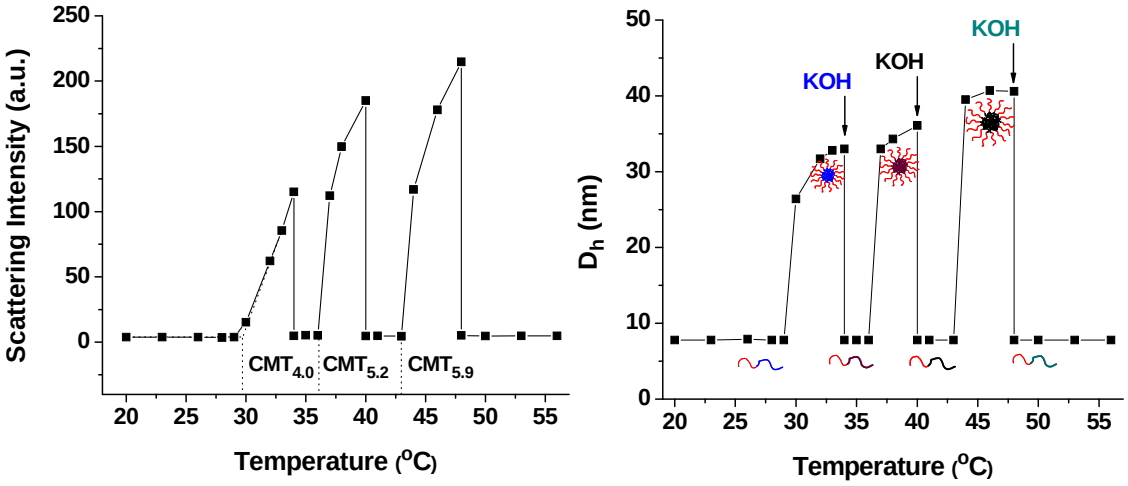
Figure 3.6. The intensity of scattered light at a scattering angle of 90° (a) and the hydrodynamic diameter (b) as a function of temperature (□ cooling, ■ heating) in a DLS study of multiple micellization/dissociation transitions of a 0.2 wt % solution of PEO-*b*-P(DEGMMA-*co*-MAA) (**BR3-H**) in 10 mM KHP buffer solution (2.50 g, the same solution used in Figure 3.3) in response to addition of HCl (19 μL of 1.00 M HCl solution at 34 °C) and subsequent temperature changes. The data points in the cooling curve from 50 to 34 °C were from the cooling process in Figure 3.3. In (b), at 30 °C in both cooling and heating processes, two size distributions were observed and the reported hydrodynamic diameters for this temperature were the average values over two hydrodynamic size distributions.

at 22 ^{o}C to 617.5 nm at 34 ^{o}C, to 614.5 nm at 45 ^{o}C, indicating the formation of micelles.

Similar results were obtained from the study of **BR4-H** by DLS and FS[82] and are summarized in Table 3.2. Note that the CMT values of **BR3-H** and **BR4-H** ($CMT_{4.0\text{-}I}$, $CMT_{5.4}$, and $CMT_{4.0\text{-}II}$) were consistently higher than the CPs of **R2-H** at the corresponding pH values by 5-7 ^{o}C and 2-3 ^{o}C, respectively. These observations support our assumption that the difference between the CMT of PEO-*b*-P(DEGMMA-*co*-MAA) and CP of **R2-H** was largely the same in the studied pH range.

3.3.6 Three Cycles of Micellization and Dissociation Transitions of Thermo- and pH-Responsive Block Copolymer PEO-*b*-P(DEGMMA-*co*-MAA) Achieved by Judiciously Controlling Temperature and pH

PEO-*b*-P(DEGMMA-*co*-MAA) was shown to undergo reversible micellization /dissociation transitions in response to temperature and pH changes. The following experiments were then conducted to pursue multiple micellization/dissociation transitions by gradually increasing the temperature and simultaneously controlling the pH. For 0.2 wt % solutions of **BR3-H** in 10 mM KHP buffer with a pH value of 4.0 (Figures 3.7 and 3.8), the block copolymer underwent micellization with the increase of temperature and the CMT at pH = 4.0 ($CMT_{4.0}$) was 30 ^{o}C, same as that found in Figure 3.2. The micelle size at 34 ^{o}C (33.0 nm) was essentially identical to that of micelles in Figures 3.2 (33.5 nm) and 3.7 (33.3 nm). As discussed earlier, to disassemble the micelles at 34 ^{o}C, the pH needs to be increased to at least 5.2, assuming that the difference between the CP of **R2-H** and the CMT of **BR3-H** at pH = 5.2 is the same as that at pH = 4.0 (6 ^{o}C). After the injection of the calculated amounts of KOH into the solutions at 34 ^{o}C to increase the pH



(a) (b)

Figure 3.7. The intensity of scattered light at a scattering angle of 90° (a) and the hydrodynamic diameter (b) as a function of temperature in a DLS study of multiple micellization and dissociation transitions of a 0.2 wt % solution of PEO-*b*-P(DEGMMA-*co*-MAA) (**BR3-H**) in 10 mM KHP buffer solution (2.50 g) in response to temperature and pH changes. At 34 °C, 16 μL of a 1.00 M KOH solution was injected into the solution (the pH changed to 5.2). At 40 °C, 11 μL of a 1.00 M KOH solution was injected (the pH changed to 5.9). At 48 °C, 7.0 μL of a 1.00 M KOH solution was injected (the pH changed to ~ 8.6). In (b), at 30 °C, two size distributions were observed, and the reported hydrodynamic diameter for this temperature was the average value over two hydrodynamic size distributions.

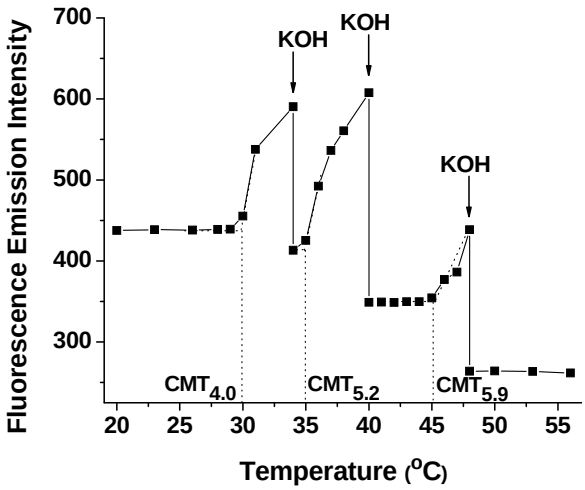


Figure 3.8. Maximum fluorescence emission intensity of Nile Red in a 0.2 wt % solution of PEO-*b*-P(DEGMMA-*co*-MAA) (**BR3-H**) in 10 mM KHP buffer solution in response to the temperature and pH changes. At 34 ^{o}C, 6.3 μmol of KOH was injected into the solution (the pH changed to 5.2); the λ_{max} shifted from 617 to 621.5 nm. At 40 ^{o}C, 4.5 μL of 1.00 M KOH was added (the pH changed to 5.9); the λ_{max} changed from 615.5 nm to 623 nm. At 48 ^{o}C: 2.7 μL of 1.00 M KOH was injected (the pH changed to ~ 8.6); the λ_{max} shifted from 616.5 nm to 625 nm.

to 5.2, the DLS results (the intensity of scattered light at scattering angle of 90^{o} and the hydrodynamic size) and the FS data (fluorescence emission intensity and the maximum peak position) showed that the micelles were dissociated into the molecularly dissolved unimers.

The solutions were then gradually heated up from 34 ^{o}C, and it was found from DLS and FS that the micelles re-formed when the temperature was above a critical point ($CMT_{5.2}$ = 36 ^{o}C from DLS and 35 ^{o}C from FS). The size of the micelles at 40 ^{o}C was 36.1 nm, virtually identical to that of the micelles of **BR3-H** at pH = 4.0 and T = 39 ^{o}C (36.0 nm in Figure 3.2b), which implied that the increase of pH from 4.0 to 5.2 had little effect on the micelle size. To dissociate the micelles at 40 ^{o}C, the pH needs to be increased to a value at which the CP of **R2-H** is 34 ^{o}C assuming that the difference between the CP of **R2-H** and the CMT of **BR3-H** at the new pH is the same as that at pH = 4.0. From Figure 3.1b, a CP of 34 ^{o}C for **R2-H** corresponds to a pH value of 5.7, which means that a minimal amount of 25 μmol of KOH needs to be injected into 2.50 g of the solution based on Figure 3.3. To ensure that the micelles were disrupted, 11 μmol of KOH (a total of 27 μmol of KOH including the amount of KOH added at T = 34 ^{o}C and pH = 4.0) was injected into the DLS tube that contained 2.50 g of the polymer solution to increase the pH to 5.9, or 4.5 μmol of KOH into 1.00 g of the polymer solution for FS study. The DLS and FS data showed that the micelles were completely disrupted. Further increasing the temperature induced the micellization again ($CMT_{5.9}$ is 43 ^{o}C from DLS and 45 ^{o}C from FS, Figures 3.7 and 3.8). The size of micelles at pH = 5.9 and T = 44 - 48 ^{o}C (~ 40 nm) was noticeably larger than those at the lower pH values, which is believed

to result from the higher degree of ionization of carboxylic acid groups at pH = 5.9 than at pH = 5.2 and 4.0.

To break the micelles at 48 ^{o}C, a similar consideration showed that the pH needs to be increased from 5.9 to at least 6.2, which from Figure 3.3 corresponds to the addition of 30 μmol of KOH into 2.50 g of a polymer solution with pH = 4.0. 7 μmol of KOH was injected into the solution, bringing the total amount of KOH to 34 μmol that made the solution pH = ~ 8.6. Similarly, a calculated amount of KOH was injected into the FS quartz cuvette to increase the pH to ~ 8.6. The DLS and FS data showed that the micelles were dissociated into the unimers (Figures 3.7 and 3.8). In a similar way, three cycles of micellization and dissociation transitions of **BR4-H** were achieved by using the same pH values but different temperatures for micelle dissociation.[82] Table 3.3 summarizes the results for both **BR3-H** and **BR4-H** obtained from three micellization and dissociation cycles, including the CMT and micelle characteristics at representative temperature at each pH. It is worth noting here that the values of CMT of **BR3-H** and **BR4-H** obtained by DLS and FS at each pH were consistently higher than the CP of **R2-H** by 6-8 ^{o}C and 2-5 ^{o}C, respectively. Although for both block copolymers the values of CMT at pH 4.0 and 5.2 determined by DLS and FS were essentially identical, the CMT from FS at pH 5.9 was 2 ^{o}C higher than that from DLS for both polymers. Since the core of the micelles contained more ionized carboxylic acid groups at pH = 5.9 and the fluorescence intensity of Nile Red is sensitive to the polarity of the microenvironment, a higher temperature is believed to be required for the fluorescence emission intensity of the dye to begin to increase.

Table 3.3. Critical Micellization Temperatures (CMT) and Micelle Characteristics of PEO-*b*-P(DEGMMA-*co*-MAA) Obtained from Three Cycles of Micellization and Dissociation Transitions as Well as Critical Micelle Concentrations (CMC) at Different pH Values

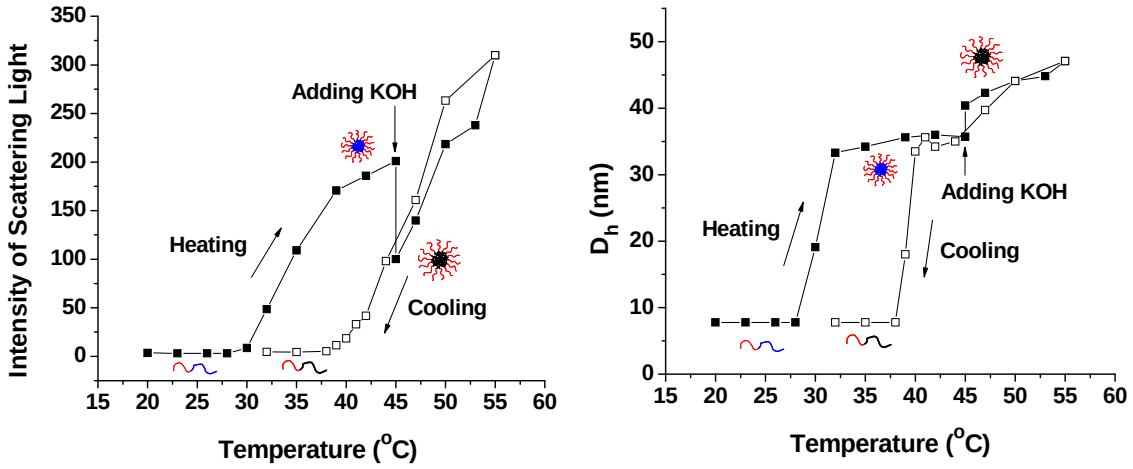
	BH3-H	**BH4-H**
$CMT_{4.0}$ at pH = 4.0 (DLS, FS)	30 °C,[a] 30 °C[b]	26 °C,[a] 26 °C[b]
Micelle size[c] and PD[d] at pH = 4.0	33.0 nm, 0.034 (34 °C)	41.0 nm and 0.006 (30 °C)
$CMC_{4.0}$ at pH = 4.0 and T = 50 °C[e]	0.031 mg/mL	0.023 mg/mL
$CMT_{5.2}$ at pH = 5.2 (DLS, FS)	36 °C,[a] 35 °C[b]	31 °C,[a] 31 °C[b]
Micelle size[c] and PD[d] at pH = 5.2	36.1 nm, 0.015 (40 °C)	47.9 nm and 0.035 (37 °C)
$CMC_{5.2}$ at pH = 5.2 and T = 50 °C	0.032 mg/mL	0.024 mg/mL
$CMT_{5.9}$ at pH = 5.9 (DLS, FS)	43 °C,[a] 45 °C[b]	40 °C,[a] 42 °C[b]
Micelle size[c] and PD[d] at pH = 5.9	40.6 nm, 0.008 (48 °C)	84.6 nm and 0.046 (45 °C)
$CMC_{5.9}$ at pH = 5.9 and T = 50 °C	0.039 mg/mL	0.037 mg/mL

[a] CMT determined by dynamic light scattering (DLS); [b] CMT determined by fluorescence spectroscopy (FS); [c] the average hydrodynamic diameter of micelles at a specific temperature was obtained by the use of the CONTIN method; [d] The polydispersity (PD) of micelles at a specific temperature obtained by the use of the CONTIN method. [e] CMC: critical micelle concentration at a particular pH and temperature, determined by FS using Nile Red as fluorescence probe. The polymer concentration in the buffer was 0.2 wt %. Note that the CP of **R2-H** is 24 °C at pH = 4.0, 28 °C at pH = 5.2, and 37 °C at pH = 5.9 (from Figure 3.1b).

With the increase of pH, the LCST transition temperature of the thermosensitive block of PEO-*b*-P(DEGMMA-*co*-MAA) increases and the polymer becomes more hydrophilic, which is expected to result in a higher critical micelle concentration (CMC). By the use of FS with Nile Red as fluorescence probe, the CMCs of **BR3-H** and **BR4-H** were determined at pH = 4.0, 5.2, and 5.9, same pH values as in the experiments of three cycles of micellization and dissociation transitions of the two block copolymers. The results are included in Table 3.3. Although the CMCs at pH = 4.0 and 5.2 were very close for both **BR3-H** (0.031 and 0.032 mg/mL, respectively) and **BR4-H** (0.023 and 0.024 mg/mL, respectively), the CMCs at pH 5.9 were appreciably higher (0.039 mg/mL for **BR3-H** and 0.037 mg/mL for **BR4-H**), consistent with the anticipated trend. Note that at any of the three pH values, the CMC of **BR4-H** was consistently lower than that of **BR3-H**, which can be attributed to the longer chain length of the thermosensitive block of **BR4-H** compared with that of **BR3-H**.

3.3.7 Control Experiment

In the preceding section, three cycles of micellization and dissociation transitions of PEO-*b*-P(DEGMMA-*co*-MAA) were achieved by gradually heating the polymer solution from 20 to 57 ^{o}C and rationally changing the pH. It should be emphasized here that it is important to judiciously choose both temperature and pH using Figures 3.1b and 3.3 as a guide for designing micellization/dissociation transitions. To further demonstrate this point, a control experiment was carried out. 2.50 g of a 0.2 wt % buffer solution of **BR3-H** with a pH of 4.0 was gradually heated to 45 ^{o}C (Figure 3.9). The micellization occurred as expected, and the size of the micelles at 45 ^{o}C was 35.7 nm, which was



(a) (b)

Figure 3.9. The intensity of scattered light at a scattering angle of 90° (a) and the hydrodynamic diameter (b) as a function of temperature in a DLS study of a 0.2 wt % solution of PEO-*b*-P(DEGMMA-*co*-MAA) (**BR3-H**) in 10 mM KHP buffer solution (2.50 g) in response to temperature and pH changes. At 45 °C, 25 μL of 1.00 M KOH solution was injected to bring the pH to 5.7 from 4.0. In (b), at 30 °C in the heating process and at 39 and 40 °C during the cooling process, two size distributions were observed, and the reported hydrodynamic diameters for these temperatures were the average values over two hydrodynamic size distributions.

essentially identical to the result shown in Figure 3.2 (36.1 nm at pH = 4.0 and T = 44 ^{o}C). 25 μL of 1.00 M KOH solution was injected into the DLS tube, which was then taken out, shaken for a few seconds, and placed back into the tube holder of the instrument. The micelles did not disassemble into the unimers, but were swelled from 35.7 nm to 40.4 nm at the same temperature (Figure 3.9). Interestingly, the scattering intensity decreased by 50 %, indicating that the micelles were not as tight as those before the injection of KOH. Apparently, the amount of added KOH was not enough to break the micelles, but the increase in pH caused more carboxylic acid groups to ionize and hence introduced more charge-charge interactions in the micelle core. From Figure 3.3, one can find out that the pH of the polymer solution increased to 5.7 after the addition of 25 μmol of KOH, which is expected to be able to break the micelles at 40 ^{o}C but not at 45 ^{o}C (to break the micelles at 45 ^{o}C, the CP of **R2-H** needs to be 39 ^{o}C, corresponding to a pH value of 6.0 and 28 μmol of KOH). Further increasing the temperature from 45 to 50 ^{o}C, the scattering intensity increased significantly, suggesting that the thermosensitive block in the core underwent continuous dehydration with the increase of temperature. When the solution was cooled from 50 to 44 ^{o}C, the size of the micelles became smaller (35 nm at 44 ^{o}C), similar to that of the micelles at the original pH value (35.7 nm at 45 ^{o}C and pH = 4.0). This is probably due to rearrangement of the micelles and the change in the number of association of molecules in each micelle.

3.4 Conclusion

In summary, this work demonstrated that thermo- and pH-sensitive block copolymers PEO-*b*-P(DEGMMA-*co*-MAA) can undergo multiple, reversible

micellization and dissociation in response to temperature and pH changes. A random copolymer P(DEGMMA-*co*-*t*BMA) and two samples of PEO-*b*-P(DEGMMA-*co*-*t*BMA) with controlled molecular weights and narrow polydispersities were synthesized by ATRP; hydrolysis with CF_3COOH produced the corresponding P(DEGMMA-*co*-MAA) and PEO-*b*-P(DEGMMA-*co*-MAA). The cloud point of P(DEGMMA-*co*-MAA) in aqueous KHP buffer solutions can be tuned from 24 to 60 ^oC by changing the pH from 4.0 to 6.7. The block copolymers underwent reversible thermo-induced micellization and dissociation transitions in 10 mM KHP buffer solutions at relatively low pH values, and the micelles had narrow polydispersities and a spherical shape. For the micelles formed at pH = 4.0, it was observed that by injection of a predetermined amount of KOH the micelles were rapidly dissociated into the unimers, which re-formed micelles by injection of the same amount of HCl at the same temperature or by heating to a higher temperature. By gradually raising temperature and simultaneously controlling the pH, three cycles of micellization and dissociation transitions were realized, demonstrating the possibility of achieving on-demand micellization and dissociation transition in the studied pH and temperature ranges. Fluorescence spectroscopy studies showed that Nile Red can be repeatedly encapsulated and released by the block copolymers. Note that the obtained plots of CMT of **BR3-H** and **BR4-H** versus pH can be used as a guide along with Figure 3.3 for designing micellization and dissociation transitions. The method reported in this article for tuning multiple micellziation and dissociation transitions may find applications in controlled encapsulation and triggered release of substances.

References:

1. Rijcken, C. J. F.; Soga, O.; Hennink, W. E.; van Nostrum, C. F. *J. Controlled Release* **2007**, *120*, 131-148.
2. Dimitrov, I.; Trzebicka, B.; Müller, A. H. E.; Dworak, A.; Tsvetanov, C. B. *Prog. Polym. Sci.* **2007**, *32*, 1275-1343.
3. Gil, E. S; Hudson, S. M. *Prog. Polym. Sci.* **2004**, *29*, 1173-1222.
4. Bütün, V.; Billingham, N. C.; Armes, S. P. *J. Am. Chem. Soc.* **1998**, *120*, 11818-11819.
5. Bütün, V.; Armes, S. P.; Billingham, N. C.; Tuzar, Z.; Rankin, A.; Eastoe, J.; Heenan, R. K. *Macromolecules* **2001**, *34*, 1503-1511.
6. Liu, S. Y.; Armes, S. P. *Angew. Chem. Int. Ed.* **2002**, *41*, 1413-1416.
7. Liu, S. Y.; Billingham, N. C.; Armes, S. P. *Angew. Chem. Int. Ed.* **2001**, *40*, 2328-2331.
8. Gohy, J. F.; Antoun, S.; Jérome, R. *Macromolecules* **2001**, *34*, 7435-7440.
9. Schilli, C. M.; Zhang, M. F.; Rizzardo, E.; Thang, S. H.; Chong, Y. K.; Edwards, K.; Karlsson, G.; Müller, A. H. E. *Macromolecules* **2004**, *37*, 7861-7866.
10. André, X.; Zhang, M. F.; Müller, A. H. E *Macromol. Rapid Commun.* **2005**, *26*, 558-563.
11. Bellomo, E. G.; Wyrsta, M. D.; Pakstis, L.; Pochan, D. J.; Deming, T. J. *Nature Materials* **2004**, *3*, 244-248.
12. Borchert, U.; Lipprandt, U.; Bilang, M.; Kimpfler, A.; Rank, A.; Peschka, R.; Schubert, R.; Lindner, P.; Forster, S. *Langmuir* **2006**, *22*, 5843-5847.

13. Xu, J.; Ge, Z. S.; Zhu, Z. Y.; Luo, S. Z.; Liu, H. W.; Liu, S. Y. *Macromolecules* **2006**, *39*, 8178-8185.

14. Wang, D.; Yin, J.; Zhu, Z.; Ge, Z.; Liu, H.; Armes, S. P.; Liu, S. Y. *Macromolecules* **2006**, *39*, 7378-7385.

15. Zhang, W.; Shi, L. Ma, R.; An, Y.; Xu, Y.; Wu, K. *Macromolecules* **2005**, *38*, 8850-8852.

16. Gillies, E. R.; Fréchet, J. M. J. *Chem. Commun.* **2003**, *14*, 1640-1641.

17. Gillies, E. R.; Jonsson, T. B.; Fréchet, J. M. J. *J. Am. Chem. Soc.* **2004**, *126*, 11936-11943.

18. Gillies, E. R.; Fréchet, J. M. J. *Bioconjugate Chem.* **2005**, *16*, 361-368.

19. Bae, Y.; Fukushima, S.; Harada, A.; Kataoka, K. *Angew. Chem. Int. Ed.* **2003**, *42*, 4640-4643.

20. Bae, Y.; Nishiyama, N.; Fukushima, S.; Hoyama, H.; Yasuhori, M.; Kataoka, K. *Bioconjugate Chem.* **2005**, *16*, 122-130.

21. Lee, Y.; Fukushima, S.; Bae, Y.; Hiki, S.; Ishii, T.; Kataoka, K. *J. Am. Chem. Soc.* **2007**, *129*, 5362-5363.

22. Zhang, L.; Bernard, J.; Davis, T. P.; Barner-Kowollik, C.; Stenzel, M. H. *Macromol. Rapid Commun.* **2008**, *29*, 123-129.

23. Chan, Y.; Wong, T.; Byrne, F.; Kavallaris, M.; Bulmus, V. *Biomacromolecules* **2008**, *9*, 1826-1836.

24. Aoshima, S.; Sugihara, S. *J. Polym. Sci. Part A: Polym. Chem.* **2000**, *38*, 3962-3965.

25. Sugihara, S.; Kanaoka, S.; Aoshima, S. *J. Polym. Sci. Part A: Polym. Chem.* **2004**, *42*, 2601-2611.

26. Sugihara, S.; Kanaoka, S.; Aoshima, S. *Macromolecules* **2005**, *38*, 1919-1927.

27. Arotcarena, M.; Heise, B.; Ishaya, S.; Laschewsky, A. *J. Am. Chem. Soc.* **2002**, *124*, 3787-3793.

28. Mertoglu, M.; Garnier, S.; Laschewsky, A.; Skrabania, K.; Sorsberg, J. *Polymer* **2005**, *46*, 7726-7740.

29. Skrabania, K.; Juliane, K.; Laschewsky, A.; Akdemir, O.; Hoth, A. ; Lutz, J.-F. *Langmuir* **2007**, *23*, 84-93.

30. Hua, F. J.; Jiang, X. G.; Zhao, B. *Macromolecules* **2006,** *39*, 3476-3479.

31. Qin, S. H.; Geng, Y.; Discher, D. E.; Yang, S. *Adv. Mater.* **2006**, *18*, 2905-2909.

32. Zhang, W. Q.; Shi, L. Q.; Wu, K.; An. Y. G. *Macromolecules* **2005**, *38*, 5743-5747.

33. Dimitrov, P.; Rangelov, S.; Dworak, A.; Tsvetanov, C. B. *Macromolecules* **2004**, *37*, 1000-1008.

34. Convertine, A. J.; Lokitz, B. S.; Vasileva, Y.; Myrick, L. J.; Scales, C. W.; Lowe, A. B.; McCormick, C. L. *Macromolecules* **2006**, *39*, 1724-1730.

35. Li, Y. T.; Lokitz, B. S.; McCormick, C. L. *Macromolecules* **2006**, *39*, 81-89.

36. Jiang, J. Q.; Tong, X.; Zhao, Y. *J. Am. Chem. Soc.* **2005**, *127*, 8290-8291.

37. Jiang, J. Q.; Tong, X.; Morris, D.; Zhao. Y. *Macromolecules* **2006**, *39*, 4633-4640.

38. Jiang, Y.; Wang, Y.; Ma, N.; Wang, Z.; Smet, M.; Zhang, X. *Langmuir* **2007**, *23*, 4029-4034.

39. Lee, H-I; Wu, W.; Oh, J. K.; Mueller, L.; Sherwood, G.; Peteanu, L.; Kowalewski, T.; Matyjaszewski, K. *Angew. Chem. Int. Ed.* **2007**, *46*, 2453-2457.

40. Jiang, X. G.; Lavender, C. A.; Woodcock, J. W.; Zhao, B. *Macromolecules* **2008**, *41*, 2632-2643.

41. Katayama, Y.; Sonoda, T.; Maeda, M. *Macromolecules* **2001**, *34*, 8569-8573.

42. Ishihara, Y.; Bazzi, H. S.; Toader, V.; Godin, F.; Sleiman, H. F. *Chem. Eur. J.* **2007**, *13*, 4560-4570.

43. Joseph, J.; Dreiss, C. A.; Cosgrove, T. *Langmuir* **2007**, *23*, 460-466.

44. Napoli, A.; Valentini, M.; Tirelli, N.; Muller, M.; Hubbell, J. A. *Nature Materials* **2004**, *3*, 183-189.

45. Napoli, A.; Boerakker, M. J.; Tirelli, N.; Muller, M.; Sommerdijk, N. A.; Hubbell, J. A. *Langmuir* **2004**, *20*, 3487-3491.

46. Wu, C.; Wang, X. H. *Phys. Rev. Lett.* **1998**, *80*, 4092-4094.

47. Plamper, F. A.; Schmalz, A.; Ballauff, M.; Müller, A. H. E. *J. Am. Chem. Soc.* **2007**, *129*, 14538-14539.

48. Schild , H. G. *Prog. Polym. Sci.* **1992**, *17*, 163-249.

49. Huang, X. N.; Du, F. S.; Ju, R.; Li, Z. C. *Macromol. Rapid Commun.* **2007**, *28*, 597-603.

50. Neradovic, D.; van Nostrum, C. F.; Hennink, W. E. *Macromolecules* **2001**, *34*, 7589-7591.

51. Neradovic, D.; van Steenbergen, M. J.; Vansteelant, L.; Meijer, Y. J.; van Nostrum, C. F.; Hennink, W. E. *Macromolecules* **2003**, *36*, 7491-7498.

52. Soga, O.; van Nostrum, C. F.; Ramzi, A.; Visser, T.; Soulimani, F.; Frederik, P. M.; Bomans, P. H. H.; Hennink, W. E. *Langmuir* **2004**, *20*, 9388-9395.

53. Rijicken, C. J. F.; Veldhuis, T. F. J.; Ramzi, A.; Meeldijk, J. D.; van Nostrum, C. F.; Hennink, W. E. *Biomacromolecules* **2005**, *6*, 2343-2351.

54. Kohori, F.; Sakai, K.; Aoyagi, T.; Yokoyama, M.; Yamato, M.; Sakurai, Y.; Okano, T. *Colloids and Surfaces B: Biointerfaces* **1999**, *16*, 195-205.

55. Gotzamanis, G.; Tsitsilianis, C. *Polymer* **2007**, *48*, 6226-6233.

56. Lutz, J.-F.; Hoth, A. *Macromolecules* **2006**, *39*, 893-896.

57. Lutz, J. F.; Weichenhan, K.; Akdemir, O.; Hoth, A. *Macromolecules* **2007**, *40*, 2503-2508.

58. Yin, X.; Hoffman, A. S.; Stayton, P. S. *Biomacromolecules* **2006**, *7*, 1381-1385.

59. Chen, G.; Hoffman, A. S. *Nature* **1995**, *373*, 49-52.

60. Feil, H.; Bae, Y. H.; Feijen, J.; Kim, S. W. *Macromolecules* **1992**, *25*, 5528-5530.

61. Bulmus, V.; Ding, Z.; Long, C. J.; Stayton, P. S.; Hoffman, A. S. *Bioconjugate Chem.* **2000**, *11*, 78-83.

62. Zhou, S. Q.; Chu, B. *J. Phys. Chem. B.* **1998**, *102*, 1364-1371.

63. Olea, A. F.; Thomas, J. K. *Macromolecules* **1989**, *22*, 1165-1169.

64. Murthy, N.; Robichaud, J. R.; Tirrell, D. A.; Stayton, P. S.; Hoffman, A. S. *J. Controlled Release* **1999**, *61*, 137-143.

66. Lokitz, B. S.; York, A. W.; Stempka, J. E.; Treat, N. D.; Li, Y.; Jarrett, W. L.; McCormick, C. L. *Macromolecules* **2007**, *40*, 6473-6480.

67. Han, S.; Hagiwara, M.; Ishizone, T. *Macromolecules* **2003**, *36*, 8312-8319.

68. Li, D. J.; Jones, G. J.; Dunlap, J. R.; Hua, F. J.; Zhao, B. *Langmuir* **2006**, *22*, 3344-3351.

69. Li, D. J.; Zhao, B. *Langmuir* **2007**, *23*, 2208-2217.

70. Zhao, B.; Li, D. J.; Hua, F. J.; Green, D. R. *Macromolecules* **2005**, *38*, 9509-9517.

71. Hua, F. J.; Jiang, X.G.; Li, D. J.; Zhao, B. *J. Polym. Sci. Part A: Polym. Chem.* **2006**, *44*, 2454-2467.

72. Jiang, X. G.; Zhao, B. *J. Polym. Sci. Part A: Polym. Chem.* **2007**, *45*, 3707-3721.

73. Li, D. J.; Zhao, B. *Langmuir* **2008**, *24*, 5911-5918.

74. Lutz, J.-F.; Andrieu, J.; Uzgun, S.; Rudolph, C.; Agarwal, S. *Macromolecules* **2007**, *40*, 8540-8543.

75. Aathimanikandan, S. V.; Savariar, E. N. Thayumanavan, S. *J. Am. Chem. Soc.* **2005**, *127*, 14922-14929.

76. Chang, Y.; Powell, E. S.; Allcock, H. R.; Park, S. M.; Kim, C. *Macromolecules* **2003**, *36*, 2568-2570.

77. Allcock, H. R.; Dudley, G. K. *Macromolecules* **1996**, *29*, 1313-1319.

78. Yamamoto, S.-I.; Pietrasik, J.; Matyjaszewski, K. *J. Polym. Sci. Part A: Polym. Chem.* **2008**, *46*, 194-202.

79. Jiang, X. W.; Smith, M. R.; Baker, G. L. *Macromolecules* **2008**, *41*, 318-324.

80. Wang, N.; Dong, A.; Radosz, M.; Shen, Y. Q. *J. Biomed. Mater. Res. Part A.* **2008**, *84A*, 148-157.

81. Andruzzi, L.; Senaratne, W.; Hexemer, A.; Sheets, E. D.; Ilic, B.; Kramer, E. J.; Baird, B.; Ober, C. J. *Langmuir* **2005**, *21*, 2495-2504.

82. Details can be found in appendix B.

83. Urry, D. W. *J. Phys. Chem. B* **1997**, *101*, 11007-11028.

Chapter 4. Stimuli-Induced Multiple Sol-Gel-Sol Transitions of Aqueous Solution of a Thermo- and Light-Sensitive Hydrophilic Block Copolymer

Abstract

A 20.0 wt % aqueous solution of a thermo- and light-sensitive hydrophilic block copolymer, poly(ethylene oxide)-*b*-poly(ethoxytri(ethylene glycol) acrylate)-*co*-*o*-nitrobenzyl acrylate) (PEO-*b*-P(TEGEA-*co*-NBA)), can undergo multiple sol-gel-sol transitions in response to temperature changes and UV irradiation. The 20.0 wt % block copolymer solution was a free-flowing liquid at low temperatures. Upon heating above the lower critical solution temperature (LCST) of the thermo- and light-sensitive P(TEGEA-*co*-NBA) block, micellization occurred with the P(TEGEA-*co*-NBA) block associating into the core and the PEO block forming the corona. The solution turned into an immobile, optically isotropic gel at 33 °C. The gel exhibited a finite yield stress and its dynamic storage modulus was essentially independent of frequency, suggesting that the gel was composed of cubic-packed micelles. With further increasing temperature to 50 °C, the gel flowed under its weight. This is because the PEO corona shrank at elevated temperatures and thus the structural constraint among micelles was released. At 33 °C, we irradiated the micellar gel with 365 nm UV light. The *o*-nitrobenzyl group of NBA was cleaved, resulting in an increase in the LCST of the thermosensitive block and the dissociation of micelles. Consequently, the gel was transformed into a free-flowing liquid, which upon heating underwent sol-gel-sol transitions, similar to the solution before UV irradiation.

4.1 Introduction

Block copolymers can self-assemble into, often spherical, micelles in a selective solvent with the solvophobic block associating into the core and the solvophilic block forming the corona.[1,2] When the effective volume fraction of micelles exceeds a critical value, micelles are packed into an ordered, usually cubic, structure and the free-flowing solution is transformed into a free-standing micellar gel.[1-25] The sol-to-gel/gel-to-sol transitions of block copolymer solutions, especially aqueous solutions of thermosensitive hydrophilic block copolymers,[12-34] have been intensively studied in the past decades because of the intriguing changes in structures and rheological properties and the potential uses in technological applications.[35-39]

Considerable effort has been invested on poly(ethylene oxide) (PEO)-based block copolymers, particularly block copolymers of PEO and poly(propylene oxide) (PPO) or poly(butylene oxide) (PBO).[1-3,12-25] At a sufficiently high concentration, aqueous solutions of these block copolymers can undergo sol-gel-sol transitions upon heating. The hard gel boundary at low/moderate concentrations in a phase diagram is usually a C-shaped curve. The lower temperature sol-gel boundary is driven by the enhancement of micellization and the ordering of micelles with increasing temperature, while the upper gel-sol boundary results from the shrinking of PEO corona at elevated temperatures.[1-3] Besides the PEO-containing copolymers, other thermosensitive water-soluble block copolymers that can form micellar gels in water have also been reported.[28-34] For example, Aoshima et al. synthesized a series of block copolymers composed of two or more thermosensitive blocks with different lower critical solution temperatures (LCSTs) by a

living cationic polymerization technique.[30-33] They observed that 20 wt % aqueous solutions of these block copolymers underwent multi-stage transitions from clear liquids to transparent gels, to hot clear liquids, to phase separated opaque mixtures with the increase of temperature. The sol-to-gel and gel-to-sol transition temperatures corresponded to the LCSTs of the thermosensitive blocks.

Of great interest are aqueous block copolymer micellar gels that can respond to more than one external stimulus.[39-47] Up to date, there are only a few reports on such micellar gels and they are thermo- and pH-responsive. These block copolymers were prepared by either growing pH-responsive blocks from or introducing carboxylic acid groups to the chain ends of an ABA triblock copolymer that can form thermoreversible gels in water (e.g., PEO-*b*-PPO-*b*-PEO),[39-45] or using pyromellitic dianhydride to couple PEO-*b*-PPO-*b*-PEO to make multiblock copolymers with carboxylic acid groups being incorporated at the junction points.[46]

This chapter presents that a 20.0 wt % aqueous solution of a thermo- and light-sensitive block copolymer, poly(ethylene oxide)-*b*-poly(ethoxytri(ethylene glycol) acrylate-*co*-*o*-nitrobenzyl acrylate) (PEO-*b*-P(TEGEA-*co*-NBA)), can undergo multiple sol-gel-sol transitions in response to temperature changes and UV irradiation. PTEGEA is a thermosensitive water-soluble polymer with a LCST of 36 ^{o}C in water;[48] it belongs to a new family of thermoresponsive hydrophilic polymers.[48-60] The *o*-nitrobenzyl group is known to undergo a photo-cleavage reaction when exposed to long wavelength UV light.[48,61,62] The key feature of this type of doubly responsive hydrophilic block copolymers is that the LCST of the thermosensitive block can be modified by a second

external stimulus. Chapter 2 shows that PEO-*b*-P(TEGEA-*co*-NBA) dissolved molecularly in a 0.2 wt % aqueous solution at temperatures below 25 ^{o}C and self-assembled into micelles at elevated temperatures. Upon UV irradiation, the *o*-nitrobenzyl group was cleaved and the LCST of the thermosensitive block was increased, causing the micelles to dissociate into unimers. Further increasing the temperature induced the formation of micelles again. In the present work, the solution behavior of a 20.0 wt % aqueous solution of PEO-*b*-P(TEGEA-*co*-NBA) under various conditions was examined by visual inspection (the vial inversion test), rheological measurements, polarized light microscopy, and dynamic light scattering. The sol-gel phase diagrams of the block copolymer in water before and after UV irradiation were mapped out by the vial inversion method.

4.2 Experimental Section

4.2.1 Materials

The thermo- and light-sensitive block copolymer used in this work, PEO-*b*-P(TEGEA-*co*-NBA), was synthesized by atom transfer radical polymerization of a mixture of TEGEA and NBA with a molar ratio of 100 : 10 from a PEO macroinitiator with a molecular weight of 5000 Da. The details of synthesis were described in chapter 2. Size exclusion chromatography analysis using polystyrene standards showed that the number average molecular weight ($M_{n,SEC}$) was 21600 Da and the polydispersity index was 1.12. The numbers of TEGEA and NBA units in the thermosensitive block were 88 and 11, respectively, which were determined by the analysis of the ^{1}H NMR spectrum

based on the fact that the molecular weight of the PEO block was 5000 Da, i.e., the degree of polymerization of the PEO block was 113.

4.2.2 General Characterization

Gel permeation chromatography (GPC) was carried out at room temperature using PL-GPC 20 (an integrated GPC system from Polymer Laboratories, Inc) with a refractive index detector, one PLgel 5 μm guard column (50 × 7.5 mm), and two PLgel 5 μm mixed-C columns (each 300 × 7.5 mm, linear range of molecular weight from 200 to 2,000,000 Da according to Polymer Laboratories). The data were processed using Cirrus^{TM} GPC/SEC software (Polymer Laboratories). Tetrahydrofuran was used as a carrier solvent at a flow rate of 1.0 mL/min. Standard monodisperse polystyrenes (Polymer Laboratories, Inc.) were used for calibration. The ^{1}H (300 MHz) spectra were recorded on a Varian Mercury 300 NMR spectrometer and the residual solvent proton signal was used as the internal standard.

4.2.3 Preparation of 20.0 wt % Aqueous Solution of PEO-*b*-P(TEGEA-*co*-NBA)

The block copolymer was added into a pre-weighed 3.7 mL vial with an inner diameter of 12 mm. The vial was then placed in a large flask and dried in high vacuum at 55 ^{o}C for at least 3 h. The mass of the dried polymer inside the vial was 0.478 g. Milli-Q water (1.917 g) was added into the vial. The mixture was then sonicated in an ice/water ultrasonic bath (Fisher Scientific Model B200 Ultrasonic Cleaner) until the block copolymer was dissolved. The vial was then stored in a refrigerator (~ 4 ^{o}C) overnight to ensure that a homogeneous solution was obtained.

4.2.4 Rheological Measurements

Rheological experiments were conducted using a stress-controlled rheometer (TA Instruments Model TA AR2000). A cone-plate geometry with a cone diameter of 20 mm and an angle of 2 ^{o} (truncation 57 μm) was employed; the temperature was controlled by the bottom Peltier plate. In each measurement, 90 μL of a polymer solution was loaded onto the plate by a micropipette. The solvent trap was filled with water and a solvent trap cover was used to minimize water evaporation. Dynamic viscoelastic properties (dynamic storage modulus G' and loss modulus G") of a polymer solution were measured by oscillatory shear experiments performed at a fixed frequency of 1 Hz in a heating ramp at a heating rate of 3 ^{o}C/min. The frequency dependences of G' and G" of a polymer solution at selected temperatures were obtained by frequency sweep tests from 0.1 to 100 Hz. A strain amplitude of γ = 0.2 % was used in all dynamic tests to ensure that the deformation was within the linear viscoelastic regime. At each temperature, the solution was equilibrated for at least 2 min prior to data recording. The flow properties (shear stress-shear rate curves) of a polymer solution at selected temperatures were measured by a shear rate ramp from 12 to 300 s^{-1} for duration of 3 min. The apparent viscosities of a polymer solution at different temperatures were measured by a temperature ramp experiment performed at a heating rate of 3 ^{o}C/min and a shear rate of 10 s^{-1}.

4.2.5 Photocleavage of *o*-Nitrobenzyl Group of NBA in PEO-*b*-P(TEGEA-*co*-NBA)

The long wavelength (365 nm) UV light from a Spectroline ENF-240C hand-held UV lamp equipped with one 4-watt long wavelength tube filtered at 365 nm and one short wavelength tube filtered at 254 nm was used for the photocleavage of *o*-nitrobenzyl

group of NBA in PEO-*b*-P(TEGEA-*co*-NBA). A 3.7 mL vial that contained a 20.0 wt % aqueous solution of PEO-*b*-P(TEGEA-*co*-NBA) (1.650 g) was placed in a water bath with a preset temperature of 33 °C. After the solution turned into a transparent gel, the gel was irradiated with 365 nm UV light at a distance of ~ 1 cm for 6 days. The irradiated polymer solution was then analyzed with rheological and dynamic light scattering experiments.

4.2.6 Polarized Light Microscopy Experiments

Polarized light microscopy experiments were conducted on a Leica (DM LB2) polarized light microscope coupled with a Mettler hot stage (FP-90). A 20.0 wt % aqueous solution of PEO-*b*-P(TEGEA-*co*-NBA) and the irradiated solution (a 18.9 wt % aqueous solution of PEO-*b*-P(TEGEA-*co*-acrylic acid) (PEO-*b*-P(TEGEA-*co*-AA)) were added into a thin (0.5 mm) quartz demountable cell. The temperature of the cell was controlled by a Mettler hot stage (FP-90).

4.2.7 Dynamic Light Scattering Studies of Aqueous Solutions of PEO-*b*-P(TEGEA-*co*-NBA) and PEO-*b*-P(TEGEA-*co*-AA)

Dynamic light scattering (DLS) studies of aqueous solutions of PEO-*b*-P(TEGEA-*co*-NBA) and PEO-*b*-P(TEGEA-*co*-AA) were conducted with a Brookhaven Instruments BI-200SM goniometer equipped with a PCI BI-9000AT digital correlator, a temperature controller, and a solid-state laser (model 25-LHP-928-249, λ = 633 nm) at a scattering angle of 90^{o}. For studies of dilute aqueous solutions, a 20.0 wt % solution of PEO-*b*-P(TEGEA-*co*-NBA) and the UV-irradiated solution (i.e., a 18.9 wt % aqueous solution of

PEO-*b*-P(TEGEA-*co*-AA)) were diluted with Milli-Q water to a concentration of 0.20 wt %. The diluted solutions were filtered into borosilicate glass tubes with an inner diameter of 7.5 mm using Millipore hydrophilic PTFE filters (0.2 μm pore size) and the glass tubes were sealed with PE stoppers. The DLS tube was placed in the cell holder of the light scattering instrument and gradually heated. At each temperature, the solution was equilibrated for 15 min prior to data recording. The time intensity-intensity correlation functions were analyzed with a Laplace inversion program (CONTIN).

For studies of concentrated solutions, a 20.0 wt % aqueous solution of PEO-*b*-P(TEGEA-*co*-NBA) and the irradiated solution were filtered into DLS tubes with Millipore hydrophilic PTFE filters (0.2 μm pore size) and sealed with PE stoppers. The tube was placed in the cell holder of the DLS instrument and gradually heated. At each temperature, the solution was equilibrated for 15 min before the scattered light intensity was recorded over duration of 5 min. For each measurement, the sampling position of the DLS tube was changed randomly every 15 s.[29]

4.2.8 Determination of Phase Diagrams of PEO-*b*-P(TEGEA-*co*-NBA) and PEO-*b*-P(TEGEA-*co*-AA) in Water by the Vial Inversion Test

A 3.7 mL vial that contained an aqueous solution of PEO-*b*-P(TEGEA-*co*-NBA) or PEO-*b*-P(TEGEA-*co*-AA) with a known concentration was placed in the water bath of a Fisher Scientific Isotemp refrigerated circulator. The temperature was increased at a step of 1 ^{o}C. At each temperature, the solution was equilibrated for 10 min before the vial was tilted or inverted to visually examine if the solution was a mobile liquid or an immobile gel under its own weight. The temperature at which the solution changed from a mobile

to an immobile state (or vice versus) was taken as the sol-to-gel (or gel-to-sol) transition temperature. Polymer solutions with different concentrations were obtained by adding a predetermined amount of water into the vial or evaporating water from the solution; their sol-to-gel/gel-to-sol transition temperatures were determined by the vial inversion method described above.

4.3 Results and Discussion

4.3.1 Multiple Sol-Gel-Sol Transitions of a 20.0 wt % Aqueous Solution of PEO-*b*-P(TEGEA-*co*-NBA) in Response to Temperature Changes and UV Irradiation

For study of sol-gel-sol transitions, a 20.0 wt % aqueous solution was made by dissolving PEO-*b*-P(TEGEA-*co*-NBA) in Milli-Q water in a vial with an inner diameter of 12 mm and heated at a step of 1 ^{o}C in a water bath. At each temperature, the solution was equilibrated for 10 min and the vial was tilted or inverted to visually examine if the solution was a flowing liquid or an immobile gel. Figure 4.1 shows the digital pictures of the block copolymer solution under different conditions. Evidently, the polymer solution was a free-flowing liquid at 20 °C (Figure 4.1a). Upon gradually heating to 33 °C, the solution turned into a free-standing gel (Figure 4.1b), which remained immobile even if the vial was inverted. With further increasing the temperature to 50 °C, the gel again flowed. Figure 4.1c shows the picture of the vial at 52 °C; the solution was a free-flowing liquid again. Note that throughout the studied temperature range from ~ 0 to ~ 60 °C, the polymer solution remained clear.

The DLS study showed that in a 0.20 wt % aqueous solution, the critical micellization temperature (CMT) of PEO-*b*-P(TEGEA-*co*-NBA) was 25 °C and micelles with an

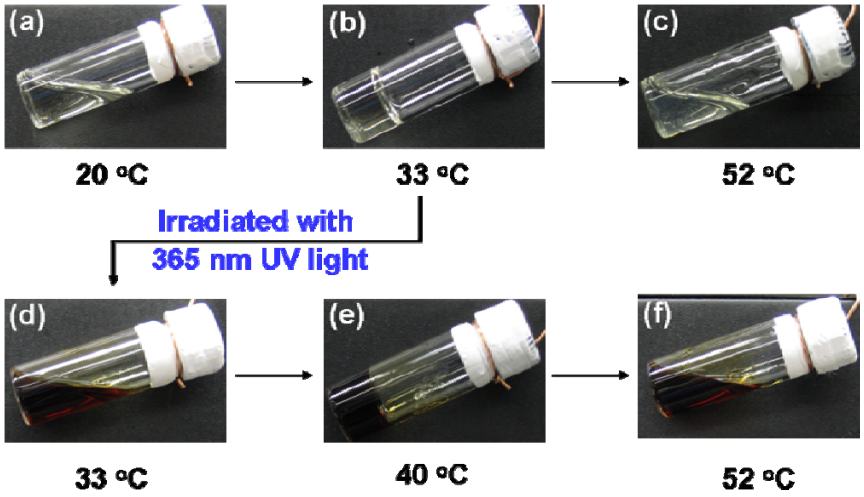


Figure 4.1. Digital optical pictures of a 20.0 wt % aqueous solution of poly(ethylene oxide)-*b*-poly(ethoxytri(ethylene oxide) acrylate-*co*-*o*-nitrobenzyl acrylate) (PEO-*b*-P(TEGEA-*co*-NBA) at (a) 20 ^{o}C, (b) 33 ^{o}C, and (c) 52 ^{o}C before UV irradiation, and at (d) 33 ^{o}C, (e) 40 ^{o}C, and (f) 52 ^{o}C after UV irradiation. At 33 ^{o}C, the 20.0 wt % aqueous solution of PEO-*b*-P(TEGEA-*co*-NBA) was irradiated for six days with 365 nm UV light from a Spectroline ENF-240C hand-held UV lamp.

apparent hydrodynamic diameter of ~ 30 nm were observed at temperatures ≥ 29 °C. From the previous work, the CMT of a 0.20 wt % aqueous solution of a block copolymer with essentially the same chemical composition in the thermosensitive block as the present one increased from 25 to 36 °C after the *o*-nitrobenzyl groups of NBA units were photo-cleaved.[48] Thus, in principle, the gel at 33 °C shown in Figure 4.1b can be converted to a free-flowing solution if the CMT of the present sample increases by the same or a similar magnitude after UV irradiation. In light of this consideration, the gel was irradiated at 33 ^{o}C with 365 nm UV light. After several hours, a brown-red color appeared, indicating that the photochemical reaction occurred. The solution became a free-flowing liquid after 2 days. To achieve a maximum degree of photocleavage of *o*-nitrobenzyl groups in the block copolymer, the irradiation was kept for additional 4 days. The final solution was a deep-red but clear, free-flowing liquid with a very low viscosity at 33 °C (Figure 4.1d).[63] ^{1}H NMR spectroscopy analysis showed that the peak at 5.45 ppm, a characteristic peak of NBA (-OCH_2(CH)$_2$), almost disappeared after UV irradiation (Figure 4.2). A quantitative analysis indicated that ~ 95 % of *o*-nitrobenzyl groups were cleaved. The CMT of PEO-*b*-P(TEGEA-*co*-acrylic acid) (PEO-*b*-P(TEGEA-*co*-AA), formed from PEO-*b*-P(TEGEA-*co*-NBA) after the UV irradiation) in a 0.20 wt % aqueous solution was 35 °C, close to the predicted CMT (36 °C). The irradiated solution turned into an immobile gel when the temperature was increased to 40 °C (Figure 4.1e). Upon further heating, the gel started to flow at 48 °C, which was slightly lower than the gel-to-sol transition temperature (50 °C) of the non-irradiated solution. Figure 1f shows that the solution was a free-flowing liquid at 52 °C. Thus, the 20.0 wt % aqueous solution of PEO-*b*-P(TEGEA-*co*-NBA) can undergo multiple sol-gel-

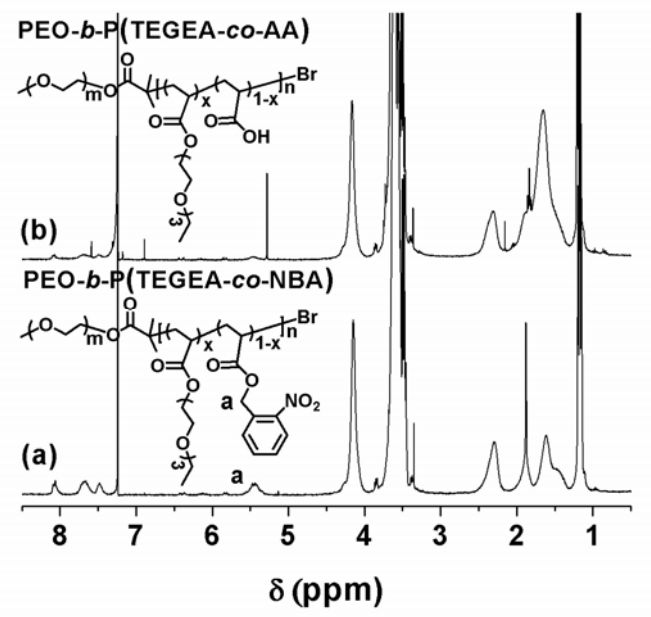
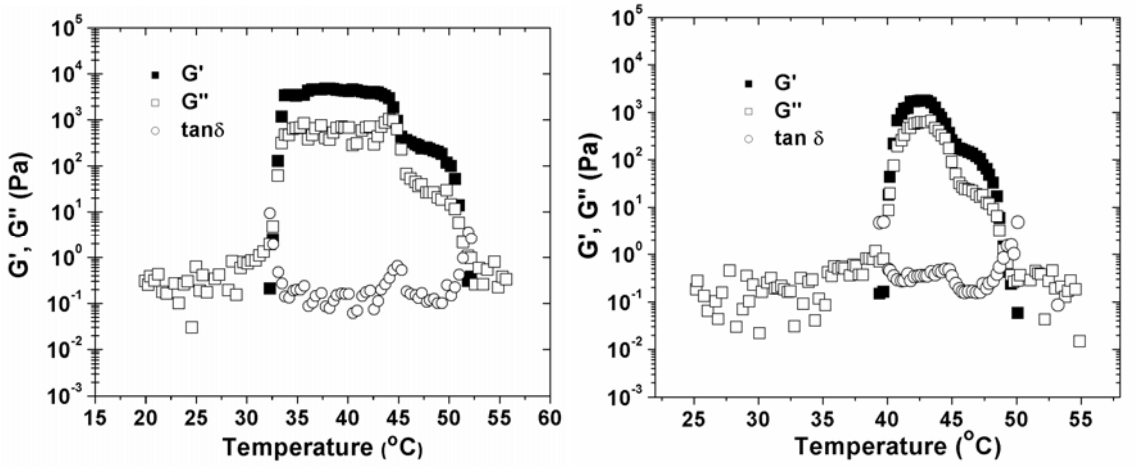


Figure 4.2. ^{1}H NMR spectra of (a) PEO-*b*-P(TEGEA-*co*-NBA) and (b) PEO-*b*-P(TEGEA-*co*-AA), which was formed from PEO-*b*-P(TEGEA-*co*-NBA) after UV irradiation at 33 ^{o}C for 6 days. $CDCl_3$ was used as the solvent.

sol transitions under different conditions in response to temperature changes and UV irradiation.

4.3.2 Rheological Properties of the 20.0 wt % Aqueous Solution of PEO-*b*-P(TEGEA-*co*-NBA) and the UV-Irradiated Solution

To quantitatively study the solution property changes in the sol-gel-sol transitions shown in Figure 4.1, rheological measurements were conducted. Figure 4.3 shows the dynamic viscoelastic properties of the 20.0 wt % aqueous solution before and after UV irradiation at a constant frequency of 1 Hz in a heating ramp with a heating rate of 3 °C/min. A strain amplitude of γ = 0.2 % was used to ensure that the measurements were taken in the linear viscoelastic regime. For the solution before UV irradiation, when the temperature was raised from 32 to 33 °C, both dynamic storage G' and loss modulus G" increased dramatically and G' became larger than G", indicating that the solution turned into a gel.[1-3] From 33 to 51 °C, G' remained greater than G", suggesting that the solution was in the gel state in this temperature range. At T > 51 °C, both G' and G" decreased sharply and G" became larger than G', which is a characteristic of a free-flowing liquid. The crossover point, G' = G", is commonly used as an indicator of the sol-to-gel or gel-to-sol transition.[1-3] Using this criteria, the sol-gel and gel-sol transition temperatures determined from rheological measurements were 33 and 51 °C, respectively, essentially the same as those estimated by the vial inversion method (33 and 50 °C). A similar phenomenon was observed for the irradiated polymer solution except that the two transitions occurred at 40 and 49 °C, which were again in good agreement with those determined by the vial inversion test (40 and 48 °C). The gel zone of the irradiated



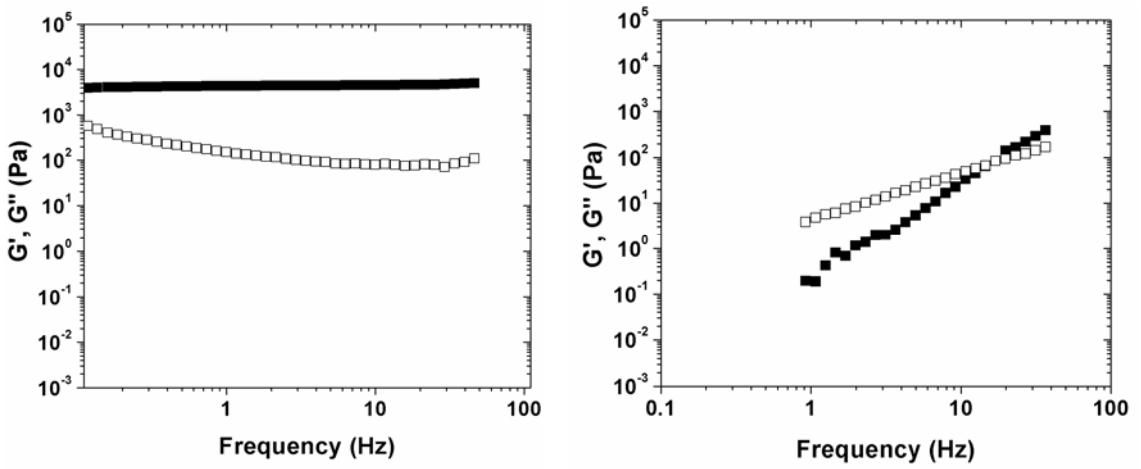
(a) (b)

Figure 4.3. Plot of dynamic storage modulus G' (■), loss modulus G" (□), and tan δ versus temperature for (a) the 20.0 wt % aqueous solution of PEO-*b*-P(TEGEA-*co*-NBA) and (b) the UV-irradiated solution (a 18.9 wt % aqueous solution of PEO-*b*-P(TEGEA-*co*-AA). The data were collected from temperature ramp experiments with a heating rate of 3 ^{o}C/min. A strain amplitude of 0.2 % and an oscillation frequency of 1 Hz were used.

solution, from 40 to 49 °C, was narrower than that of the solution before UV irradiation, from 33 to 51 °C. A closer examination showed that the highest value of G' (4.7 kPa) for the solution before UV irradiation was much higher than that of the irradiated solution (1.7 kPa). A possible reason for this observation is that the concentration of the block copolymer decreased from 20.0 wt % to 18.9 wt % after UV irradiation because of the removal of *o*-nitrobenzyl groups. Thus, the packing of micelles in the gel of the irradiated sample was not as tight as in the gel of the 20.0 wt % solution before UV irradiation.

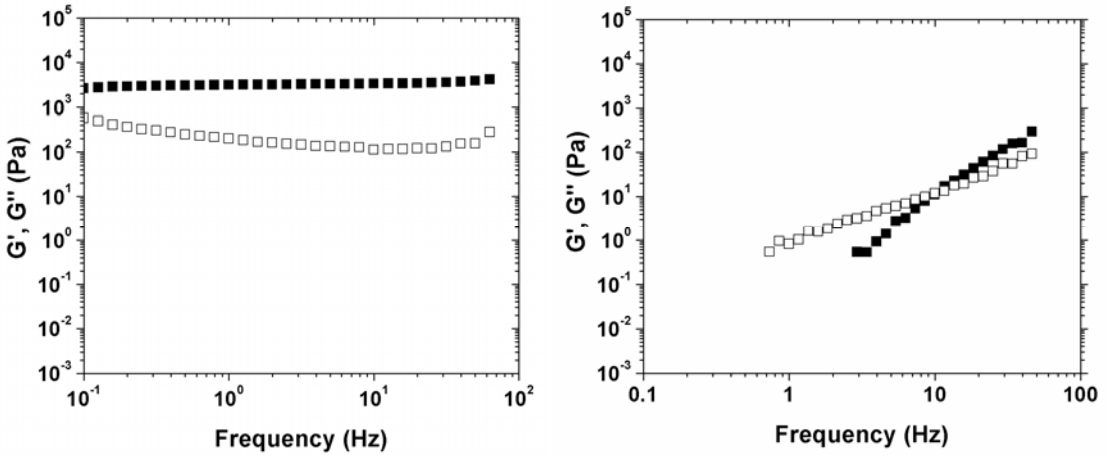
Interestingly, when the temperature reached 45 °C, G' and G" of both non-irradiated and irradiated solutions decreased noticeably (Figure 4.3), but G' was still larger than G" in the temperature range from 45 to 51 °C for the non-irradiated sample and from 45 to 49 °C for the irradiated sample. A similar phenomenon was observed by Li et al. in a study of the rheological properties of a 27 wt % aqueous solution of PEO-*b*-PBO.[64] Such a gel with lower values of G' and G" is commonly called a soft gel, which presumably comprised a dynamic network of weakly interacting spherical micelles.[1-3,15,64]

The formation of micellar gels was also evidenced by the data from frequency sweep experiments (Figures 4.4a and 4.5a). For the non-irradiated solution at 33 °C, the dynamic storage modulus G' was essentially independent of frequency (Figure 4.4a), while G" varied slightly, with a minimum at an intermediate frequency. In addition, G' was about one order of magnitude larger than G" in the studied frequency range from ~ 0.1 to ~ 100 s^{-1}. Similar properties were observed for the irradiated sample at 41 °C (Figure 4.5a). These are the characteristics of elastic solids with a cubic structure,[1-3,65] suggesting that the micelles in both solutions were packed into a cubic lattice. This is also



(a) (b)

Figure 4.4. Frequency dependences of dynamic storage modulus G' (■) and dynamic loss modulus G'' (□) of the 20.0 wt % aqueous solution of PEO-*b*-P(TEGEA-*co*-NBA) at (a) 33 °C and (b) 31 °C. A strain amplitude of 0.2 % was used in the frequency sweep experiments.

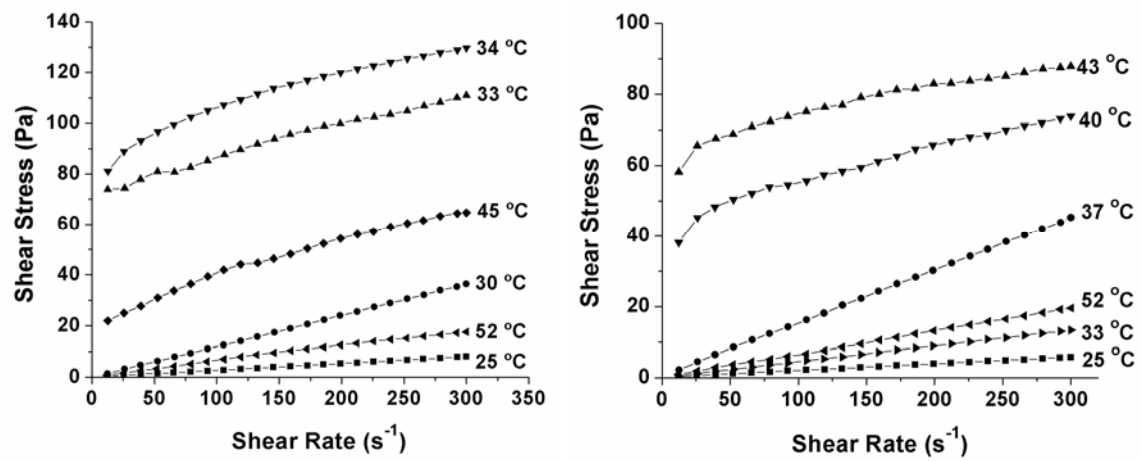


(a) (b)

Figure 4.5. Frequency dependences of dynamic storage modulus G' (■) and dynamic loss modulus G'' (□) of the UV-irradiated solution (a 18.9 wt % aqueous solution of PEO-*b*-P(TEGEA-*co*-AA)) at (a) 41 °C and (b) 37 °C. A strain amplitude of 0.2 % was used in the frequency sweep experiments.

supported by polarized light microscopy results. In the gel zones, both solutions were completely dark under a polarized light microscope with crossed polarizers, demonstrating that the gels were optically isotropic. Note that among all ordered structures, only a cubic lattice is optically isotropic. In contrast to the frequency dependences of G' and G" in the gel zones, for the non-irradiated solution at 31 °C and the irradiated solution at 37 °C, G' and G" scaled to the second and first power of frequency, respectively (Figures 4.4b and 4.5b), which is typical for a viscoelastic fluid.[1-3,29]

The flow properties of both solutions were further studied under steady shear conditions. Figure 4.6 shows the flow curves of the 20.0 wt % aqueous solution of PEO-*b*-P(TEGEA-*co*-NBA) and the irradiated solution at various temperatures. For the non-irradiated solution at 25 °C, the shear stress σ was proportional to the shear rate $d\gamma/dt$, indicating that the solution behaved as a Newtonian liquid. At 30 °C, the solution was still a Newtonian liquid, but the viscosity was slightly higher, presumably because of the presence of micelles in the solution. At 33, 34, and 45 °C, the solution exhibited a plastic flow behavior with a finite yield stress of ~ 70, 75, and 20 Pa, respectively. Clearly, once the initial resistance was overcome, the shear stress was essentially proportional to the shear rate. Therefore, the flow behavior can be described by the equation: $\sigma = \sigma_o + \eta d\gamma/dt$, where σ_o is the yield stress and η is the viscosity. At 52 °C, the solution became a Newtonian liquid with a low viscosity (Figure 4.6a). Similarly, the irradiated solution exhibited a plastic flow behavior with a finite yield stress of ~ 40 and 60 Pa at 40 and 43 °C, respectively. Below 40 °C and above 49 °C, the polymer solution behaved as a



(a) (b)

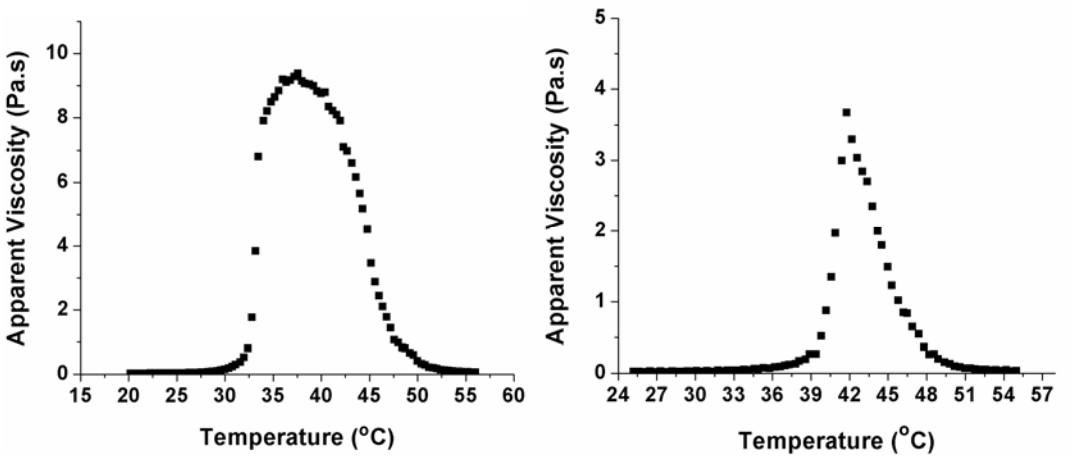
Figure 4.6. Flow curves of (a) a 20.0 wt % aqueous solution of block copolymer PEO-*b*-P(TEGEA-*co*-NBA) and (b) the UV-irradiated solution (a 18.9 wt % aqueous solution of PEO-*b*-P(TEGEA-*co*-AA) at various temperatures).

Newtonian liquid.

Figure 4.7 shows the temperature dependence of apparent viscosity of the 20.0 wt % aqueous solution of PEO-*b*-P(TEGEA-*co*-NBA) before and after UV irradiation at a shear rate of 10 s^{-1}. For the solution before UV irradiation, when the temperature was below 26 °C, the viscosity was < 0.040 Pa·s and there was essentially no change when the temperature was increased from 20 to 25 °C. A sharp increase in the apparent viscosity was observed when the temperature was raised to ~ 33 °C. After reaching the highest value, 9.38 Pa·s, at 38 °C, the apparent viscosity began to decrease with the further increase of temperature. At 56 °C, the apparent viscosity was only 0.063 Pa·s. For the irradiated solution, the apparent viscosity was very low at temperatures below 36 °C and increased rapidly at ~ 40 °C, where the solution turned into a gel. Upon further heating, the viscosity began to decrease; at 55 °C, the apparent viscosity was only 0.034 Pa·s. These results matched those obtained from dynamic viscoelastic measurements and the vial inversion tests. It was noticed that the highest apparent viscosity of the irradiated solution, 3.66 Pa·s observed at 42 °C, was much smaller than that of the non-irradiated solution (9.38 Pa·s at 38 °C). This is likely due to the decreased polymer concentration after UV irradiation as discussed earlier.

4.3.3 Sol-Gel Phase Diagrams of PEO-*b*-P(TEGEA-*co*-NBA) and PEO-*b*-P(TEGEA-*co*-AA) in Water at Moderate Concentrations

The sol-gel phase diagram of an aqueous solution of a thermosensitive diblock copolymer at low/moderate concentrations is usually a C-shaped curve,[1-3] which can be conveniently mapped out by the tube or vial inversion test. This simple method has been



(a) (b)

Figure 4.7. Temperature dependence of the apparent viscosity of (a) the 20.0 wt % aqueous solution of PEO-*b*-P(TEGEA-*co*-NBA) and (b) the irradiated solution at a shear rate of 10 s^{-1}.

reported to give results in good agreement with those from rheology studies.[1-3] The results presented above also demonstrated this agreement. Therefore, the vial inversion method was used to determine the sol-gel phase diagrams of aqueous solutions of PEO-*b*-P(TEGEA-*co*-NBA) and PEO-*b*-P(TEGEA-*co*-AA), formed from PEO-*b*-P(TEGEA-*co*-NBA) after UV irradiation, at moderate concentrations. The results are shown in Figure 4.8. The lowest concentration (critical gelation concentration, CGC) of PEO-*b*-P(TEGEA-*co*-NBA) in water that can form a micellar gel was 17.5 wt %. After the cleavage of *o*-nitrobenzyl groups by UV irradiation, the CGC increased slightly to 18.3 wt %, which might result from the increased hydrophilicity of the thermosensitive block of PEO-*b*-P(TEGEA-*co*-AA). It is known that for PEO-based thermosensitive diblock copolymers, the lower temperature sol-gel boundary corresponds to the enhanced micellization of the block copolymer with the increase of temperature and the ordering of spherical micelles onto a cubic macrolattice. Since this boundary was related to the LCST of the thermosensitive block, the gelation temperature did not change much with the concentration. From Figure 4.8, one can see that the sol-gel transition temperature for the concentration of 18.9 wt % was 34 °C, which was ~ 3 °C higher than that for the 22.9 wt % concentration. The upper temperature boundary is due to the negative coefficient of the PEO solubility in water.[1-3] The gel-sol transition temperature increased sharply from 40 to 60 °C with the increase of concentration from 18.3 wt % to 22.9 wt %. After the UV irradiation, the lower boundary shifted up by ~ 7 °C and the slope of the upper boundary was less steep than that for the polymer before UV irradiation.

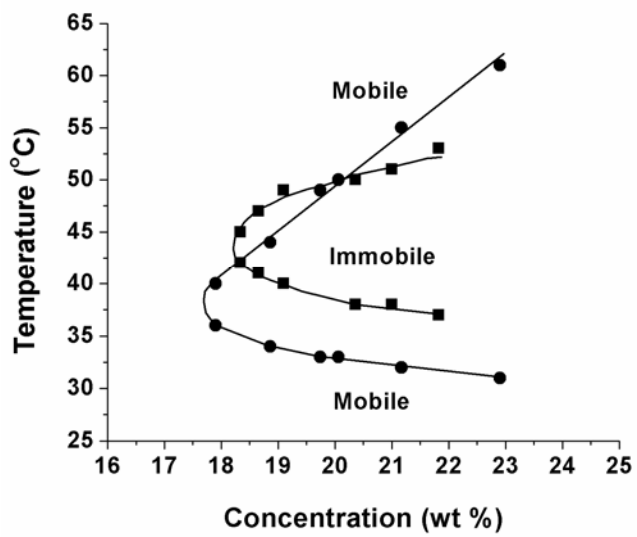
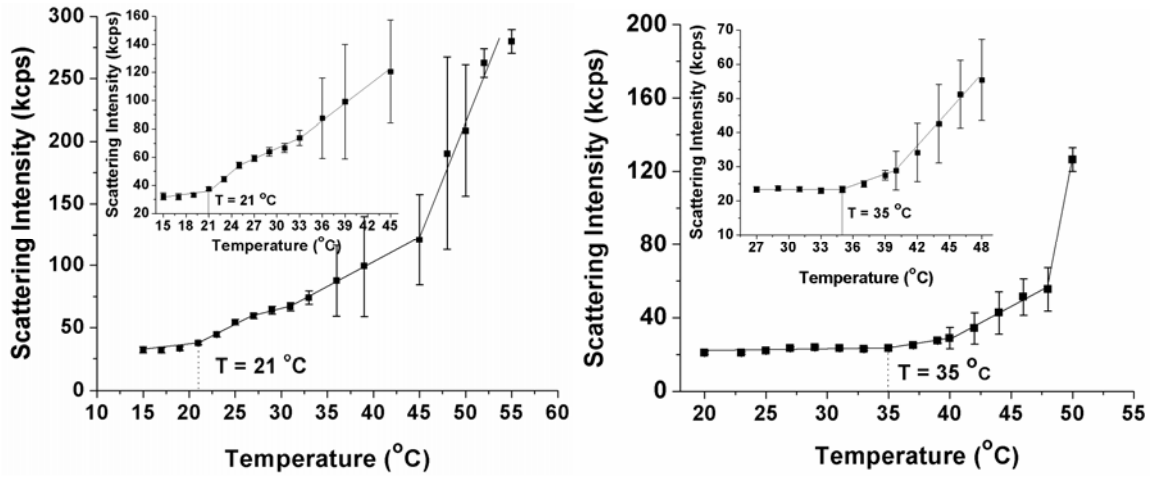


Figure 4.8. Sol-Gel phase diagrams for aqueous solutions of PEO-*b*-P(TEGEA-*co*-NBA) (●) and PEO-*b*-P(TEGEA-*co*-AA) (■), formed from PEO-*b*-P(TEGEA-*co*-NBA) after UV irradiation at 33 °C for six days, at moderate concentrations.

4.3.4 Mechanisms of Sol-to-Gel/Gel-to-Sol Transitions of the 20.0 wt % Aqueous Solution of the Thermo- and Light-Sensitive Block Copolymer Induced by Temperature Changes and UV Irradiation

As shown in Figure 4.1, the 20.0 wt % aqueous solution of PEO-*b*-P(TEGEA-*co*-NBA) can undergo multiple sol-gel-sol transitions in response to temperature changes and UV irradiation. This is because the LCST transition temperature of the thermosensitive block of PEO-*b*-P(TEGEA-*co*-NBA) can be modified by UV irradiation and the PEO solubility in water decreases with an increase in temperature.

As mentioned earlier, the CMT of PEO-*b*-P(TEGEA-*co*-NBA) in a 0.20 wt % aqueous solution was 25 °C and spherical micelles with an apparent hydrodynamic diameter of ~ 30 nm were observed at temperatures ≥ 29 °C. Since the CMT of the block copolymer in the 20.0 wt % aqueous solution could be slightly different from that in a 0.20 wt % solution, the concentrated solution was also studied by DLS experiment. Figure 4.9a shows the scattering intensity of the 20.0 wt % aqueous solution of PEO-*b*-P(TEGEA-*co*-NBA) at a scattering angle of 90° as a function of temperature. In this experiment, the increase in scattering intensity correlates to an increase in density correlations on the length scale of $d \sim 450$ nm, where this relationship is derived from $d = 2\pi/q$ where $q = 4\pi/\lambda \sin(\theta/2)$; θ is the scattering angle, and is the wavelength of the scattered light. Thus, the increase in scattering intensity that is observed at 21 °C can be interpreted as an increase in aggregation and ordering due to micellization and therefore, light scattering defines the CMT to be 21 °C, about 4 °C lower than in a 0.20 wt % aqueous solution. Note that in the studies of thermosensitive block copolymers of vinyl



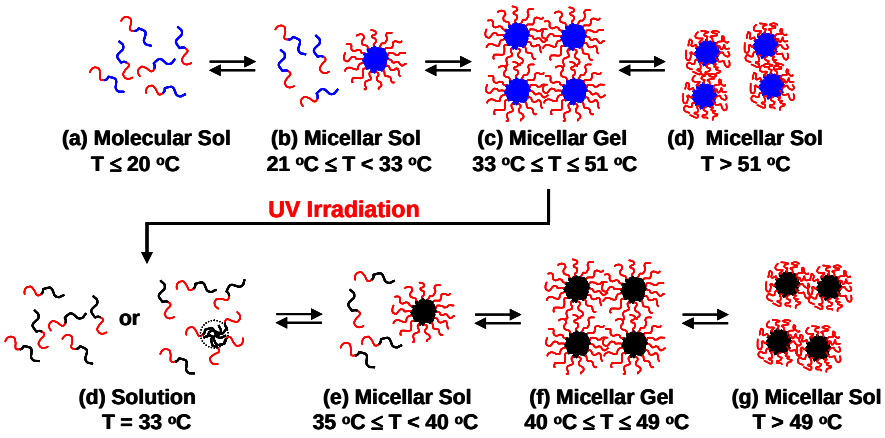
(a) (b)

Figure 4.9. Scattered light intensity of (a) the 20.0 wt % aqueous solution of PEO-*b*-P(TEGEA-*co*-NBA) and (b) the 18.9 wt % aqueous solution of PEO-*b*-P(TEGEA-*co*-AA) at a scattering angle of 90° as a function of temperature.[66] The data were collected from dynamic light scattering studies. The 18.9 wt % solution of PEO-*b*-P(TEGEA-*co*-AA) was obtained from the 20.0 wt % aqueous solution of PEO-*b*-P(TEGEA-*co*-NBA) after UV irradiation at 33 °C for six days. The insets in (a) and (b) show the enlarged plots of scattering intensity versus temperature.

ethers in water, Aoshima et al. found that the CMT of a block copolymer in a concentrated aqueous solution was either the same as or a few degree lower than that in a dilute solution.[29,33,34] Additionally, the increased scattering that occurred at ~ 48 °C indicates further increase in density correlations on the length scale of 450 nm at this temperature.

Thus, the combination of experimental results presented in this work allows us to propose a mechanism for the sol-gel/gel-sol transitions of this 20.0 % solution. It is believed that PEO-*b*-P(TEGEA-*co*-NBA) was dissolved molecularly at T ≤ 20 °C as schematically illustrated in Scheme 4.1a. Above ~ 20 °C, micellization occurred with the thermosensitive P(TEGEA-*co*-NBA) block associating into the core and the PEO block forming the corona. The fraction of polymer molecules in the micelles increased with temperature. At 33 °C, the volume fraction of micelles in the solution reached a critical value and the micellar solution was transformed into a cubic-packed micellar gel (Scheme 4.1b). The cubic structure was manifested in the frequency independence of G' of the solution at 33 °C in the dynamic rheological measurements and the optical isotropy in the polarized light microscopy experiments.[1-3,65] Upon further heating, the PEO corona shrinks as the solvent quality decreases, which results in the break up of the gel to a sol, where the increase in light scattering suggests that particles are micelle aggregates. This makes sense, as the relatively poor solvent quality of the water for both the core and corona of the micelle would imply that the micelles will aggregate to minimize PEO-water contacts. Regardless, the structural change causes the release of the structural constraint and the conversion of the gel to a micellar sol (Scheme 4.1c).

Scheme 4.1. Schematic Illustration of Thermo- and Light-Induced Multiple Sol-to-gel/gel-to-sol Transitions of the 20.0 wt % Aqueous Solution of PEO-*b*-P(TEGEA-*co*-NBA) under Different Conditions



As mentioned in Chapter 2, at a carefully chosen temperature, UV irradiation can dissociate the micelles into the unimers.[48] In the present work, the micellar gel was irradiated at 33 °C to cleave the *o*-nitrobenzyl groups. After six days, ~ 95 % of *o*-nitrobenzyl groups were cleaved and the gel became a free-flowing liquid with an apparent viscosity of 0.026 Pa·s at 33 °C (Figure 4.7). Note that the apparent viscosity of the solution before UV irradiation was 3.84 Pa·s at 33 °C, which was nearly 150 times higher than the apparent viscosity of the irradiated solution at the same temperature. The CMT of a 0.20 wt % aqueous solution of PEO-b-P(TEGEA-*co*-AA), formed from the PEO-*b*-P(TEGEA-*co*-NBA) after UV irradiation, was 35 °C. Figure 4.9b shows the plot of scattering intensity of the irradiated solution versus temperature. It appears that the scattering intensity began to increase slightly at 35 °C. As described above, the scattering at one angle cannot provide sufficient information to characterize the state of PEO-*b*-P(TEGEA-*co*-AA) in the irradiated solution at 33 °C. However, it is very likely that the block copolymer was either in the unimer state or in the early stage of the micellization transition zone at 33 °C. For the latter case, some polymer chains might form interchain clusters or ill-defined micellar aggregates,[29] but a significant amount of PEO-*b*-P(TEGEA-*co*-AA) should be in the unimer state (Scheme 4.1d). Note that the thermosensitive block P(TEGEA-*co*-AA) of the resultant block copolymer contained ionizable carboxylic acid groups, the LCST of P(TEGEA-*co*-AA) and thus the CMT of PEO-*b*-P(TEGEA-*co*-AA) could be tuned by adjusting the pH.[57] With the further increase of temperature, the solution underwent sol-gel-sol transitions (Scheme 4.1e and 4.1f), similar to the thermo-induced phase transitions of the solution before UV irradiation.

From the results of rheology and polarized light microscopy studies, the gel at 41 °C was composed of cubic-packed micelles.

4.4 Conclusion

It was demonstrated in this chapter that a 20.0 wt % aqueous solution of a thermo- and light-sensitive hydrophilic block copolymer, PEO-*b*-P(TEGEA-*co*-NBA), can undergo multiple sol-gel-sol transitions under different conditions in response to temperature changes and UV irradiation. The solution was a free-flowing Newtonian liquid with a low viscosity at low temperatures. Upon gradually heating to 33 °C, the solution was transformed into a transparent gel, which exhibited a plastic flow with a finite yield stress under a steady shear condition. The gel flowed under its own weight when the temperature reached 50 °C. At 33 °C, the 20.0 wt % solution was irradiated with 365 nm UV light; the gel was converted to a free-flowing, deep-red liquid. ^{1}H NMR spectroscopy analysis showed that ~ 95 % *o*-nitrobenzyl groups were cleaved. The irradiated solution underwent similar thermo-induced sol-gel-sol transitions except that the sol-to-gel and gel-to-sol transitions shifted to 40 and 48 °C, respectively. Dynamic rheological measurements showed that G' was essentially independent of frequency for the gel at 33 °C before UV irradiation and 41 °C after UV irradiation, suggesting that both gels were composed of cubic-packed micelles, which was also supported by the results from polarized light microscopy studies. The sol-gel/gel-sol transition temperatures determined from rheological measurements were in good agreement with those from visual inspection. The phase diagrams of the block copolymer in water before and after UV irradiation at moderate concentrations were mapped out by the vial

inversion method. While the upper boundary did not change much, the lower temperature boundary shifted up by ~ 7 °C after UV irradiation. The principle used in this work, that is, the sol-gel transition temperatures can be tuned by changing the LCST of a thermosensitive block via a second external stimulus, can be extended to other block copolymer systems. For example, by incorporating ionizable carboxylic acid groups into the thermosensitive block of a block copolymer, the LCST transition temperatures can be reversibly and precisely tuned by changing the pH,[57] making it possible to precisely control sol-gel-sol transitions.

References and Footnote

1. Hamley, I. W. *Block Copolymers in Solution: Fundamentals and Applications*, John Wiley & Sons: Chichester, 2005.
2. Hamley, I. W. *The Physics of Block Copolymers*, Oxford University Press: Oxford, 1998.
3. Hamley, I. W. *Philosophical Transaction of the Royal Society of London Series A-Mathematical Physical and Engineering Sciences* **2001**, *359*, 1017-1044.
4. Watanabe, H.; Kotaka, T.; Hashimoto, T.; Shibayama, M.; Kawai, H. *J. Rheology* **1982**, *26*, 153-179.
5. Shibayama, M.; Hashimoto, T.; Kawai, H. *Macromolecules* **1983**, *16*, 16-28.
6. Hashimoto, T.; Shibayama, M.; Kawai, H.; Watanabe, H.; Kotaka, T. *Macromolecules* **1983**, *16*, 361-371.
7. McConnell, G. A.; Gast, A. P.; Huang, J. S.; Smith, S. D. *Phys. Rev. Lett.* **1993**, *71*, 2102-2105.
8. Hanley, K. J.; Lodge, T. P.; Huang, C.-I. *Macromolecules* **2000**, *33*, 5918-5931.
9. Lodge, T. P.; Pudil, B.; Hanley, K. J. *Macromolecules* **2002**, *35*, 4707-4717.
10. Lodge, T. P.; Hanley, K. J.; Pudil, B.; Alahapperuma, V. *Macromolecules* **2003**, *36*, 816-822.
11. Willet, N.; Gohy, J. F.; Lei, L. C.; Heinrich, M.; Auvray, L.; Varshney, S.; Jérôme, R.; Leyh, B. *Angew. Chem. Int. Ed.* **2007**, *46*, 7988-7992.
12. Luo, Y. Z.; Nicholas, C. V.; Attwood, D.; Collett, J. H.; Price, C.; Booth, C. *Colloid Polym. Sci.* **1992**, *270*, 1094-1105.

13. Hvidt, S.; Jørgensen, E. B.; Schillén, K.; Brown, W. *J. Phys. Chem.* **1994**, *98*, 12320-12328.

14. Kelarakis, A.; Mingvanish, W.; Daniel, C.; Li, H.; Havredaki, V.; Booth, C.; Hamley, I. W.; Ryan, A. J. *Phys. Chem. Chem. Phys.* **2000**, *2*, 2755-2763.

15. Li, H.; Yu, G. -E.; Price, C.; Booth, C.; Hecht, E.; Hoffmann, H. *Macromolecules* **1997**, *30*, 1347-1354.

16. Deng, N.-J.; Luo, Y.-Z.; Tanodekaew, S.; Binham, N.; Attwood, D.; and Booth, C. *J. Polym. Sci. Part B: Polym. Phys.* **1995**, *33*, 1085-1096.

17. Mingvanish, W.; Mai, S.-M.; Heatley, F.; Booth, C.; Attwood, D. *J. Phys. Chem. B.* **1999**, *103*, 11269-11274.

18. Hamley, I. W.; Pople, J. A.; Fairclough, J. P. A.; Ryan, A. J.; Booth, C.; Yang, Y.-W. *Macromolecules* **1998**, *31*, 3906-3911.

19. Hamley, I. W.; Daniel, C.; Mingvanish, W.; Mai, S.-M.; Booth, C.; Messe, L.; Ryan, A. J. *Langmuir* **2000**, *16*, 2508-2514.

20. Mortensen, K.; Brown, W.; Norden, B. *Phys. Rev. Lett.* **1992**, *68*, 2340-2343.

21. Mortensen, K. *Europhys. Lett.* **1992**, *19*, 599-604.

22. Alexandridis, P.; Hatton, T. A. *Colloids and Surfaces A – Physicochemical and Engineering Aspects*, **1995**, *96*, 1-46.

23. Alexandridis, P.; Olsson, U.; Kindman, B. *Langmuir* **1997**, *12*, 23-34.

24. Wanka, G.; Hoffmann, H.; Ulbricht, W. *Macromolecules* **1994**, *27*, 4145-4159.

25. Zhou, Z; Chu, B. *Macromolecules* **1994**, *27*, 2025-2033.

26. Lin, H. H.; Cheng, Y. L. *Macromolecules* **2001**, *34*, 3710-3715.

27. Motokawa, R.; Morishita, K.; Koizumi, S.; Nakahira, T.; Annaka, M. *Macromolecules* **2005**, *38*, 5748-5760.

28. Okabe, S.; Sugihara, S.; Aoshima, S.; Shibayama, M. *Macromolecules* **2002**, *35*, 8139-8146.

29. Okabe, S.; Sugihara, S.; Aoshima, S.; Shibayama, M. *Macromolecules* **2003**, *36*, 4099-4106.

30. Aoshima, S.; Sugihara, S. *J. Polym. Sci. Part A: Polym. Chem.* **2000**, *38*, 3962-3965.

31. Aoshima, S.; Sugihara, S.; Shibayama, M.; Kanaoka, S. *Macromol. Symp.* **2004**, *215*, 151-163.

32. Sugihara, S. Kanaoka, S.; Aoshima, S. *J. Polym. Sci. Part A: Polym. Chem.* **2004**, *42*, 2601-2611.

33. Sugihara, S.; Kanaoka, S.; Aoshima, S. *Macromolecules* **2005**, *38*, 1919-1927.

34. Sugihara, S.; Hashimoto, K.; Okabe, S.; Shibayama, M.; Kanaoka, S.; Aoshima, S. *Macromolecules* **2004**, *37*, 336-343.

35. Jeong, B. M.; Bae, Y. H.; Lee, D. S.; Kim, S. W. *Nature* **1997**, *388*, 860-862.

36. Yoshioka, H.; Mori, Y.; Tsukikawa, S.; Kubota, S. *Polymers for Advanced Technologies* **1998**, *9*, 155-158.

37. Bromberg, L. E.; Ron, E. S. *Advanced Drug Delivery Reviews* **1998**, *31*, 197-221.

38. Gil, E. S.; Hudson, S. M. *Prog. Polym. Sci.* **2004**, *29*, 1173-1222.

39. He, C. L.; Kim, S. W.; Lee, D. S. *J. Controlled Release* **2008**, *127*, 189-207.

40. Anderson, B. C.; Cox, S. M.; Bloom, P. D.; Sheares, V. V.; Mallapragada, S. K. *Macromolecules* **2003**, *36*, 1670-1676.

41. Determan, M. D.; Cox, J. P.; Seifert, S.; Thiyagarajan, P.; Mallapragada, S. K. *Polymer* **2005**, *46*, 6933-6946.

42. Shim, W. S.; Yoo, J. S.; Bae, Y. H.; Lee, D. S. *Biomacromolecules* **2005**, *6*, 2930-2934.

43. Shim, W. S.; Kim, S. W.; Lee, D. S. *Biomacromolecules* **2006**, *7*, 1935-1941.

44. Dayananda, K.; Pi, B. S.; Kim, B. S.; Park, T. G.; Lee, D. S. *Polymer* **2007**, *48*, 758-762.

45. Park, S. Y.; Lee, Y.; Bae, K. H.; Ahn, C. H.; Park, T. G. *Macromol. Rapid Commun.* **2007**, *28*, 1172-1176.

46. Suh, J. M.; Bae, S. J.; Jeong, B. *Adv. Mater.* **2005**, *17*, 118-120.

47. Joo, M. K.; Park, M. H.; Choi, B. G.; Jeong, B. *J. Mater. Chem.* **2009**, *19*, 5891-5905.

48. Jiang, X. G., Lavender, C. A.; Woodcock, J. W.; Zhao, B. *Macromolecules* **2008**, *41*, 2632-2643.

49. Han, S.; Hagiwara, M.; Ishizone, T. *Macromolecules* **2003**, *36*, 8312-8319.

50. Ishizone, T.; Seki, A.; Hagiwara, M.; Han, S.; Yokoyama, H.; Oyane, A.; Deffieux, A.; Carlotti, S. *Macromolecules* **2008**, *41*, 2963-2967.

51. Zhao, B.; Li, D. J.; Hua, F. J.; Green, D. R. *Macromolecules* **2005**, *38*, 9509-9517.

52. Hua, F. J.; Jiang, X. G.; Li, D. J.; Zhao, B. *J. Polym. Sci. Part A: Polym. Chem.* **2006**, *44*, 2454-2467.

53. Li, D. J.; Jones, G. L.; Dunlap, J. R.; Hua, F. J.; Zhao, B. *Langmuir* **2006**, 22, 3344-3351.

54. Li, D. J.; Zhao, B. *Langmuir* **2007**, *23*, 2208-2217.

55. Li, D. J.; Dunlap, J. R.; Zhao, B. *Langmuir* **2008**, 24, 5911-5918.

56. Jiang, X. G.; Zhao, B. *J. Polym. Sci. Part A: Polym. Chem.* **2007**, *45*, 3707-3721.

57. Jiang X. G.; Zhao, B. *Macromolecules* **2008**, *41*, 9366-9375.

58. O'Lenick, T. G.; Jiang, X. M.; Zhao, B. *Polymer* **2009**, *50*, 4363-4371.

59. Lutz, J.-F.; Hoth, A. *Macromolecules* **2006**, *39*, 893-896.

60. Lutz, J. F.; Weichenhan, K.; Akdemir, O.; Hoth, A. *Macromolecules* **2007**, *40*, 2503-2508.

61. Zhao, B.; Moore, J. S.; Beebe, D. J. *Science* **2001**, *291*, 1023-1026.

62. Jiang, J. Q.; Tong, X.; Morris, D.; Zhao. Y. *Macromolecules* **2006**, *39*, 4633-4640.

63. It should be noted here that by visual inspection and dynamic light scattering, no insoluble crosslinked polymer was observed in a 0.2 wt % aqueous solution that was made by diluting the irradiated sample. To further investigate if chain degradation or crosslinking occurred during the UV irradiation, two control experiments were conducted. In the first one, a 21.9 % aqueous solution of PEO-*b*-PTEGEA ($M_{n,GPC}$ = 20.9 kDa and PDI = 1.12) that contained *o*-nitrobenzyl alcohol (concentration: 4 mg/mL) was prepared to mimic the 20.0 wt % aqueous solution of PEO-*b*-P(TEGEA-*co*-NBA). The solution was irradiated at 30 °C for 6 days with 365 nm UV light from the same UV lamp used for the 20.0 wt % aqueous solution of PEO-*b*-P(TEGEA-*co*-NBA). There were no any changes in the ^{1}H NMR spectrum and in the molecular weight and molecular weight distribution from GPC analysis. The sol-to-gel transition temperature of this solution after UV irradiation was 41 °C, which was identical to that before UV irradiation. In the second experiment, a 19.5 wt % aqueous solution of PEO_{113}-*b*-P($TEGEA_{89}$-*co*-(2-(*o*-

nitrobenzyloxy)ethyl acrylate)$_{10}$) (PEO$_{113}$-*b*-P(TEGEA$_{89}$-*co*-EGNBA$_{10}$), $M_{n,SEC}$ = 20.4 kDa, PDI = 1.13) was irradiated at 30 °C for 6 days with the same UV lamp. ^{1}H NMR spectroscopy analysis showed that the photocleavage was complete. There were essentially no changes in the molecular weight and molecular weight distribution from GPC analysis. Thus, these experiments proved that the chain degradation or crosslinking of the block copolymer did not occur during the UV irradiation.

64. Contrary to the report by Li et al. in reference 15 that the soft gel zone could not be located by the tube inversion method, our block copolymer solution did not flow in the tilted/inverted vial in the temperature range of 45 to 51 ^{o}C before UV irradiation and of 45 to 49 ^{o}C after UV irradiation, presumably because our vial had a smaller inner diameter and the gel could support its own weight.

65. Kossuth, M. B.; Morse, D. C.; Bates, F. S. *J. Rheol.* **1999**, *43*, 167-196.

66. Each data point in these two plots represents the average of 300 values of scattered light intensity collected at a scattering angle of 90^o over a period of 5 min at a constant temperature (one value per second). The fluctuation of scattered light intensity for each data point is the standard deviation. Note that the gel is a nonergodic system and the scattering intensity is position-dependent. Therefore, the sampling position of the DLS tube was changed randomly every 15 sec. Clearly, the fluctuation of scattering intensity before the sol-to-gel transition temperature is extremely small. The sol-to-gel and gel-to-sol transitions can also be seen from the changes in the magnitude of the fluctuation of scattered light intensity.

Chapter 5. Summary and Future Work

5.1 Summary

Well-defined thermosensitive water-soluble polystyrenics and doubly responsive hydrophilic block copolymers were synthesized by "living"/controlled radical polymerization (NMRP and ATRP). Polystyrenics with a short oligo(ethylene glycol) pendant from each repeat unit exhibit LCST transitions in water. To study the effect of polymer chain end groups on cloud point, a series of well-defined thermosensitive polystyrenics with two hydrophobic end groups, one hydrophobic end group, and "no" end groups were prepared and their cloud points in water were determined. We found that the hydrophobic end groups can decrease the cloud point appreciably, especially in the lower molecular weight range, and can even reverse the molecular weight dependence of cloud point. By incorporating a small amount of stimuli-responsive groups into the thermosensitive block of a hydrophilic block copolymer, the LCST of the thermosensitive block can be modified by a stimulus and multiple micellization/dissociation transitions can be achieved by combining two external triggers. For example, thermo- and light-sensitive PEO-*b*-(PTEGEA-*co*-NBA) underwent multiple micellization/dissociation transitions in water in response to temperature changes and UV irradiation. When the polymer concentration was high enough (e.g., 20.0 wt %), aqueous solutions of PEO-*b*-(PTEGEA-*co*-NBA) exhibited multiple sol-gel/gel-sol transitions upon temperature changes and light irradiation. PEO-*b*-P(DEGMMA-*co*-AA) that contained a small amount of carboxylic acids in the thermosensitive block underwent thermo- and pH-induced reversible micellization/dissociation transitions in aqueous buffers.

Dissolution of our thermosensitive polymers in water is believed to involve hydrophilic hydration, which comes from hydrogen bonding between oligo(ethylene glycol) pendants and water, and hydrophobic hydration of polymer chains.[1] Aoshima et al. observed from differential scanning calorimetry analysis that the LCST transitions of thermosensitive poly(vinyl ether)s with short oligo(ethylene glycol) pendants, which are similar in structure to our thermosensitive polystyrenics and polyacrylates, were endothermic. Thus, the entropy changes of the systems must be positive. Since the entropy of polymer chains decreases during the demixing, the overall entropy gain of the system is likely because the hydrated water that surrounds polymer chains is released into bulk water. It can be concluded from this research that the LCST transition temperature increases with the decrease of polymer concentration, molecular weight (for polymers with "no" hydrophobic groups at chain ends), and the hydrophobicity of polymer chains. The observed molecular weight dependence of cloud points of thermosensitive polystyrenics with hydrophobic chain ends (Chapter 1) is because the hydrophobic end groups have a larger effect on low molecular weight polymers. For a thermosensitive polymer that is incorporated with a small amount of stimuli-responsive groups, the LCST can be modified by changing the hydrophobicity of polymer chains through an external stimulus. In Chapter 2, the cleavage of hydrophobic *o*-nitrobenzyl groups increased the hydrophilicity and thus the LCST of the thermosensitive block, raised the critical micellization temperature to above the experimental temperature, and induced the dissociation of micelles. The LCST of the thermosensitive block of PEO-*b*-P(DEGMMA-*co*-MAA) in Chapter 3 can be continuously and reversibly altered by changing the solution pH. It is possible to use our thermo- and pH-sensitive block copolymers to

achieve on-demand micellization and dissociation transitions in certain pH and temperature ranges. For the concentrated solution studied in Chapter 4, the thermo-induced sol-gel-sol transitions resulted from the volume fraction changes of micelles in water. The light-induced gel-sol transition was due to the LCST increase of the thermosensitive block.

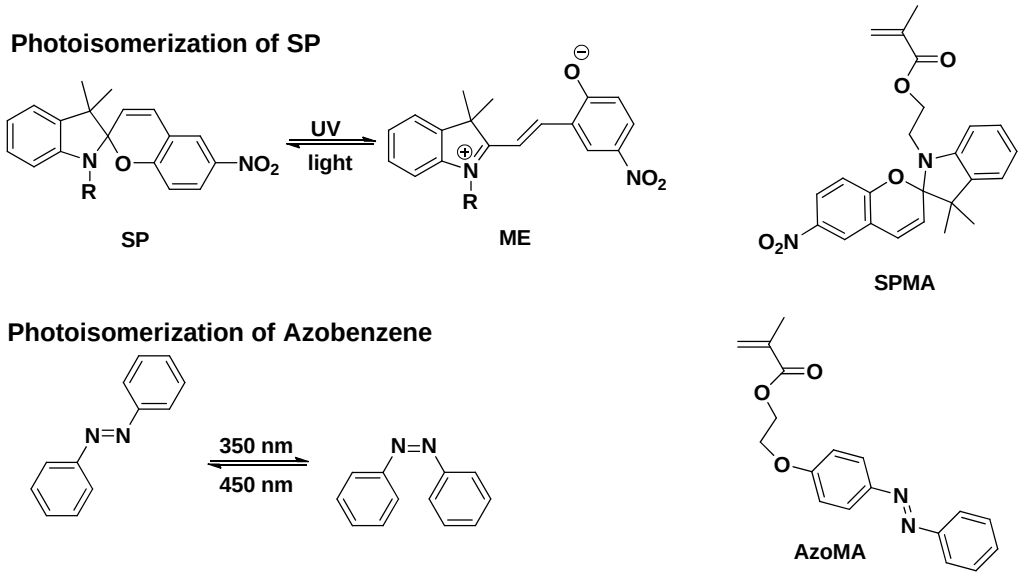
5.2 Future Work

5.2.1 Light-Induced Reversible Micellization/Dissociation Transitions of Thermo- and Light-Sensitive Block Copolymer in Water

Light is a very attractive external stimulus for modifying the LCST of a thermosensitive copolymer and for effecting micellization and dissociation transitions of responsive block copolymers in water. Chapter 2 presented the synthesis of thermo- and light-sensitive PEO-*b*-P(TEGEA-*co*-NBA) and their solution behavior under various environmental conditions. Although the thermo-induced micellization and dissociation transition was reversible, the UV-triggered dissociation of micelles was not because of the irreversible cleavage of *o*-nitrobenzyl groups. For many applications, light-induced reversible micellization is desired and more advantageous. This can be achieved by using photochromic moieties that can undergo light-induced reversible isomerization as responsive groups. We will use spiropyran and azobenzene detailed below.

Spiropyran derivatives are known to undergo reversible isomerization between the closed-ring and open structures (Scheme 5.1). Under the visible light, these photochromic compounds are in the neutral spiropyran form (SP). Upon UV irradiation, they change to the merocyanine (ME) form and become more hydrophilic. The distinct colors of these

Scheme 5.1. Photoisomerization of spiropyran and azobenzene compounds and monomer structures of SPMA and AzoMA



photochromic units in different forms make them very attractive. Aloson et al. attached spiropyran groups onto amino acid polymers and observed the changes in their inverse temperature transitions under different light conditions.[2] Lee et al. recently reported light-induced reversible formation of micelles of block copolymer PEO-*b*-poly(SPMA) (the molecular structure of SPMA is shown in Scheme 5.1).[3] We will synthesize thermo- and light-responsive hydrophilic block copolymers with the thermosensitive block containing a small amount of SPMA. Since the SP isomerization is also sensitive to temperature and pH changes, it is desired to conduct experiments around room temperature and at a fixed pH. Therefore, we choose to use DEGMMA and SPMA to make the thermosensitive block, because the LCST of PDEGMMA is 25 °C. Following the procedure described in Chapter 2, a series of random copolymers will be synthesized first by copolymerizing DEGMMA and SPMA with different molar ratios (100 : 5, 100 : 10, and 100 : 15) from small molecule initiator ethyl 2-bromisobutyrate (Chapter 3). The LCST changes of their aqueous solutions in response to light will be determined and the copolymer that exhibits the largest LCST change will be identified. Using the PEO macroinitiator described in Chapter 2, we will then prepare three block copolymers with different block lengths for the thermosensitive block (DP = 50, 100, and 150). The molar ratio of the two monomers in the thermosensitive block will be kept the same as that of the random copolymer that exhibited the largest LCST change. The solution behavior of these block copolymers under different environmental conditions will be studied by dynamic light scattering and fluorescence spectroscopy.

Azobenzene is known to isomerize reversibly between the *trans* and *cis* forms when irradiated with light of different wavelengths (Scheme 5.1); *trans*-azobenzene formed

under 450 nm light is less polar than the *cis*-azobenzne formed under 350 nm light. Housni et al. recently reported that the LCST of poly(*N,N*-dimethylacrylamide-*co*-*N*-4-phenylazophenylacrylamide) can be reversibly changed between ~ 34 and ~ 20 °C.[4] We will incorporate azobenzene groups into the thermosensitive blocks of block copolymers for effecting light-induced reversible micellization/dissociation transitions in water. Again, we will synthesize a series of random copolymers with different ratios of AzoMA (see Scheme 5.1) to DEGMMA and study their LCST changes. The block copolymers with different molecular weights but the same molar ratio of two monomers that corresponds to the largest LCST change for the random copolymer will be synthesized and their aqueous solutions will be investigated.

5.2.2 Structural Studies of Aqueous Solutions of Doubly Responsive Hydrophilic Block Copolymers by Small-Angle Neutron Scattering

Our doubly responsive hydrophilic block copolymers can undergo multiple micellization/dissociation transitions in water in response to external stimuli. In a concentrated solution, when the volume fraction of micelles reaches a critical value, the micelles pack into a gel and the free-flowing solution become immobile. From the frequency sweeps of micellar gels and sols shown in Chapter 4, the gels were similar to the elastic solids with a cubic structure and the disordered sols contained heterogeneous assembilies. To understand the mechanisms of sol-gel/gel-sol transitions, further work is needed to elucidate the nanostructures of micelles formed by the self-assembly of block copolymer molecules and the ordered hierarchical macrolattices formed by the self-organization of micelles. Small angle neutron scattering (SANS) can provide information

on the structural change of a thermo-sensitive block copolymer solution upon heating, from molecular solution, to micellar solution, to micellar gel/macrolattice, and to micellar solution again.[5,6] For example, Okabe et al. used SANS to study the sol-gel-sol transitions of poly(2-ethoxyethyl vinyl ether-*b*-2-hydroxyethyl vinyl ether).[6] By varying the D_2O/H_2O ratio, the nanostructure of block copolymer micelles can be obtained.[7] In our future work, the SANS instrument should have at least two capabilities: precise temperature control and shearing alignment. 0.2 wt % and 20 wt % solutions of PEO-*b*-P(TEGEA-*co*-NBA) in mixtures of D_2O/H_2O with various ratios will be prepared. The thermo-induced micellization and gelation will be studied first. We will also monitor the structural change of the solution under the UV irradiation in situ if all is possible.

References:

1. Urry, D. W. *J. Phys. Chem. B* **1997**, *101*, 11007-11028.
2. Alonso, M.; Reboto, V.; Guiscardo, L.; San Martin, A.; Rodriguez-Cabello, J. C. *Macromolecules* **2000**, *33*, 9480-9482.
3. Li, H.; Wu, W.; Oh, J. K.; Mueller, L.; Sherwood, G.; Peteanu, L.; Kowalewski, T.; Matyjaszewski, K. *Angew. Chem. Int. Ed.* **2007**, *46*, 2453-2457.
4. Housni, A.; Zhao, Y.; Zhao, Y. *Langmuir* **2010**, *26*, 12366-12370.
5. Mortensen, K. *J. Phys.: Condens. Matter* **1996**, *8*, A103-A124.
6. Okabe, S.; Sugihara, S.; Aoshima, S.; Shibayama, M. *Macromolecules* **2002**, *35*, 8139-8146.
7. Pederson, J. S.; Hamley, I. W.; Ryu, C. Y.; Lodge, T. P. *Macromolecules* **2000**, *33*, 542-550.

Appendix A. Multiple Micellization and Dissociation Transitions of Thermo- and Light-Sensitive Poly(ethylene oxide)-*b*-Poly(ethoxytri(ethylene glycol) acrylate-*co*-*o*-nitrobenzyl acrylate) in Dilute Aqueous Solution

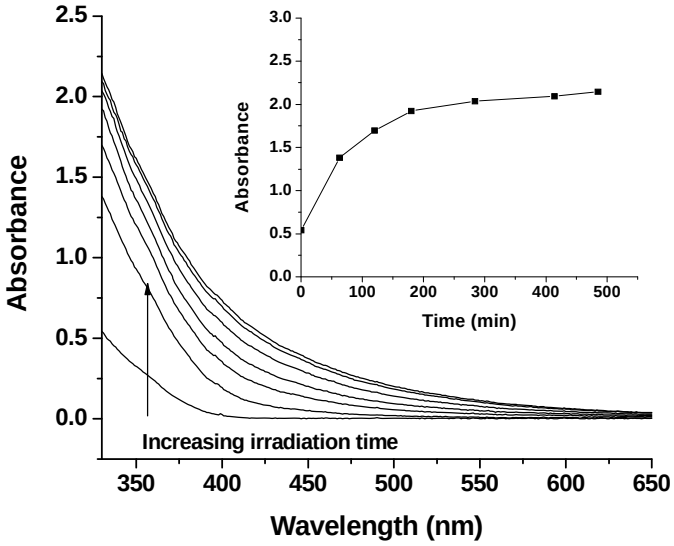


Figure A.1. UV-vis spectra of an aqueous solution of P(TEGEA-*co*-NBA) ($M_{n,GPC}$ = 13,900 g/mol and PDI = 1.13) with a concentration of 0.2 wt % after irradiation with 365 nm UV light at 13 ^{o}C for 0, 63, 120, 180, 284, 414, and 485 min. The inset is the plot of the absorbance of polymer solution at wavelength of 330 nm versus UV irradiation time.

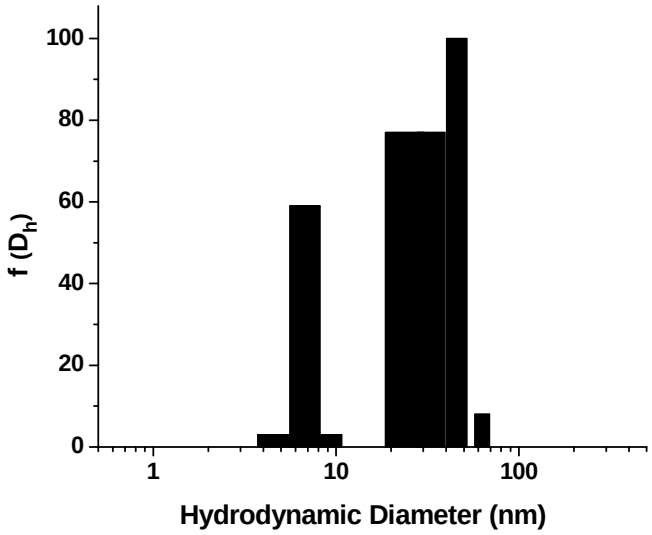


Figure A.2. Hydrodynamic diameter (D_h) distribution function of PEO-*b*-P(TEGEA-*co*-NBA) (BR-**4**, $M_{n,GPC}$ = 18,300 g/mol, PDI = 1.07, 0.2 wt % aqueous solution) at 27 ^{o}C in the cooling process.

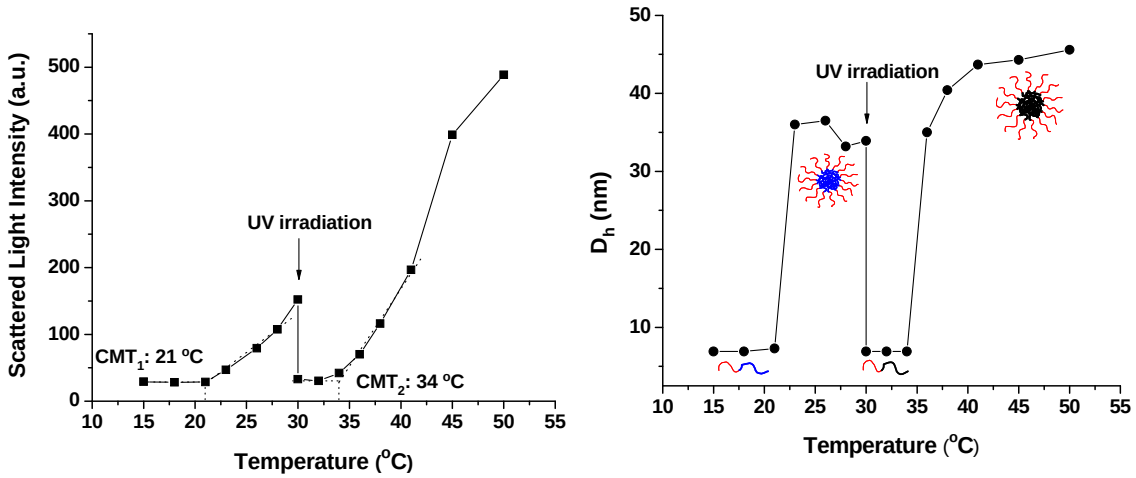
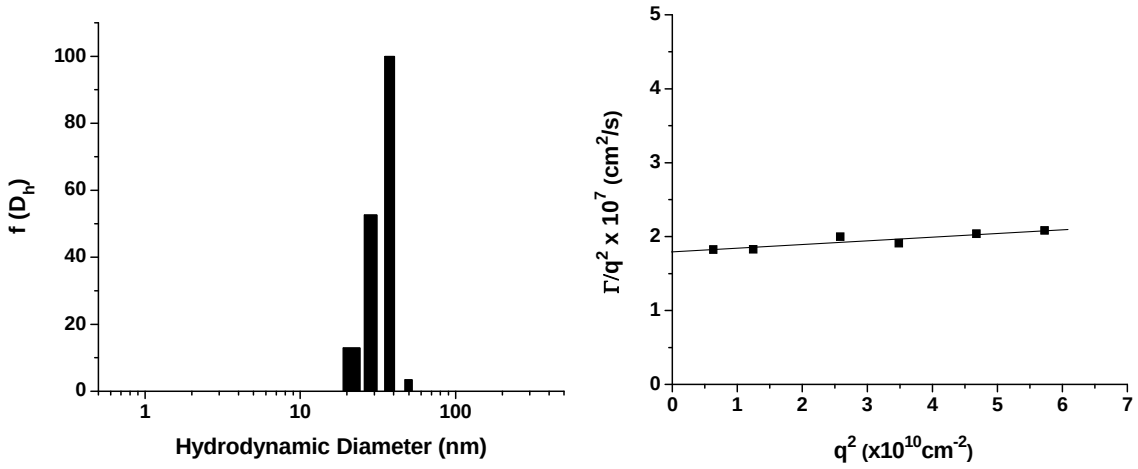
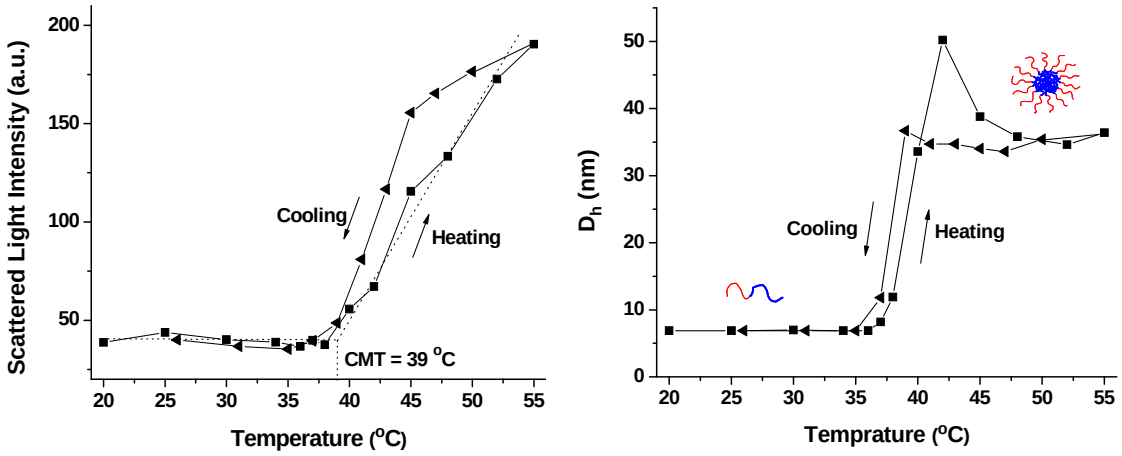


Figure A.3. The intensity of scattered light at scattering angle of 90° (a) and hydrodynamic diameter (b) as a function of temperature in a dynamic light scattering study of multiple micellization and dissociation transitions of PEO-*b*-P(TEGEA-*co*-NBA) (BR-**5**, $M_{n,GPC}$ = 24,700 g/mol, PDI = 1.11, 0.2 wt %) in water in response to temperature changes and UV irradiation. At 30 °C, the polymer solution was irradiated with 365 nm UV light for 480 min. The collection of light scattering data was resumed thereafter.



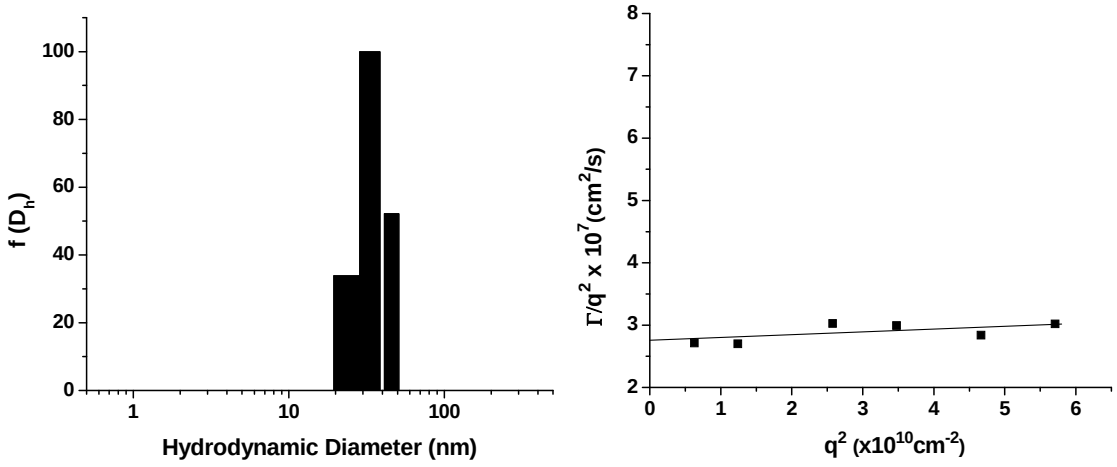
(a) (b)

Figure A.4. (a) Hydrodynamic diameter (D_h) distribution function of PEO-*b*-P(TEGEA-*co*-NBA) (BR-**5**, $M_{n,GPC}$ = 24,700 g/mol, PDI = 1.11, 0.2 wt % aqueous solution) at 30 ^{o}C in the heating process and (b) plot of Γ/q^2 of micelles of BR-**5** versus q^2 at 30 ^{o}C. The polydispersity of micelles of BR-**5** was 0.030 at 30 ^{o}C.



(a) (b)

Figure A.5. The intensity of scattered light at scattering angle of 90° (a) and hydrodynamic diameter (b) as a function of temperature in both heating and cooling processes in a dynamic light scattering study of thermo-induced formation and dissociation of micelles of PEO-*b*-PTEGEA (B-**3**, $M_{n,GPC}$ = 21,400 g/mol, PDI = 1.07, 0.2 wt %) in water.



(a) (b)

Figure A.6. (a) Hydrodynamic diameter (D_h) distribution function of micelles of PEO-*b*-PTEGEA (B-**3**, $M_{n,GPC}$ = 21,400 g/mol, PDI = 1.07) at 50 ^oC and (b) plot of Γ/q^2 of micelles of B-**3** versus q^2 at 50 ^oC. The polydispersity of micelles at 50 ^oC was 0.044.

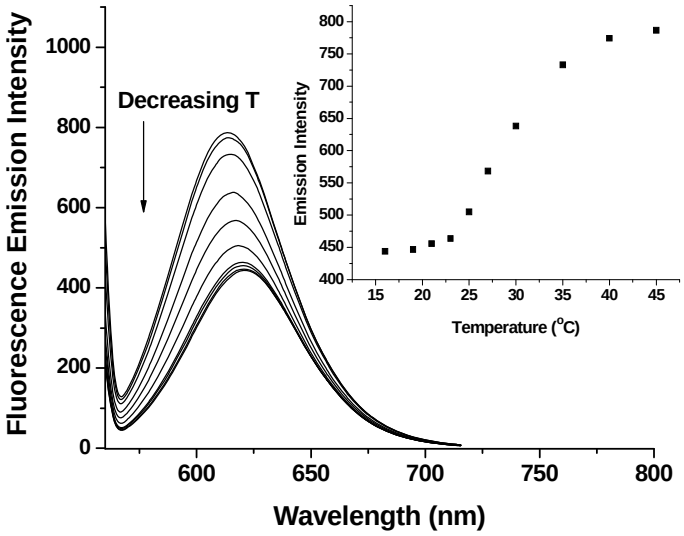
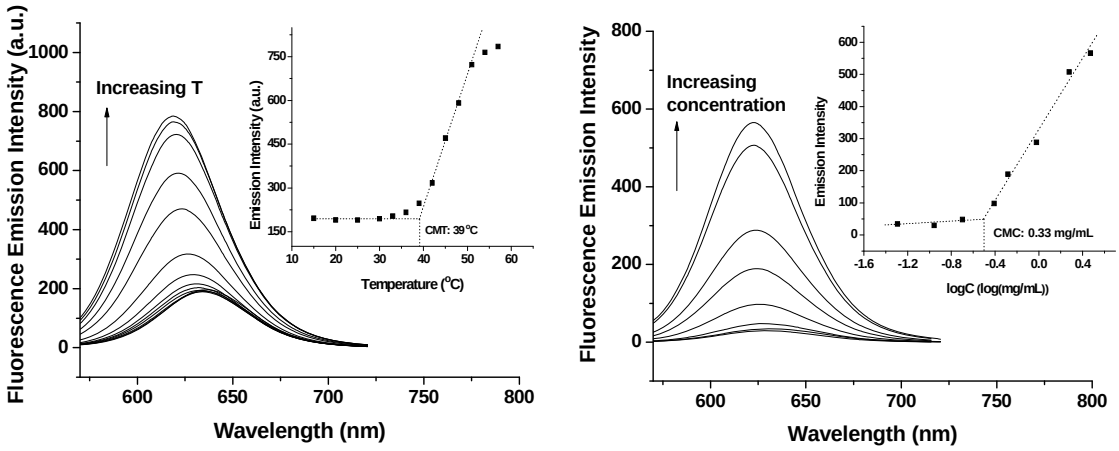


Figure A.7. Fluorescence emission spectra of Nile Red in a 0.2 wt % aqueous solution of PEO-*b*-P(TEGEA-*co*-NBA) (BR-**4**, $M_{n,GPC}$ = 18,300 g/mol, PDI = 1.07) at different temperatures during the cooling process. The inset is the plot of maximum fluorescence emission intensity versus temperature.



(a) (b)

Figure A.8. Fluorescence spectra of Nile Red (a) in a 0.2 wt % aqueous solution of PEO-*b*-PTEGEA) (B-**3**, $M_{n,GPC}$ = 21,400 g/mol, PDI = 1.07) at various temperatures during the heating process and (b) in a series of aqueous solutions of B-**3** with different concentrations at 45 ^{o}C. The inset in (a) is the plot of maximum fluorescence intensity versus temperature, from which the critical micellization temperature (CMT) was determined. The inset in (b) is the plot of maximum fluorescence emission intensity versus the logarithm of polymer concentration at 45 ^{o}C, from which the critical micelle concentration (CMC) was determined.

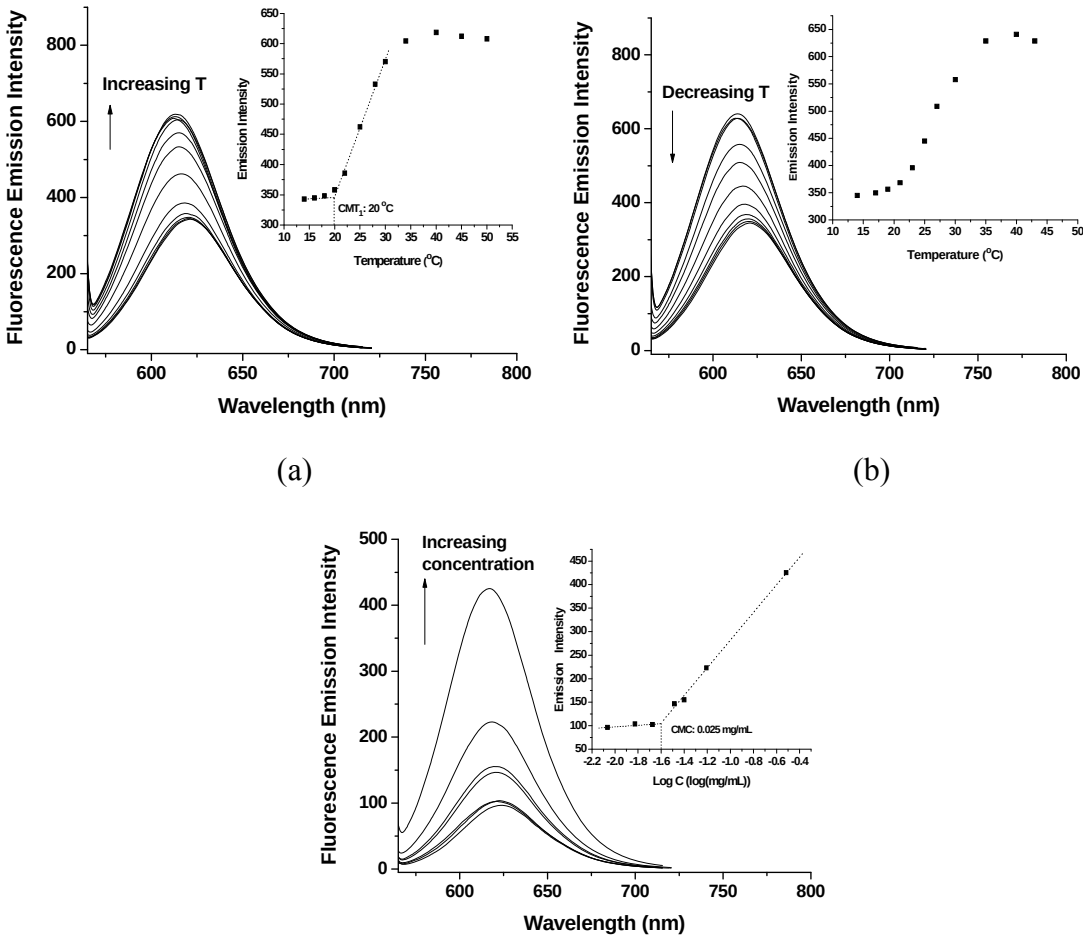


Figure A.9. Fluorescence spectra of Nile Red (a) in a 0.2 wt % aqueous solution of PEO-*b*-P(TEGEA-*co*-NBA) (BR-**5**, $M_{n,GPC}$ = 24,700 g/mol, PDI = 1.11) at various temperatures during the (a) heating and (b) cooling processes, and (c) in a series of aqueous solutions of BR-**5** with different concentrations at 30 ^{o}C. The insets in (a) and (b) are the plots of maximum fluorescence emission intensity versus temperature, from which the critical micellization temperature (CMT) was determined. The inset in (c) is the plot of maximum fluorescence emission intensity versus the logarithm of polymer concentration at 30 ^{o}C, from which the critical micelle concentration (CMC) was determined.

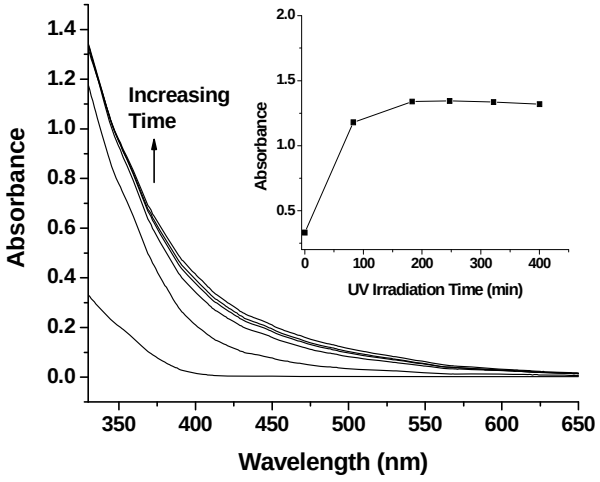


Figure A.10. UV-vis spectra of an aqueous solution of PEO-*b*-P(TEGEA-*co*-NBA) (BR-**4**, $M_{n,GPC}$ = 18,300 g/mol, PDI = 1.07) with a concentration of 0.2 wt % after irradiation with 365 nm UV light for 0, 83, 183, 247, 322, and 400 min at 32 ^{o}C. The inset is the plot of the absorbance of polymer solution at wavelength of 330 nm versus UV irradiation time.

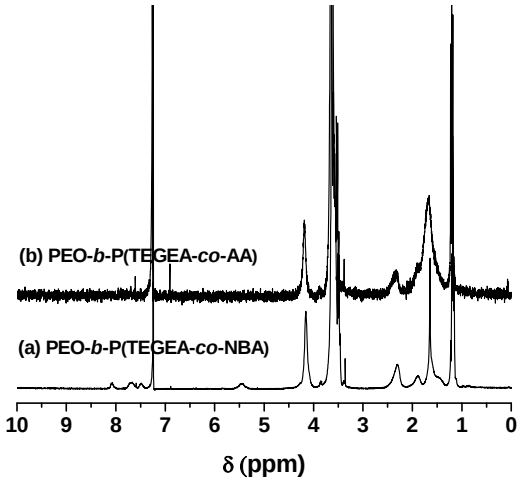


Figure A.11. ^{1}H NMR spectra of block copolymer PEO-*b*-P(TEGEA-*co*-NBA) (BR-**4**, $M_{n,GPC}$ = 18,300 g/mol, PDI = 1.07) and the corresponding polymer PEO-*b*-P(TEGEA-*co*-AA) obtained after UV irradiation at 32 ^{o}C for 400 min.

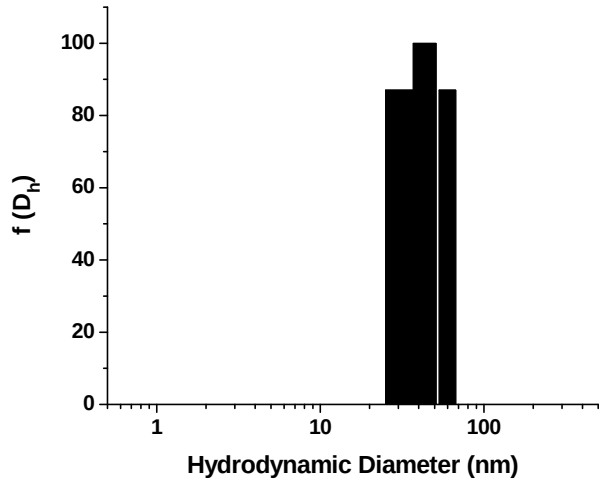


Figure A.12. Hydrodynamic diameter (D_h) distribution function of micelles of PEO-*b*-P(TEGEA-*co*-AA) at 50 ^{o}C. The polymer solution was obtained in situ from the UV irradiation of a 0.2 wt % aqueous solution of BR-**4** ($M_{n,GPC}$ = 18,300 g/mol, PDI = 1.07) at 32 ^{o}C for 480 min. The hydrodynamic diameter was calculated by use of the CONTIN method. The polydispersity of micelles at 50 ^{o}C was 0.062.

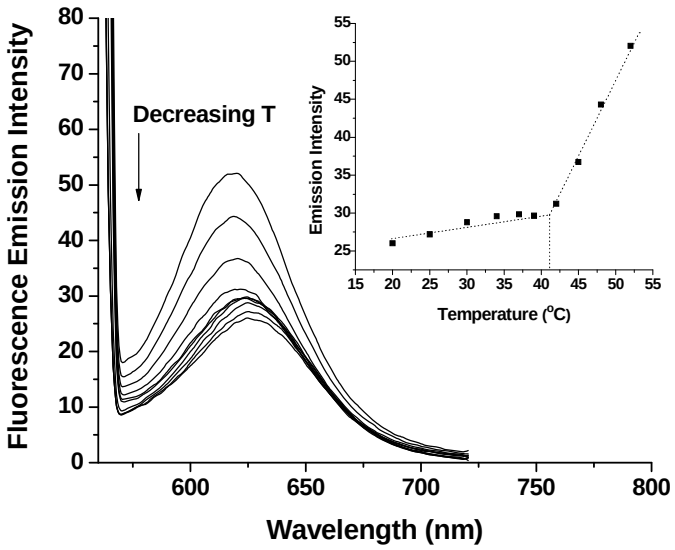


Figure A.13. Fluorescence spectra of photobleached Nile Red in the aqueous solution of PEO-*b*-P(TEGEA-*co*-AA) at various temperatures in the cooling process. The aqueous solution of PEO-*b*-P(TEGEA-*co*-AA) was obtained in situ by UV irradiation of a 0.2 wt % aqueous solution of PEO-*b*-P(TEGEA-*co*-NBA) (BR-**4**, $M_{n,GPC}$ = 18,300 g/mol, PDI = 1.07) at 32 ^{o}C for 480 min. The inset is the plot of emission intensity of the maximum peak versus temperature.

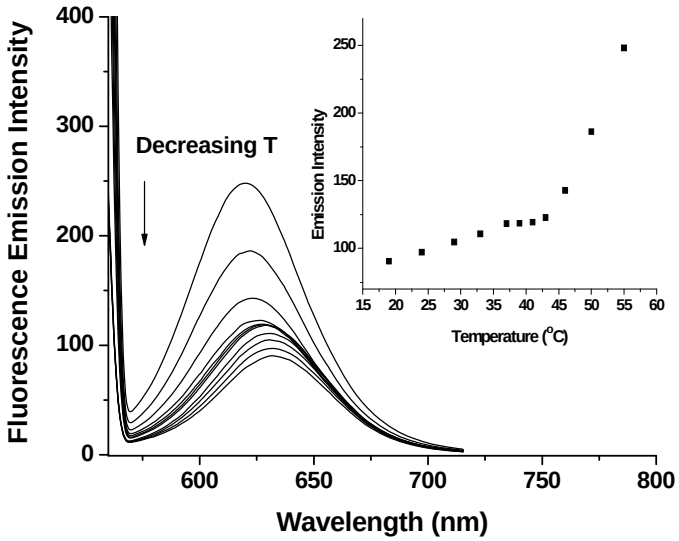
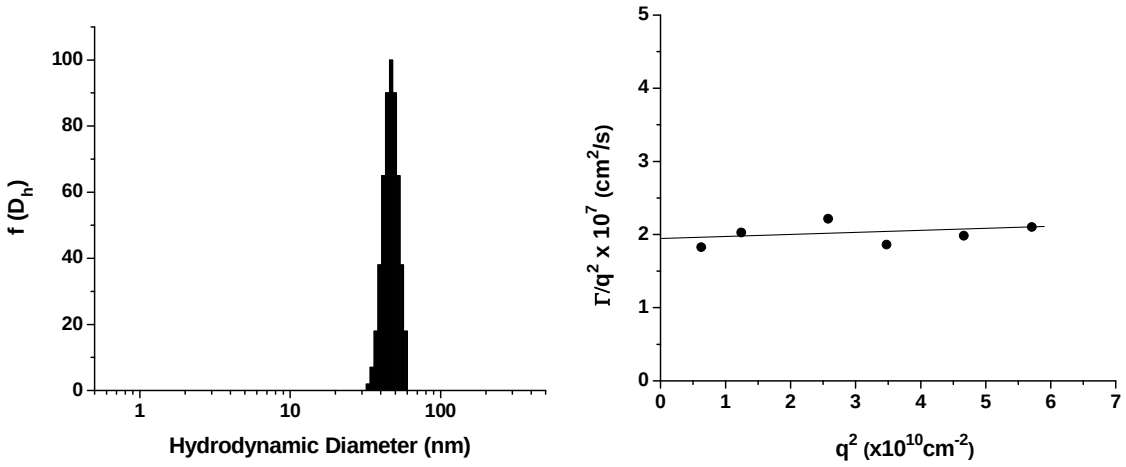
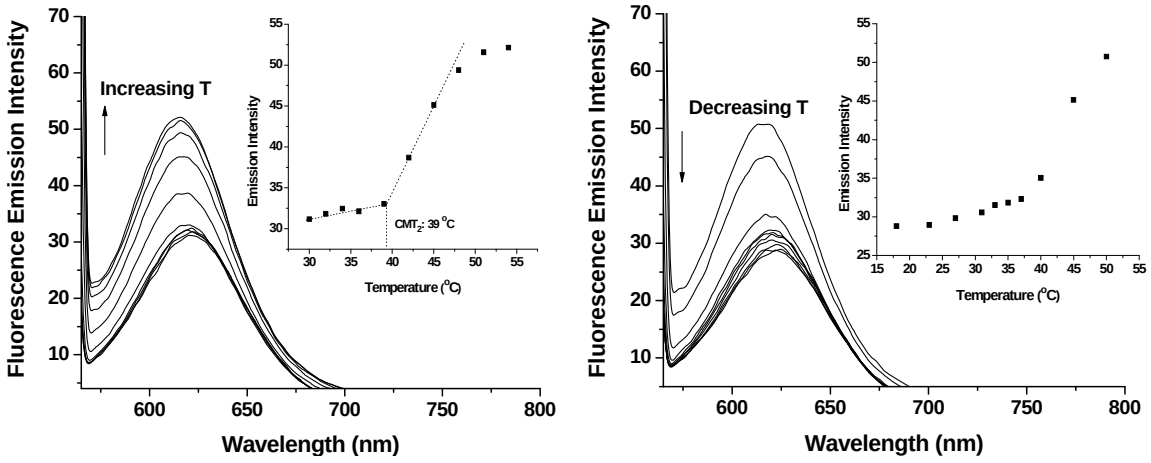


Figure A.14. Fluorescence spectra of Nile Red (photobleached dye plus reloaded fresh Nile Red dye) in the aqueous solution of PEO-*b*-P(TEGEA-*co*-AA) at various temperatures in the cooling process. The aqueous solution of PEO-*b*-P(TEGEA-*co*-AA) was obtained in situ by UV irradiation of a 0.2 wt % aqueous solution of PEO-*b*-P(TEGEA-*co*-NBA) (BR-**4**, $M_{n,GPC}$ = 18,300 g/mol, PDI = 1.07) at 32 ^{o}C for 480 min. The inset is the plot of emission intensity of the maximum peak versus temperature.



(a) (b)

Figure A.15. (a) Hydrodynamic diameter (D_h) distribution function of PEO-*b*-P(TEGEA-*co*-AA) at 50 ^oC in the heating process and (b) plot of Γ/q^2 of micelles of PEO-*b*-P(TEGEA-*co*-AA) versus q^2 at 50 ^oC. The aqueous solution of PEO-*b*-P(TEGEA-*co*-AA) was obtained in situ by UV irradiation of a 0.2 wt % aqueous solution of PEO-*b*-P(TEGEA-*co*-NBA) (BR-**5**, $M_{n,GPC}$ = 24,700 g/mol, PDI = 1.11) loaded with Nile Red at 30 ^oC for 480 min. The polydispersity of micelles at 50 ^oC was 0.013.



(a) (b)

Figure A.16. Fluorescence spectra of photobleached Nile Red in the aqueous solution of PEO-*b*-P(TEGEA-*co*-AA) at various temperatures in (a) the heating process and (b) the cooling process. The aqueous solution of PEO-*b*-P(TEGEA-*co*-AA) was obtained in situ by UV irradiation of a 0.2 wt % aqueous solution of PEO-*b*-P(TEGEA-*co*-NBA) (BR-**5**, $M_{n,GPC}$ = 24,700 g/mol, PDI = 1.11) loaded with Nile Red at 30 ^{o}C for 480 min. The inset is the plot of emission intensity of the maximum peak versus temperature.

Appendix B. Tuning Micellization and Dissociation Transitions of Thermo- and pH-Sensitive Poly(ethylene oxide)-*b*-poly(methoxydi(ethylene glycol) methacrylate-*co*-methacrylic acid) in Aqueous Solution by Combining Temperature and pH Triggers

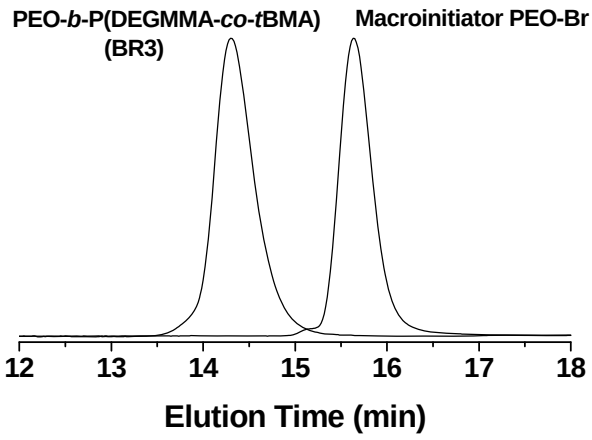


Figure B.1. Gel permeation chromatography traces of macroinitiator PEO-Br and a block copolymer PEO-*b*-P(DEGMMA-*co*-*t*BMA) (**BR3** in Table 3.1).

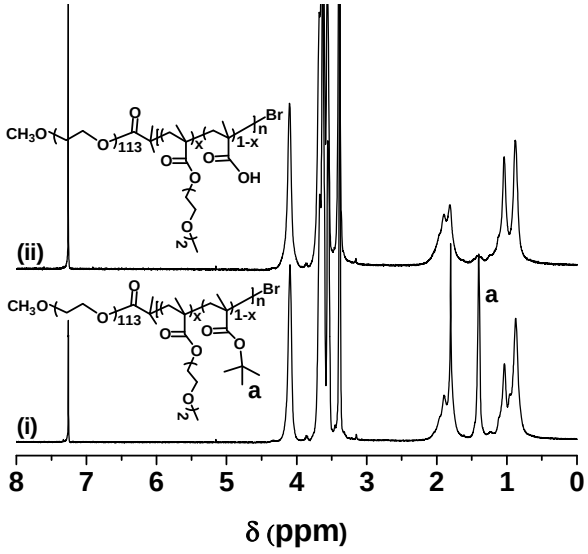


Figure B.2. ^{1}H NMR spectra of (i) PEO-*b*-P(DEGMMA-*co*-*t*BMA) (**BR3**, $M_{n,GPC}$ = 21800 Da, PDI = 1.06) and (ii) PEO-*b*-P(DEGMMA-*co*-MAA) (**BR3-H**). $CDCl_3$ was used as solvent in the ^{1}H NMR spectroscopy analysis.

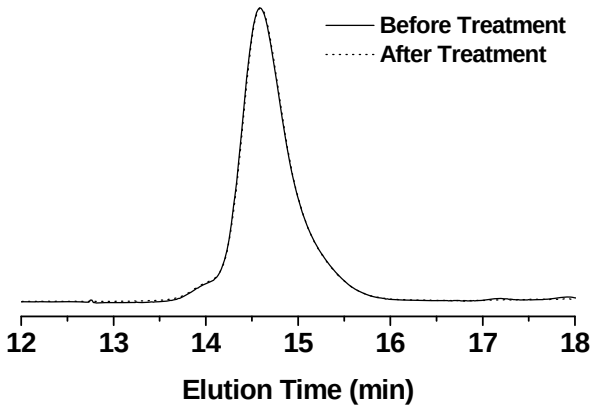


Figure B.3. Gel permeation chromatography traces of PDEGMMA (**H1**, $M_{n,GPC}$ = 16200 Da, PDI = 1.11) before and after treatment with CF_3COOH in a control experiment.

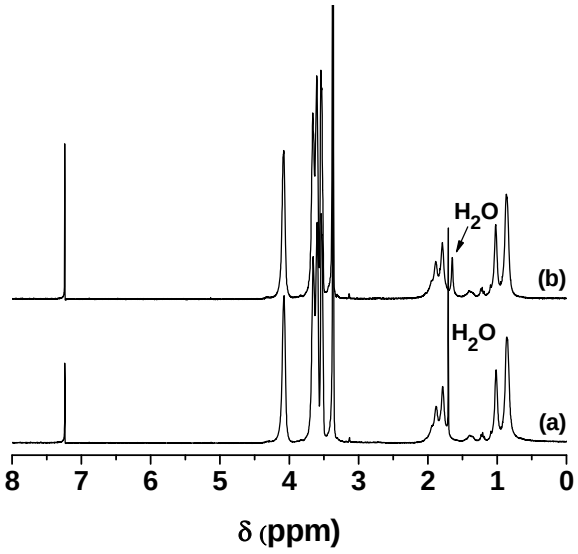


Figure B.4. ^{1}H NMR spectra of PDEGMMA (**H1**, $M_{n,GPC}$ = 16200 Da, PDI = 1.11) before (a) and after treatment with CF_3COOH (b) in a control experiment.

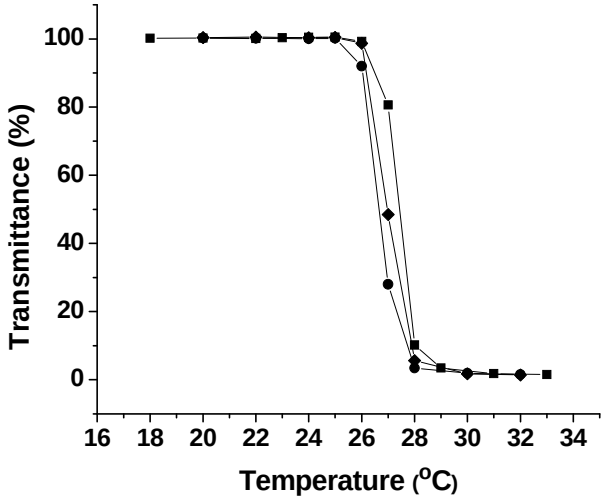
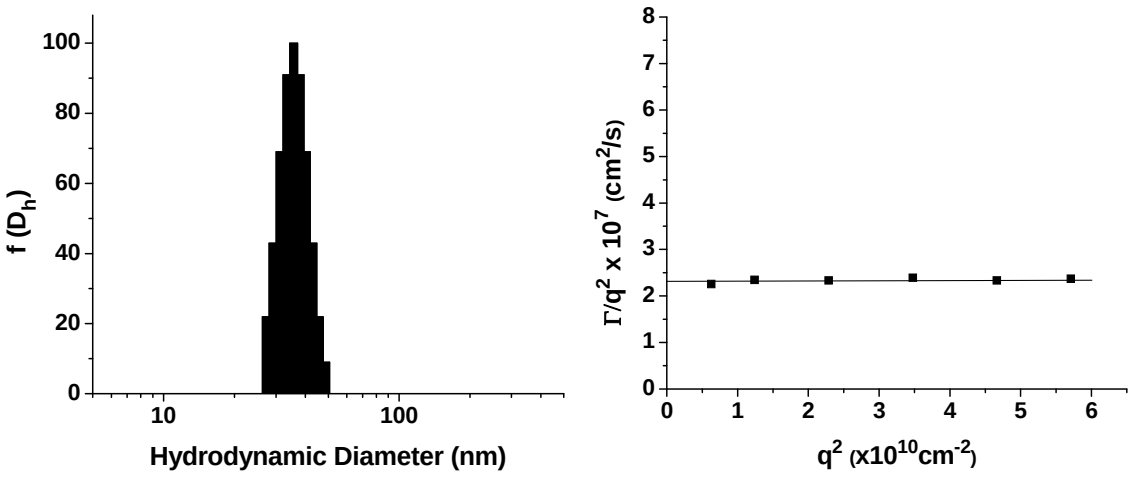
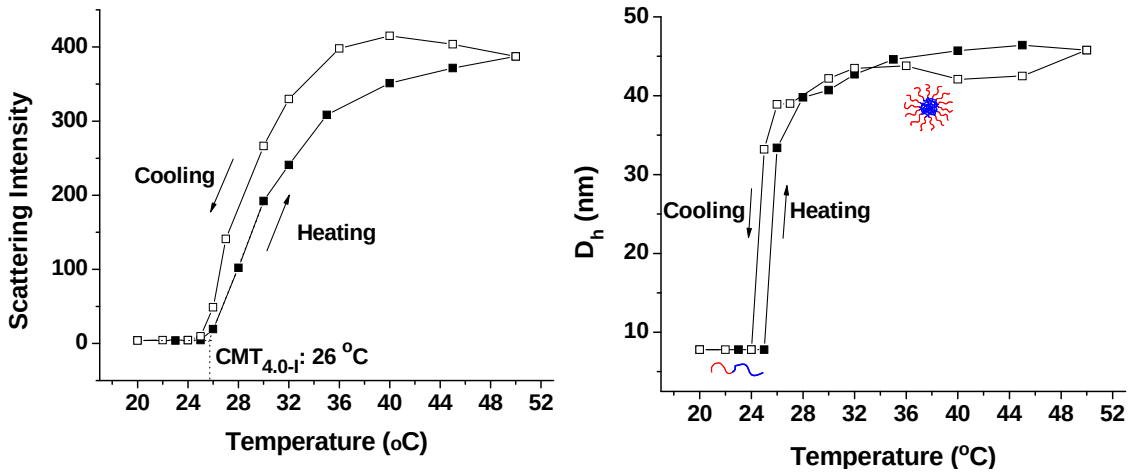


Figure B.5. Optical transmittances at wavelength of 550 nm of 0.2 wt % aqueous solutions of PDEGMMA (**H1**, $M_{n,GPC}$ = 16200 Da, PDI = 1.11) in 10 mM potassium hydrogen phthalate buffer with pH values of 4.1 (■), 5.3 (◆),and 6.1 (●) as a function of temperature upon heating. The transmittances were recorded with a UV-visible spectrometer.



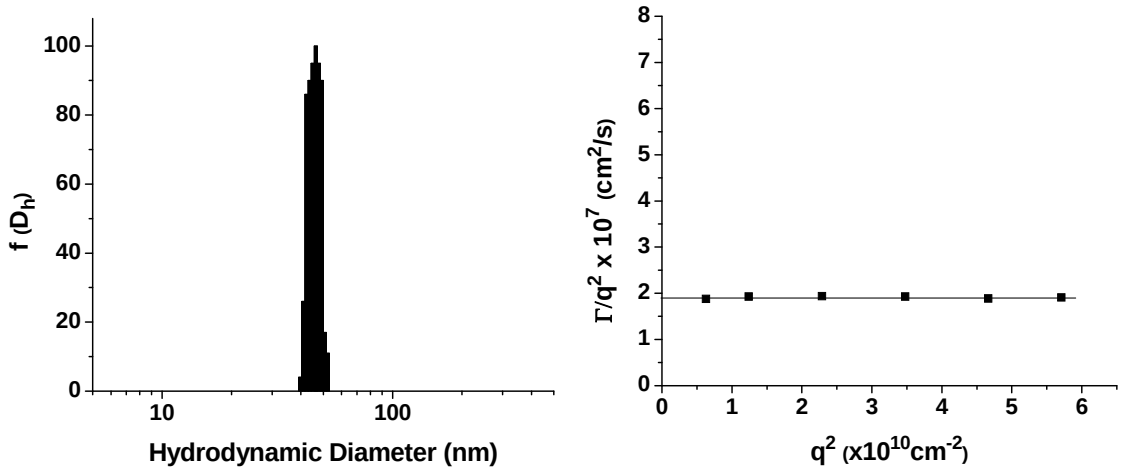
(a) (b)

Figure B.6. (a) Hydrodynamic diameter (D_h) distribution of micelles of PEO-*b*-P(DEGMMA-*co*-MAA) (**BR3-H**) at pH = 4.0 and T = 50 ^{o}C and (b) plot of Γ/q^2 of micelles of **BR3-H** vs. q^2 at pH = 4.0 and T = 50 ^{o}C. The polydispersity of micelles at 50 ^{o}C was 0.018.



(a) (b)

Figure B.7. The intensity of scattered light at scattering angle of 90° (a) and the hydrodynamic diameter (b) as a function of temperature (■ heating, □ cooling) in a dynamic light scattering study of a 0.2 wt % aqueous buffer solution of PEO-*b*-P(DEGMMA-*co*-MAA) (**BR4-H**) at pH = 4.0. In (b), at 26 °C in the heating process and at 25 °C in the cooling process, two size distributions, one ascribed to the unimers and one to the micelles, were observed and the reported hydrodynamic diameters for these temperatures were the average values over two hydrodynamic size distributions.



(a) (b)

Figure B.8. (a) Hydrodynamic diameter (D_h) distribution of micelles of PEO-*b*-P(DEGMMA-*co*-MAA) (**BR4-H**) at pH = 4.0 and T = 50 ^{o}C and (b) plot of Γ/q^2 of micelles of **BR4-H** vs. q^2 at pH = 4.0 and T = 50 ^{o}C. The polydispersity of micelles at 50 ^{o}C was 0.004.

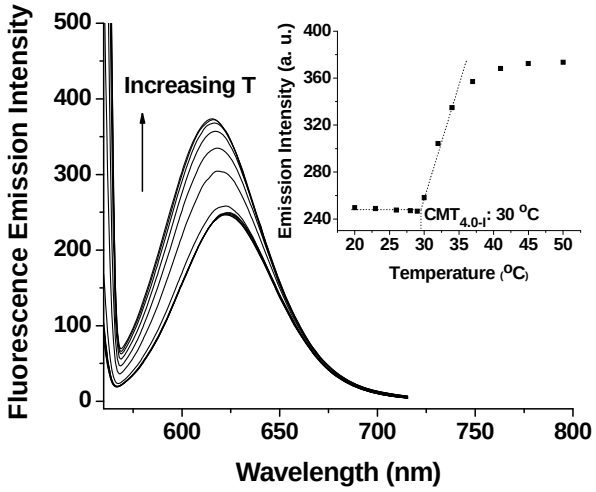


Figure B.9. Fluorescence emission spectra of Nile Red in a 0.2 wt % aqueous buffer solution of PEO-*b*-P(DEGMMA-*co*-MAA) (**BR3-H**) with a pH of 4.0 at various temperatures during heating. The inset is the plot of maximum fluorescence intensity versus temperature, from which the critical micellization temperature ($CMT_{4.0\text{-}I}$) was determined. The excitation wavelength was 550 nm.

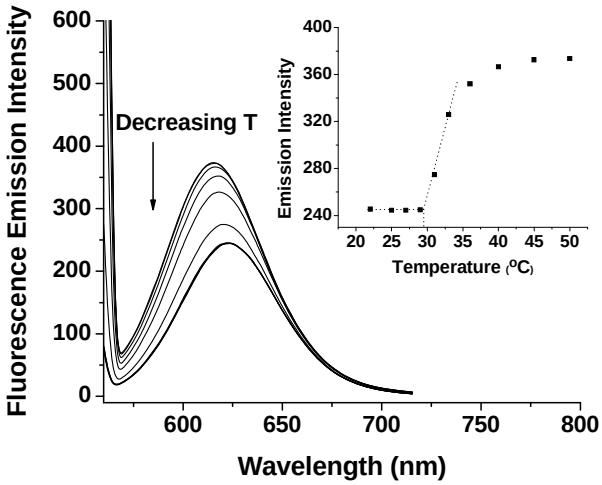


Figure B.10. Fluorescence emission spectra of Nile Red in a 0.2 wt % solution of PEO-*b*-P(DEGMMA-*co*-MAA) (**BR3-H**) in 10 mM KHP buffer with a pH of 4.0 at various temperatures during cooling. The inset is the plot of maximum fluorescence intensity versus temperature, from which the critical micellization temperature was determined. The excitation wavelength is 550 nm.

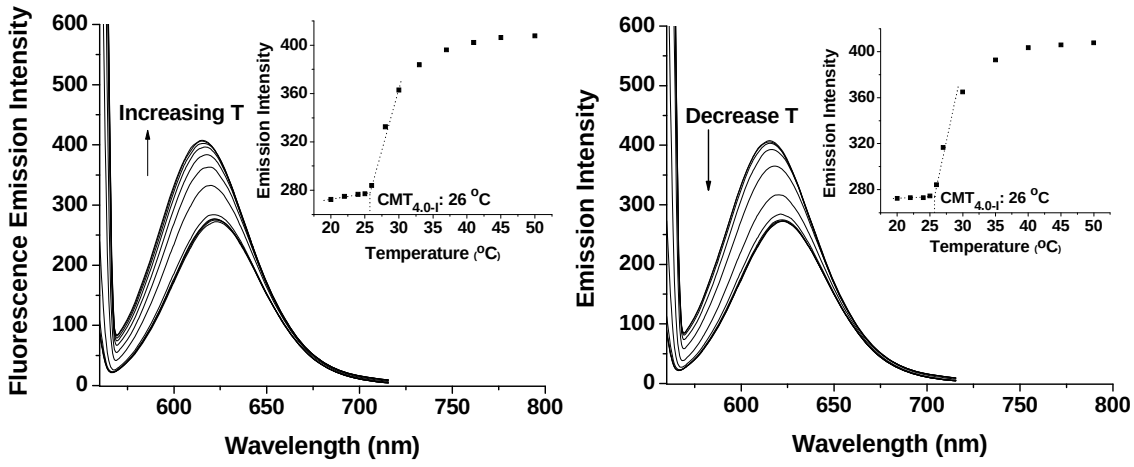


Figure B.11. Fluorescence emission spectra of Nile Red in a 0.2 wt % solution of PEO-*b*-P(DEGMMA-*co*-MAA) (**BR4-H**) in 10 mM KHP buffer with a pH of 4.0 at various temperatures in both heating (a) and cooling (b) processes. The insets are the plots of maximum fluorescence intensity versus temperature, from which the critical micellization temperature ($CMT_{4.0\text{-}I}$) was determined. The excitation wavelength is 550 nm.

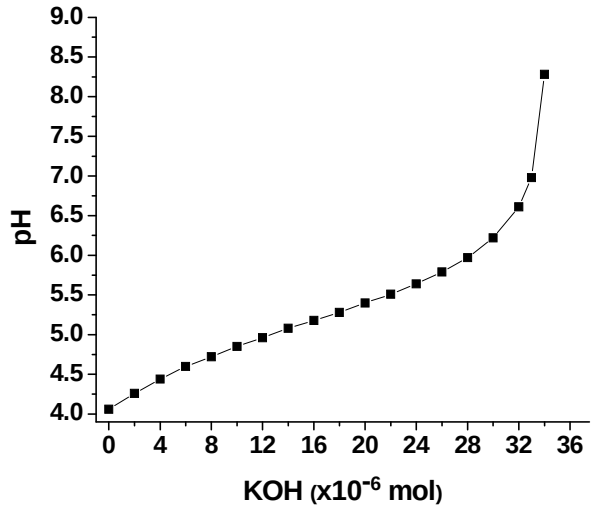
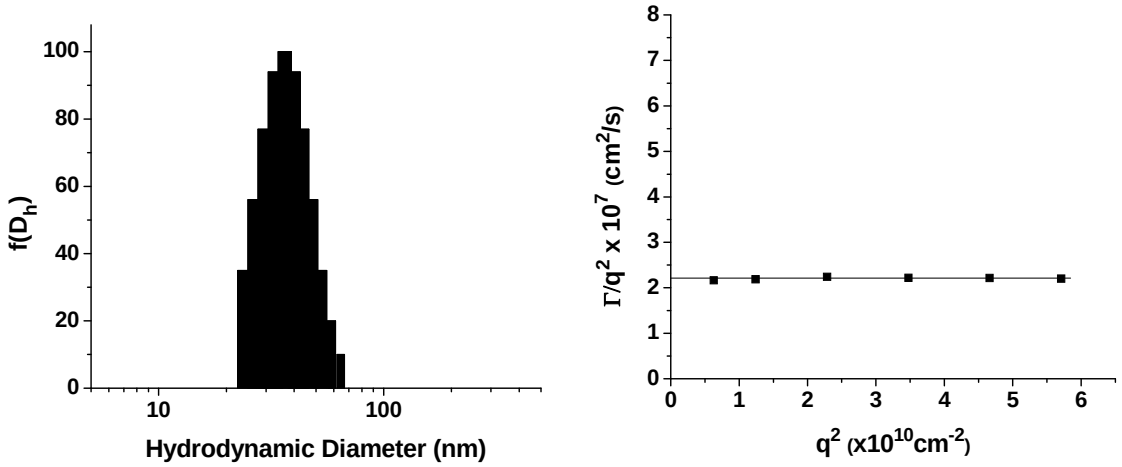


Figure B.12. The plot of solution pH versus number of μmols of KOH injected into a 0.2 wt % solution of PEO-*b*-P(DEGMMA-*co*-MAA) (**BR4-H**) in 10 mM KHP buffer (2.50 g). The KOH solution was added stepwise; each time, 10 μL of a 0.20 M aqueous KOH solution was injected via a microsyringe, followed by the measurement of pH with a pH meter. The volume of the solution increased by 6.8 % after the titration was finished.



(a) (b)

Figure B.13. (a) Hydrodynamic diameter (D_h) distribution of micelles of PEO-*b*-P(DEGMMA-*co*-MAA) (**BR3-H**) at pH = 5.4 and T = 50 ^{o}C and (b) plot of Γ/q^2 of micelles of **BR3-H** vs. q^2 at pH = 5.4 and T = 50 ^{o}C. The polydispersity of micelles at 50 ^{o}C was 0.055.

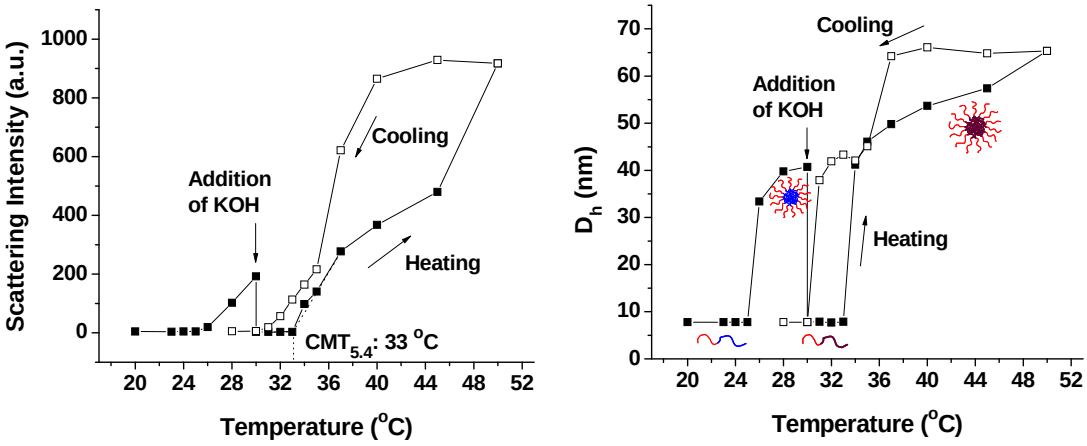


Figure B.14. The intensity of scattered light at scattering angle of 90° (a) and the hydrodynamic diameter (b) as a function of temperature (■ heating, □ cooling) in a dynamic light scattering study of multiple micellization/dissociation transitions of 0.2 wt % PEO-*b*-P(DEGMMA-*co*-MAA) (**BR4-H**) in 10 mM KHP buffer solution (the same solution used in Figure B.7) in response to addition of KOH and subsequent temperature changes. At 30 °C, 19 μmol of KOH (19 μL 1.00 M KOH) was injected into the polymer solution (2.50 g) to break the micelles in situ. The data points from 20 °C to 30 °C were from the heating process in Figure B.7. In (b), at 26 °C in the heating process, two size distributions were observed and the reported hydrodynamic diameter for this temperature was the average value over two hydrodynamic size distributions.

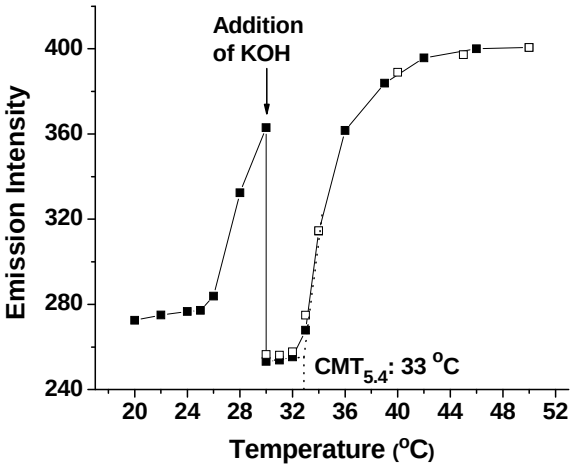
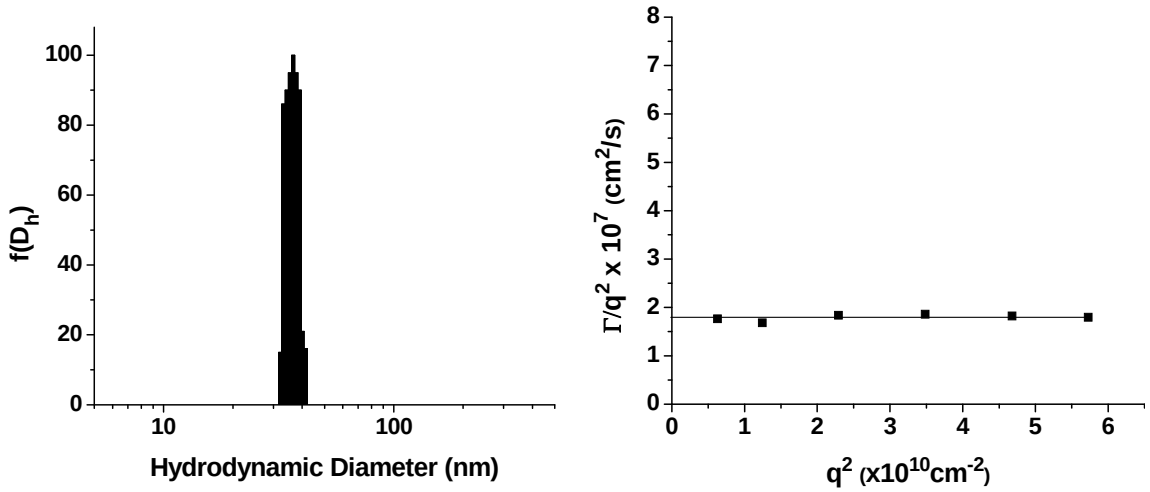
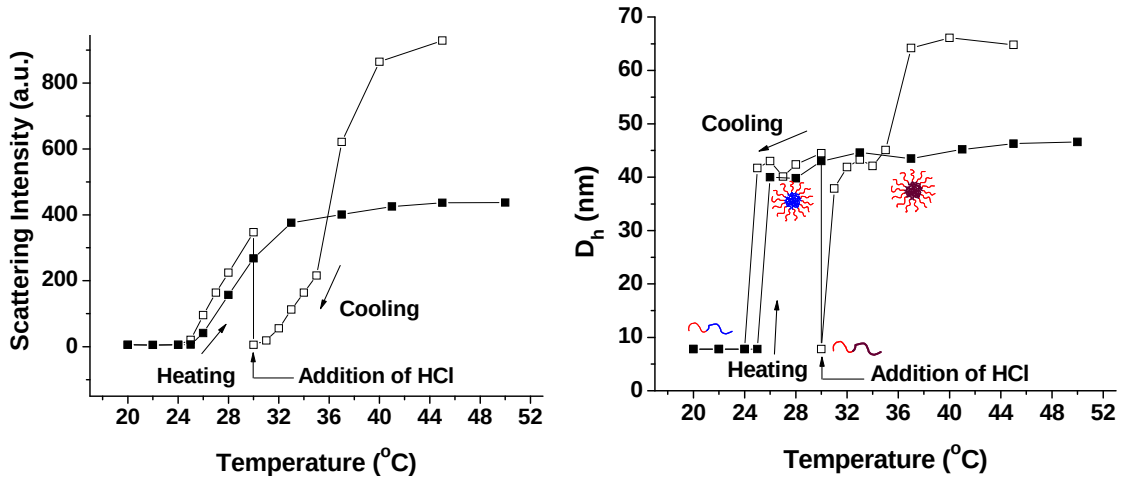


Figure B.15. Fluorescence emission intensity of Nile Red in a 0.2 wt % solution of **BR4-H** (PEO-*b*-P(DEGMMA-*co*-MAA)) in 10 mM KHP buffer (the same solution used in Figure B.11) in response to addition of KOH and subsequent temperature changes. The data points from 20 to 30 ^{o}C were from the heating process in Figure B.11. At 30 ^{o}C, 7.6 μmol of KOH (7.6 μL 1.00 M KOH) was injected into the fluorescence quartz cuvette that contained 1.00 g of a 0.2 wt % polymer buffer solution (the pH increased from 4.0 to 5.4) and the fluorescence emission intensity was recorded at a function of temperature (■ heating, □ cooling). The excitation wavelength was 550 nm.



(a) (b)

Figure B.16. (a) Hydrodynamic diameter (D_h) distribution of micelles of PEO-*b*-P(DEGMMA-*co*-MAA) (**BR3-H**) at pH = 4.0 and T = 50 ^oC and (b) plot of Γ/q^2 of micelles of **BR3-H** vs. q^2 at pH = 4.0 and T = 34 ^oC. The polydispersity of micelles at 50 ^oC was 0.004. A predetermined amount of HCl (7.5 μmol) was added into the polymer solution to change the pH back to 4.0 from 5.4 and subsequent cooling and heating to 50 ^oC.



(a) (b)

Figure B.17. The intensity of scattered light at a scattering angle of 90° (a) and the hydrodynamic diameter (b) as a function of temperature (□ cooling, ■ heating) in a dynamic light scattering study of multiple micellization/dissociation transitions of a 0.2 wt % solution of PEO-*b*-P(DEGMMA-*co*-MAA) (**BR4-H**) in 10 mM KHP buffer solution (the same solution used in Figure B.14) in response to addition of HCl and subsequent temperature changes. At 30 °C, 19 μL of 1.00 M HCl solution was injected into the DLS tube which contained 2.50 g of the polymer solution. The data points in the cooling curve from 50 to 30 °C were from the cooling curve of Figure B.14.

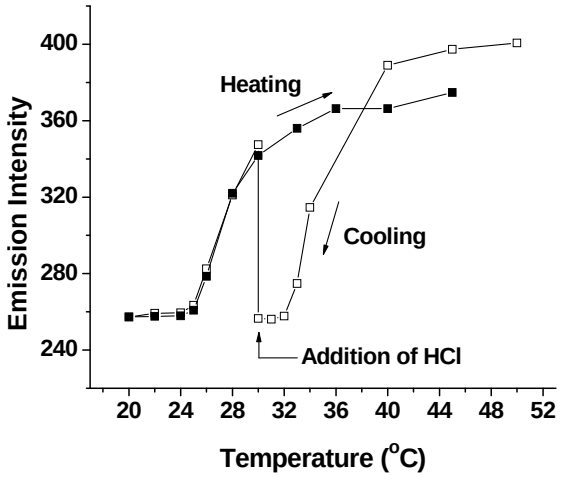
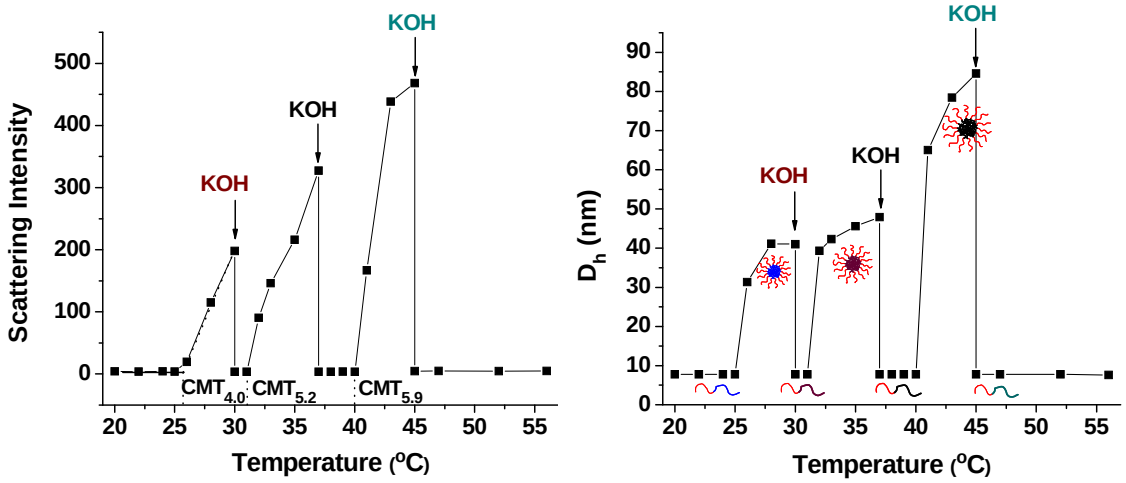


Figure B.18. Fluorescence emission intensity of Nile Red in a 0.2 wt % solution of PEO-*b*-P(DEGMMA-*co*-MAA) (**BR4-H**) in 10 mM KHP buffer (the same solution used in Figure B.15) in response to addition of HCl and subsequent temperature changes. The data points from 50 to 30 ^{o}C were from the cooling process in Figure B.15. At 30 ^{o}C, 7.6 μmol of HCl (7.6 μL of 1.00 M HCl) was injected into the solution (1.00 g) to change the pH from 5.4 to 4.0 and the fluorescence emission intensity was recorded at a function of temperature (□ cooling, ■ heating). The excitation wavelength was 550 nm.



(a) (b)

Figure B.19. The intensity of scattered light at a scattering angle of 90° (a) and the hydrodynamic diameter (b) as a function of temperature in a dynamic light scattering study of multiple micellization/dissociation transitions of a 0.2 wt % solution of PEO-*b*-P(DEGMMA-*co*-MAA) (**BR4-H**) in 10 mM KHP buffer (2.50 g) in response to temperature and pH changes. At 30 °C, 16 μL of 1.00 M KOH solution was injected into the solution (the pH changed to 5.2). At 37 °C, 11.0 μL of 1.00 M KOH solution was injected (the pH changed to 5.9). At 45 °C, 7.0 μL of 1.00 M KOH solution was injected into the solution (the pH changed to ~ 8.3). In (b), at 26 °C, two size distributions were observed and the reported hydrodynamic diameter for this temperature was the average value over two hydrodynamic size distributions.

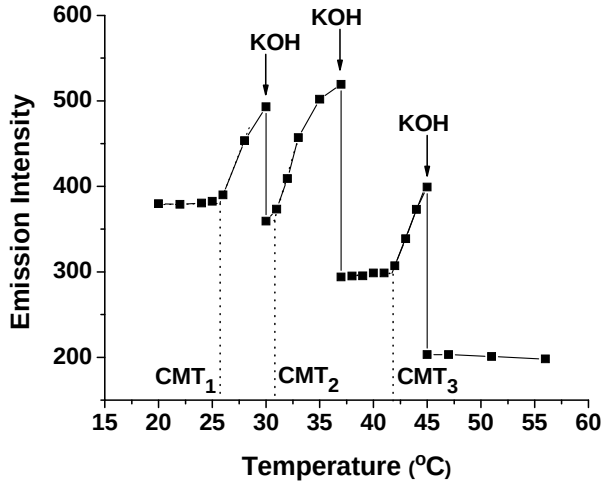


Figure B.20. Fluorescence emission intensity of Nile Red in a 10 mM KHP buffer solution that contained 0.2 wt % PEO-*b*-P(DEGMMA-*co*-MAA) (**BR4-H**) in response to the temperature and pH changes. The excitation wavelength was 550 nm. At 30 ^{o}C, 6.6 μL of a 1.00 M KOH solution was injected into the solution (the pH changed to 5.2). At 37 ^{o}C, 4.5 μL of 1.00 M KOH was added (the pH changed to 5.9). At 45 ^{o}C: 3.0 μL of 1.00 M KOH was injected (the pH changed to ~ 8.3).

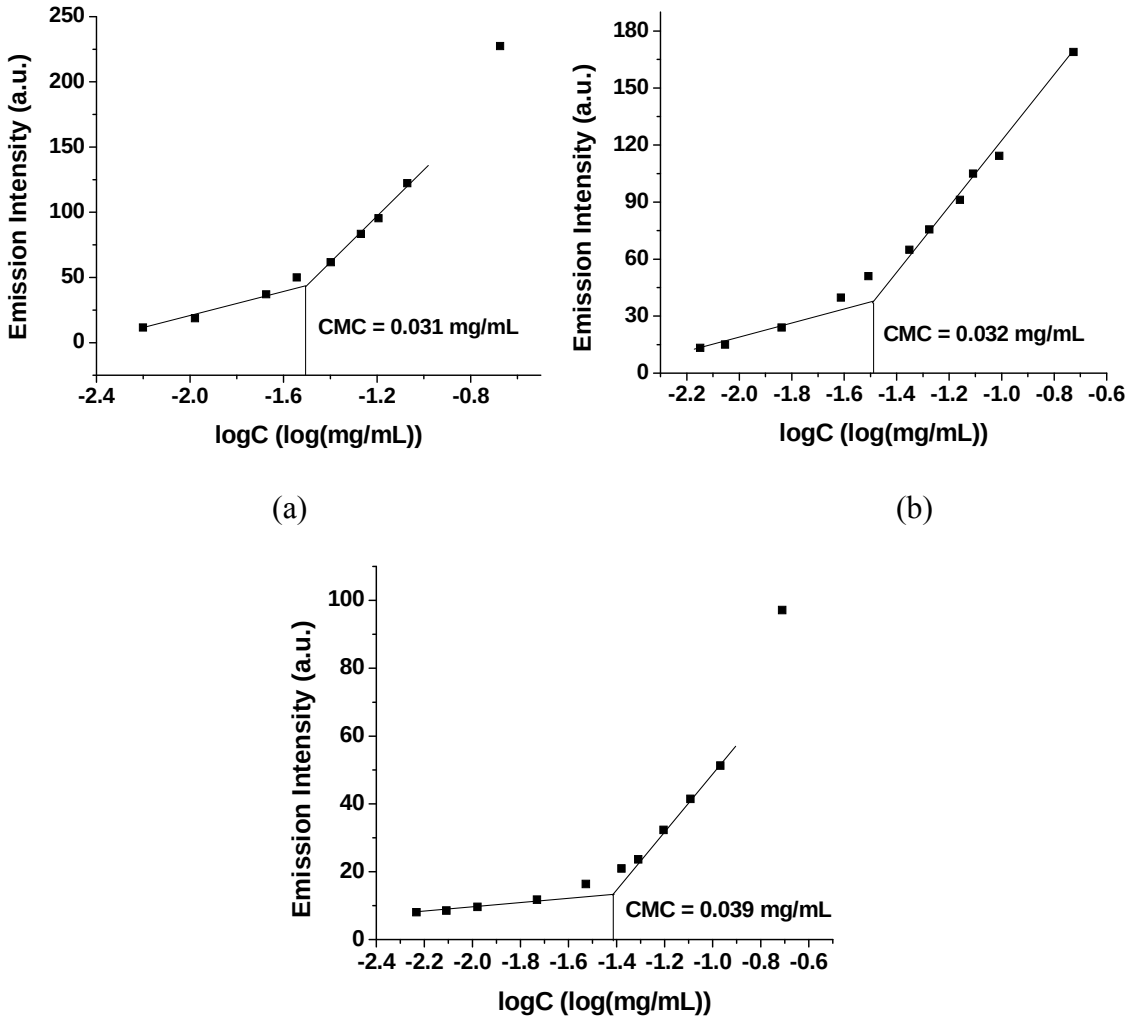
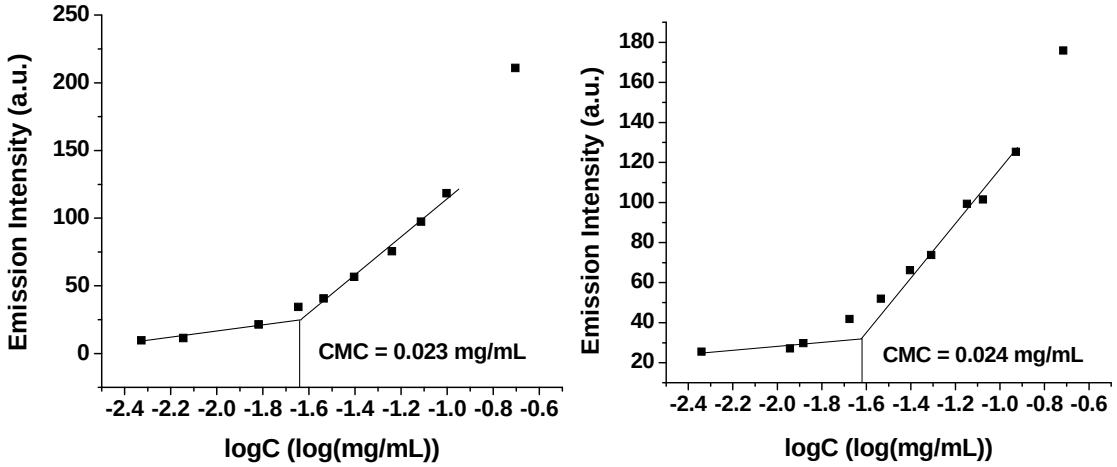
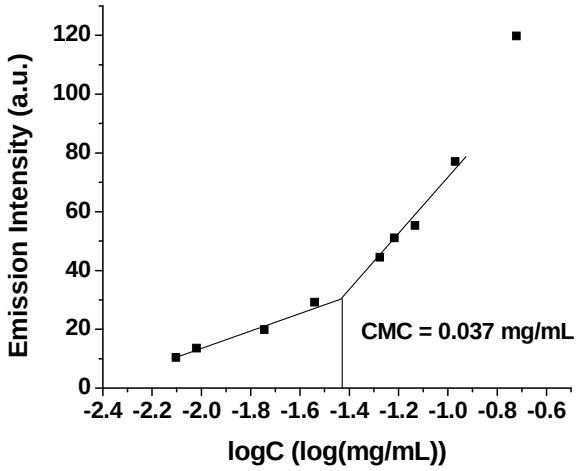


Figure B.21. Plots of maximum fluorescence emission intensity of Nile Red in 10 mM KHP buffer solutions of **BR3-H** at T= 50 ^{o}C and pH = 4.0 (a), T = 50 ^{o}C and pH = 5.2 (b), T = 50 ^{o}C and pH = 5.9 (c) versus the logarithm of polymer concentration, from which the critical micelle concentrations (CMC) were determined.



(a)

(b)



(c)

Figure B.22. Plots of maximum fluorescence emission intensity of Nile Red in 10 mM KHP buffer solutions of **BR4-H** at T= 50 ^{o}C and pH = 4.0 (a), T = 50 ^{o}C and pH = 5.2 (b), T = 50 ^{o}C and pH = 5.9 (c) versus the logarithm of polymer concentration, from which the critical micelle concentrations (CMC) were determined.

Vita

Xueguang Jiang was born in Rushan, China. He attended the University of Science and Technology of China in Anhui from 1997 to 2002, where he received a B.S. degree in Chemistry. In August, 2005, he enrolled as a graduate student in the Department of Chemistry at the University of Tennessee, Knoxville and joined Dr. Bin Zhao's group working on stimuli-responsive hydrophilic polymers. Xueguang Jiang received a Doctor of Philosophy Degree in Chemistry from the University of Tennessee in August, 2010.